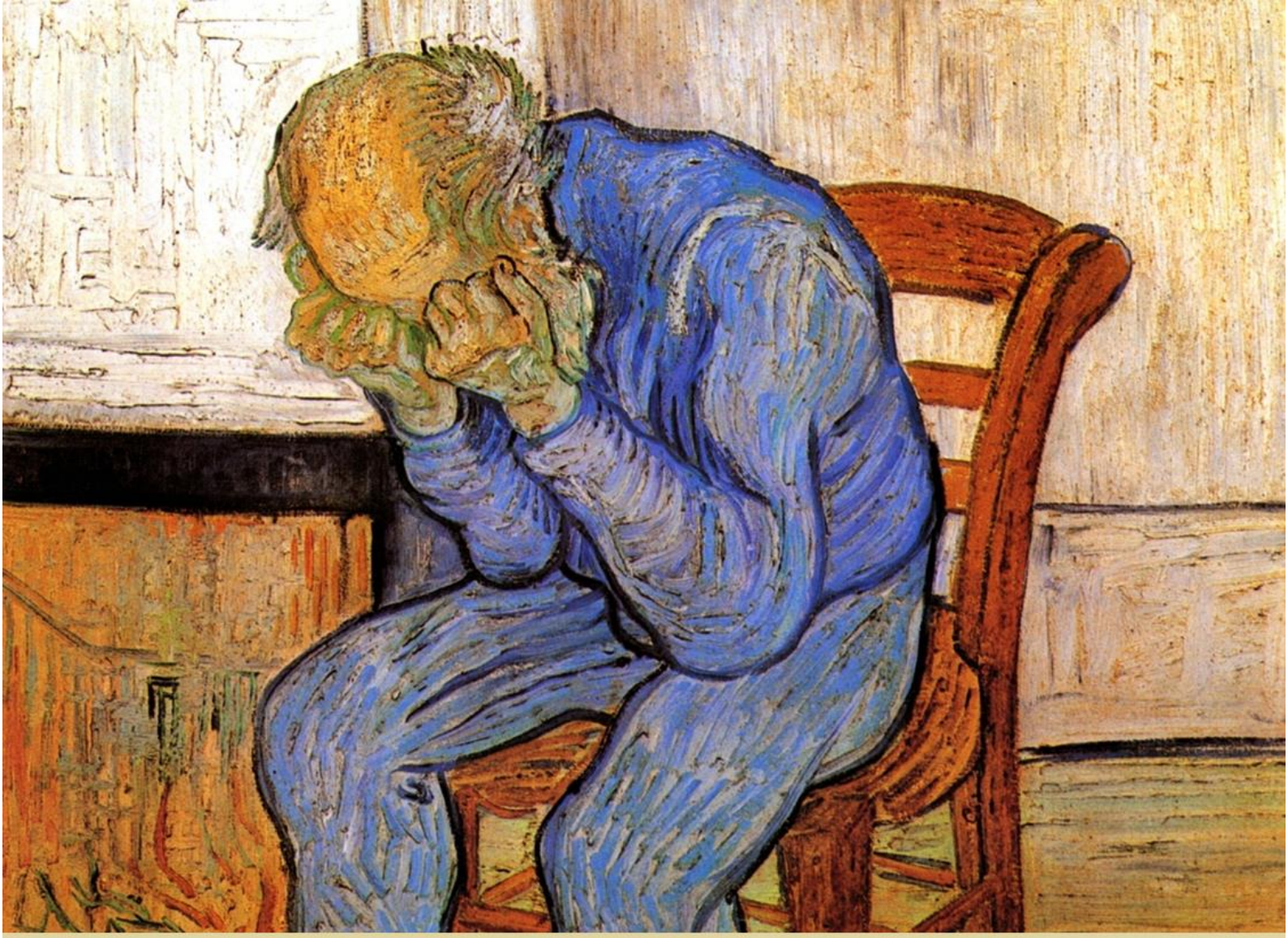

Carlos Adriano Albuquerque Andrade de Matos

Regulation of ataxin-3 by phosphorylation: Relevance for Machado-Joseph disease

Tese de Doutoramento em Biologia, na especialidade de Biologia Celular, orientada pela Professora Doutora Ana Luísa Monteiro de Carvalho e pela Professora Doutora Sandra de Macedo Ribeiro e apresentada ao Departamento de Ciências da Vida da Faculdade de Ciências e Tecnologia da Universidade de Coimbra

Julho de 2014

· U C ·

UNIVERSIDADE DE COIMBRA

Carlos Adriano Albuquerque Andrade de Matos

Regulation of ataxin-3 by phosphorylation: Relevance for Machado-Joseph disease

Tese de Doutoramento em Biologia, na especialidade de Biologia Celular, orientada pela Professora Doutora Ana Luísa Monteiro de Carvalho e pela Professora Doutora Sandra de Macedo Ribeiro e apresentada ao Departamento de Ciências da Vida da Faculdade de Ciências e Tecnologia da Universidade de Coimbra

Julho de 2014

UNIVERSIDADE DE COIMBRA

O trabalho aqui apresentado foi realizado no Centro de Neurociências e Biologia Celular – CNC, Universidade de Coimbra, Portugal e no Instituto de Biologia Molecular e Celular – IBMC, Porto, Portugal e financiado pela Fundação para a Ciência e Tecnologia.

The work hereby presented was performed at the Center for Neuroscience and Cell Biology – CNC, University of Coimbra, Coimbra, Portugal and at the Institute for Molecular and Cell Biology – IBMC, Porto, Portugal and funded by the Portuguese Foundation for Science and Technology.

SFRH/BD/47160/2008; PTDC/SAU-NMC/110602/2009; PEst-C/SAU/LA0001/2013-2014

Nota de capa

Pormenor de *Sorrowing Old Man (At Eternity's Gate)*, de Vincent van Gogh. A imagem encontra-se no domínio público.

Cover nove

Detail of *Sorrowing Old Man (At Eternity's Gate)*, by Vincent van Gogh. The image is in the public domain.

A toda a minha família

e em especial aos Andrades

“He no longer saw the face of his friend Siddhartha, instead he saw other faces, many, a long sequence, a flowing river of faces, of hundreds, of thousands, which all came and disappeared, and yet all seemed to be there simultaneously, which all constantly changed and renewed themselves, and which were still all Siddhartha. He saw (…) all of these figures and faces in a thousand relationships with one another, each one helping the other, loving it, hating it, destroying it, giving re-birth to it, each one was a will to die, a passionately painful confession of transitoriness, and yet none of them died, each one only transformed, was always re-born, received evermore a new face, without any time having passed between the one and the other face—and all of these figures and faces rested, flowed, generated themselves, floated along and merged with each other (…).”

in *Shiddhartha* by Hermann Hess

“All we have to decide is what to do with the time that is given to us.”

- Gandalf, in *The Lord of the Rings* By J.R.R. Tolkien

Agradecimentos

Quando se procura agradecer a alguém por uma contribuição para um trabalho de anos (cinco, neste caso), poderá torna-se difícil escolher a pessoa a quem se dirigem as primeiras palavras. No meu caso, porém, considero-me com sorte, pois a escolha foi sempre clara para mim desde o início. Começo, pois, por agradecer à minha orientadora, a Professora Ana Luísa Carvalho. Em primeiro – em primeiríssimo – lugar, agradeço-lhe pelas aulas de Biologia Celular e Molecular a que tive o prazer de assistir no anfiteatro do antigo Departamento de Zoologia, há quase dez anos. Quando decidi entrar na Universidade de Coimbra para estudar Biologia, o meu gosto por esta ciência estava muito direccionado para as áreas da Biodiversidade e da Ecologia, embora me tenham sempre fascinado e interessado também as áreas mais moleculares da Biologia. Foram talvez (ou talvez certamente) as suas aulas que me começaram a direccionar para aquele que viria a ser um percurso académico voltado para a Biologia Celular e Molecular, na esperança de um dia poder vir eu próprio a fazer investigação e a contribuir para esta área do conhecimento científico. Em segundo lugar agradeço-lhe assim a oportunidade que me deu de trabalhar consigo durante o meu projecto de Mestrado e de me ter permitido expandir esse trabalho para o Doutoramento sobre cujo trabalho versa esta tese. Agradeço-lhe todos os conselhos, todas as observações pertinentes, todas as sugestões certeiras, todo o conhecimento que me transmitiu e todo o espírito científico que procura incutir aos seus alunos e que tão bem exemplifica. Agradeço a motivação que sempre me transmitiu, o ânimo, a confiança nas minhas capacidades que sempre reconheci e que espero honrar com o presente trabalho. Finalmente, ficarei para sempre grato pelo facto de ter sempre tolerado os meus erros, as minhas falhas e as minhas incertezas e por ter sempre reconhecido que, não obstante o dever do trabalho que desenvolvemos, é importante viver também outras coisas. Graças a isso tive a oportunidade de perseguir outros sonhos, e de cumprir um ou dois.

Agradeço de igual modo à Doutora Sandra Ribeiro, cuja distância durante este período de Doutoramento foi unicamente física, estando na verdade sempre presente durante todo o processo. Agradeço-lhe toda a orientação que me deu durante estes anos, bem como o facto de me ter permitido obter alguns dos materiais cruciais para muitas das experiências aqui mencionadas. Agradeço-lhe a confiança que depositou em mim e o seu modo inspirador de olhar para os problemas científicos. Não posso deixar também de agradecer a oportunidade que me deu de trabalhar noutros projectos para além daquele que aqui apresento.

Devo o maior dos agradecimentos aos meus pais. Para além de serem os responsáveis por eu ter tido as condições e a oportunidade para estudar e para ingressar no Douramento, são sem dúvida os principais responsáveis pelo meu gosto pela ciência e pela liberdade que tive em escolher as vias que escolhi. Agradeço-lhes o modo como cuidam de mim e se preocupam e me fazem sentir amado e capaz de fazer qualquer coisa neste mundo. Vocês são os maiores e esta tese é para vocês.

À minha maninha Marcela agradeço o apoio, a preocupação, a alegria, a sensatez e a ligação que sempre manteve comigo e que é única. Agradeço-lhe as risadas, as conversas sérias e a introspecção que delas deriva. Um grande abraço fica aqui também para o Eduardo, a quem agradeço toda a amizade e ajuda para tantas coisas. Ao meu maninho João estarei sempre grato pelo companheirismo, pela amizade, pela boa energia que transmite a quem o rodeia e em especial a mim. Sempre foi o meu melhor amigo, e assim vai continuar a ser. Manos, esta tese é para vocês também.

À minha avó Ilda agradeço um amor que nunca lhe conseguirei agradecer por palavras, à minha avó Fernanda o cuidado de tantos anos, às minhas tias Ni e Zi a vivacidade e o interesse com que fazem tudo e com que me motivaram para a ciência (ainda que talvez não o saibam). Agradeço a todo o resto da minha família o omnipresente apoio e interesse e um amor puro e único, nomeadamente ao meu tio Cá, à minha tia Anabela, à minha tia Lúcia, ao Acácio e a todos os meus primos que menciono aqui por ordem meramente etária e de quem lamento não ter estado mais próximo nestes anos que passaram: Inês, João, Beatriz, Ana Carolina, Maria Inês, Maria Carolina.

A ti, Clévio, agradeço por muito mais do que seria possível conter nesta página. Obrigado por tudo o que fizeste por mim nestes últimos anos, por todo o companheirismo, pela amizade, pela aventura, pela alegria e pelo gosto de viver. Obrigado por me teres suportado nestes últimos tempos, por seres compreensivo e teres contribuído para que eu tenho acabado a escrita desta tese sem ter perdido o juízo. Obrigado pelas partidas de squash, pelos jantares e pelos momentos de diversão. Agradeço-te também por acreditares em mim e por seres um grande exemplo de competência e de espírito de trabalho. E agradeço, claro está, pela ajuda – pela enorme ajuda – com as experiências com o modelo lentiviral de rato. Sem o teu auxílio esta tese seria bem mais pobre.

Agradeço ao Doutor Carlos Duarte tudo que me ensinou acerca de Neurobiologia, todo o contributo técnico para o trabalho aqui apresentado e a boa disposição com que sempre me motivou a investir nos meus sonhos. Estou muito grato também ao Doutor Ramiro Almeida e ao Doutor João Peça pela discussão interessante e perspicaz do meu trabalho. Ao Doutor Luís almeida agradeço a oportunidade que tive no seu laboratório com o modelo lentiviral de MJD em ratos, pelo seu interesse, pela sua apreciação e pela sua boa disposição.

Devo o maior agradecimento a todos os meus colegas de laboratório, sem excepção. A todos vós estou grato pelo ânimo, pela energia criadora e compassiva que todos demonstraram para comigo nestes quase 6 anos. Agradeço à Tatiana as palhaçadas e as conversas construtivas, ao Luís o seu companheirismo e o exemplo da sua dedicação ao trabalho, à Sandra a alegria e toda a ajuda e interesse, ao Graciano (*o pórpio*) a boa disposição, ao Rui, ao Michelle e ao Ivan a amizade, à Miranda, à Gladys, à Dominique e à Mariline a simpatia, à Marta as risadas e ao Pedro Afonso a sua boa disposição contagiante e a sua sinceridade. Deixo um agradecimento também à Joana Ferreira pelo seu interesse, pela sua ajuda, pela grande paciência e pelo facto de ter estado quase sempre a meu lado, literalmente. Devo um agradecimento especial também à Joana Fernandes, pela amizade que tivemos e da qual espero continuar a ser merecedor. Agradeço à Susana o enorme interesse que sempre

demonstrou no meu trabalho, a paciência, e o modo crucial como me ajudou com as experiências que utilizaram as culturas de córtex. Sem ti esta tese estaria incompleta. Agradeço à Rita o facto de me ter ensinado a fazer os ensaios com a Ub-AMC e a Ub-VS e à Doutora Luísa Cortes a ajuda com a microscopia. Um obrigado não fica esquecido para a Mariliza e a sua contribuição para os estudos de agregação. Fica aqui ainda um grande beijinho para a Dona Céu e para a Elisabete, por toda a simpatia e pelo facto de tornarem o trabalho no laboratório mais fácil.

Agradeço às princesas Mariana, Marisa e Sara a boa disposição e a preocupação e à Célia a alegria e a ajuda na formatação desta tese. Deixo também um agradecimento ao Mário Laço pela ajuda com os ensaios de actividade com cadeias de polyUb e à Joana Santos e ao Bruno Almeida pelo auxílio com a produção e atx3 recombinante. Agradeço à Doutora Patrícia Maciel a oportunidade para aprender e trabalhar no seu laboratório, à Andreia Castro e à Ana Jalles toda a ajuda com as *C. elegans* e à Dulce Almeida, à Fátima Ramalhosa, à Francisca e às outras meninas do Minho o modo como me acarinharam.

Agradeço aos meus grandes amigos Carlos, por acreditar em mim e nas minhas capacidades, pelos momentos de alegria e diversão e pelas conversas sobre trabalho e sobre os mistérios do mundo. Ao Pedro serei sempre grato pelo companheirismo e pela sabedoria e pela grande e eterna amizade. Deixo um obrigado à Renata, por ser uma amiga tão antiga mas sempre tão presente e à Joana Vindeirinho pela alegria e por ser sempre compincha. Para o maior viola de fado, Alexis Simões, para o maior guitarrista, Hugo Paiva de Carvalho, e para o rouxinol José Branco fica um grande e Minervino abraço de obrigado pela vossa amizade e pelo vosso interesse no meu trabalho.

Finalmente, agradeço a todas as pessoas que fazem de mim uma pessoa feliz e que eventualmente não estejam mencionados nos parágrafos acima incluídos. Deste modo, e muito resumidamente, um obrigado à malta de Biologia por me ligarem a um passado saudoso, à malta do japonês, aos meus amigos do Japão e, claro está, aos meus amigos de sempre e para sempre: André, Bekas, Filipe, Joana, Joana.

☸

ओं मणिपद्मे हूं

Table of contents

Abbreviations

6His	hexahistidine
ALP	alkaline phosphatase
AMPA	α-amino-3-hydroxy-5-methyl-4-isoxazolepropionic acid
AMPAR	AMPA receptor
ANOVA	analysis of variance
AR	androgen receptor
ATM	protein kinase ataxia-telangiectasia mutated
atx3	ataxin-3
atx3L	ataxin-3-like protein
BACE457Δ	β-sile amyloid precursor protein cleaving enzyme
BCA	bicinchoninic acid
BLAST	Basic Local Alignment Seach Tool
BSA	bovine serum albumin
CAA	cytosine-adenine-adenine
$CACNA1_A$	calcium channel, voltage dependent, P/Q type, α1A subunit
CAG	cytosine-adenine-guanine
CaMK	calcium/calmodulin-dependent protein kinase
CaMK2	calcium/calmodulin-dependent protein kinase 2
CBP	CREB-binding protein
Cdc2	cell division cycle 2 kinase
Cdk1	cycling-dependent kinase 1
Cdk5	cyclin-dependent kinase 5
CHIP	C-terminus of Hsp70-interacting protein
CK1	casein kinase 1
CK2	casein kinase 2
CLAP	chymostatin, pepstatin, antipain and leupeptin
CNS	central nervous system
CREB	cAMP response element-binding protein
CRM1	chromosome region maintenance 1
CRMP-2	collapsing response mediator protein-2
DARPP-32	dopamine- and cyclic AMP-regulated phosphoprotein of 32 kDa
DIV	days *in vitro*
DMEM	Dulbecco's Modified Eagle's Medium
DNA PK	DNA-dependent protein kinase
DRPLA	dentatorubral-pallidoluysian atrophy
DTT	dithiothreitol
DUB	deubiquitinase; deubiquitinating enzyme
DUB-1	Ub C-terminal hydrolase
DUBA	deubiquitinating enzyme A
ECF	Enhanced Chemifluorescence substrate
EMBL-EBI	European Molecular Biology Laboratory – European Bioinformatics Institute

ER	endoplasmic reticulum (in figures, only)
ERAD	endoplasmic reticulum-associated degradation
FBS	fetal bovine serum
FOXO	forkhead box class O
FOXO4	FOXO transcription factor 4
FRAP	fluorescence recovery after photobleaching
FSK	forskolin
GABA	γ-aminobutyric acid
GABAR	GABA receptor
GFP	green fluorescent protein
GluR6	glutamate receptor channel subunit β2
GSK3	glycogen synthase kinase 3
GSK3β	glycogen synthase kinase 3β
HBSS	Hank's balanced salt solution
HD	Huntington's disease
HDAC3	histone deacetylase 3
HDAC6	histone deacetylase 6
HEK	human embryonic kidney
HEPES	4-(2-hydroxyethyl)-1-piperazineethanesulfonic acid
Hsp70	70 kDa heat shock protein
htt	huntingtin
IGF1	insulin-like growth factor
IgG	immunoglobulin G
IH	immunohistochemistry (in figures, only)
IKK	IκB kinase
InsP3R1	type 1 inositol 1,4,5-trisphosphate receptor
IPB	immunoprecipitation buffer
iPSCs	induced pluripotent stem cells
JAMM	JAB1/MPN/MOV34 metalloenzymes
JD	Josephin domain
JNK	c-Jun N-terminal kinase
KLH	keyhole limpet hemocyanin
KO	knockout
LB	Lysogeny Broth
LC	liquid chromatography
LC-ES-MS	LC followed by ion spray MS
LTF	long-term synaptic facilitation
MAP	mitogen-activated protein
MAP2	microtubule-associated protein 2
MAPK	MAP-kinase
MEM	Minimum Essential Medium
mGluR1	metabotropic glutamate receptor subtype 1
MITOL	mitochondrial Ub ligase
MJD	Machado-Joseph disease
MMP2	matrix-metalloproteinase 2
mono.	monoclonal
monoUb	monoubiquitin
mRNA	messenger RNA
MS	mass spectrometry
MTOC	microtubule-organizing center

n.d.	none described
NCBI	National Center for Biotechnology Information
NCor	nuclear receptor co-repressor
NEAA	non-essential amino acids
NEDD8	neural precursor cell expressed developmentally downregulated gene 8
NES	nuclear export signals
NF-κB	nuclear factor kappa-light-chain-enhancer of activated B cells
NI	nuclear inclusion
NLS	nuclear localization signal
NMDA	N-methyl-D-aspartate receptors
NMDAR	NMDA receptor
NMR	nuclear magnetic resonance
OA	okadaic acid
ON	overnight
OTU	ovarian tumor protease
p38MAPK	p38 mitogen-activated protein kinase
Patx3	atx3 phosphorylated at S12 (when referring to the phospho-specific antibody)
PBS	phosphate buffer saline
PCAF	p300/CBP-associated factor
PDB	Protein Data Bank
PICK1	protein interacting with C kinase
PKA	protein kinase A
PKB	Protein kinase B
PKC	protein kinase C
PKG	protein kinase G
PMA	phorbol 12-myristate 13-acetate
PMSF	phenylmethanesulphonyl fluoride
poly.	polyclonal
polyQ	polyglutamine
polyUb	polyubiquitin
PP	phosphatases (in figures, only)
PP1	protein phosphatase 1
PP2A	protein phosphatase 2A
PSD	postsynaptic density
PSD-95	postsynaptic density protein 95
PTM	post-translation modification
PVDF	polyvinylidene difluoride
RCSB	Research Collaboratory for Structural Bioinformatics
RFU	relative fluorescence units
RIPA	radioimmunoprecipitation buffer
RSK	ribosomal s6 kinase
RT	room temperature
SBMA	spinal and bulbar muscular atrophy
SCA	spinocerebellar ataxia
SCA1,2,3,6,7,17	spinocerebellar ataxia type 1, 2, 3, 6, 7 or 17
SDS	sodium dodecyl sulfate
SDS-PAGE	SDS-polyacrylamide gel electrophoresis
SEM	standard error of the mean

SGK	serum/glucocorticoid regulated kinase
shRNA	short hairpin RNA
SOD2	manganese superoxide dismutase
SOV	sodium orthovanadate
STS	staurosporine
SYK	spleen tyrosine kinase
TARF2	tumor necrosis factor receptor-associated factor 2
TBP	TATA box binding protein
TBS-T	Tris-buffered saline-Tween 20
TCRα	T-cell receptor α
TEV	tobacco etch virus
UAF	USP1-associated factor
Ub	ubiquitin
Ub-AMC	Ub-C-terminal 7-amino-4-methylcoumarin
UBP2	Ub C-terminal hydrolase 2
Ub-VS	Ub-vinylsulfone
UCH	Ub C-terminal hydrolase
UCHL1	Ub C-terminal hydrolase isozyme L1
UIMs	Ub-interacting motifs
UPP	Ub-proteasome pathway
USP	Ub-specific processing protease
USP1,2,4,7,8,10,14,21,25,33,36	Ub C-terminal hydrolase 1, 2, 4, 7, 8, 10, 14, 21, 25, 33 or 36
USP9X	Ub-specific peptidase 9
VCP	valosin-containing protein
VGLUT1	vesicular glutamate transporter subtype 1
VGLUT2	vesicular glutamate transporter subtype 2
WB	Western blot (in figures, only)
WT	wild-type (in respect to residue at position 12 of atx3)
YAC	yeast artificial chromosome
λPP	lambda phosphatase (in figures, only)

Resumo

A doença de Machado-Joseph (DMJ), também designada por ataxia espinocerebelosa tipo 3, é a forma mais comum de ataxia hereditária dominante no mundo. Apesar de ser uma doença neurodegenerativa rara, apresenta considerável prevalência em Portugal, especialmente em algumas regiões do vale do Tejo e no arquipélago dos Açores. A DMJ manifesta-se clinicamente por uma perda progressiva da capacidade de coordenação de movimentos voluntários e por outros sintomas motores e posturais que se agravam progressivamente; a doença é invariavelmente fatal e nenhum tratamento eficaz foi até hoje desenvolvido.

O factor genético responsável pela DMJ é conhecido desde há décadas: uma expansão anormal de uma sequência repetitiva de CAG na região codificante do gene MJD1. O gene codifica a ataxina-3 (atx3), uma enzima com actividade de desubiquitinase (DUB) que contém uma sequência de poliglutaminas (poliQ) resultante dos trinucleótidos de CAG, que quando expandida para lá de um valor crítico torna a atx3 tóxica. Embora os mecanismos que estabelecem a ligação entre esta expansão anormal da atx3 e as características neurodegenerativas da DMJ sejam ainda grandemente desconhecidos, acredita-se que o estabelecimento de interacções aberrantes entre proteínas e a agregação de atx3 serão importantes intervenientes na patogénese da DMJ, levando possivelmente ao compromisso de sistemas celulares importantes. Com efeito, apesar de a atx3 ser ubiquamente expressa em diferentes tecidos e tipos celulares, a toxicidade da atx3 expandida afecta unicamente células neuronais, o que indica que os mecanismos patogénicos ocorrem especificamente em neurónios. Sabe-se que a mutação que causa a DMJ – a expansão de poliQ – é também responsável por outras doenças neurodegenerativas, mas as proteínas nelas envolvidas não partilham qualquer homologia para lá da sequência de poliQ. Tendo em conta que cada uma das nove doenças de poliQ é caracterizada por uma degeneração neuronal selectiva que ocorre segundo um padrão distinto, considera-se que a função biológica de cada uma das proteínas que as causam seja um factor importante na definição das consequências toxicas da expansão. Deste modo, os domínios proteicos para lá da sequência de polyQ deverão ser moduladores importantes na toxidade e poderão estar envolvidos nas vias responsáveis pela selectividade celular. O papel biológico da atx3 continua por apurar, mas as informações disponíveis sugerem que esta proteína participa em mecanismos celulares que utilizam sinais de ubiquitinação, como sejam sistemas de controlo de qualidade, ou na regulação da transcrição genética. As modificações pós-traducionais (MPTs) são mecanismos que regulam diversas funções das proteínas e por este motivo acredita-se que possam influenciar a toxicidade das proteínas com sequências de poliQ, através da modificação de domínios que estejam fora da sequência expandida. Para além disso, uma diferente regulação destas proteínas por MPTs poderá ajudar a explicar a especificidade celular dos padrões de neurodegenração. Uma melhor compreensão da função da atx3 e do modo como a proteína é

regulada será, por estes motivos, importante para melhor definir os mecanismos patogénicos da DMJ.

A fosforilação é uma forma conhecida de MPT que se sabe modificar diversas proteínas envolvidas em doenças de poliQ e interferir com a sua agregação e toxicidade. Tendo isto em conta, procurámos caracterizar quais são os efeitos da fosforilação da serina 12 da atx3, uma MPT que identificámos recentemente por espectrometria de massa usando atx3 purificada a partir de linhas celulares humanas. Nesse sentido, gerámos um anticorpo fosfo-específico direccionado para a detecção de serina 12 fosforilada e determinámos que é possível identificar espécies fosforiladas derivadas de atx3 em linhas celulares de mamíferos e em neurónios corticais de rato. Uma análise estrutural da atx3 demonstrou que a serina 12 se encontra no domínio catalítico da proteina, próximo do local catalítico, fazendo deste resíduo um provável agente regulador da actividade da atx3. Concordantemente, ensaios *in vitro* demonstraram que mimetizando a fosforilação da serine 12 através da mutação deste resíduo para aspartato reduz a actividade da atx3 contra substratos modelo de ubiquitina, o que indica que esta MPT poderá ser importante na modulação da função da atx3.

Demonstrámos também pela primeira vez que a expressão de atx3 com uma expansão de poliQ em neurónios corticais perturba a morfologia dendrítica e diminui o número de sinapses glutamatérgicas funcionais; este tipo de alterações poderá estar envolvido na DMJ. A mimetização da fosforilação reverteu, em certa medida, aquele fenótipo neuromorfológico, o que sugere que a fosforilação da serina 12 poderá ter um papel protector, eventualmente relacionado com algum tipo de função da atx3 na manutenção da estrutura neuronal que nunca fora descrito. No mesmo modelo celular, a mutação da serina 12 para aspartato ou alanina reduz também a formação de agregados de atx3. Os efeitos que a fosforilação da serina 12 tem na toxicidade induzida pela atxs3 expandida foram ainda investigados num modelo lentiviral de DMJ em rato, no qual se demonstrou que a mutação da serina 12 leva a uma diminuição da formação de agregados e a uma redução da depleção de neurónios.

Os resultados deste estudo sugerem que a serina 12 da atx3 define a toxicidade da proteína e que a modificação deste aminoácido por fosforilação interfere com as consequências tóxicas da expansão de poliQ. Este trabalho estabeleceu um modelo de cultura de neurónios com aplicações promissoras para o estudo das modificações neuronais resultantes da expansão da atx3 e representa ainda a primeira vez em que os efeitos da fosforilação da atx3 são estudados *in vivo*.

Abstract

Machado-Joseph disease (MJD), otherwise known as spinocerebellar ataxia type 3, is the most common form of dominantly-inherited ataxia in the world. Despite being a rare neurodegenerative disease, it is remarkably prevalent in Portugal, particularly in some regions of the Tagus river valley and in the Azorean archipelago. Clinically, MJD is characterized by a progressive impairment of the coordination of voluntary movements and others motor and postural symptoms that aggravate progressively; the disease is invariably fatal and to this date no effective treatment has been developed.

The genetic cause of MJD has been known for two decades: an abnormal expansion of a CAG repeat sequence in the coding region of the MJD1 gene. The gene codifies ataxin-3 (atx3), a deubiquitinating enzyme (DUB) that contains a polyglutamine (polyQ) tract encoded by the CAG trinucleotides which upon expansion beyond a critical threshold renders the protein toxic. Though the precise mechanisms linking the abnormal polyQ expansion to the neurodegenerative features of MJD remain to be elucidated, aberrant protein interactions and aggregation are envisioned as important players in pathogenesis, possibly leading to the compromise of important cellular systems. Importantly, though atx3 displays ubiquitous expression throughout diverse tissues and cell types, polyQ-expanded atx3 toxicity affects only neuronal cells, indicating that disease mechanisms are neuronal-specific. The same type of mutation – polyQ expansion – is known to cause other neurodegenerative diseases, but the causative proteins in each of these cases share no homology outside the polyQ tract. Considering that each of the nine polyQ diseases is characterized by distinct patterns of selective neuronal demise, is it believed that the concrete biologic role of each disease-causing protein plays a role in defining toxicity outcomes. Accordingly, protein domains outside the polyQ tract are admitted to be important modulators of toxicity, participating in the mechanisms responsible for cell selectivity. The precise biologic role of atx3 remains to be elucidated, but available evidence suggest a participation in cellular mechanisms utilizing ubiquitination signals, such as protein quality control systems, or transcription regulation. Post-translational modifications (PTMs) are a group of mechanisms that regulate diverse protein functions and are consequently admitted to influence polyQ toxicity by modifying the domains outside the expanded tract. Furthermore, differential regulation of disease-causing proteins between cells by PTMs may help explain the cell-specificity patterns of polyQ-induced neurodegeneration. A better understanding of atx3 function and of how the protein is regulated is crucial for a better characterization of MJD pathogenesis mechanisms.

Phosphorylation is a well characterized PTM that has been shown to modify diverse polyQ disease-causing proteins and to interfere with aggregation and toxicity. We thus set out to characterize the effects of phosphorylation of atx3 at serine 12, a PTM we recently identified by a mass spectrometry analysis of atx3 purified from human cell lines. We generated a phospho-specific antibody directed against that modified residue and observed that atx3-derived species are phosphorylated in both mammalian cells lines and in rat cortical

neurons. Structural analysis of atx3 revealed that serine 12 is localized in the catalytic domain of the protein, close to the catalytic site, making it a good candidate for an activity regulator. Accordingly, *in vitro* assays demonstrated that mimicking phosphorylation by mutating serine 12 to aspartate decreases its activity against ubiquitin model substrates, indicating that this PTM may be important in defining atx3 function.

We demonstrated for the first time that expression of expanded atx3 is cortical neurons impairs dendritic morphology and diminishes the number of functional glutamatergic synapses, two neuron-specific alterations that may be involved in MJD. Mimicking atx3 phosphorylation limited this neuromorphologic phenotype, suggesting a protective role of serine 12 phosphorylation possibly linked to a yet undescribed function of atx3 in the maintenance of neuronal structure. In the same cell model, mutating serine 12 to aspartate or alanine also reduced atx3 aggregate formation. The effects of serine 12 phosphorylation on expanded atx3-induced toxicity were further explored in a lentiviral rat model of MJD, where mutation of the residue was shown to decrease both aggregate formation and neuronal depletion.

The results of this study suggest that serine 12 of atx3 plays a role in defining atx3 toxicity and that modification of this amino acid residue by phosphorylation interferes with the toxic outcomes of polyQ expansion. The current work established a neuronal culture model with promising applications for the further study of neuron-specific changes deriving from atx3 expansion and represents the first time the outcomes of atx3 phosphorylation are studied *in vivo*.

Keywords: Machado-Joseph disease, ataxia, neurodegenerative diseases, ataxin-3, deubiquitinases, polyglutamine diseases, phosphorylation

Chapter 1

Introduction

Chapter 1 – Introduction

1.1 Neurodegenerative diseases

Neurological diseases have a recognizable and often dramatic impact on the life of human beings. Since the nervous system is responsible for the control and coordination of a vast number of organic activities, pathology can lead to the compromise of many human functions, including body movement, cognition and sensory acquisition, expressed in patients by a wide range of symptoms and disabilities. In the last decades, the increase in longevity, observed specially in industrialized countries, along with the scientific and technical achievements witnessed in the fields of biologic sciences and medicine, have shed light into the diversity of progressive diseases of the nervous system that develop later in life. These disorders are grouped under the term of neurodegenerative diseases (Jellinger, 2009; Jennekens, 2014), and have been one of the most important focus of recent biomedical research. Diseases of the nervous system are usually considered degenerative when they involve a chronic progression of symptoms, caused by a matching progressive loss of neuronal structure and functionality (Bredesen *et al.*, 2006; Jennekens, 2014; Palop *et al.*, 2006). Some of the diseases obeying to this criterion are in fact not limited to old age, starting at earlier phases in life.

Disorders that are commonly classified as neurodegenerative include dementias such as Alzheimer's and prion diseases, movement disorders like Parkinson's, Huntington's disease (HD) and several ataxias, and motor neuron pathologies like amyotrophic lateral sclerosis. Neurodegenerative diseases usually have devastating effects and so far only symptomatic treatments have been developed. They thus remain, to this date, incurable. The lack of effective treatments may be largely due to the incomplete knowledge of the pathologic mechanisms involved, despite the effort put into investigating their causes. However, though some of these diseases are in fact described as idiopathic or as resulting from a complex interplay between genetic and environmental factors, many are known to arise from discrete genetic factors. Understanding how these pathogenic genes and their eventual protein products give rise to the observed neurodegeneration features – and how to interfere with those mechanisms – is bound to help future development of efficient treatments.

1.2 Machado-Joseph disease

Description and epidemiology

Machado-Joseph disease (MJD) is a hereditary disorder of the nervous system caused by mutation of the *ATXN3* gene (also known as *MJD* or *MJD1*), localized in the long arm of chromosome 14 (14q32.1) (Kawaguchi *et al.*, 1994; Takiyama *et al.*, 1993). The disease, also known as spinocerebellar ataxia type 3 (SCA3), was first described during the 1970s, in two families of Portuguese immigrants in the United States, both originally from two islands of the Azorean archipelago: Flores and São Miguel (Nakano *et al.*, 1972; Rosenberg *et al.*, 1976; Woods and Schaumburg, 1972). Currently, with the molecular diagnose tools now available, MJD has been identified worldwide, and in spite of being a rare disease, it is nonetheless the most common form of autosomal dominant spinocerebellar ataxia (SCA), accounting for about 21 % of cases (Figure 1A) (Schöls *et al.*, 2004). Particularly, MJD is the most predominant form of SCA in Portugal (3,1/100.000 habitants, in the mainland; Figure 1B), with the highest prevalence in the world being found in the Azores – 1/239 habitants, in the island of Flores (Bettencourt and Lima, 2011; Coutinho *et al.*, 2013). However, MJD accounts for an important fraction of SCA cases in other countries as well, not only in North America, in the United States and Canada, but also in Mexico and Brazil, in European countries such as France, the Netherlands and Germany, in Australia and in Asian countries like Japan, China, Taiwan, Singapore and India (Bettencourt and Lima, 2011; Durr, 2010; Martins *et al.*, 2007; Martins *et al.*, 2012; Ruano *et al.*, 2014).

Though the dispersal of the disease mutation was initially believed to originate from the Portuguese maritime expansion during the 15th and 16th centuries and also to latter Portuguese emigration phenomena in the last few centuries, MJD has been found in families with diverse ethnic backgrounds (Gaspar *et al.*, 2001). The characterization of those backgrounds has suggested the existence of two main genetic lineages of MJD: the most ancestral one (~6.000 years) apparently originated in Asia and later spread to Europe and to the rest of the world, while the other, more recent lineage (~1.500 years), was possibly initiated in mainland Portugal and then dispersed through Portuguese emigration (Martins *et al.*, 2007).

Clinical features and neuropathology

Patients with MJD have diverse clinical presentations, but one of the most recognized signs, and frequently one the earliest, is the hallmark ataxia, i. e., an impairment of the coordination of voluntary movements. Other symptoms include postural instability, dystonia, proprioceptive loss, tremor, paucity of movements (bradikinesia or akinesia), disorders of muscle tone and contraction (fasciculations, spasticity and rigidity), amyotrophy, neuropathy, visual (nystagmus, eyelid retraction, ophthalmoparesis, dipoplia) and speech problems

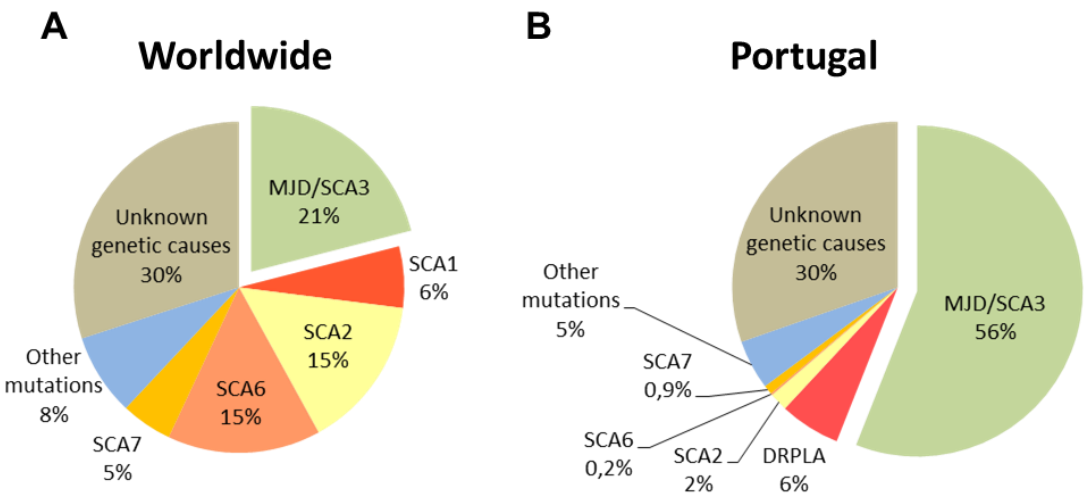

Figure 1: MJD is the most prevalent form of autosomal dominantly-inherited ataxias. ***A*** The worldwide relative prevalence of dominantly-inherited ataxias is based on the percentages presented by Schöll and collaborators (2004). ***B*** The percentages presented for Portugal were calculated based on the study by Bettencourt and coworkers (2013). SCA17 and ataxias unrelated to polyQ expansions are grouped under *other mutations*. *Unknown genetic causes* reflects diseases causes by unidentified genetic factors.

(dysarthria), swallowing difficulties (dysphagia) and weight loss without loss of appetite, incontinence, restless legs syndrome, sleep disorders and depression (Bettencourt and Lima, 2011; Colomer Gould, 2012; Riess *et al.*, 2008; Vale *et al.*, 2010). Cognitive difficulties and dementia have been rarely described (Burk *et al.*, 2003; Ishikawa *et al.*, 2002). The observance of each of the above clinical signs differs greatly between patients, including in individuals within the same family. The age of onset is also highly variable, and although MJD is often described as a late-onset disease, symptoms may in fact appear between ages of 4 and 70 years, with a mean age of onset of about 40 years (Bettencourt and Lima, 2011). The great pleomorphism of MJD has led clinicians to classify the diverse disease phenotypes into 3 to 5 clinical types, grouped according to the collection of symptoms observed, the age of onset and the degree of progressiveness (Bettencourt and Lima, 2011; Colomer Gould, 2012).

MJD is progressive in all cases and ultimately fatal; the mean survival time is 21 years (Bettencourt and Lima, 2011; Kieling *et al.*, 2007). At advanced stages patients suffer from cachexia and pulmonary complications and the major terminal illness reported is aspiration pneumonia, admittedly arising from dysphagia (Colomer Gould, 2012; Rüb *et al.*, 2006a; Schöls *et al.*, 2000).

The clinical features of MJD patients result from the structural and functional compromise of several discrete regions of the central nervous system (CNS). The observed symptoms and numerous studies investigating brain regional atrophy, changes in metabolism and functionality, neuronal loss and other pathological markers demonstrated that neurodegeneration involves predominantly a) the cerebellum, including the dentate nucleus, spinocerebellar tracts and the medial cerebellar peduncle; b) the brainstem, namely the pons and medulla oblongata (including the vestibular nucleus, the locus coeruleus, and the medial

and lateral lemniscus); c) the basal ganglia, namely the substantia nigra, the globus pallidus and the striatum (including the caudate nucleus and the putamen); d) the thalamus; e) cranial nerves, especially the oculomotor (III) and the hypoglossoal (XII) nerves; and f) the spinal cord, namely the anterior horn, the Clarke's column and the dorsal columns (Bettencourt and Lima, 2011; Matos *et al.*, 2011; Riess *et al.*, 2008; Rosenberg, 1992; Rüb *et al.*, 2013; Sudarsky and Coutinho, 1995; Wullner *et al.*, 2005). Other brain regions less frequently implicated in MJD but increasingly considered important include the cerebral and cerebellar cortices, the Purkinje cells and the inferior olive. Overall, observations have thus suggested the pathological compromise of diverse neuronal pathways, including: a) somatomotor loops (the cerebellothalamocortical and the basal ganglia-thalamocortical motor loops), dysfunctionally leading to ataxia and other motor and postural symptoms; b) sensory systems (somatosensory, visual and auditory systems); c) the vestibular system, causing impaired body balance; d) the oculomotor system, causing eye-movement related symptoms; e) the ingestion-related brainstem system; f) the precerebellar brainstem system, g) the midbrain dopaminergic system, causing the parkinsonism-like symptoms (paucity of movements and rigidity) ; h) the midbrain cholinergic system; and the i) pontine noradrenergic system (Colomer Gould, 2012; Rüb *et al.*, 2008; Rüb *et al.*, 2013).

To this date, MJD remains incurable. Apart from therapeutic strategies aiming at alleviating some of the symptoms or helping patients cope with disabilities, no effective causative treatment – capable of preventing or curing the disease, delaying its onset, or stalling progression – has been developed (Bettencourt and Lima, 2011; Riess *et al.*, 2008; Rüb *et al.*, 2013).

Genetic causes

The biologic mechanisms connecting mutation of the *ATXN3* gene to the development of the neurodegenerative features and clinical signs of MJD are still not completely understood. Nonetheless, it has been known for 2 decades that the mutation causing MJD consists of an abnormal repetition of cytosine-adenine-guanine (CAG) trinucleotides in the coding region of the gene (Kawaguchi *et al.*, 1994). In the human population, the number of CAGs trinucleotides in that particular sequence of the *ATXN3* gene varies significantly, and only the expansion beyond a critical threshold is associated with MJD. Healthy individuals have been known to carry up to 44 of those repeats, while longer sequences, with 61-87 CAG repeats, have been connected with the development of the disease (Maciel *et al.*, 2001). Alleles with CAG sequences of intermediates sizes have been rarely described and display a lower penetrance, since their pathologic outcome is not as certain. In fact, although the shortest repeat number associated with MJD was 45, healthy individuals carrying 51 CAGs have also been described (Bettencourt and Lima, 2011; Maciel *et al.*, 2001; Riess *et al.*, 2008; Rüb *et al.*, 2013).

The protein product of the *ATXN3* gene is an ubiquitous deubiquitinating enzyme (DUB) named ataxin-3 (atx3) (Kawaguchi *et al.*, 1994). Since the CAG trinucleotide codifies the amino acid glutamine, the abnormally repetitive form of the gene is translated as an aberrantly elongated protein, containing an expanded sequence of repeated glutamine residues. The way this expanded glutamine tract of atx3 leads to the development of MJD is the subject of much of the scientific research aiming at comprehending this devastating pathology.

1.3 Polyglutamine diseases

Machado-Joseph disease in the context of trinucleotide repeat disorders

MJD is not the only disorder caused by an abnormal repeat expansion. Nucleotide repeat expansions are a common genetic cause of many hereditary diseases and, in fact, the majority of autosomal dominant SCAs to which a mutation has been ascribed are known to result from this type of modification, and most of these cases correspond to trinucleotide repeat disorders (Rüb *et al.*, 2013). Out of these, apart from MJD/SCA3, five SCAs are known to result from CAG repeat expansions in coding regions of the respective causative genes; this is true for spinocerebellar ataxias type 1, 2, 6, 7 and 17 (SCA1, 2, 6, 7, 17) (Cummings and Zoghbi, 2000; Rüb *et al.*, 2013). Three other neurodegenerative diseases – HD, dentatorubral-pallidoluysian atrophy (DRPLA) and spinal and bulbar muscular atrophy (SBMA) – also arise from exaggerated CAG repetitions in genes that are translated into proteins containing sequences of expanded glutamines. For this reason, the 9 disorders are collectively known as polyglutamine (polyQ) diseases (Figure 2; Table I).

All polyQ diseases involve progressive neuronal demise restricted to selective populations of neurons, though the specific critical threshold of repeat number, the degeneration pattern and the associated clinical signs are characteristic of each disorder. In spite of the specific traits of each disease, the fact that the same type of alterations in otherwise unrelated genes and proteins lead to neurodegeneration has prompted researchers to look into polyQ diseases as a group, in search of common pathological mechanism (Bauer and Nukina, 2009; Cummings and Zoghbi, 2000; Gatchel and Zoghbi, 2005; Shao and Diamond, 2007; Zoghbi and Orr, 2000).

Repeat length and pathology

An important common feature of the group is the positive correlation existing between the CAG (or glutamine) repeat number and both the severity and precocity of symptoms: lengthier repeat sequences have been recurrently reported to be associated with aggravated clinical presentations and to earlier ages of disease onset (Zoghbi and Orr, 2000). Both aspects constitute evidence to the prominence of the expanded sequences in the disease

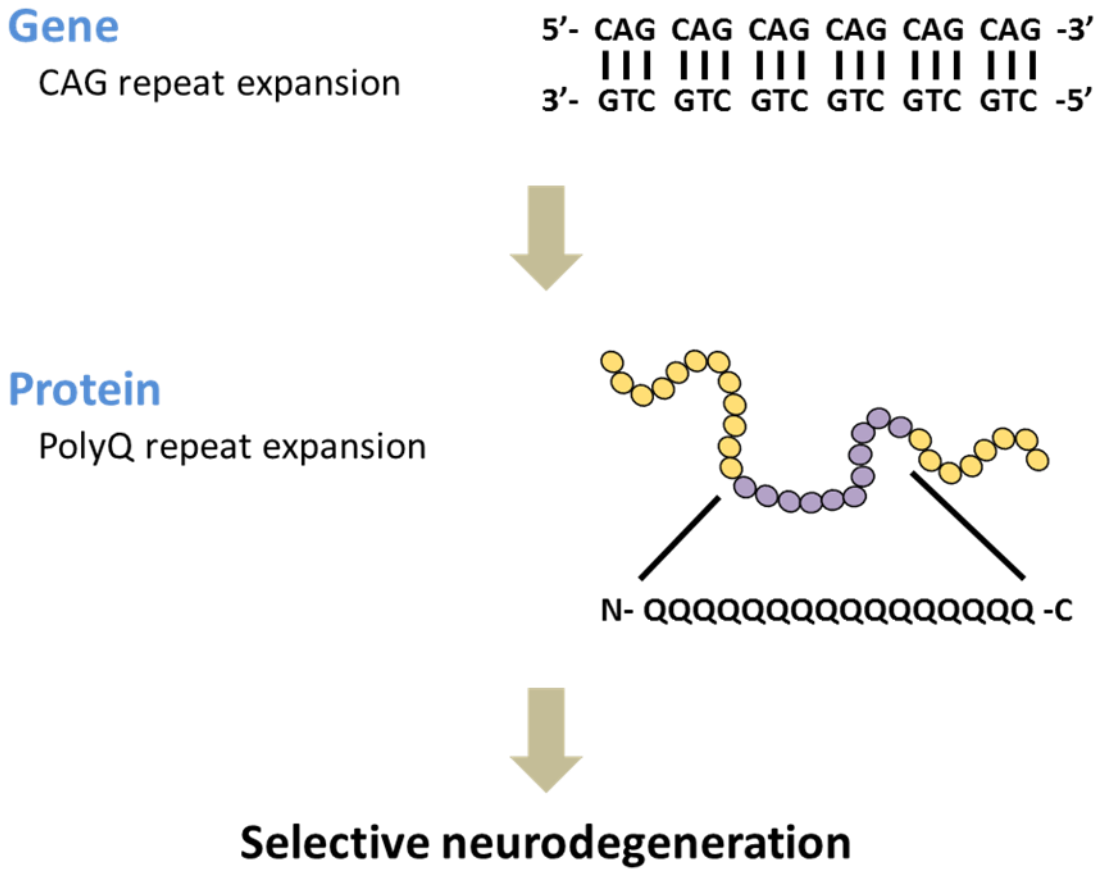

Figure 2: CAG trinucleotide repeat expansions and polyQ diseases. The genes causatively involved in polyQ diseases contain a CAG repeat sequence in their protein-coding region. The CAG trinucleotide encodes the amino acid glutamine, thus being translated into a protein product that includes a tract containing repeated glutamine residues – the polyQ sequence. When the CAG trinucleotides are repeated beyond a critical threshold the polyQ-expanded protein leads to neurodegeneration, whose regional selectivity varies depending on the particular protein involved.

mechanisms of polyQ diseases. In the case of MJD, the CAG repeat size explains 50-75% of the variation observed in the age at which symptoms first manifest and a link between the severity of clinical presentation and the number of CAG repetitions has also been suggested for the disease, with longer expansions giving rise to harsher symptoms (Bettencourt and Lima, 2011; Maciel *et al.*, 1995; Maruyama *et al.*, 1995; Riess *et al.*, 2008).

In fact, there appears to be a correlation between at least some of the described MJD clinical types and the size of CAG sequences carried by patients: considering the first three types characterized, lengthier sequences appear to associate with the most severe and earlier form – type 1 –, while smaller and intermediate sequences are associated with milder presentations – types 3 and 2, respectively (Colomer Gould, 2012; Maciel *et al.*, 1995; Maruyama *et al.*, 1995; Riess *et al.*, 2008). Cases of homozigoty of expanded *ATXN3* alleles

Table I: Biologic features of polyQ diseases

Disease name	Mutated gene	Protein product	Putative function	CAG repeat number		Regions most affected
				Normal	Pathogenic	
HD	*HD*	Huntingtin	Signalling, transport, transcription	6-34	36-121	Striatum, cerebral cortex
DRLPA	*DRPLA*	Atrophin 1	Transcription	7-34	49-88	Cerebellum, cerebral cortex, basal ganglia, Luys body
SBMA	*AR*	Androgen receptor	Steroid-hormone receptor	9-36	38-62	Anterior horn and bulbar neurons, dorsal root ganglia
SCA1	*SCA1*	Ataxin-1	Transcription	6-39	40-82	Cerebellar Purkinje cells, dentate nucleus, brainstem
SCA2	*SCA2*	Ataxin-2	RNA metabolism	15-24	32-200	Cerebellar Purkinje cells, brainstem, frontotemporal lobes
MJD/ SCA3	*ATXN3/MJD/MJD1*	Ataxin-3	Deubiquitinating activity and transcription regulation	10-51	45-87	Cerebellar dentate neurons, basal ganglia, brainstem, spinal cord
SCA6	*CACNA1A*	$CACNA1_A$	P/Q-type α1A calcium channel subunit	4-20	20-29	Cerebellar Purkinje cells, dentate nucleus, inferior olive
SCA7	*SCA7*	Ataxin-7	Transcription	4-35	37-306	Cerebellum, brainstem, macula, visual cortex
SCA17	*SCA17*	TBP	Transcription	25-42	47-63	Cerebellar Purkinje cells, inferior olive

(adapted from Gatchel and Zoghbi, 2005; Matos *et al.*, 2011; and Shao and Diamond, 2007)

Abbreviations: HD, Huntington's disease; DRPLA, dentatorubral-pallidoluysian atrophy; SBMA, spinal and bulbar muscular atrophy; SCA, spinocerebellar ataxia; MJD, Machado-Joseph disease; $CACNA1_A$, calcium channel, voltage dependent, P/Q type, α1A subunit; TBP, TATA box binding protein.

have been described and shown to result in very early disease onsets (an onset at 4 years has been reported) and very severe clinical features, thus suggesting a gene dosage effect (Carvalho *et al.*, 2008; Lang *et al.*, 1994; Lerer *et al.*, 1996; Sobue *et al.*, 1996).

Repeat instability

Another phenomenon recurrently observed in polyQ diseases is anticipation, i. e., the propensity of successive generations to present worsened disease manifestations, involving earlier ages of onset and/or more severe symptoms (Cummings and Zoghbi, 2000; Durr, 2010; Schöls *et al.*, 2004). This is generally attributed to the further increase in CAG repeat number

that tendentially occurs with each new generation, resulting from the significant instability of the pathogenic expansion (Rüb *et al.*, 2013; Zoghbi and Orr, 2000). Interestingly, this intergenerational instability is more pronounced in the case of paternal transmissions of the disease gene, more often leading to further trinucleotide expansions. Accordingly, in MJD, non-expanded alleles are usually transmitted without modifications (Bettencourt *et al.*, 2008), but anticipation, and the increased instability and risk of further expansion by patrilineal transmission, have been observed (Bettencourt and Lima, 2011; Maruyama *et al.*, 1995; Riess *et al.*, 2008).

Furthermore, the instability of the polyQ disease alleles is not limited to the germline, extending to somatic cells as well (Riess *et al.*, 2008; Zoghbi and Orr, 2000). Somatic mosaicism has been documented in MJD, though an increased number of CAG repeats does not correlate with increased vulnerability of particular CNS structures to degeneration (Cancel *et al.*, 1998; Ito *et al.*, 1998; Lopes-Cendes *et al.*, 1996).

Aggregation and inclusion bodies

A conspicuous characteristic of every polyQ disease is the formation of microscopic intraneuronal inclusion bodies in discrete regions of the CNS of patients (Gatchel and Zoghbi, 2005; Williams and Paulson, 2008; Zoghbi and Orr, 2000). In the majority of polyQ diseases, inclusions are found in the nucleus (nuclear inclusions – NIs), but in some cases also in the cytoplasm (HD, SBMA, SCA2 and MJD) or exclusively in the cytoplasm (SCA6) (Gatchel and Zoghbi, 2005; Schöls *et al.*, 2004; Todd and Lim, 2013). These macromolecular aggregates are known to contain the pathogenic proteins related with each disorder, as well as ubiquitin (Ub) and frequently other proteins involved in quality control systems of the cell, namely other components of the Ub-proteasome pathway (UPP) and molecular chaperones, which are usually recruited in response to misfolding and protein aggregation. These observations led to the hypothesis that polyQ diseases could arise from pathologic mechanisms involving protein aggregation, caused by misfolding events triggered by the aberrant polyQ expansions (Williams and Paulson, 2008; Zoghbi and Orr, 2000). In effect, polyQ-containing proteins are prone to aggregate *in vitro*, and aggregation has been continuously defined as an important toxicity mechanism in the context of polyQ diseases. In spite of their considerable diversity, neurodegenerative disorders are often defined as protein misfolding diseases or *proteinopathies*, since they are recurrently admitted to involve protein conformation changes, aggregation and formation of protein deposits (Jellinger, 2009).

Nonetheless, though inclusion bodies undoubtedly constitute a polyQ disease hallmark, their direct causative involvement in pathogenic pathways has been a matter of long debate (Todd and Lim, 2013). Surmounting evidence from diverse studies of cell culture-based systems, animal models or polyQ disease patients have demonstrated that inclusion formation does not necessarily correlate with cell loss or atrophy – in some cases, inclusion formation is even associated with cell survival (Arrasate *et al.*, 2004; Bauer and Nukina, 2009; Gatchel and

Zoghbi, 2005; Saudou *et al.*, 1998; Schöls *et al.*, 2004; Slow *et al.*, 2005). Consequently, inclusions are now admitted to be either a byproduct of upstream toxicity events or in fact even the result of protective mechanisms moved by the cell in order to deal with the actual toxic species (Ross and Poirier, 2004; Todd and Lim, 2013; Williams and Paulson, 2008). In the case of MJD, though the presence of NIs has been known for some time (Paulson *et al.*, 1997b), this disease markers have been detected not only in regions suffering neurodegeneration, but also in structures normally considered as spared in the disease, such as the autonomic ganglia, the interstitial nucleus of Cajal and several thalamic nuclei that do not degenerate (Riess *et al.*, 2008; Rüb *et al.*, 2006b; Yamada *et al.*, 2001). The presence of inclusions in MJD patients' neurons does not predict the actual fate of the respective cells, playing no clear protective or deleterious role (Riess *et al.*, 2008).

Toxicity mechanisms

The identity of the actual toxic species causing neurodegeneration in polyQ diseases remains, to some extent, a mystery. It has been speculated that even the expanded messenger RNA (mRNA) molecules resulting from the transcription of pathogenic CAG repeat-containing genes might be toxic (Evers *et al.*, 2014; Gatchel and Zoghbi, 2005). In fact, expression of non-translated mRNAs containing CAG expansions in *Drosophila* leads to neuronal degeneration and, conversely, altering every other CAG trinucleotide to cytosine-adenine-adenine (CAA, which also codifies glutamine), in an expanded CAG-containing truncated atx3 gene, decreases its regular toxicity (Li *et al.*, 2008). However, these observations are yet to be thoroughly explored, and the involvement of mRNA toxicity in polyQ diseases is considered controversial (La Spada and Taylor, 2010). On the other hand, the theoretical and empirical body of research demonstrating the toxicity of the translated polyQ-expanded protein products of CAG-containing genes is highly and convincingly developed. Prominent observations implicating proteins in the toxicity mechanisms of polyQ diseases derive from studies exploring the role of the subcellular localization of the pathogenic proteins, the importance of their molecular interactions, the mechanisms and outcomes of aggregation and the effects elicited by interference with protein quality control systems.

The presence of an expanded polyQ stretch in the context of each disease-associated protein is believed to introduce a toxic *gain of function*, thereby turning the otherwise normal proteins into toxic entities (Bauer and Nukina, 2009; Gatchel and Zoghbi, 2005; La Spada and Taylor, 2010). The molecular and cellular consequences of the polyQ-induced alterations are believed to constitute the basis of the pathogenic mechanisms they trigger. The several changes possibly caused by polyQ expansion include: a) modifications of host protein function; b) aberrant molecular interactions; c) increase in the propensity to form toxic aggregates (distinct from the macromolecular inclusions bodies described above); d) proteolytic generation of toxic fragments; e) transcriptional alterations; f) impaired axonal transport; g) abnormalities in neurotransmission; h) proteotoxic stress resulting from disruption of quality

control systems; i) mitochondrial dysfunction, leading to oxidative stress and bioenergetic defects; j) dysregulation of intracellular calcium homeostasis; and k) impairment of DNA quality control systems (Hands *et al.*, 2008; Shao and Diamond, 2007; Takahashi *et al.*, 2010; Williams and Paulson, 2008). More than one of these mechanisms is admitted to contribute to each polyQ disease, and it is expectable that some of them (primarily changes in protein function and molecular interactions) underlie many of the others.

PolyQ-expanded proteins tend to suffer conformational changes, and, as mentioned before, they tend to aggregate, with longer polyQ sequences increasing this propensity (Williams and Paulson, 2008). Accordingly, as hinted by the putative mechanisms of polyQ toxicity stated above, the actual agents of toxicity have been variously defined as a) the full-length, monomeric, pathogenic protein; b) the oligomeric intermediates of its aggregation pathway; c) the microaggregates and protofibrils formed with the process; d) or truncated fragments of the protein, which in turn may also aggregate (Bauer and Nukina, 2009; Takahashi *et al.*, 2010; Todd and Lim, 2013; Williams and Paulson, 2008). Yet again, it is possible that all or at least some of these agents mediate toxicity pathways, though ultimately stemming from the same alterations introduced by the polyQ expansions. The general adult/late onset of polyQ diseases may be connected to these misfolding-related events. Possibly, the decline of quality control systems and the accompanying increase in protein damage that occur with ageing lead to further misfolding and aggregation of expanded polyQ proteins, causing neurodegeneration and the development of symptoms (Hands *et al.*, 2008; Kirkwood, 2008).

The role of protein context

Though it is tempting to try to envision an unifying set of mechanisms that is responsible for expansion-derived toxicity in every polyQ disease, the differences existing between them suggest that other players are also important in defining the toxicity of the expanded proteins. PolyQ-containing proteins display a widespread distribution in the CNS and other tissues, but the neurodegeneration profile and the clinical features (including symptoms and age of onset) observed in each disorder don't overlap, even in the case of the six SCAs (Rüb *et al.*, 2013; Takahashi *et al.*, 2010; Zoghbi and Orr, 2000). Additionally, the pathogenic threshold of glutamine repeat number varies between diseases, clearly showing that the expanded sequence is not the only factor defining the disease outcome (Williams and Paulson, 2008).

In fact, each polyQ disorder is caused by proteins that are otherwise unrelated, sharing no significant homology outside the polyQ stretch. For this reason, authors consensually point out another factor to be considered when addressing polyQ disease toxicity – the role of *protein context* (Gatchel and Zoghbi, 2005; Takahashi *et al.*, 2010). Each polyQ-containing protein is assumed to have varying biochemical properties and to play different cellular functions; presumably, the alterations introduced by expansion will thus have different toxic

outcomes. Toxicity has even been proposed to be actually driven by the normal function of the proteins, with the polyQ tracts playing a modulatory role (Gatchel and Zoghbi, 2005). Accordingly, in order to deepen the understanding of the pathological pathways involved in polyQ diseases and their cell type selectivity, it is important to look also at the regions outside the polyQ tract, comprehend the properties and function of each protein and explore how the polyQ expansion affects them. These aspects have frequently been the target of much of the scientific research developed in the field of polyQ diseases. Aggregation of polyQ-containing proteins, for example, has repeatedly been shown to be modulated by the sequences flanking the polyQ tract (Almeida *et al.*, 2013; Bauer and Nukina, 2009; Saunders and Bottomley, 2009).

In order to expose the hypotheses explaining the causes of MJD, the following sections will focus on what is currently known about the molecular and biologic characteristics of atx3 and address the consequences deriving from polyQ expansion of this protein. These segments are based on previously published work (Matos *et al.*, 2011), hereby appropriately expanded and updated.

1.4 Ataxin-3

Distribution and ubiquity

Atx3 is a protein of wide distribution in the Eukarya domain of Life, with homologs identified in diverse groups of eukaryotic organisms, including plants, fungi and animals – from flatworms and nematodes to mollusks, arthropods and chordates (according to the National Center for Biotechnology Information – NCBI, USA). This pervasive conservation in considerably diverse clades suggests that atx3 is a protein of important biologic role (Tzvetkov and Breuer, 2007).

In mice, rats and humans, atx3 presents an ubiquitous expression, being found in different tissues and cell types, including in the brain, despite the selective neuronal demise its mutation causes in MJD patients (Costa *et al.*, 2004; Ichikawa *et al.*, 2001; Nishiyama *et al.*, 1996; Paulson *et al.*, 1997a; Schmidt *et al.*, 1998; Trottier *et al.*, 1998). Atx3 expression varies between different brain regions and cellular types, but increased levels at the transcript or protein level do not correlate with the admitted specific vulnerability to degeneration (Bauer and Nukina, 2009; Ichikawa *et al.*, 2001; Trottier *et al.*, 1998; Zoghbi and Orr, 2000). Furthermore, mRNA levels in the brain do not differ between MJD patients and controls (Nishiyama *et al.*, 1996).

Intracellular localization

In addition to the ubiquitous distribution of atx3 among different tissues, the protein seems to be widely, though heterogeneously, distributed within the cells themselves, being found in the cytoplasm (mitochondria included) and the nucleus, with varying degrees of

predominance depending on the cell type (Macedo-Ribeiro *et al.*, 2009; Paulson *et al.*, 1997b; Pozzi *et al.*, 2008; Reina *et al.*, 2010; Tait *et al.*, 1998; Trottier *et al.*, 1998; Wang *et al.*, 1997). In human brain cells atx3 is predominantly cytoplasmic, generally displaying a somatodendritic and axonal distribution, though it is also occasionally found in the nucleus (Paulson *et al.*, 1997b; Schmidt *et al.*, 1998; Trottier *et al.*, 1998). The heterogeneity observed suggests that regulation of atx3 expression levels and localization may be functionally important (Trottier *et al.*, 1998).

Structure, domains and enzymatic activity

Atx3 is a protein of about 40-43 kDa, fundamentally constituted by a structured globular N-terminal domain, named Josephin domain (JD), followed by a more flexible C-terminal tail (Masino *et al.*, 2003). The JD (residues 1-182, in the human protein) is a catalytic subunit displaying Ub protease activity, i. e., the ability to cleave isopeptide bonds between Ub monomors. The C-terminal tail includes two or three Ub-interacting motifs (UIMs) and the polyQ stretch of variable repeat number and length, whose expansion beyond the critical threshold of about 44 glutamines has been associated with the development of MJD (Albrecht *et al.*, 2004; Burnett *et al.*, 2003; Nicastro *et al.*, 2005) (Figure 3).

Studies have reported the existence of different isoforms of atx3 (Goto *et al.*, 1997; Kawaguchi *et al.*, 1994; Schmidt *et al.*, 1998). The two most extensively characterized are undoubtedly isoforms MJD1a (also termed ataxin-3a) and MJD1-1 (otherwise known as ataxin-3c), which result from alternative splicing and differ in the architecture of their respective C-terminal tails: isoform MJD1a has only two UIMs, followed by the polyQ sequence and a C-terminal hydrophobic stretch, while the MJD1-1 isoform displays an additional UIM after the polyQ stretch instead (Colomer Gould, 2012; Goto *et al.*, 1997; Harris *et al.*, 2010; Kawaguchi *et al.*, 1994). Both forms are expressed in the human brain, though it was reported that the 3UIM-containg isoform is the predominant one (Harris *et al.*, 2010; Schmidt *et al.*, 1998). It is possible, however, that the observed prevalence is relative only to the soluble levels of the atx3. In actual fact, more than 50 transcripts of the *ATXN3* gene have been described in humans, at least a part of them admittedly deriving from alternative splicing (Bettencourt *et al.*, 2009; Ichikawa *et al.*, 2001). The actual biological relevance of all these variants remains undisclosed, but some of the uncharacterized ones have been predicted to be translated into protein products (Bettencourt and Lima, 2011).

According to its nuclear magnetic resonance (NMR) structure, the JD is mainly composed of two subdomains: a globular catalytic subdomain and a flexible helical hairpin (Figure 4A) (Mao *et al.*, 2005; Nicastro *et al.*, 2005). The surface of the JD includes two hydrophobic Ub-binding sites: site 1 is localized close to the catalytic cleft existing between the two subdomains, and site 2, contiguous to the other one, is placed on the opposite surface of the JD (Figure 4C and D) (Nicastro *et al.*, 2009). The Ub protease activity was first predicted trough an integrative bioinformatics analysis of atx3 primary sequence (Scheel *et al.*, 2003) and

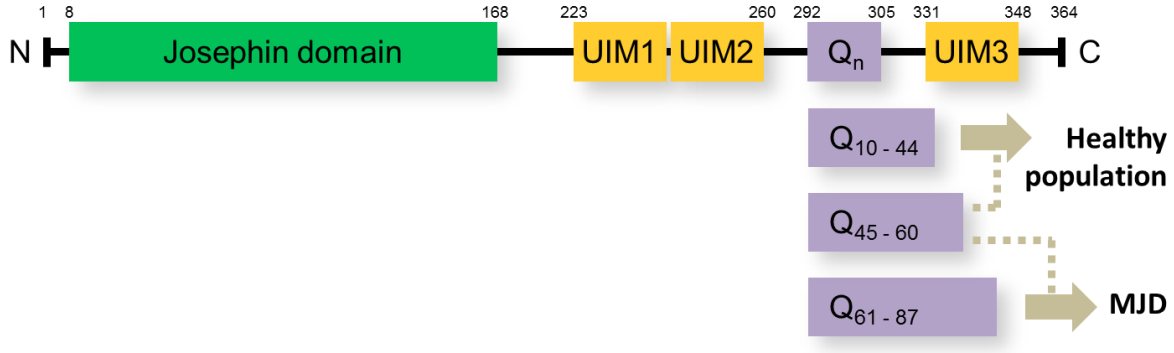

Figure 3: Domain architecture of atx3. Atx3 is mainly composed by a structured N-terminal catalytic domain with DUB activity, the JD, followed by a flexible C-terminal tail containing 2 UIMs capable of interacting with Ub and the polyQ region of variable length (Q_n). Alleles occurring in the healthy population contain up to 44 glutamine residues, while sequences with 61-87 repeats have been associated with the development of MJD. Alleles with intermediate sizes have been found in healthy individuals and in MJD patients. Depending on the isoform, a third UIM may follow the polyQ sequence. Domain mapping is based on the UniProt reference sequence of human atx3 (code P54252) with 3 UIMs and a polyQ sequence with 14 repeats and uses the annotations described by Almeida and collaborators (2013).

later attested biochemically using several Ub model substrates and Ub protease-specific inhibitors (Burnett *et al.*, 2003; Mao *et al.*, 2005; Nicastro *et al.*, 2005). The JD is a motif with a high degree of conservation between species (Albrecht *et al.*, 2003; Masino *et al.*, 2003) and, in fact, proteins other than atx3 have also been found to possess this type of catalytic domain (Nijman *et al.*, 2005). These observations have established atx3 and those other JD-containing proteins as DUBs (Burnett *et al.*, 2003; Scheel *et al.*, 2003; Tzvetkov and Breuer, 2007).

According to structural comparisons with other proteases, atx3 is a papain-like cysteine protease. The amino acids of the catalytic triad – cysteine 14, histidine 119 and asparagine 134 – are strictly conserved in relation to other groups of DUBs (see following subsection) (Mao *et al.*, 2005; Nicastro *et al.*, 2005) (Figure 4B). The glutamine residue at position 9 is also recognized as being important for the catalytic activity of atx3.

Apart from the JD, atx3 tertiary structure remains largely unknown. The C-terminal tail presents a decreased degree of conservation among species and is considered to be less structured and complex (Albrecht *et al.*, 2004; Albrecht *et al.*, 2003; Masino *et al.*, 2003). Still, NMR analysis of the two UIMs located upstream of the polyQ stretch (the ones conserved in the two major atx3 isoforms) has shown that they fold into two α-helixes, separated by a short flexible linker region (Almeida *et al.*, 2013; Song *et al.*, 2010) (Figure 5). The polyQ region is admitted to be polymorphic: while isolated polyQ sequences possibly lack regular secondary structures, it has been suggest that, when they are part of a protein, polyQ tracts may have multiple conformations, varying between α-helical structures, random coils and extended loops, depending on their size (glutamine number), the actual regions flanking them (the

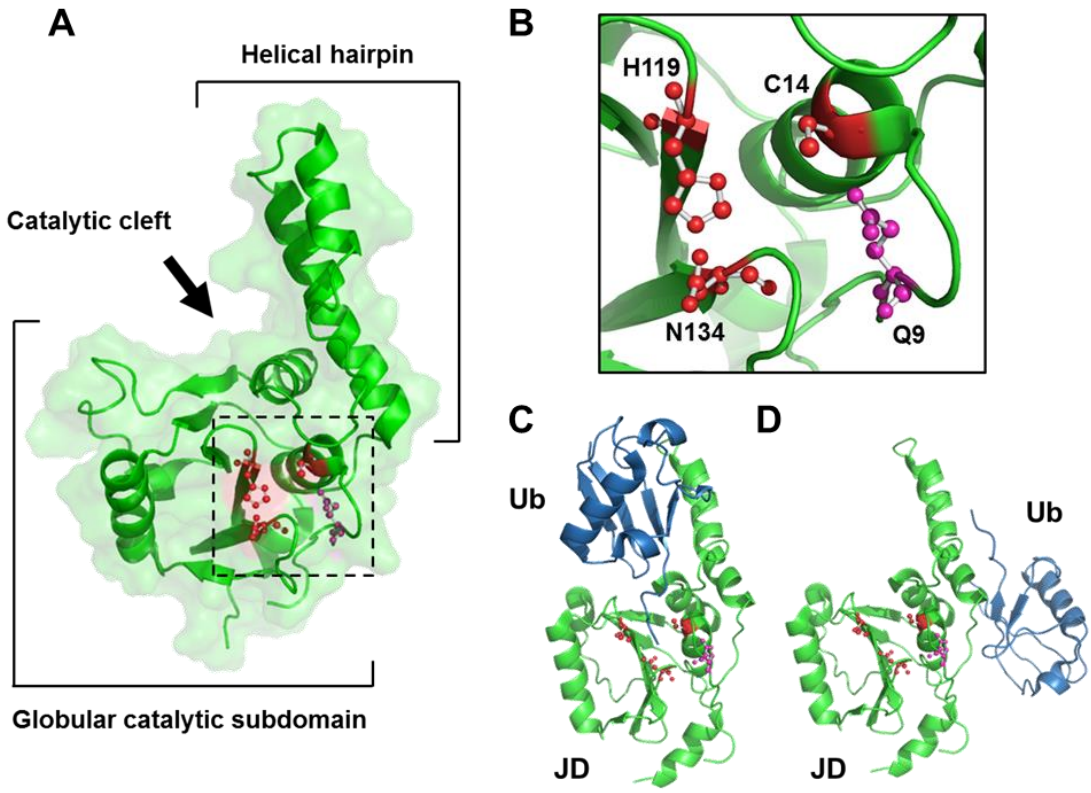

Figure 4: Tertiary strucutre of the JD. A The catalytic domain of atx3 is mainly constituted by a globular subdomain and a flexible hairpin. Between them lies the catalytic cleft (PDB code: 1YZB). **B** The arrangement of the amino acids of the catalytic triad (in red) and glutamine 9 (in purple) is presented in detail. The JD is able to interact with two Ub molecules through two Ub-binding sites: ***C*** site 1, close to the catalytic cleft, and ***D*** site 2, on the opposite surface (PDB code: 2JRI).

protein context), possible molecular interactions and the cellular environment (Almeida *et al.*, 2013; Kim *et al.*, 2009).

Clues to ataxin-3 function and biologic role

Even twenty years after atx3 was described for the first time, the precise functions of this disease-causing protein remain, to some extent, shrouded in mystery. Several hints to the cellular mechanisms with which atx3 may be involved have derived from studies exploring its enzymatic activity and its interactions, each one contributing to the drawing of the larger picture of atx3 biologic role. Currently, atx3 is admitted to participate in cellular pathways utilizing Ub signals and has been predominantly associated with protein quality control systems and transcription regulation.

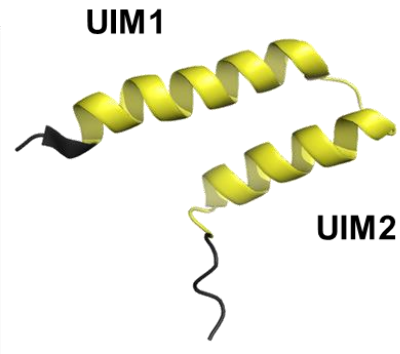

Figure 5: Tertiary structure of UIM1 and UIM2. The first two UIMs of atx3 form two α-helixes, separated by a flexible linker region (PDB code: 2KLZ).

A. Ubiquitination

Ubiquitination (or ubiquitylation) is a reversible mechanism of post-translational processing that consists on the covalent binding of Ub, a small and ubiquitous protein, to a lysine residue of another protein (Pickart and Eddins, 2004; Pickart and Fushman, 2004; Reyes-Turcu *et al.*, 2009; Wilkinson *et al.*, 2005). Conjugation of Ub is known to be implicated in the regulation of many protein properties, including enzymatic activity, stability and subcellular localization, and to have outcomes in countless cellular processes, ranging from protein degradation and endocytosis to DNA repair, chromatin remodeling and gene expression, cell cycle progression, pathway signaling, endocytosis and secretory pathway component sorting (Weissman, 2001; Welchman *et al.*, 2005).

Ub is one the most versatile molecular signals in eukaryotic cells, and the actual outcome of ubiquitination depends on the type of arrangements produced by Ub conjugation: Ub can be conjugated in a monomeric form (monoubiquitination), to one or several lysine residues of a protein, or form chains constituted by several Ub moieties (polyubiquitination) (Ikeda and Dikic, 2008). PolyUb chains are formed by isopeptide bonds established between a lysine of the last Ub monomer of a growing chain and the C-terminal glycine of a newly added monomer (Weissman, 2001). PolyUb chains are very diverse since they can have varying lengths and because conjugation between Ub monomers can be mediated by seven possible lysines. In living organisms, polyUb chains can be assembled with diverse topologies resulting from different linkage modes existing between Ub monomers. *In vivo*, the best characterized chains are the ones described as homotypic, resulting from the repetition of the linkage to a particular residue, but other types of arrangements have been also described, including chains of mixed-linkage types, branched chains and the recently uncovered linear chains, resulting from conjugation between the N-terminal methionine and the C-terminal glycine of Ub monomers (Ikeda and Dikic, 2008; Rieser *et al.*, 2013; Ye and Rape, 2009). The most familiar, *classic*, polyUb chains are the ones linked by lysine 48, whose well documented function is the targeting of proteins for proteasomal degradation; the UPP is one of the main mechanisms of

short-lived or damaged protein turnover. The *in vivo* functions of the other, *atypical*, chains are being progressively unveiled, but many have been shown to mediate non-degradative pathways, such as the ones described above. In particular, K63-linked polyUb chains, probably the best studied chains after K48-linked ones, have been implicated in DNA repair mechanisms, endocytosis and protein sorting (Ikeda and Dikic, 2008; Komander *et al.*, 2009; Weissman, 2001; Ye and Rape, 2009).

Conjugation of Ub to a target protein is a multistep process mainly involving three types of enzymes: Ub-activating (E1) enzymes, Ub-conjugating (E2) enzymes and Ub protein (E3) ligases. In brief, initially the E1 enzymes bind (or activate) Ub in a process requiring ATP, the E2 enzymes then conjugate Ub onto themselves, acting as carrier proteins, and the E3 ligases finally transfer Ub to the side chain of the targeted lysine residue of the substrate protein (Fang and Weissman, 2004; Pickart and Eddins, 2004; Weissman, 2001). E3 ligases (and E2 enzymes, to a lesser extent) are admitted to be responsible for the selectivity in substrate selection and for controlling the assembly of polyUb chains, with specific linkage types (Ikeda and Dikic, 2008). The formation of polyUb chains is widely accepted to occur by sequential addition of Ub monomers to substrate-bound Ub, but this idea is currently challenged by evidence demonstrating that polyUb chains can be assembled by E2 and E3 enzymes and only then conjugated onto substrate proteins (Li *et al.*, 2007).

B. Deubiquitinating enzymes

Ubiquitination is a regulated process that is not only reversible but also dynamic, being terminated and modulated by enzymes that counter the action of the Ub-conjugating machinery – the deubiquitinating enzymes (also termed deubiquitinases and hereby generally abbreviated as DUBs). The human genome encodes about 79 putative functional DUBs (Komander *et al.*, 2009; Nijman *et al.*, 2005). These enzymes are proteases directed at the isopeptide bonds formed by Ub, and according to the mechanism of catalysis and homology they have been subdivided into five families: i) the Ub C-terminal hydrolases (UCHs); ii) the Ub-specific processing proteases (USPs); iii) the ovarian tumor proteases (OTUs); iv) the Josephins; and v) the JAB1/MPN/Mov34 metalloenzymes (JAMMs). The Josephin family of DUBs includes atx3 and three other human proteins, all of them containing a JD: the atx3-like protein (atx3L), Josephin-1 and Josephin-2 (Tzvetkov and Breuer, 2007).

Most DUBs are cysteine proteases, the exception being the JAMM family, which is constituted by zinc metalloproteases (Komander *et al.*, 2009; Nijman *et al.*, 2005). Although cysteine protease DUBs of different families share only a limited sequence and structural similarity, the structure of the catalytic core and the active site amino acids closely resemble those of the classical cysteine protease papain (Eletr and Wilkinson, 2014; Nijman *et al.*, 2005). The conserved catalytic triad is constituted by a cysteine, a histidine and an aspartate. Catalysis is mediated by the thiol group of cysteine, whose deprotonation is assisted by the histidine residue, in turn polarized and oriented by the aspartate. The cysteine performs a nucleophilic

attack on the carbonyl of the peptide bond and the intermediate is stabilized in an oxyanion hole, generally provided by hydrogen bond donors (glutamine, in the case of atx3), and the catalytic cysteine. The target protein is released and a covalent intermediate is formed between the enzyme and, in the case of DUBs, Ub, which is then release upon reaction of the intermediate with water (Eletr and Wilkinson, 2014; Nijman *et al.*, 2005).

DUBs may play different roles: a) they may remove Ub from substrates, terminating a Ub signal (possibly rescuing them from degradation); b) they are responsible for shortening polyUb chains, editing an ubiquitination arrangement and exchanging Ub signals; c) they may modulate the rate of ubiquitination, d) they may recognize and regulate entry of proteins into the proteasome (*proofreading*); e) they disassemble bound and unbound polyUb-chains and recycle Ub; f) and they are even implicated in processing immature Ub, which is synthetized as different fusion proproteins (Komander *et al.*, 2009; Weissman, 2001). In the cell, DUBs are subject to several mechanisms of regulation that define the timing and localization of cleavage and that modulate their enzymatic activity (usually low *in vitro*) in order to avoid cleavage of unwanted bonds, being generally considered to take part in multiprotein complexes that define and coordinate and their actions (Marfany and Denuc, 2008; Reyes-Turcu *et al.*, 2009). The tight regulation of deubiquitination is also illustrated by the specificity or preferences that some DUBs display, in terms of both ubiquitinated substrates and particular types of Ub signals (Komander *et al.*, 2009). Given the fact that DUBs participate in the control of Ub signals, it is not surprising that this group of enzymes plays a part in several cellular pathways, though current evidence demonstrates that most individual DUBs are involved in a limited number of systems (Nijman *et al.*, 2005). Over the years, DUBs have been implicated in regulating the stability of other proteins (by interfering with the UPP and lysosomal degradation), cell cycle regulation, gene expression, DNA repair, enzyme activation, endocytosis, modulation of kinases and signal transduction pathways (Clague and Urbe, 2006; Eletr and Wilkinson, 2014; Nijman *et al.*, 2005; Reyes-Turcu *et al.*, 2009).

C. Ataxin-3 deubiquitinase activity and ubiquitin binding – possible involvement with the ubiquitin-proteasome pathway

The fact that atx3 displays DUB activity and possesses regions able to interact with Ub points out to an involvement in pathways that rely on Ub signals, and starting from the first studies trying to explore atx3 function, significant evidence has connected atx3 to the UPP (Doss-Pepe *et al.*, 2003). Atx3 interacts with ubiquitinated species (Doss-Pepe *et al.*, 2003) and is able to bind polyUb chains trough the UIMs located in the C-terminal tail, being capable of interacting with both K48 and K63-linked chains (Burnett *et al.*, 2003; Chai *et al.*, 2004; Donaldson *et al.*, 2003; Winborn *et al.*, 2008). When binding mono- or polyUb, the affinity of the first two tandem UIMs is greater than that of each individual UIM, suggesting a cooperative action. The binding is stronger with lengthier polyUb chains, likely resulting from structural modifications of the linker region existing between the UIMs and that may also

modulate the interaction with chains of different linkage type (Song *et al.*, 2010). Additionally, there is a preference for chains of at least four Ub monomers and, perhaps not coincidently, K48-linked polyUb chains of four and more monomers are the ones involved in targeting proteins for proteasomal degradation (Burnett *et al.*, 2003; Mao *et al.*, 2005; Winborn *et al.*, 2008). Importantly, atx3 has been shown to be able to bind polyubiquitinated proteins in both non-neural and neural cell lines (Berke *et al.*, 2005).

Regarding its activity as a DUB, results suggest that atx3 functions as a protease directed at editing polyUb chains, rather than favoring their complete disassembly (Burnett *et al.*, 2003; Burnett and Pittman, 2005; Kuhlbrodt *et al.*, 2011; Mao *et al.*, 2005; Nicastro *et al.*, 2010; Winborn *et al.*, 2008). *In vitro* assays with isolated polyUb chains or ubiquitinated proteins reveal that atx3 decreases the levels of lengthier species, shortening Ub chains rather than promoting the recycling of free monoUb (Burnett *et al.*, 2003; Kuhlbrodt *et al.*, 2011; Nicastro *et al.*, 2010; Winborn *et al.*, 2008). Additionally, atx3 shows a preference for cleaving K63-linked chains or chains of mixed K48 and K63 linkage, compared to pure K48-linked chains, *in vitro* (Winborn *et al.*, 2008).

The first *in vivo* clues to atx3 function derive from the characterization of an atx3 knockout (KO) mouse (Schmitt *et al.*, 2007). These animals showed no significant morphological or behavioral differences, compared to wild-type animals, but had a notable increase in the levels of ubiquitinated proteins, detectable in the testis and in the brain. This establishes atx3 as an active DUB, *in vivo*. The absence of deleterious physiological consequences was suggested to result from possible redundancy existing among DUBs (Schmitt *et al.*, 2007).

In cells, when atx3 activity is inhibited through mutation of its catalytic cysteine to an aspartate residue, there is an accumulation of polyubiquitinated proteins (Berke *et al.*, 2005; Mao *et al.*, 2005). This effect requires intact UIMs, indicating that the accumulation results from *substrate trapping* by the catalytic inactive atx3, and thus suggesting a link between the catalytic activity of the JD and the UIMs. These motifs are admitted to help recruit the polyubiquitinated substrates and present them to the catalytic site in a way that allows for sequential editing (Mao *et al.*, 2005; Winborn *et al.*, 2008). Accordingly, it was also observed that the UIMs are required for atx3 to exhibit the cleavage polyUb linkage type preferences reported (Winborn *et al.*, 2008). The particular contribution of the possible third UIM is not very clear, considering that, *in vitro*, the two major isoforms (MJD1a and MJD1-1) have similar Ub protease activity (Harris *et al.*, 2010).

The two Ub-interacting surfaces present in the JD display a low level of affinity, but are nonetheless important in binding polyUb chains and positioning them for cleavage (Nicastro *et al.*, 2009; Nicastro *et al.*, 2010). Experiments using mutants of these sites revealed that site 1, next to the catalytic cleft, is indispensable for cleavage of polyUb chains, being possibly required for the correct placing of Ub relatively to the catalytic site. Its negative charge may facilitate the docking of the positively-charged C-terminus of Ub (Almeida *et al.*, 2013; Nicastro *et al.*, 2010; Todi *et al.*, 2010). Site 2 is not as critical for enzymatic activity and acts differently depending on the Ub linkage type: mutation does not alter the cleavage of K63-linked chains,

but impairs activity against K48-linked ones. This suggests that site 2 is probably more involved in determining cleaving preferences. Additionally, the cooperative interplay between these two Ub-binding sites of the JD and the UIMs is admitted to be crucial for the cleavage of Ub chains by atx3, in cells. The UIMs may recruit and bind polyUb chains, while the two sites at the JD surface may adjust the position of the isopeptide bonds relatively to the catalytic site, allowing proteolysis (Nicastro *et al.*, 2009; Nicastro *et al.*, 2010). Curiously, the structure of the JD apparently only accommodates K48-linked polyUb and, in fact, the isolated JD associates more strongly with K48-linked polyUb chains and cleaves them more efficiently than K63-linked ones, in contrast to the full-length protein (Nicastro *et al.*, 2010; Winborn *et al.*, 2008). This particularity of the free JD may be related to the observation that the activity of full-length atx3 was greatest against polyUb chains of mixed K48 and K63 linkage (Nicastro *et al.*, 2010; Winborn *et al.*, 2008).

In the experiments described before, when atx3 DUB activity is inhibited by mutation, there is an increase in polyubiquitinated species of a considerable range of molecular sizes, localized primarily in the nucleus (Berke *et al.*, 2005). This indicates that atx3 presumably binds and eventually acts upon a broad range of ubiquitinated substrates. Furthermore, the changes provoked by the mutation are reportedly similar to what is elicited when the proteasome is pharmacologically inhibited (Berke *et al.*, 2005), suggesting that atx3 is possibly involved with ubiquitinated proteins that are targeted for degradation by the UPP. Intriguingly though, current studies present contradictory results regarding the actual effect of atx3 on protein turnover. Atx3 is able to edit K48-linked polyUb chains conjugated to a model protein (lysozyme) *in vitro*, at the same time blocking its proteasome-dependent degradation (Burnett and Pittman, 2005). The authors of this report proposed that atx3 may partially deubiquitinate proteins and prevent their degradation by binding through the UIMs, while maintaining their degradation signals. The same group had previously reported that, in cells, expression of atx3 increased the stability of a short-lived green fluorescent protein (GFP)-tagged with a sequence that targets it for proteasomal degradation (Burnett *et al.*, 2003). However, it has also been reported that lysates from *Caenorhabditis elegans* lacking the worm atx3 ortholog were better at stabilizing GFP-tagged Ub-fusion degradation substrate (UbiV-GFP) (Kuhlbrodt *et al.*, 2011).

The preference for atypical polyUb chains suggests that atx3 may function as a regulator of topologically complex polyUb chains (Winborn *et al.*, 2008), but it is challenging to draw any definite conclusion regarding the particular systems in which atx3 DUB activity is involved, seeing as the actual physiologic targets of atx3 enzymatic activity are yet to be determined. DUBs are known to display specificity at several levels, being able to distinguish not only between different Ub linkage types and chain structures, but also between different ubiquitinated substrates (Komander *et al.*, 2009; Reyes-Turcu *et al.*, 2009). Importantly, the *in vitro* assays evaluating atx3-mediated proteolysis usually only employ model substrates such as Ub derivatives, Ub fusion proteins or polyUb chains, and the observed activity is generally low (Burnett *et al.*, 2003; Chow *et al.*, 2004b; Durcan *et al.*, 2011; Nicastro *et al.*, 2010; Weeks *et al.*, 2011; Winborn *et al.*, 2008). This suggests that external factors or the association with the endogenous substrate(s) of atx3 may be required for optimal proteolysis. Most DUBs are

known to be *cryptic*, requiring proper substrate(s) in order to acquire a catalytic-competent conformation (Komander *et al.*, 2009; Reyes-Turcu *et al.*, 2009; Reyes-Turcu and Wilkinson, 2009). As detailed below, growing evidence from recent studies exploring atx3 molecular interactions is starting to suggest that some E3 Ub ligases may interact with atx3 in a substrate-like manner (see section below).

D. Ataxin-3 interactors and protein homeostasis systems

Atx3 has been shown to interact with several other proteins (Figure 6). The studies describing the outcomes of these interactions have provided additional hints into the possible participation of atx3 in protein homeostasis systems.

Atx3 was initially shown to associate with the proteasome through its N-terminal region (Doss-Pepe *et al.*, 2003), though a latter study reported that this interaction may not be very strong or even direct (Todi *et al.*, 2007). Another report described an *in vitro* direct interaction with the p45 subunit of the proteasome, but related it with the turnover of atx3 itself (Wang *et al.*, 2007). Regardless, two of the best characterized atx3 interactions favor the idea of a functional involvement with the UPP: the ones atx3 establishes directly with valosin-containing protein (VCP)/p97 and with the human homologs of the yeast DNA repair protein Rad23 A and B (HHR23A/B) (Burnett *et al.*, 2003; Doss-Pepe *et al.*, 2003; Laço *et al.*, 2012a; Mao *et al.*, 2005). Atx3 interacts with VCP/p97 through its C-terminal region (Boeddrich *et al.*, 2006; Hirabayashi *et al.*, 2001; Mao *et al.*, 2005; Matsumoto *et al.*, 2004; Zhong and Pittman, 2006) and with Ub-like domains of HHR23A/B through the Ub-binding site 2 of the JD (Figure 6) (Nicastro *et al.*, 2005; Wang *et al.*, 2000). Both proteins have been implicated in diverse biological processes, including the UPP, as they have both been linked to the shuttling of polyubiquitinated substrates to the proteasome for degradation (Albrecht *et al.*, 2004; Burnett *et al.*, 2003; Doss-Pepe *et al.*, 2003). It has been proposed that, functioning with these interactors, atx3 may act in a number of different ways: a) trimming polyUb chains of a substrate, thus facilitating the subsequent disassembly of the chain by proteasome-associated DUBs; b) editing polyUb chains in order to guarantee that the substrate is correctly targeted for degradation; or c) functioning as a transiently-associated subunit of the proteasome and recognizing some of its substrates (Boeddrich *et al.*, 2006; Doss-Pepe *et al.*, 2003; Wang *et al.*, 2008). The interaction with VCP/p97 (but not with hHR23A) was recently shown to enhance atx3 DUB activity *in vitro*, against both K48- and K63-lined polyUb chains (Laço *et al.*, 2012a; Nicastro *et al.*, 2010). It was proposed that, in a cellular context, VCP-p97 could activate atx3, which would preferentially process K63 linkages present in polyubiquitinated substrates, yielding polyUb chains enriched in K48 linkages that would target those substrates for transference to the proteasome (Laço *et al.*, 2012a). In *C. elegans*, the majority of UbiV-GFP-derived polyubiquitinated species that accumulated when both atx3 and VCP/p97 orthologs were knocked down do not present K48-linkages, supporting the idea that atx3 prefers chains of atypical topology (Kuhlbrodt *et al.*, 2011).

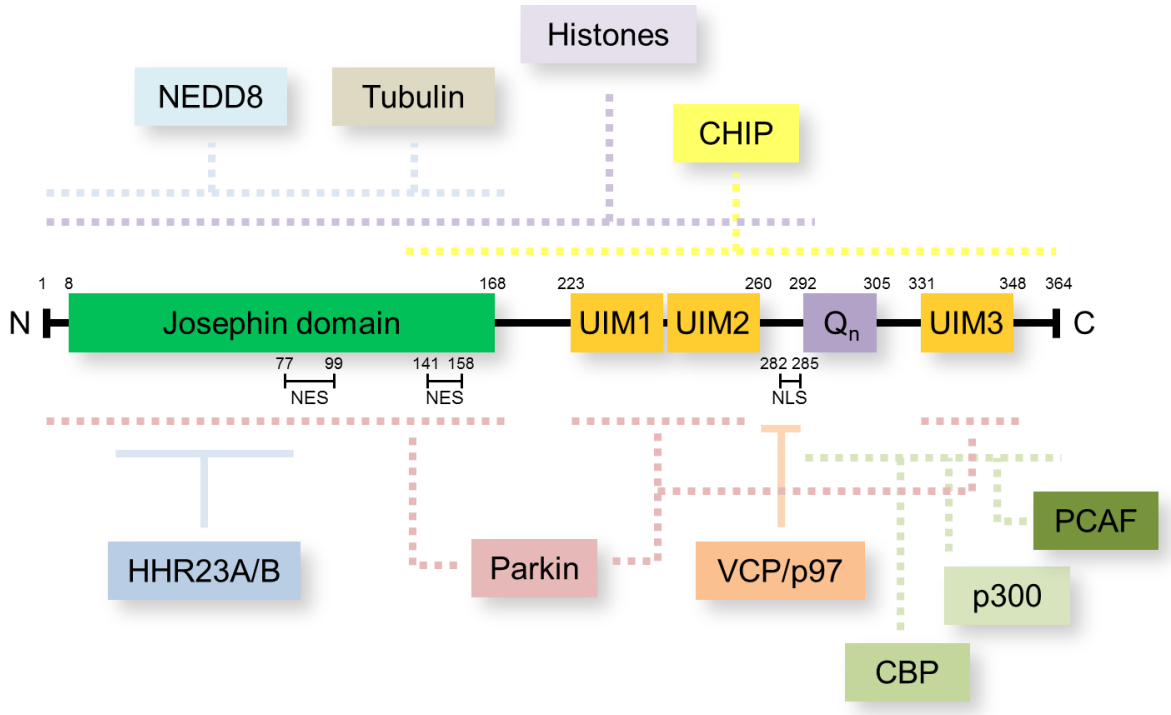

Figure 6: Mapping of atx3 direct interactions and subcellular targeting sequences. Atx3 has been shown to interact directly with several proteins. The figure uses continuous lines to represent interactions known to be mediated by limited regions within atx3 domains: HHR23A/B interacts with Ub-binding site 2 of the JD, while VCP/p97 interacts with a part of the linker region between UIM2 and the polyQ sequence (Q_n). Interrupted lines represent interactions which have been mapped with lesser detail: NEDD8 and tubulin have been demonstrated to interact with atx3 JD, histones bind atx3 sequence N-terminally of the polyQ region, CHIP interacts with atx3 C-terminally of amino acid 133, PCAF, p300 and CBP bind a polyQ-containing C-terminal region and parkin interacts with both the JD and the UIMs. One functional NLS was described in the vicinity of the region interacting with VCP/p97 and two NES were reported in the JD. The figure uses the same domain annotations as figure 3.

Particularly, VCP/p97 and HHR23A/B constitute important players in the endoplasmic reticulum-associated degradation (ERAD), the system mediating the ubiquitination of misfolded proteins and unassembled complex constituents present in the secretory pathway and consequent exportation to the cytosol for degradation by the proteasome (Amm *et al.*, 2014; Hirsch *et al.*, 2009; Meusser *et al.*, 2005). While atx3 has been described to be involved with the ERAD, once again there are contradictory results regarding whether it promotes or decreases degradation by this pathway. In transfected cells, while one study showed that atx3 decreases the degradation of CD3δ, a transmembrane ERAD substrate (Zhong and Pittman, 2006), other authors reported instead that inactivation of atx3 by C14A mutation produced a better stabilization of other ERAD substrates – transmembrane T-cell receptor α (TCRα) and the luminal β-sile amyloid precursor protein cleaving enzyme (BACE457Δ) (Wang *et al.*, 2006). Nonetheless, results point out a role for atx3 in regulating the flow of substrates through the ERAD pathway. It was recently proposed that DUB activity in general, regardless of its agent, may be an important player imparting discrimination between putative substrates of the ERAD (Zhang *et al.*, 2013). Targeting for degradation involves several factors, including the encounter

of the substrate with the enzymatic machinery mediating ubiquitination, the length of time of the interaction between them, the action of countering DUBs and several downstream steps. The interplay between ubiquitination and deubiquitination may dynamically define the length of dwell time of the Ub chains, thus dynamically defining the degradation signals. It was further suggested that, considering that DUBs may be important in downstream events after commitment to degradation, modulation of deubiquitination in slightly different ways (possibly through different procedures such as in the experiments mentioned above) can have different outcomes in terms of substrate degradation (Zhang *et al.*, 2013).

Neural precursor cell expressed developmentally downregulated gene 8 (NEDD8), a Ub-like protein, interacts with atx3 in a substrate-like manner (Ferro *et al.*, 2007; Mori *et al.*, 2005). NEDD8 is conjugated to other proteins in a way reminiscent of ubiquitination and this attachment, termed neddylation, has been reported to regulate target protein's functions (van der Veen and Ploegh, 2012). The interaction between atx3 and NEDD8, along with the observed deneddylase activity of atx3, may interfere with the neddylation state of other proteins, influencing the processes with which this modification is involved (Ferro *et al.*, 2007).

Atx3 has also been linked to aggresome formation. Aggresomes are misfolded protein aggregates that form near the microtubule-organizing center (MTOC) when the proteasome is not able to deal with misfolded proteins. These structures seem to be of physiologic importance, since they concentrate defective proteins that are then degraded by lysosomes, contributing to the maintenance of cellular homeostasis (Kopito, 2000; Markossian and Kurganov, 2004). Endogenous atx3 seems to play a role in the regulation of aggresome formation, having been shown to colocalize with aggresome and preaggresome particles and to be important in the formation of aggresomes themselves (Burnett and Pittman, 2005). Both atx3 catalytic activity and UIMs mediate this last function. Atx3 was additionally shown to associate with: dynein and histone deacetylase 6 (HDAC6), two known constituents of the complex responsible for the transport of misfolded protein to the MTOC (Burnett and Pittman, 2005), ubiquilin-1, a recently described player in aggresome formation (Heir *et al.*, 2006), and directly with tubulin, one of the main constituents of the cytoskeleton (Mazzucchelli *et al.*, 2009; Zhong and Pittman, 2006). Though it has been proposed that atx3 may protect misfolded protein before they reach the MTOC or stabilizes proteins involved in that transport (Burnett and Pittman, 2005), atx3 was recently shown to play a role in generating unanchored Ub chains, whose C-terminal region binds to HDAC6, signalizing misfolding proteins for transport to forming aggresomes (Ouyang *et al.*, 2012).

E. Ataxin-3 and E3 ubiquitin ligases

DUBs are frequently found to interact with E3 Ub ligases (Eletr and Wilkinson, 2014; Sowa *et al.*, 2009; Ventii and Wilkinson, 2008), the enzymes responsible for the formation of the isopeptide bonds between an Ub moiety and a lysine residue of the target protein – promoting ubiquitination – or of another Ub molecule – forming polyUb chains (Pickart and

Eddins, 2004). E3 ligases are very diverse and specific, partly accounting for the selectivity of the ubiquitination mechanisms. Atx3 (or polyQ-expanded fragments of the protein) have been shown to interact with several Ub ligases (Durcan and Fon, 2013): C-terminus of 70 kDa heat shock protein (Hsp70)-interacting protein (CHIP), parkin, E4B, mitochondrial Ub ligase (MITOL – a protein from the outer mitochondrial membrane), Hrd1 and gp78 (both associated with the endoplasmic reticulum and with the ERAD). Furthermore, with the exception of Hrd1, these enzymes have been reported to promote atx3 ubiquitination and degradation (Durcan *et al.*, 2011; Jana *et al.*, 2005; Matsumoto *et al.*, 2004; Miller *et al.*, 2005; Sugiura *et al.*, 2010; Tsai *et al.*, 2003; Wang *et al.*, 2006; Ying *et al.*, 2009). Attending to what has been seen for other pairs of DUBs and E3 enzymes, it can be speculated that atx3 and the Ub ligases with which it interacts may transregulate each other as part of their normal function (Wada and Kamitani, 2006). The E3 enzymes may be responsible for regulating atx3 activity or targeting it to degradation through promotion of its ubiquitination, while atx3 may edit polyUb chains added to other E3 ligase substrates and regulate the ubiquitination state of the E3 ligases themselves (Durcan and Fon, 2013; Reyes-Turcu *et al.*, 2009; Todi *et al.*, 2009; Wada and Kamitani, 2006; Weissman *et al.*, 2011).

Atx3 was the first DUB described to interact with the E3 ligase parkin, the most commonly mutated protein in familial Parkinson's disease. They interact in cells and were shown to bind directly *in vitro*, in an interaction that increases when parkin is polyubiquitinated and that is mediated by the JD and the UIMs of atx3 (Figure 6) (Durcan *et al.*, 2011). Parkin-mediated ubiquitination of atx3 is controversial (Tsai *et al.*, 2003), but atx3 was shown to deubiquitinate self-ubiquitinated parkin, though non-expanded atx3 had no effect on its stability or turnover (Durcan *et al.*, 2011). Curiously, atx3 appears to reduce parkin ubiquitination through a more unconventional method than Ub hydrolysis, actively opposing the ligation of Ub to parkin, rather than removing Ub moieties or chains (Durcan *et al.*, 2012). Atx3 interacts transiently with the E2s used by parkin to self-ubiquitinate, and, when the three interact, atx3 apparently promotes the transference of Ub onto itself, through an undisclosed mechanism mediated by C14 of the catalytic site (Durcan and Fon, 2013).

The interaction between atx3 and CHIP was also detected in cells and further observed to be direct, *in vitro* (Jana *et al.*, 2005; Scaglione *et al.*, 2011). CHIP interacts with the C-terminal region of atx3 and their association is stabilized in cells when CHIP is monoubiquitinated, a modification that was shown to be mediated by Ube2w, an initiator E2 Ub-conjugating enzyme, and to enhance the ability of CHIP to target substrates for degradation (Scaglione *et al.*, 2011). Atx3 deubiquitinates CHIP *in vitro* (Winborn *et al.*, 2008), and though this does not affect its degradation in cells (Durcan and Fon, 2013), in ubiquitination assays mediated by CHIP, atx3 limits the length of Ub chains attached to CHIP substrates to a critical point (Scaglione *et al.*, 2011). *In vitro*, when substrate polyubiquitination reaches a certain point, atx3 deubiquitinates CHIP, terminating the reaction. CHIP is an important enzyme in quality control systems, linking molecular chaperons to the UPP. It was suggested that, together with E2 enzymes like Ube2w, atx3 regulates CHIP ubiquitination status and thus CHIP-mediated ubiquitination and degradation of misfolded protein substrates

(Scaglione *et al.*, 2011). Atx3 may be important in limiting the length of the polyUb chain to the minimum needed for degradation (four monomers) or modulate the rate of proteasomal degradation through the interplay between cycles of Ub conjugation and removal. Interestingly, though atx3 has been shown to cleave long Ub chains preferentially, in this case it is able to remove Ub from monoubiquitinated CHIP, though only in the presence of a CHIP polyubiquitinated substrate. This suggests that atx3 may be recruited when a substrate is polyubiquitinated, in order to deubiquitinate CHIP and terminate the process (Scaglione *et al.*, 2011).

F. Ataxin-3 and transcription regulation

A different aspect of atx3 function concerns its involvement in transcription regulation. Characterization of glutamine repeat-containing proteins has demonstrated that many of them are involved in regulating signalling at the transcriptional level, the polyQ sequence mediating important molecular interactions (Hands *et al.*, 2008). Atx3 has been shown to influence the regulation of the expression of many genes (Evert *et al.*, 2003; Rodrigues *et al.*, 2007). A microarray analysis using two different *C. elegans* KO strains lacking the worm ortholog of atx3 identified 290 genes (1.4% of the worm total genome) that are differentially expressed comparing to wild-type animals. 143 of these had unknown function, but the other 147 genes were grouped according to their proposed biological roles: cell structure and mobility components (50%), signal transduction (20%), the UPP (8%), and other cell processes (22%), which include genes encoding enzymes, transporters, receptors and channels involved in diverse pathways. Of the 290 differentially expressed genes, 253 were upregulated and 37 were downregulated in KO animals (Rodrigues *et al.*, 2007). Even though there was a clear transcriptional dysregulation in the KO strains, in resemblance with the KO mice mentioned above, the animals were viable and had no overt phenotype, possibly due to functional redundancy and adaptative modifications.

Atx3 function as a transcription regulator is supported by *in vitro* and *in situ* molecular interactions studies. Atx3 is known to interact with: a) three transcription activators – cAMP response element-binding protein (CREB)-binding protein (CBP), p300 and p300/CBP-associated factor (PCAF) – through its C-terminal region (Li *et al.*, 2002); b) two transcription repressors – histone deacetylase 3 (HDAC3) and nuclear receptor co-repressor (NCor) – through an interaction involving its UIMs (Evert *et al.*, 2006a); and histones, mainly through the N-terminal region (Li *et al.*, 2002). Interaction with CBP, p300, PCF and histones was demonstrated to be direct (Figure 6) (Li *et al.*, 2002). The same studies report that atx3 represses the transcription mechanisms mediated by these proteins through different processes. CBP, p300 and PCAF are transcriptional co-activators that form complexes with other co-activators and proteins with acetyltransferase activity and acetylate histones; atx3 seems to repress transcription mediated by these co-activators by binding them through its C-terminal region. Furthermore, binding of histones through the N-terminal of atx3 seems to

repress acetylation by blocking the access to histone acetylation sites (Li *et al.*, 2002; Nicastro *et al.*, 2005). Atx3 interaction with HDAC3 and NCor was also reported to lead to a decrease in histone acetylation and consequent transcription repression (Evert *et al.*, 2006a). In particular, atx3 was shown to repress matrix-metalloproteinase 2 (MMP2) gene expression in luciferase reporter assays.

A recent study implicated atx3 in the transcriptional activation of a particular gene – manganese superoxide dismutase (SOD2), which is related to oxidative stress responses (Araujo *et al.*, 2011). Atx3 interacts with the forkhead box class O (FOXO) transcription factor 4 (FOXO4) in the human pons, apparently through the JD, and both proteins bind chromatin at the level of the human SOD2 gene promotor containing a FOXO4-binding element, in human-derived lymphoblastoid cell lines. Atx3 coactivates FOXO4-dependent gene transcription, including the transcription of the SOD2 gene; atx3 knockdown decreases the levels of the SOD2 gene. Interestingly, in the human cell lines, binding of atx3 increases in response to oxidative stress stimuli. These observations suggest that atx3 is important in regulating FOXO4-dependent antioxidant responses.

Although there are some studies that suggest an association between transcription regulation and the UPP, there is no clear evidence for such connection in the case of atx3 (Burnett *et al.*, 2003). It has been hypothesized, however, that atx3 DUB activity may interfere with the turnover of transcription regulators with which it interacts, thereby influencing repressor complex formation and activity (Evert *et al.*, 2006a; Rodrigues *et al.*, 2007). Nonetheless, the effects of atx3 in the FOXO4-dependent transcription are not accompanied by deubiquitination of FOXO4 (Araujo *et al.*, 2011).

G. Roles of ataxin-3 in the organization of the cytoskeleton and myogenesis

The importance of atx3 interactions with components of the cytoskeleton such as tubulin, microtubule-associated protein 2 (MAP2) and dynein may not be limited to its possible role in aggresome formation (Burnett and Pittman, 2005; Mazzucchelli *et al.*, 2009). Atx3 may play a role in the organization of the cytoskeleton itself, since its absence leads to morphologic alterations in cell lines, which are accompanied by the disorganization of the several cytoskeleton constituents (microtubules, microfilaments and intermediate filaments) and a loss of cell adhesions (Rodrigues *et al.*, 2010). Though an increase in cell death was observed when atx3 levels were reduced, there was no proof of significant mitotic alterations.

Interestingly, *in vitro* silencing of atx3 in differentiating mouse myoblasts not only leads to the generation of an immature cytoskeleton, but also compromises myoblasts transition into muscle fibers, thus suggesting a potential role for atx3 in myogenesis (do Carmo Costa *et al.*, 2010). This process comprises several events where remodeling of the cytoskeleton as well as of cell-cell and cell-extracellular matrix interactions are of crucial importance, with a tight control of protein expression and turnover (frequently by the UPP) being essential (Baylies and Michelson, 2001; Bryson-Richardson and Currie, 2008). The

observed effect of atx3 silencing was proposed to be mediated by integrins and, in agreement, silencing atx3 decreases the levels of a5 and a7 integrin subunits, which are known participants in myogenesis (do Carmo Costa *et al.*, 2010; Mayer, 2003). Furthermore, atx3 interacts with integrin subunit a5 and represses its degradation, and several proteins related to integrin-mediated responses were reported to have altered levels in myoblasts when atx3 was silenced (do Carmo Costa *et al.*, 2010). It is noteworthy, however, that no overt phenotype concerning cytoskeleton organization or muscle differentiation was reported in atx3 KO animals. This may be due to compensation or to subtle changes in the cytoskeleton that were not identified in the analyses performed (do Carmo Costa *et al.*, 2010; Rodrigues *et al.*, 2007; Rodrigues *et al.*, 2010; Schmitt *et al.*, 2007).

H. Summary of ataxin-3 proposed roles

The biochemical characteristics of atx3, the interactions described so far and the cellular outcomes of both features suggest that the biological role of atx3 may be connected to three major processes: a) protein homeostasis pathways; b) transcription regulation; c) cytoskeleton organization and myogenesis (Figure 7). Considering in particular the participation of the protein in quality control systems, atx3 may be important in: (i) regulating the formation, maintenance and termination of Ub signals, namely in polyUb chains of atypical morphology and possibly involving interactions with E3 enzymes like parkin and CHIP; (ii) shuttling substrates to the proteasome for degradation or, conversely, (iii) protecting them from proteasomal degradation; (iv) modulating the targeting and flux of ERAD substrates; and (v) aggresome formation.

As discussed above, atx3 participation in these diverse pathways may result from a more limited cell role, in a restricted number of mechanisms and interactions. For example, atx3 participation in the UPP may make it responsible for the regulation of the half-life of several different targets, which in turn take part in diverse cell functions (do Carmo Costa *et al.*, 2010; Evert *et al.*, 2006a; Rodrigues *et al.*, 2007; Rodrigues *et al.*, 2010). The fine-tuning of Ub signals, with outcomes possibly unrelated to degradation, may also be a promising mechanism through which atx3 mediates several cellular functions. Ubiquitination is increasingly regarded as a very complex and dynamic process, resulting from the intricate balances between Ub conjugation and deubiquitination (Komander *et al.*, 2009; Marfany and Denuc, 2008; Nguyen *et al.*, 2014; Zhang *et al.*, 2013). The observed preference for processing of atypical chains, the opposing effects in actual protein degradation described, and the mechanistic interaction between atx3 and E3 in ligases polyUb chains support this hypothesis. Considering the complexity of Ub signals and the myriad of pathways they intervene, regulation mediated by atx3 possibly may be also relevant in mechanisms in which atx3 has thus far not been implicated, such as DNA repair mechanisms, endocytosis and transport (Eletr and Wilkinson, 2014; Nijman *et al.*, 2005; Reyes-Turcu *et al.*, 2009). Interestingly, atx3 regulates protein stress responses, protein degradation and ageing in *C. elegans*, and the observed effects were

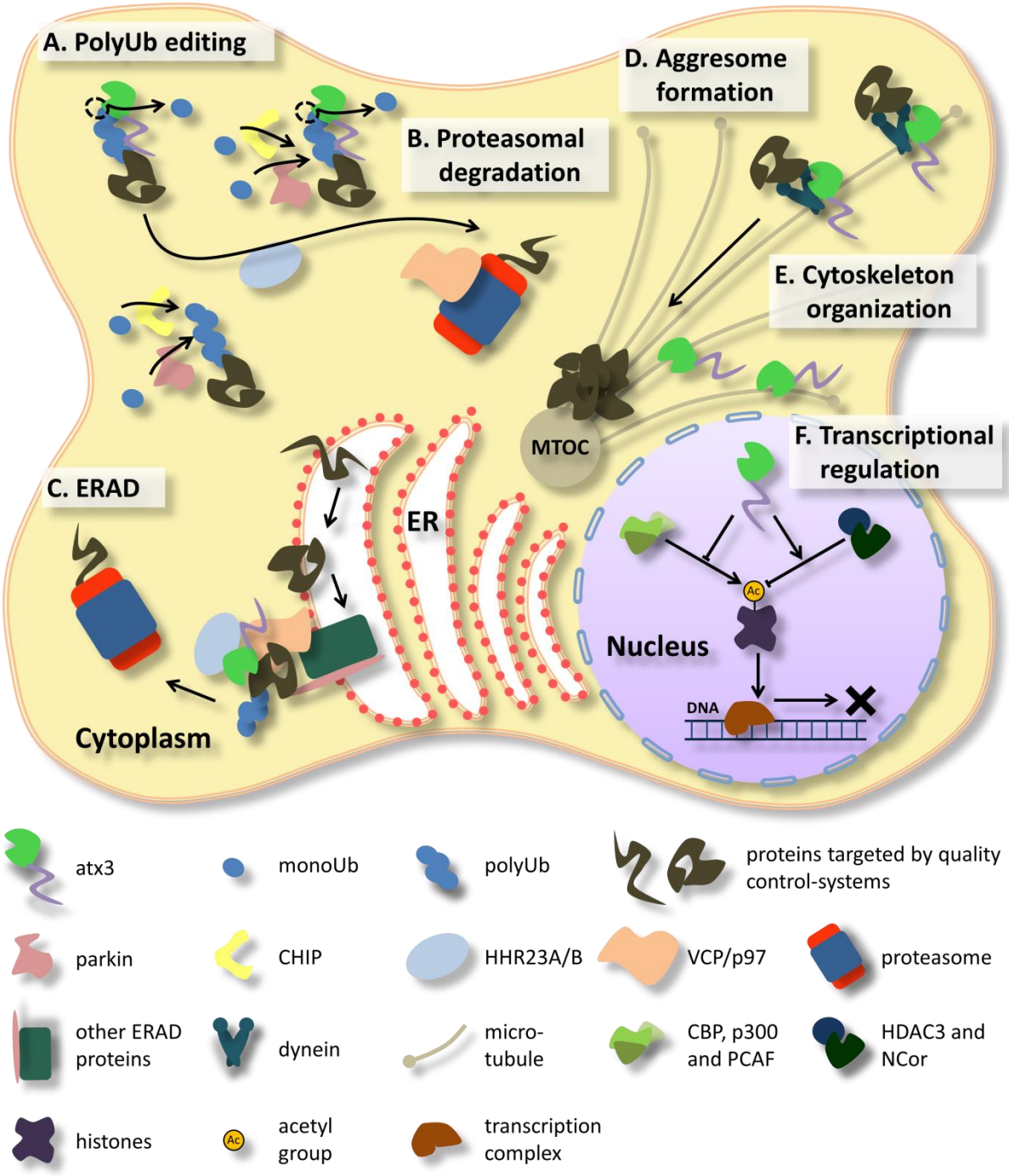

Figure 7: Atx3 activity, interactions and proposed biologic roles. ***A*** Atx3 displays DUB activity and has been shown to be able to edit polyUb chains, possibly regulating Ub signals in tandem with E3 ligases such as parkin and CHIP. Atx3 is believed to participate in quality control systems, interfering with ***B*** proteasomal degradation particularly in ***C*** the ERAD, by means of its interaction with HHR23A/B and VCP/p97. ***D*** Atx3 has been further linked to aggresome formation, interacting with tubulin and dynein, and with ***E*** the organization of the cytoskeleton itself. ***F*** Interactions with regulators of histone acetylation support many reports describing atx3 as a participant in transcription regulation.

described to require the synergistic action of VCP and involve the editing the ubiquitination state of substrates of the insulin/insulin-like growth factor (IGF1) (Kuhlbrodt *et al.*, 2011). This

suggests that regulation of Ub signals by atx3 may be very important in specific biological mechanisms (Scaglione *et al.*, 2011).

Intracellular transport and shuttling

As mentioned before, atx3 is found in both the cytoplasm and the nucleus. Several studies demonstrated that atx3 is actively transported across the nuclear envelope, being actively shuttled from the cytoplasm to the nucleus and vice versa (Antony *et al.*, 2009; Chai *et al.*, 2002; Macedo-Ribeiro *et al.*, 2009).

Regarding nuclear importation, a functional nuclear localization signal (NLS) upstream of the polyQ sequence (R282-R285) has been predicted (Boeddrich *et al.*, 2006; Tait *et al.*, 1998) and later shown to be active, promoting atx3 transport to the cell nucleus (Figure 6) (Macedo-Ribeiro *et al.*, 2009). Nuclear exportation appears to integrate both chromosome region maintenance 1 (CRM1)-dependent and independent mechanisms (Macedo-Ribeiro *et al.*, 2009) and, as of yet, two apparently functional nuclear export signals (NES) have been reported (I77-Y99 and E141-E158), though without consensus (Figure 6) (Antony *et al.*, 2009; Macedo-Ribeiro *et al.*, 2009). There is compelling evidence supporting the idea that at least the CMR1-independent mechanism of nuclear export is mediated by a N-terminal conformational motif comprised by regions in both the JD and the UIMs (Macedo-Ribeiro *et al.*, 2009).

Atx3 shifts to the nucleus in response to proteotoxic stimuli, such as oxidative stress (Araujo *et al.*, 2011) and heat shock, but independently from the identified NLS (Reina *et al.*, 2010). Two other regions seem important for this transport instead: the JD, namely S111, and the C-terminal region comprising the polyQ sequence and the rest of the C-terminal (but not the UIMs) (Reina *et al.*, 2010). This observation adds to other recent evidence suggesting that atx3 biological function may be important in cellular systems of stress response (Araujo *et al.*, 2011; Kuhlbrodt *et al.*, 2011; Mueller *et al.*, 2009; Todi *et al.*, 2009). Atx3 activity as a DUB participating in protein homeostasis pathways is in agreement with this possibility, as atx3 is likely important in dealing with misfolded proteins that arise as a consequence of stress, or that may also exacerbate cellular stress. The responses may also be triggered at a transcriptional level, considering the observed coactivation of FOXO4-mediated SOD2 expression by atx3 (Araujo *et al.*, 2011).

Atx3 degradation and turnover

Both the UPP and autophagy, two of the main protein degradation pathways existing in animal cells, have been shown to modulate atx3 turnover (Harris *et al.*, 2010). Atx3 has been shown to be polyubiquitinated and to be degraded by the proteasome (Berke *et al.*, 2005; Jana *et al.*, 2005; Matsumoto *et al.*, 2004; Todi *et al.*, 2007; Tsai *et al.*, 2003; Wang *et al.*, 2007); as

mentioned above, many E3 Ub ligases were reported to interact with atx3 and to promote its ubiquitination and degradation. However, the proportional importance of the UPP apparently depends on the particular atx3 isoform in question. It was suggested that proteasomal degradation is more important only in the case of the atx3 isoform lacking the third UIM (MJD1a), which is a less stable isoform. The three UIM-containing atx3 is more stable and is mainly degraded by autophagy (Harris *et al.*, 2010).

Interestingly, atx3 catalytic activity appears to regulate its turnover, since catalytically inactive atx3 has higher steady state levels in cells, partially resulting from a reduction on proteasomal degradation (Todi *et al.*, 2007). Strikingly, however, in this case and in several other studies (Berke *et al.*, 2005; Matsumoto *et al.*, 2004; Miller *et al.*, 2004), increased ubiquitination did not correlate with increased degradation, thereby indicating that proteasomal degradation independent of ubiquitination may also be relevant (Todi *et al.*, 2007).

1.5 Toxic consequences of ataxin-3 polyglutamine expansion

Polyglutamine sequences as causes of toxicity

The physiologic role of homopeptidic repeats such as polyQ sequences is not clearly understood, but it has been pointed out that this type of motives is usually associated with multimolecular complexes and that they are most likely important in regulating or mediating molecular interactions (Almeida *et al.*, 2013; Fiumara *et al.*, 2010; Hands *et al.*, 2008; Schaefer *et al.*, 2012). Homopeptidic regions are considered to be unstructured, becoming structured when establishing molecular interactions (Almeida *et al.*, 2013). It has recently been shown that polyQ tracts and adjacent regions have a propensity to engage in intermolecular interactions via formation of coiled-coils, in every disease-associated polyQ protein (Fiumara *et al.*, 2010). The flexibility of the polyQ sequence may facilitate the establishment of protein-protein interactions with the polyQ tract itself or with other protein regions, and stabilize them (Schaefer *et al.*, 2012).

To date, the mechanisms by which polyQ-expand atx3 leads to MJD pathogenesis have not been clarified, though, as for every other polyQ disease, the unstable polyQ expansion is considered to be of causal importance. There are several observations supporting this idea: a) the polyQ disease protein sequences are dissimilar outside the polyQ tract; b) disease severity increases with glutamine repeat number; c) age of onset decreases with the increase of repeat number; d) several transgenic models expressing polyQ sequences outside the natural gene context present neurodegenerative phenotypes (Ordway *et al.*, 1999; Takahashi *et al.*, 2010; Williams and Paulson, 2008; Zoghbi and Orr, 2000). As stated above, however, though the polyQ sequence expansion appears to be the triggering factor leading to the development of MJD, atx3 regions outside the polyQ region and the protein properties they determine are sure

to define the development of MJD and to determine its particular aspects (Gatchel and Zoghbi, 2005; Robertson and Bottomley, 2010).

Intracellular inclusion bodies

The formation of large inclusion bodies containing the pathogenic protein is one hallmark of every polyQ expansion disease. Even though wild-type atx3 displays a wide distribution within cells and is predominantly cytoplasmic in neurons, in MJD patients' brains, atx3 is commonly known to amass in the form of NIs present only in neurons (Paulson *et al.*, 1997b). Cytoplasmic inclusions have occasionally been reported (Hayashi *et al.*, 2003; Paulson *et al.*, 1997b; Yamada *et al.*, 2001) and recently axonal inclusions have also been observed in patients brains, in fibers known to degenerate in MJD (Seidel *et al.*, 2010). Apart from the polyQ-expanded atx3, NIs and the axonal inclusions contain several other proteins, including members of the cell quality control systems, like proteasome constituents, Ub and molecular chaperones, which may be mobilized against atx3 misfolding and aggregation (Chai *et al.*, 1999a; Chai *et al.*, 1999b; Chow *et al.*, 2004a; Paulson *et al.*, 1997b; Schmidt *et al.*, 2002; Seidel *et al.*, 2010).

Intracellular inclusions have been often linked to the pathogenesis of polyQ diseases as a major means of polyQ toxicity because of their ability to sequester different molecules, provoking cytotoxicity through several possible mechanisms: a) hindrance of transcription, through sequestration of molecules involved in transcription regulation (Chai *et al.*, 2002; McCampbell *et al.*, 2000); b) a general disturbance of the quality control systems of the cells, due to sequestration of proteasome constituents and molecular chaperones (Chai *et al.*, 1999a; Chai *et al.*, 1999b; Ferrigno and Silver, 2000; Muchowski *et al.*, 2000; Paulson *et al.*, 1997b; Schmidt *et al.*, 2002; Warrick *et al.*, 1999); c) hindrance of axonal transport, resulting from motor protein titration and physical blocking (Gunawardena *et al.*, 2003); d) other disturbances caused by recruitment of Ub-binding proteins (since inclusions are heavily ubiquitinated) or other polyQ-containing proteins (Donaldson *et al.*, 2003; Perez *et al.*, 1998).

As explained before, the importance of these large microscope-visible macromolecular aggregates to disease pathogenesis is now disputed and many authors suggest that they are in fact just the result of protective mechanisms moved by the cell in order to cope with the toxicity of the expanded proteins (Ross and Poirier, 2004; Todd and Lim, 2013; Williams and Paulson, 2008). However, studies concerning MJD demonstrate that there is no perfect overlap between the brain regions that degenerate and the regions presenting NIs (Riess *et al.*, 2008; Rüb *et al.*, 2006b; Yamada *et al.*, 2001). Additionally, it was also shown that, in the pons, patients with more severe neuronal loss presented a smaller amount of neurons with NIs (Evert *et al.*, 2006b).

Polyglutamine aggregation and toxicity

Studies suggest that expanded atx3 and every other polyQ-expanded protein tend to form aggregates, as a result of polyQ expansion-induced misfolding and consequent transition to aggregation-prone conformations (Bevivino and Loll, 2001; Chow *et al.*, 2004c; Jana and Nukina, 2004; Muchowski and Wacker, 2005; Nagai *et al.*, 2007; Tanaka *et al.*, 2001; Williams and Paulson, 2008). Aggregates formed by atx3 or other polyQ-containing proteins were shown to contain β-rich fibrillar structures of amyloid nature, reminiscent of the amyloid aggregates observed in Alzheimer's and prion diseases (Almeida *et al.*, 2013; Bevivino and Loll, 2001; Chen *et al.*, 2002). As for most amyloid-forming proteins, several pathways may drive the conversion of the soluble protein to amyloid aggregates, through the formation of different conformationally altered monomeric or self-assembled multimeric species (Uversky, 2010), being the small aggregates or oligomers the ones most commonly envisioned as the actual toxic species causing cytotoxicity (Takahashi *et al.*, 2010). It is suggested that the soluble amyloid oligomers have an inherent toxicity caused by mechanisms common to all of them (Kayed *et al.*, 2003), for example being able to destabilize the lipid bilayer, increasing its conductivity, or to sequester quality control system components and transcription factors, causing proteotoxic stress and transcriptional dysregulation (Figure 8) (Demuro *et al.*, 2005; Kayed *et al.*, 2004; Schaffar *et al.*, 2004; Shao and Diamond, 2007). It is also possible that the cell-mediated formation of NIs, though directed as an adaptive response, may trigger a snowball effect, in which important proteins are sequestered and more cellular systems become dysfunctional.

Mechanisms of ataxin-3 aggregation

Investigation has focused on a search to comprehend the mechanisms underlying atx3 aggregation and on trying to identify the toxic misfolded monomeric or oligomeric species (Takahashi *et al.*, 2010). *In vitro*, polyQ-expanded atx3 aggregates into amyloid-like fibrils (Bevivino and Loll, 2001; Ellisdon *et al.*, 2007; Ellisdon *et al.*, 2006) but, curiously, even non-expanded atx3 and the JD alone display a tendency to aggregate (albeit at slower rates than the expanded forms), underlying the relevance of regions outside the polyQ tract for protein self-assembly and aggregate formation (Chow *et al.*, 2004a; Chow *et al.*, 2004b; Gales *et al.*, 2005; Masino *et al.*, 2011; Masino *et al.*, 2004). Aggregation of atx3 is admitted to consist of two steps: the first step is independent from the polyQ sequence and involves a monomeric thermodynamic nucleus formed by a single misfolded protein to which monomers are added, consequently leading to elongation and fibril formation; in the case of the expanded protein there is a second aggregation step that leads to the formation of more stable sodium dodecyl sulfate (SDS)-insoluble aggregates (Ellisdon *et al.*, 2007; Saunders and Bottomley, 2009).

The JD plays a central role in the early conformational changes (Gales *et al.*, 2005), modulating the aggregation of both expanded and non-expanded atx3 (Ellisdon *et al.*, 2006;

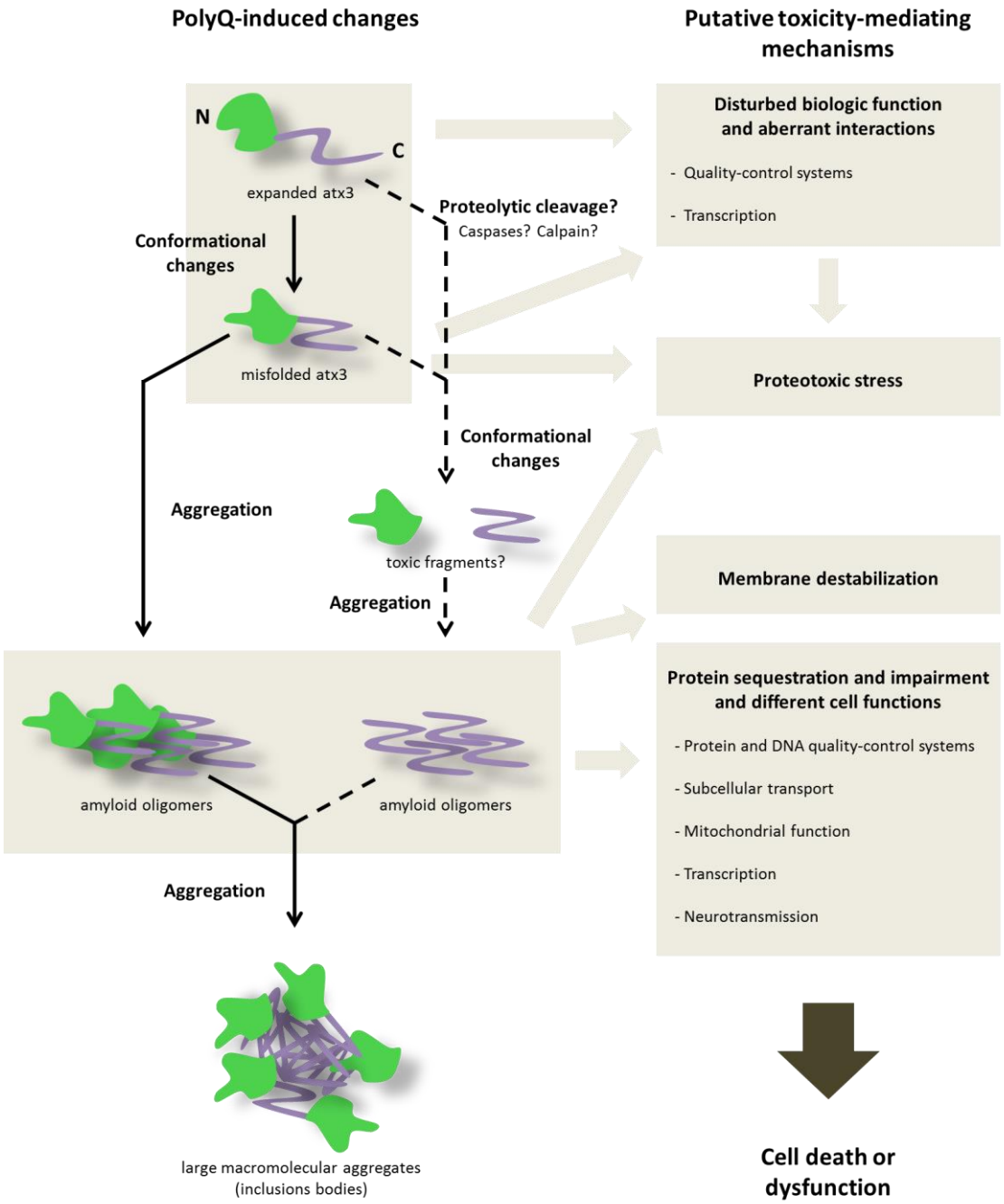

Figure 8: Putative mechanisms mediating expanded atx3 toxicity. PolyQ expansion of atx3 beyond 45 glutamines is known to lead to the development of MJD, though the identity of the actual toxic species is still a matter of debate. The effect the pathogenic mutation may have on the physiological function of atx3, be it at the level of protein quality control or transcription regulation, could affect important cellular activities and lead to cellular demise. Expanded atx3 is known to aggregate and produce large macromolecular aggregates, and it is believed that soluble amyloid-like oligomers that serve as intermediaries of the self-aggregation pathway may be deleterious to the cells, possibly destabilizing the cell membrane and/or recruiting important proteins with consequent disruption of important cellular systems. Proteotoxic stress may arise from atx3 misfolding, aggregation, aberrant interactions or the compromise of its native function as a player in protein homeostasis maintenance. Though without consensus, proteolytic cleavage of atx3 and generation of toxic protein fragments may be an important step contributing to toxic events such as oligomerization. The figure uses continuous black lines to represent changes produced on atx3 upon polyQ expansion and interrupted black lines to represent events related with proteolytic cleavage. The gray arrows link putative toxic species to some of mechanisms that might make them deleterious.

Masino *et al.*, 2004; Saunders and Bottomley, 2009). Interestingly, the surfaces involved in self-association of this domain overlap with the functionally relevant Ub binding sites 1 and 2 (Masino *et al.*, 2011; Nicastro *et al.*, 2009). These observations provide a direct link between protein function and aggregation and expose a role for intracellular interactors in protecting against atx3 self-assembly, especially given the fact that Ub reduces *in vitro* aggregation of the JD (Masino *et al.*, 2011). The C-terminal region of atx3 may also represent a bridge between physiological interactions and aggregation. In atx3, the regions predicted to form coiled-coils partially includes the α-helical UIMs and regions shown to interact with molecular partners such as VCP domains (Boeddrich *et al.*, 2006; Fiumara *et al.*, 2010; Song *et al.*, 2010). When expanded, the polyQ region may provoke aberrant protein interactions leading to atx3 aggregation. Overall, the regions outside the polyQ tract seem to predispose atx3 to aggregation, and the expansion of the polyQ sequence precipitates the formation of highly stable amyloid aggregates (Almeida *et al.*, 2013). The connection between normal molecular interactions and aggregation may help explain the failure of non-expanded atx3 to self-aggregate in the crowded cell environment and provide clues to understand the delayed onset of symptoms in patients (Gales *et al.*, 2005).

Taking these observations into account, one can speculate about the possible causes for the persistent atx3 aggregation occurring in MJD patients' brain and for the adult/late onset of the disease. In healthy people, the slow aggregation kinetics of the non-expanded atx3, the interaction with its macromolecular partners, and the high instability of the aggregates formed ensure an effective break down by the cell's intrinsic quality control mechanisms. Conversely, in MJD patients, the enhanced kinetics of the expanded atx3 aggregation, eventual polyQ expansion-induced alterations in protein-protein interactions, as well as the great stability of the aggregates formed lead to their aberrant accumulation inside the cells. This accumulation may increase with aging, as a result of the progressive failure of quality control mechanisms (Ellisdon *et al.*, 2007; Ellisdon *et al.*, 2006; Gales *et al.*, 2005; Masino *et al.*, 2011; Masino *et al.*, 2004).

Proteolytic cleavage and toxic fragment hypothesis

Several studies suggest that the proteolytic cleavage of polyQ disease proteins contributes to pathogenesis, the resulting fragments being of crucial importance for their aggregation and cytotoxicity. This idea is referred to as the *toxic fragment hypothesis* (Takahashi *et al.*, 2010; Tarlac and Storey, 2003; Wellington *et al.*, 1998). Proteolytic cleavage of atx3 has been reported in several cell and animal models and in MJD patients' brains, though results are considerably diverse.

Atx3 has been shown to produce polyQ-containing C-terminal fragments of about 34-37 kDa (Goti *et al.*, 2004; Jung *et al.*, 2009; Simões *et al.*, 2012; Simões *et al.*, 2014). In transgenic mice, a 36 kDa fragment was enriched in the nuclear fraction of expanded atx3-expressing animals' brain homogenates, but was not detected in other tissues (Goti *et al.*,

2004). A fragment with similar characteristics was also enriched in the nuclear fraction of MJD patients' brains and was even identified as more abundant in the dentante nuclei and the substantia nigra, two brain regions known to be affected in the disease (Goti *et al.*, 2004). Furthermore, studies using transfected cell lines reported that expression of C-terminal fragments of atx3 containing the expanded polyQ sequence leads to strong atx3 aggregation and cell death (Breuer *et al.*, 2010; Goti *et al.*, 2004; Haacke *et al.*, 2006; Ikeda *et al.*, 1996; Paulson *et al.*, 1997b; Yoshizawa *et al.*, 2000). Severe toxicity, characterized by neurodegeneration and motor phenotypes, is observed in animal models expressing C-terminal fragments of atx3 containing expanded polyQ regions (Ikeda *et al.*, 1996; Torashima *et al.*, 2008; Warrick *et al.*, 1998).

Fragments of other molecular sizes and/or composition have been also described, albeit more varyingly. In COS-7 cells, endogenous atx3 was shown to generate a 28 kDa fragment described to contain the C-terminal region of atx3 and including the polyQ tract (Berke *et al.*, 2004), possibly corresponding to a non-expanded form of the 34-37 kDa fragment mentioned above. Another study, using transfected COS-7 cells, mentioned a greater variety of fragments. Non-expanded atx3 was shown to generate four C-terminal fragments (with about 18, 21, 28 and 42 kDa) and two N-terminal fragments (with 37 and 42 kDa), while the expanded protein generated only two C-terminal fragments (a 37 kDa fragment and another with about 50 kDa). The 42 kDa fragments were found only in the cytoplasm, but the other ones were found also in the nucleus (Pozzi *et al.*, 2008). In an *in vitro* proteolysis of purified non-expanded human atx3 using a postnuclear supernatant preparation derived from a mice neural cell line, five main atx3 fragments were identified: one, with about 29 kDa, derived from the endogenous mouse protein, and four others derived from the human protein, with about 16, 20, 24 and 34 kDa respectively (at least some of them containing N-terminal regions) (Haacke *et al.*, 2007). Recent reports described an atx3 fragment of about 26 kDa present in the brain of lentiviral MJD mouse models, that includes the N-terminus of the protein that is also detected in the brains of animals transduced with non-expanded atx3 (Simões *et al.*, 2012; Simões *et al.*, 2014). Another report observed that incubation of lysates with calpains gives rise to an N-terminal fragment of ~30 kDa in both transfected human cell lines and a transgenic model, derived from either expanded and non-expanded overexpressed human atx3, in the cell lines, as well as from the endogenous mouse protein and expanded atx3, in the model (Hübener *et al.*, 2013). Studies performed in neuronal cultures generated from human-derived induced pluripotent stem cells (iPSCs) revealed a 34 kDa atx3 fragment, which was curiously present (and had the same size) in both MJD patients and controls, possibly indicating that it is a N-terminal fragment (Koch *et al.*, 2011). Other fragments, of diverse molecular sizes (25-45 kDa) were also shown to be generated and to aggregate, but only in patient-derived neurons. The great diversity of fragments mentioned here may be overstated, and some of them may admittedly result from common proteolytic processes, though yielding apparently different products in the corresponding studies. These differences may result from the employment of considerably different experimental models, and possibly from different sampling conditions.

Nonetheless, this diversity illustrates the fact that atx3 may be proteolytic cleaved in different ways.

Concerning the enzymes responsible for the proteolytic processing of atx3, in cell lines, atx3 was shown to be cleaved by caspases (predominantly caspase-1) (Berke *et al.*, 2004; Jung *et al.*, 2009) and calcium-dependent calpain proteases (Haacke *et al.*, 2007) and these proteolytic events were reported to increase the aggregation of polyQ-expanded atx3. *In vitro* assays with cell lines and brain homogenates indicate that the calcium-dependent cleavage is more efficient with calpain-2 (Hübener *et al.*, 2013). The particular mapping of cleavage sites of atx3 is yet inconclusive, but some putative regions have been identified so far. For caspases, cleavage apparently occurs near the UIMs (amino acids 223-260), apparently between amino acids 171-228 (Goti *et al.*, 2004; Jung *et al.*, 2009) and/or 241-248 (Berke *et al.*, 2004). For calpains, the cleavage sites suggested are localized around residues 60, 154, 220 and 260 (Haacke *et al.*, 2007; Hübener *et al.*, 2013; Simões *et al.*, 2012). Curiously, an *in vitro* study also reported evidence for an autoproteolytic cleavage of atx3, catalyzed by the C14 of atx3 active site. This cleavage targeted the C-terminal region of the protein, while the JD domain was preserved (Mauri *et al.*, 2006).

Some studies demonstrate that cleavage by caspases and calpains is important for the pathogenic mechanisms, *in vivo*. In a *Drosophila* model, mutating six putative caspase cleavage sites reduced formation of the ~37 kDa C-terminal fragment of atx3, at the same time reducing protein aggregation and neural toxicity; NI formation was, however, unaffected (Jung *et al.*, 2009). In lentiviral mouse models, calpain inhibition was shown to reduce fragmentation of expanded atx3, as well as aggregation and neurodegeneration caused by expanded atx3 expression in the striatum, and to ameliorate motor symptoms in animals expressing the protein in the cerebellum (Simões *et al.*, 2012; Simões *et al.*, 2014). Knocking down calpastatin (an endogenous calpain inhibitor) in a transgenic MJD mouse model had opposite effects (Hübener *et al.*, 2013). In the neuronal cultures derived from patients' iPSCs, atx3 fragmentation was stimulated by glutamate (the main excitatory neurotransmitter) and led to aggregation, in a process that was reported to depend on calpains (Koch *et al.*, 2011).

Taken together, these results suggest that proteolytic cleavage of atx3 may indeed play a part in MJD pathogenesis, being important for atx3 aggregation and toxicity. It is conceivable that atx3 proteolysis is required (or at least is important) for the changes in atx3 properties that make the protein toxic: separation from the JD may either increase the ability of the polyQ-containing C-terminal region to form toxic oligomers or otherwise disturb atx3 normal functions or interactions, thus perturbing normal cellular mechanisms (Chow *et al.*, 2004c; Haacke *et al.*, 2006; Jung *et al.*, 2009; Yoshizawa *et al.*, 2000, see section below). Interistingly, in a gene trap mouse model expressing a fusion protein including a N-terminal portion of atx3 (including the JD and the first UIM), animals presented extranuclear neuronal inclusion bodies, neurodegeneration and age-dependent motor symptoms, suggesting that putative fragments containing the N-terminal region of atx3, possibly derived from proteolytic cleavage, may also induce toxicity (Hübener *et al.*, 2011). The region used partially mimics a putative calpain-derived fragment resulting from cleavage at position 260.

Contrastingly though, Pozzi and collaborators observed that expanded atx3 is cleaved to a lesser extent when compared with the normal protein, in COS-7 cells (Pozzi *et al.*, 2008). The authors suggested that the expanded polyQ stretch can mask some cleavage sites and that pathogenesis can result from accumulation of uncleaved expanded atx3.

Polyglutamine expansion-induced changes in ataxin-3 features

Apart from inducing the formation of aggregates, the polyQ expansion of atx3 may interfere with the protein at the singular level, producing changes in its function, interactions or localization that lead to cellular toxicity and thereby play a part in the development of MJD.

A. Effects on deubiquitinase activity and ubiquitin interaction

It has initially been hypothesized that atx3 expansion leads to a loss of protein function and that this would be sufficiently significant to cause the MJD. However, the mouse and *C. elegans* atx3 KOs present no detectable overt phenotype, indicating that atx3 function is not crucial or at least that it can been overcome by other proteins, in these systems (Rodrigues *et al.*, 2007; Schmitt *et al.*, 2007). Another hypothesis, with better experimental support, is that the expanded polyQ affects the protein's function in a way that alters its cellular activity, actively promoting cell toxicity.

Atx3 has been linked to protein homeostasis pathways and, in line with what has been said above, disturbance of these mechanisms is a possible cause of toxicity as it might interfere with the normal turnover and degradation of important molecules. Generally, studies have demonstrated that there are not many significant differences in the deubiquitinating activity between normal and expanded atx3 and that there is no change in polyUb chain linkage preferences depending on polyQ length (Berke *et al.*, 2004; Burnett *et al.*, 2003; Winborn *et al.*, 2008). One study (Winborn *et al.*, 2008), however, described that the ability of expanded atx3 to reduce general cellular protein ubiquitination was decreased, when compared to that of the non-expanded form. This decrease can have consequences in the cellular pathways that use Ub signals influenced by atx3 DUB activity. In yeast, expression of expanded atx3 (but not the non-expanded protein) stabilized an ubiquitinated model substrate degraded by the UPP (Doss-Pepe *et al.*, 2003). Expanded atx3 retains its ability to bind polyubiquitinated substrates in a UIM-dependent manner, with no global differences comparing to the normal protein (Berke *et al.*, 2004) but, nonetheless, the possibility that the two forms may differentially bind and/or proteolyse particular substrates is not ruled out.

Atx3 participation in protein homeostasis systems adds an interesting aspect to MJD: atx3 could interact with misfolded and aggregated proteins as part of its normal function, but possible stable interactions between them and the expanded protein may potentiate protein aggregation and constitute a cause for disturbance of those systems (Burnett *et al.*, 2003;

Burnett and Pittman, 2005). Interestingly, the presence of Ub and proteasome constituents in atx3 inclusions can partially be explained by their physiologically relevant interactions with atx3 (Doss-Pepe *et al.*, 2003).

B. Effects on ataxin-3 interactions

Another aspect where an expanded polyQ tract may alter atx3 properties, possibly influencing its physiological role, is in the interactions atx3 establishes. HHR23A and HHR23B binding is not affected by the polyQ expansion, but HHR23A colocalizes with expanded atx3-containing aggregates in cell lines (Wang *et al.*, 2000). PolyQ expansion of atx3 increases the extent of the interaction with VCP/p97, which also colocalizes with the NIs in MJD patients (Boeddrich *et al.*, 2006). These changes are likely to cause an altered distribution pattern for these proteins and influence their activity and other molecular interactions (Boeddrich *et al.*, 2006; Higashiyama *et al.*, 2002; Hirabayashi *et al.*, 2001; Wang *et al.*, 2000). Interestingly, the enhancement of atx3 DUB activity elicited by VCP/p97 is abrogated when atx3 is expanded (Laço *et al.*, 2012a). Impairment of the ERAD caused by expansion of atx3 may induce endoplasmic reticulum proteotoxic stress that may contribute to the degenerative mechanisms (Wang *et al.*, 2006; Zhong and Pittman, 2006). Curiously, mice expressing an atx3 fusion protein containing just its N-terminal region (including the JD, but lacking the region that interacts with VCP/p97) display an increased susceptibility to endoplasmic reticulum stress (Hübener *et al.*, 2011).

In spite of the many studies unable to detect polyQ-induced changes in atx3 enzymatic activity, expanded atx3 was recently shown to deubiquitinate parkin to a greater extent than non-expanded atx3 and to induce its degradation by autophagy through an unknown mechanism (Durcan *et al.*, 2011). Interestingly, the increase in deubiquitination was specially directed against chains of K27- and K29-linkage, which may be important in the mechanisms leading to degradation. Parkin levels were also reduced in an expanded atx3-expressing mouse model. Considering that parkin has been described as having neuroprotective effects and the fact that its mutation causes a familial form of Parkinson's disease, the expanded atx3-induced decrease of parkin levels may be related to symptoms of Parkinsonism observed in some MJD patients. PolyQ expansion of atx3 does not change atx3 enzymatic activity towards CHIP, but alters their interaction, increasing the affinity of their binding but turning the potentiating effect of ubiquitination of CHIP redundant (Scaglione *et al.*, 2011). Furthermore, the levels of CHIP were also reduced in the brain of the above transgenic model, comparing to wild-type animals and to atx3 KOs. This could be the result of the altered dynamics in the atx3-CHIP interaction, caused by the polyQ-induced increase in affinity (Scaglione *et al.*, 2011). These observations indicate that disturbances caused by polyQ expansion of atx3 may have a negative impact on the cellular homeostasis mechanisms mediated by parkin and CHIP, which have been otherwise shown to be protectors against polyQ-induced toxicity (Durcan and Fon, 2013; Miller *et al.*, 2005; Tsai *et al.*, 2003).

C. Effects on transcription regulation

PolyQ expansion might also affect the proposed function of atx3 as a transcription regulator. Expansion may alter atx3 binding properties and compromise its ability to establish transcription repressor complexes, leading to the increased expression of certain genes, some of which may contribute to MJD development.

When compared to non-expanded atx3, expanded atx3 appears to bind chromatin in different regions and to aberrantly increase transcription in cells (Evert *et al.*, 2006a; Evert *et al.*, 2003). Histone acetylation is increased in cells expressing expanded atx3 and in human MJD brain, although both normal and expanded forms associate with HDAC3 and NCoR (Evert *et al.*, 2006a). Interestingly, however, though this interaction is normally mediated by the UIMs of atx3, the aberrant transcriptional activation is instead mediated by cysteine 14 of atx3 catalytic site. Expanded atx3 is also reported to bind transcriptional co-activators (CBP, p300 and PCAF) to a greater extent than the non-expanded form, though its inhibitory effect on transcription was similar (Li *et al.*, 2002).

Importantly, MJD patients' brains have been reported to show transcriptional dysregulation of several genes (Evert *et al.*, 2006a; Evert *et al.*, 2001; Wen *et al.*, 2003). A direct example of the negative effect on transcription regulation comes from studies relating apoptosis with the cell loss observed in MJD, as expanded atx3 was reported to upregulate the Bax protein (a pro-apoptotic protein), while downregulating Bcl-xL levels (an anti-apoptotic protein), in cultured neurons (Chou *et al.*, 2006).

Expression of several genes involved in cell signaling and synaptic transmission was also shown to be altered in the brain of MJD model mice expressing expanded atx3, suggesting that synaptic dysfunction resulting from transcription dysregulation may play a part in toxicity mechanisms of MJD (Chou *et al.*, 2008). Importantly, in accordance with the mechanisms proposed for atx3-mediated genetic repression – but contrasting to studies of human MJD brain (Evert *et al.*, 2006a) –, these transcriptional alterations have been related to decreased histone acetylation, and the pharmacological reversal of this state by administration of the deacetylase inhibitor sodium butyrate was reported to counter transcriptional dysregulation and simultaneously ameliorate the disease phenotype of this MJD model mice (Chou *et al.*, 2011).

In the case of the FOXO4-mediated coactivation of SOD2, though atx3 interacts with FOXO4 independently from the polyQ tract length, the expanded form shows an impaired effect on transcription and, concordantly, SOD2 has a decreased expression in MJD patients' pons (Araujo *et al.*, 2011). SOD2 expression is normally activated by FOXO transcription factors in response to oxidative stress, and, accordingly, in patient-derived lymphoblastoid cell lines, there is an increased susceptibility to reactive oxygen species formation and decreased viability upon oxidative stress stimuli. Binding of atx3 to the SOD2 gene promoter region is increased in patient-derived cells, and both FOXO4 and atx3 binding becames unresponsive to the oxidative stress stimuli, indicating that these oxidative stress responses involve binding of

both FOXO4 and atx3 to SOD2 gene promoter, and suggesting that expanded atx3 prevents the FOXO4 upregulation of SOD2 upon oxidative stress (Araujo *et al.*, 2011).

D. Aberrant interactions as the source of toxicity

Though the deleterious effects on transcription and quality control systems may logically derive from modifications of atx3 endogenous functions, through its effect in modulating Ub signals, it is tempting to hypothesize that all the cellular changes originate actually from aggregation and aberrant interactions that destabilize not only atx3 function but other cellular systems as well. In fact, all the toxicity mechanisms caused by polyQ expansion, including aggregation itself, are increasingly envisioned as ultimately stemming from the tendency of the pathogenic proteins to interact aberrantly (Schaefer *et al.*, 2012; Williams and Paulson, 2008). Some interactions with physiologic partners may be enhanced and others diminished, and the advent of abnormal associations may recruit different proteins and disturb a wide range of cellular systems (Gatchel and Zoghbi, 2005; Williams and Paulson, 2008). Aggregation would arise from aberrant interactions between specimens of a particular polyQ-expanded protein.

Misfolding of the expanded polyQ-containing proteins may alter interactions that are mediated by different protein regions, including the polyQ tract and, in fact, the propensity of the polyQ tracts and adjacent regions to engage in intermolecular interactions via formation of coiled-coils is significantly increased upon polyQ expansion (Fiumara *et al.*, 2010). These regions may also be implicated in protein aggregation, likely representing a transition state between normal protein conformation and aberrant β-sheath aggregation. Aberrant interactions with other coiled-coil forming proteins (e.g., CHIP) might recruit them and destabilize cellular homeostasis (Fiumara *et al.*, 2010).

Ataxin-3 as a protector against polyglutamine toxicity

It has been determined that, apart from expanded atx3, protein aggregates seen in MJD also contain normal, non-expanded protein (Fujigasaki *et al.*, 2000). This is possible because MJD is an autosomal dominant disease, and so both normal and expanded forms can be present in the same cell, in the case of heterozygous individuals. The co-aggregation of non-expanded atx3 may reflect the importance of regions outside the polyQ tract in the aggregation mechanism or result from conformational changes that the misfolded expanded atx3 induces in the non-expanded protein, leading to its recruitment to the assembling aggregates (Chow *et al.*, 2004a).

Another possibility, however, is that atx3 is recruited to aggregates because of UIM-mediated recruitment to the highly ubiquitinated inclusions and/or because of its involvement in the UPP and other protein homeostasis systems (Burnett *et al.*, 2003; Burnett and Pittman,

2005; Donaldson *et al.*, 2003; Fujigasaki *et al.*, 2001; Warrick *et al.*, 2005) . Consistent with this, a striking feature of atx3 is that it normally colocalizes with aggregates (or inclusion bodies) formed in other polyQ expansion diseases (Uchihara *et al.*, 2001) and other neurodegenerative states (Burnett *et al.*, 2003; Fujigasaki *et al.*, 2000; Pountney *et al.*, 2003; Seilhean *et al.*, 2004; Takahashi *et al.*, 2001). Warrick and collaborators (2005) made important observations that strongly suggested this protective role of atx3 against polyQ toxicity. They reported that flies expressing both non-expanded and expanded atx3 (or non-expanded atx3 and other expanded polyQ-disease proteins) did not present the phenotypes that result from expression of the expanded polyQ protein. This suggested that atx3 was able to mitigate toxicity in several *Drosophila* polyQ diseases models, including a MJD model. The protective activity is apparently linked to atx3 involvement in quality control mechanisms such as the UPP, as it requires normal proteasome functionality and atx3 Ub-associated activities, including Ub protease activity and UIM functionality. These considerations may further explain why MJD patients with two pathogenic alleles have a more severe phenotype than heterozygous patients (Carvalho *et al.*, 2008; Lang *et al.*, 1994; Lerer *et al.*, 1996; Sobue *et al.*, 1996). The worsened phenotype of homozygous patients may result not only from the presence of two pathogenic alleles but also from a loss of the protective function of non-pathogenic atx3 (Warrick *et al.*, 2005)

Nonetheless, the idea of atx3 functioning as a protector against polyQ toxicity was recently challenged by several research groups. In contrast to the observations in flies, a double transgenic mouse coexpressing both expanded and non-expanded atx3 had a similar disease phenotype (including neurological symptoms and brain NIs) to that of mice expressing only the extended form of the protein (Hübener and Riess, 2010). Similarly, overexpression of non-expanded atx3 in a lentiviral rat model of MJD expressing expanded atx3 does not prevent development of the MJD-related phenotype caused by the pathogenic form of the protein (Alves *et al.*, 2010). However, the possibility that the contrasting results obtained in flies and rodents may reflect the use of different animal models cannot be excluded. Until further studies come to light, it is not possible to conclude if, in humans, the milder phenotype of heterozygous individuals is due to the protective effect of atx3 or simply to gene dosage.

The role of the nuclear environment

The nucleus is an important player in the pathogenesis of MJD and other polyQ diseases, seeing as nuclear localization of polyQ proteins is repeatedly reported as important for the development of polyQ disease-related phenomena (Schöls *et al.*, 2004; Shao and Diamond, 2007). As mentioned before, though, in neurons atx3 distributes mainly in the cytoplasm, whereas the most conspicuous atx3 aggregates, the macromolecular inclusions, are mainly observed in the nucleus (Paulson *et al.*, 1997b; Schmidt *et al.*, 1998). Whether they are toxic themselves or are formed as a response to the toxicity of other expanded atx3-derived

species, their presence may be indicative of the negative effects of atx3 in this cellular compartment.

Considering that atx3 is detected in both the cytoplasm and the nucleus, that it is actively shuttled between the two compartments and that its biological function has been related to transcription regulation, the normal cellular role of atx3 appears to involve the nucleus (Antony *et al.*, 2009; Evert *et al.*, 2006b; Evert *et al.*, 2001; Macedo-Ribeiro *et al.*, 2009; Wen *et al.*, 2003). Consequently, expanded polyQ-derived modifications of this nuclear role may be deleterious to the cell. In transgenic mice, it was demonstrated that artificially targeting expanded atx3 to the nucleus indeed aggravates the disease phenotype, while forcing nuclear export reduces it (Bichelmeier *et al.*, 2007). Furthermore, inhibition of calpains, which was observed to reduced toxicity in MJD lentiviral mouse models, was also reported to prevent nuclear translocation of atx3 in MJD transgenic mice (Simões *et al.*, 2012). These observations strongly imply that nuclear localization of atx3 is critically important for the manifestation of MJD symptoms, *in vivo*.

Clearly, the simple nuclear localization of atx3 is not sufficient to cause MJD, as the endogenous protein itself is detected in the nucleus (Trottier *et al.*, 1998), but several studies reported that non-expanded atx3 fragments (Perez *et al.*, 1998) and full-length atx3 (Macedo-Ribeiro *et al.*, 2009) targeted to the nucleus lead to aggregate formation, suggesting that the nuclear environment may be important in this event. Moreover, non-expanded atx3 was found to adopt a unique conformation once in the nucleus, and to bind to the nuclear matrix (Perez *et al.*, 1999). It was also proposed that the formation of large atx3 aggregates in the nucleus may be due to a less efficient degradation of the protein in this compartment, when compared to the cytoplasm (Breuer *et al.*, 2010; Goellner and Rechsteiner, 2003).

Stress-induced nuclear transport of expanded atx3 as a part of its normal physiologic function would be expected to have deleterious effects on the cell, protecting it from degradation and accelerating toxicity (Bichelmeier *et al.*, 2007; Breuer *et al.*, 2010; Reina *et al.*, 2010). Aging and a possible dysfunction of atx3 caused by the unstable expansion may culminate in an inability for atx3 to protect against proteotoxic stress, leading to cell toxicity (Reina *et al.*, 2010). Remarkably, the presence of misfolded and/or aggregated expanded atx3, which may constitute a proteotoxic stimulus by itself, will likely increase nuclear localization of the protein and thus be responsible for triggering and/or enhancing those effects (Mueller *et al.*, 2009).

1.6 Ataxin-3 toxicity mechanisms, cellular context and neuronal damage

Mechanisms of cellular toxicity

The considerations presented above demonstrate how toxicity derived from polyQ expansion of atx3 has been related with diverse biochemical and cellular mechanisms. In short, and in parallel with the plethora of putative toxic changes involved in polyQ disease

pathogenesis that were presented before, atx3 expansion has been variously shown to: alter atx3 DUB activity against parkin and other unidentified ubiquitinated species; cause aberrant interactions, increasing the association with VCP/p97 and CHIP; lead to the formation of toxic aggregates and toxic fragments; and elicit transcriptional alterations. Induction of proteotoxic stress is admittedly caused by misfolding and aggregation of expanded atx3, but can also result from alterations of atx3 interaction with CHIP or changes in the UPP, the ERAD or aggresome formation (Figure 8).

Other mechanisms of cellular toxicity, apparently less related to atx3 proposed roles, have also been suggested and supported by growing experimental evidence. Components of the autophagic pathway have been shown to accumulate in MJD patients' brains, suggesting also a compromise of autophagy (Nascimento-Ferreira *et al.*, 2011). Mitochondrial activity is compromised in several cell-based MJD model systems (Laço *et al.*, 2012b) and expression of expanded atx3 was shown to cause a decrease in the activity of antioxidant enzymes, which may be a cause of oxidative stress (Yu *et al.*, 2009). Furthermore, there is evidence for DNA damage (a possible consequence of oxidative stress) in cellular and animal MJD models and in patients' brains (Kazachkova *et al.*, 2013; Yu *et al.*, 2009). Together, these observations propose a role for mitochondrial dysfunction and oxidative stress in MJD, whose effects may include impaired bioenergetics and oxidative damage (Evers *et al.*, 2014). Considering the effects of expanded atx3 in the FOXO4-mediated transcription of the antioxidant enzyme SOD2, oxidative damage may also arise from impaired stress responses at a transcriptional level (Araujo *et al.*, 2011). Finally, considering that Ub signals are implicated in a great variety of cellular systems, changes in undisclosed aspects of atx3 role caused by polyQ expansion possibly influence other processes, with negative consequences for cell function and survival.

Neuronal toxicity and dysfunction

In spite of the diversity of cellular pathways demonstrated or suggested to be altered due to atx3 polyQ expansion, it is challenging to try to define a particular cascade of mechanisms and point out a limited group of upstream players. As exposed before, many authors believe that aberrant interactions resulting from misfolding are the ulterior source of toxicity, but the intricacies of MJD pathogenesis (and of the other polyQ diseases) remain largely undisclosed. What is more, the majority of the proposed mechanisms represent general toxicity pathways that would affect any cell, independently of type, and are thus unable to explain why neurons are specifically targeted in MJD. It is conceivable that neurons might be particularly sensitive to misfolded proteins and the consequences of aberrant interactions and aggregation, being highly specialized postmitotic cells (Williams and Paulson, 2008). In fact, some studies demonstrate fragmentation and aggregation limited to neuronal systems (Goti *et al.*, 2004; Koch *et al.*, 2011). It could also be the case that neurons are more sensitive to the particular proteotoxic stresses, transcriptional aberrations or other cellular dysfunctions caused by pathogenic atx3.

Reports exploring cellular mechanisms that would be specifically deleterious for neurons are relatively scarce. Additionally, being a neurodegenerative disorder, MJD as well as the other polyQ diseases are often studied in a context where cell loss is envisioned as both the result of protein toxicity and the cause of the observed clinical symptoms, but recent studies suggest that MJD symptoms may arise before significant cell death occurs (Bichelmeier *et al.*, 2007; Boy *et al.*, 2009; Chou *et al.*, 2008; Goti *et al.*, 2004; Shakkottai *et al.*, 2011; Silva-Fernandes *et al.*, 2010). The pathogenic mechanisms may include not only pathways that lead to neuronal death, but also to neuronal dysfunction. Supporting this idea, neuronal dysfunction has been increasingly linked to many neurodegenerative disorders, including Alzheimer's disease (Terry *et al.*, 1991) and polyQ diseases such as HD (Fan and Raymond, 2007). Defects in physiology occurring before actual neuronal loss are admittedly contributing to clinical presentations and might constitute the actual basis of neuronal damage. The hypothesis that symptoms develop even before severe neuronal death occurs encourages the search for therapies that may act before irreversible damage, ideally avoiding it (Boy *et al.*, 2009; Shakkottai *et al.*, 2011).

According to the alterations observed in a MJD mouse model expressing atx3 in the CNS, cell signaling and synaptic transmission deficiencies may arise from transcriptional alterations (Chou *et al.*, 2008). Even before prominent cell loss occurs, mice displayed altered decreased expression of genes involved in calcium signaling and mitogen-activated protein (MAP) kinases pathways, as well as glutamatergic (including glutamate receptor channel subunit β2 – GluR6 – and vesicular glutamate transporter subtype 2 – VGLUT2) and γ-aminobutyric acid (GABA) neurotransmission. Another study employing a yeast artificial chromosome (YAC) MJD mouse model, generated using the whole human expanded ATXN3 gene and expressing atx3 throughout the body (Cemal *et al.*, 2002), suggested that a direct disturbance of calcium signaling, an important player in neurotransmission, may play a role in MJD (Chen *et al.*, 2008). PolyQ-expanded atx3 (but not the non-expanded form) was found to associate with the type 1 inositol 1,4,5-trisphosphate receptor ($InsP_3R1$) in cortical lysates, and to potentiate $InsP_3$-mediated calcium release in both transfected cells and patients fibroblasts. Treatment of the transgenic mice with dantrolene, a stabilizer of calcium signaling, was shown to ameliorate many symptoms of the YAC MJD mouse model and to decrease neuronal loss (Chen *et al.*, 2008).

Impaired axonal transport is one other mechanism that would specifically target neurons. Neuronal inclusion bodies have been seldom described outside the nucleus, but were recently observed in axons of human MJD patients' brains, in fiber tracts connecting regions known to degenerate in MJD (Seidel *et al.*, 2010). As with NIs, these axonal inclusions colocalize with proteins involved in regulation of protein turnover, such as Ub. The correlation between the areas displaying axonal inclusions and the ones that degenerate supports the idea that axonal aggregates play a role in pathogenesis, possibly interfering with axonal transport and consequently with delivery of proteins to the synapses, with negative outcomes for cell function and survival (Gunawardena *et al.*, 2003; Seidel *et al.*, 2010).

In neural cell models expressing human atx3, the expanded protein caused disturbances of electrophysiological properties – reduction of resting membrane potential and hyperpolarizing shift of the activation curve of delayed rectifier potassium currents – even before the onset of drastic cell demise (Jeub *et al.*, 2006). A recently published report using model mice expressing a C-terminal fragment of polyQ-expanded atx3 showed a severe compromised dendritic morphology and capacitance in Purkinje cells. This was accompanied by an altered subcellular distribution of metabotropic glutamate receptor subtype 1 (mGluR1), which formed unusual dendritic clusters, and an impairment of mGluR signaling (Konno *et al.*, 2014). The model used presents several limitations: expression is directed uniquely at Purkinje cells, whose involvement in the disease is disputed; only a fragment of atx3 is being expressed; and comparison was made with wild-type animals. Nonetheless, it illustrates the putative contribution of neuronal functionality and synaptic transmission in MJD disease mechanisms. Interestingly though, in the YAC MJD mouse model expressing atx3 throughout the body, Purkinje cells exhibited abnormal spontaneous firing, even before neurodegeneration was observed but concomitantly with mild gait symptoms (Shakkottai *et al.*, 2011). The electrophysiological changes involved depolarization block, reflecting a reduction in repolarizing potassium currents associated with a decrease in voltage-activated potassium channels currents. Interestingly, expanded atx3 was found to affect the kinetics of voltage-activated potassium channels in cell lines, in a polyQ length-dependent manner.

The pivotal study using cultured neurons generated from human-derived iPSCs demonstrated that the increased fragmentation and aggregation observed in patient-derived neurons required stimulation with glutamate and was neuron-specific, since it was not observed in MJD patients-derived glia, fibroblasts or iPSCs (Koch *et al.*, 2011). Furthermore, it was also dependent on availability of extracellular calcium, and the functionality of sodium channels and ionotropic glutamate receptors (α-amino-3-hydroxy-5-methyl-4-isoxazolepropionic acid receptors – AMPAR – and N-methyl-D-aspartate receptors – NMDAR). This led the authors to propose a mechanism whereby depolarization-induced calcium influx and activation of calpains (described to be necessary for the process) leads to cleavage and aggregation of pathogenic atx3, specifically in neurons (Koch *et al.*, 2011).

Deubiquitinases and ubiquitination in the nervous system

Observing that atx3 is widely expressed in different tissues, the specific targeting of neurons by the pathological effects of the expanded protein can also be regarded as resulting from the fact that atx3 is particularly important in this type of cells. Expansion of atx3 and consequent disturbance of its functions and those of the systems with which atx3 interacts in neurons could then help explain why they are selectivity affected in MJD. Glutamine repeat regions are the most prevalent amino acid repetition in humans, and although they have not been shown to be specially represented in neurologically specialized proteins (Hands *et al.*, 2008; Huntley and Golding, 2004), they have been found to be significantly represented in

neurodevelopmental genes (Almeida *et al.*, 2013). In atx3 KO mice, the observed increase on ubiquitinated proteins is detected in both brain and testis lysates, but curiously the change is more pronounced in the latter samples (Schmitt *et al.*, 2007). Though this can lead to the hastened conclusion that atx3 DUB activity is more important in the testis than in the brain, it illustrates how atx3-mediated regulation of ubiquitination can vary between the brain and other tissues. Except for this observation and the neuron-specific toxic mechanisms presented above, the importance of atx3 function in neurons has not been fully explored.

Nonetheless, other clues to the particular relevance of atx3 in neuronal tissues may be suggested by the particular role of other DUBs and Ub signals in the nervous system, namely through mechanisms of protein sorting and degradation. Ub-mediated pathways have been diversely implicated in events that are crucial for neuronal structure and function, such as neuronal growth and development, synaptic function and plasticity, and neuronal survival (Hamilton and Zito, 2013; Yi and Ehlers, 2007).

A. Deubiquitinases and neuronal structure

Mutation or knockdown of several components of Ub ligase complexes have been described to produce changes in the rate and orientation of axonal growth, along with some morphological aberrations, in neuronal cell cultures and model organisms. The UPP is probably important in regulating the surface expression of important players determining axonal growth patterns (like transmembrane receptors) and in controlling the localized dynamics of the cytoskeleton, necessary for the polarized extension of neurites (Yi and Ehlers, 2007). In vertebrates, components of the UPP such as Ub, E1 enzymes and the proteasomal machinery have been implicated in the formation of new growth cones after lesions as well as in the responsivity of growth cones to external guidance cues, both of which are admitted to rely on rapid protein synthesis and degradation (Campbell and Holt, 2001; Verma *et al.*, 2005). The UPP is also important in neuronal pruning, i. e., the phenomenon whereby excessively branched axonal projections generated during development are refined and matured by elimination of some of the branches and synapses (Yi and Ehlers, 2007). Interestingly, overexpression of the yeast DUB Ub C-terminal hydrolase 2 (UBP2) causes loss of pruning in *Drosophila*, in a process reported to result from impairment of protein degradation by the proteasome (Watts *et al.*, 2003). In vertebrates, Ub C-terminal hydrolase 33 (USP33) interacts with Roundabout 1, a receptor implicated in axonal pathfinding, and silencing of that DUB destabilizes regular axonal growth patterns (Yuasa-Kawada *et al.*, 2009).

The correct balance between ubiquitination and deubiquitination is important for the formation of synapses with correct structure and functionality, seeing as the compromise of cellular components involved in ubiquitination may lead to morphologically aberrant and dysfunctional synapses (Yi and Ehlers, 2007). Additionally, the UPP is also implicated in synapse maintenance, as proteasomal degradation of important synaptic components is known to lead no synaptic loss (Pak and Sheng, 2003).

B. Deubiquitinases and synaptic transmission

Ubiquitination is involved in mediating synapse function itself, possibly through the regulation of the turnover of synaptic proteins and control of vesicle traffic. The UPP has been variously demonstrated to play a role in the turnover of several neurotransmitter receptors, such as glutamate and GABA receptors (GABARs), and degradation of receptors during the ERAD is predicted to influence the posterior trafficking of synaptic receptors (Yi and Ehlers, 2007). Proteins involved in ubiquitination, such as adaptor proteins and Ub ligases have been reported to be implicated also in the presentation and endocytosis of neurotransmitter receptors; for example, proteosomal functionality and ubiquitination of scaffolding proteins of the synapses have been implicated in activity-dependent endocytosis of AMPAR (Colledge *et al.*, 2003; Patrick *et al.*, 2003).

Proteasomal degradation is also known to regulate the turnover of presynaptic proteins, with likely effects on synaptic vesicle priming, release and recycling, but faster mechanism linking ubiquitination signals to the function of presynaptic terminals may be at play as well (Yi and Ehlers, 2007). Interestingly, depolarization of synaptosomes (biochemically isolated synaptic terminals) in the presence of calcium leads to a rapid decrease of ubiquitinated species, apparently resulting from protein deubiquitination rather than degradation (Chen *et al.*, 2003a). In epithelial cells, pharmacologically-provoked entry of calcium also reduces the amount of Ub conjugates, and one of the proteins whose ubiquitinated state decreases is epsin-1, a protein involved in vesicle formation. Silencing the DUB FAM/Ub-specific peptidase 9 (USP9X) in epithelial cells causes epsin-1 to remain monoubiquitinated, which was suggested to affect epsin-1 interactions and, consequently, the dynamics and sorting of presynaptic vesicles (Chen *et al.*, 2003a). These results point out a possible mechanism of fast synaptic regulation by ubiquitination. Curiously, in *Drosophila*, overexpression of FAM/USP9X ortholog Faf leads to defects in synapse morphology at neuromuscular junctions, though this effect was regarded as resulting from changes in development (DiAntonio *et al.*, 2001).

The observation of neurological symptoms in animals that are deficient in certain DUBs finely illustrates the importance of these enzymes in neuronal mechanisms. Mutant mice with decreased levels of USP14 (Ub C-terminal hydrolase 14), a proteasome-associated DUB implicated in yielding exclusively monoUB from substrates (Komander *et al.*, 2009), display an ataxic phenotype and several defects in synaptic transmission, accompanied by a reduction in free monoUb, but show no neuronal loss (Crimmins *et al.*, 2006; Wilson *et al.*, 2002). The observations made in this model support the idea that DUBs and Ub availability play relevant roles in regulating synaptic activity. Loss of USP14 leads to neurodevelopment defects in the neuronal part of neuromuscular junctions, including nerve terminal sprouting and impaired arborization, accompanied by altered morphology of postsynaptic acetylcholine receptor clusters (Chen *et al.*, 2009). The observed decrease of monoUb in synaptosomal fractions

suggested that the developmental aberrations result from diminished protein turnover at the synapse (Chen *et al.*, 2009). Interestingly, the Purkinje cells of mice deficient in USP14 have an altered GABAergic transmission, with increased levels of GABAergic receptors at the cell surface and increased GABA-mediated currents. USP14 was shown to interact with a GABAR subunit, leading to the hypothesis that the observed changes result from decrease in receptor turnover caused by USP14 subexpression (Lappe-Siefke *et al.*, 2009; Todi and Paulson, 2011). In fact, increased ubiquitination of GABARs resulting from blockade of neuronal activity has been reported to lead to a decrease in surface expression dependent on the proteasome, rooted in a decreased stability at the level of the endoplasmic reticulum (Saliba *et al.*, 2007).

Ub C-terminal hydrolase isozyme L1 (UCHL1), a DUB that is known to stabilize monoUb (Osaka *et al.*, 2003), is one of the most abundant proteins in the brain (Leroy *et al.*, 1998) and it has been suggested that its role in maintaining the levels of free Ub is important for the maintenance of structure and function of the nervous system, particularly at the level of the synapse (Todi and Paulson, 2011). UCHL1 has been associated with familial forms of PD (Chen *et al.*, 2010; Leroy *et al.*, 1998) and mice lacking UCHL1 functionality show reduced levels of monoUb in the brain and develop motor ataxia (Osaka *et al.*, 2003; Saigoh *et al.*, 1999). In hippocampal cultures, NMDAR activation upregulates UCHL1 and increases the levels of free Ub, while pharmacological inhibition of this DUB decreases the levels of monoUb and decreases dendritic spine density but increases both spine size and the size of protein clusters in both the postsynaptic and presynaptic regions. UCHL1 inhibition was further shown to decrease protein degradation by the UPP, admittedly through the decrease of monoUb levels (Cartier *et al.*, 2009). KO mice for UCHL1 develop spasticity and paralysis and display impairment in synaptic transmission at the neuromuscular junctions, accompanied by loss of synaptic vesicles and other structural defects (Chen *et al.*, 2010). The authors of this report suggested that synaptic defects may result from the decreased levels of free Ub, that would hinder the role of this signalling molecule in membrane protein endocytosis (Chen *et al.*, 2010). Interestingly, in the sea slug *Aplysia*, the UCHL1 ortholog AP-Uch has been shown to be upregulated during long-term synaptic facilitation (LTF), a synaptic plasticity mechanism related to memory formation and cognition, and to be required for this phenomenon (Hegde *et al.*, 1997). It has been suggested that AP-Uch potentiates proteasomal degradation of proteins that would otherwise inhibit the establishment of LTF (Hegde *et al.*, 1997), or that this effect is due to its action in recycling Ub during degradation of proteins involved in LTF (Todi and Paulson, 2011).

C. Possible links between ataxin-3 biologic role and neuronal function

Many reports have identified several other DUBs at the synapse, some of which were demonstrated to be associated with the synaptic proteasome (Kowalski and Juo, 2012). Other studies employing DUB mutants or protein silencing have variously associated DUBs with neurodevelopmental changes, neurological symptoms and neuronal survival (Todi and Paulson,

2011). Taking all the observations into consideration, it becomes clear that ubiquitination, and the opposing activity of DUBs, are required for several events that are necessary for the establishment of normal neuronal structure and function, including at the level of the synapse. The particular effects of each DUB are admittedly distinct, but their role in protein degradation, endocytosis and in yielding free Ub shall be crucial for many neuronal processes.

In the case of atx3, until now no particular neuron-specific function has been described, though it is unlikely that its role is linked to recycling of monoUb, considering that atx3 DUB activity is preferentially associated with polyUb chain editing. Atx3 functions may putatively be related to protein stabilization or regulation of protein turnover; if the yet-unknown atx3 substrates are important in neuronal activities, this could help explain the deleterious effect of atx3, when its polyQ stretch is expanded and its interactions possibly altered. Even if this is not the case, the preference of atx3 for atypical polyUb chains may make it an exchanger of different Ub signals, and possibly relate this protein with cellular systems mediating endocytosis or signaling pathways (Mukhopadhyay and Riezman, 2007), admittedly important in neurons. Both monoubiquitination and K63-linked polyubiquitination have been recognized as important signals mediating internalization and further sorting of plasma membrane proteins (Tanno and Komada, 2013). Additionally, considering that cytoskeletal specializations largely underlie the morphological particularities of neurons (including the organization of both pre- and postsynaptic terminals, for example), atx3 putative role in cytoskeletal organization may negatively affect neuronal structure (and consequently function) if that role is altered upon polyQ expansion (Rodrigues *et al.*, 2010). The importance of neuronal dysfunction in the context of the symptoms and progression of neurodegenerative diseases is increasingly recognized (Palop *et al.*, 2006); considering the versatility of Ub signals and their logical relevance for neuronal structure and functionality, changes derived from the unbalanced actions of expanded atx3 may underlie important mechanisms leading to dysfunction in MJD.

1.7 Post-translational modifications as regulators of protein activity and toxicity

Cell context and post-translational modifications

The unraveling of the neuron-specific mechanisms of expanded atx3 toxicity is crucial for the understanding of the pathogenesis of MJD. However, if the same set of mechanisms applied equally to all neurons, it would be expected that cell demise would affect neurons indiscriminately. Neurodegeneration in MJD and the other polyQ diseases occurs in specific patterns, i. e., there are others levels of cell specificity in polyQ diseases, considering that even among neurons only certain populations are affected in each disease, while others are apparently spared. Both in MJD patients and in animal MJD models (Colomer Gould, 2012), expression of expanded atx3 in the CNS does not correlate with the observed

neurodegeneration profiles, meaning that the toxicity mechanisms are either specific of certain cell populations, or that different cell populations show varying degree of resistance to the effects of expanded atx3. Protein properties and neuronal particularities may conjugate, so that toxicity spares some neurons but damages others. Additionally, though studies often describe neurodegeneration as encompassing regional atrophy, cell loss and other morphological signs of demise, it is increasingly important to consider that cells that have no visible changes in structure may be dysfunctional and thus contribute to the disease as well. This is possibly the case, for instance, of Purkinje cells, which have been classically considered to be spared in MJD, but were reported to be dysfunctional in symptomatic YAC MJD model (Shakkottai *et al.*, 2011). The same may be true for cell populations presenting aggregates, but displaying no other overt morphologic defects.

The differential effect of atx3 in different neuronal cell types is undoubtedly mediated by the protein regions outside the polyQ tract, considering that the other polyQ-containing proteins associated with neurodegenerative disease lead to different neurodegeneration profiles, despite the wide distribution and the common pathological expansion. Each of those proteins shares no homology outside the polyQ tract, and it is logical to consider these regions as responsible for the specificities of each pathology. Interestingly, a recent study employing a *C. elegans* model of MJD expressing expanded atx3 in neurons described that even in this organism aggregation occurs only in specific neuronal subtypes (Teixeira-Castro *et al.*, 2011), but the profile was different from what was elicited by expression of isolated polyQ sequences. Additionally, polyQ sequences of 40 residues produced stronger locomotor deficits than atx3 containing 75 glutamines.

Differential regulation of proteins in different cell types may be mediated by post-translation modifications (PTMs), a diverse set of mechanisms that regulate protein properties, frequently in a reversible way (Cohen, 2002; La Spada and Taylor, 2003; Pennuto *et al.*, 2009). Among the most prevalent (and best studied) PTMs is the covalent conjugation of small protein modifiers, as is the case of ubiquitination but also of others Ub-like proteins, such as NEDD8 and small Ub-like modifiers (SUMO), which are added to lysine residues of substrate proteins through an enzymatic cascade largely resembling that of Ub conjugation (van der Veen and Ploegh, 2012; Welchman *et al.*, 2005). Many other PTMs exist in eukaryotic cells, and among the numerous modifications involving conjugation of chemical groups to amino acid side chains, the most acknowledged is phosphorylation. This modification usually consists in the addition of a phosphate group to the side chains of amino acids containing a hydroxyl group. In eukaryotes, phosphorylation normally occurs in serine, threonine and tyrosine residues, and is catalyzed by enzymes designates as kinases; the reverse effect, termed dephosphorylation, is catalyzed by phosphatases (Cohen, 2002).

PTMs regulate many different properties of a protein, including enzymatic activity, molecular interactions, subcellular localization and stability. The changes produced are considered to result from steric or charge effects or to derive from possible alterations in protein interactions (Hunter, 2007). PTMs are the basis of many regulatory pathways of the cell and are consequently implicated in a myriad of biological phenomena. Phosphorylation, in

particular, is considered the most general regulatory device in eukaryotic cells and has been demonstrated to mediate mechanisms in almost every physiologic event (Cohen, 2002; Hunter, 2012; Pawson and Scott, 2005). Strikingly, it has been predicted that around 30 % of the human proteins are phosphorylated and that, at any time point in a eukaryotic cell, one-third of all proteins are phosphorylated (Cohen, 2002). For this reasons, it is logical to hypothesize that at least some of atx3 features are regulated by PTMs. Furthermore, it is also possible that PTMs influence the toxicity mechanisms moved upon polyQ expansion of the protein, either by playing particular roles in atx3 biological function that become deleterious to neurons upon mutation, or by directly influencing toxic phenomena, such as aggregation, proteolytic processing or abnormal interactions. Understanding how atx3 PTMs affect the properties of the protein may thus help decipher the biological role of this protein, but is probably also bound to contribute to the understanding of MJD pathogenic mechanisms.

Regulation of deubiquitinating enzymes by post-translational modifications

DUBs are themselves responsible for the modulation of one diverse and complex PTM that is implicated in several cellular mechanisms – ubiquitination. For this reason, these enzymes are highly regulated, by means of different strategies. The activity of DUBs is known to be regulated in cells by the proteins with which they interact (including the proper substrates and scaffolding proteins), by changes in their subcellular localization and, remarkably, by PTMs that target them (Komander *et al.*, 2009). Understanding the possible effects that PTMs have on DUBs is perhaps the best way to envisage the possible outcomes of atx3 modifications.

Proteases are frequently regulated by phosphorylation, a modification that can either activate or inactivate these enzymes, depending on the particular sites and proteins that are targeted (Renatus and Farady, 2012). Largely due to high-throughput proteomic studies, many DUBs are currently known to be phosphorylated, some of them in more than one residue (Kessler and Edelmann, 2011). However, only a small fraction of these modifications has been biochemically characterized and their outcomes explored. Phosphorylation of many DUBs has been demonstrated to modify their enzymatic activity, contributing to the extensive crosstalk recognized to exist between phospho and Ub signaling (Komander *et al.*, 2009). The majority of available studies describes phosphorylation events with negative consequences for DUB activity; this is the case of phosphorylation of Ub C-terminal hydrolase 8 (USP8), cylindromatosis-associated USP CYLD and otubain-1, OTU enzyme, at amino acids S680, S418 and Y26, respectively (Edelmann *et al.*, 2010; Hutti *et al.*, 2007; Mizuno *et al.*, 2007; Reiley *et al.*, 2005). The conclusions of these studies were based on observations obtained with phosphomutated DUBs, where the phosphorylation sites are either mutated to negatively charged amino acids so as to resemble constitutive phosphorylation states, or to alanine residues, in order to block phosphorylation. The evaluation of activity was performed through various methods: USP8 reacted *ex vivo* against polyUb chains (Mizuno *et al.*, 2007), CYLD

activity was evaluated in cell extracts through the ubiquitination pattern of an overexpressed substrate (see below) (Reiley *et al.*, 2005), and otubain-1 reaction with Ub was observed by formation of adducts with a Ub derivative (Edelmann *et al.*, 2010).

It is believed that the molecular effects of protein phosphorylation range from the establishment of electrostatic point charges that influence protein conformation to the creation of binding surfaces for protein interaction (Tarrant and Cole, 2009). The structural alterations underlying the changes in proteolytic activity produced by phosphate conjugation are not clearly understood, though they are increasingly regarded as being rather subtle (Renatus and Farady, 2012) A recent study describing the activation of deubiquitinating enzyme A (DUBA), an OTU, shed light into the molecular mechanisms mediating the changes in protease activity elicited by phosphorylation, with possible clues to the regulation of the activity of other DUBs (Huang *et al.*, 2012). When *in vitro*-produced DUBA is not phosphorylated, the enzyme is unable to process Ub model substrates, but *in vitro* phosphorylation of S177 by casein kinase 2 (CK2) is sufficient to render it active. The crystal structure of phosphorylated DUBA complexed with Ub-aldehyde revealed that, instead of an alteration of the catalytic residues, S177 phosphorylation contributes to a structural stabilization of the complex formed by the enzyme and the substrate. Ligand-free DUBA is believed to rest in an inactive conformation, and correct alignment of the substrate-binding site is only induced upon Ub binding; the phosphate group stabilizes the structure of DUBA and also interacts with the C-terminal region of Ub (Huang *et al.*, 2012; Renatus and Farady, 2012).

The downstream consequences of activity changes caused by phosphorylation of DUBs remain unidentified in many cases, but are nonetheless considered to be diverse (Kessler and Edelmann, 2011). The possible outcomes are hereby exemplified by the role of DUB phosphorylation in regulating the nuclear factor kappa-light-chain-enhancer of activated B cells (NF-κB) pathway, which is implicated in DNA transcription regulation. CYLD, whose DUB activity downregulates the NF-κB pathway through cleavage of K63-linked chains from certain components of the pathway, is known to be phosphorylated in response to NF-κB-inducing factors. Mimicking constitutive phosphorylation of CYLD at one residue, S418, decreases its DUB enzymatic activity against tumor necrosis factor receptor-associated factor 2 (TARF2), a component of the NF-κB-inducing pathway, and the availability of this and other putatively phosphorylatable sites was reported to be important for adequate downstream responses of this pathway (Reiley *et al.*, 2005). A20 is an OTU also known to cleave K63-linked chains from several components of the NK-kB pathway, but additionally leading to conjugation of K48-linked chains that target them for degradation, through means of a Ub ligase domain also contained in A20. Phosphorylation of A20 at S381 increases its ability to downregulate this pathway, though it is not known if phosphorylation affects its DUB activity or the Ub ligase activity (Hutti *et al.*, 2007). Phosphorylation of both CYLD and A20 was associated with the activity of IκB kinase (IKK) β (Hutti *et al.*, 2007; Reiley *et al.*, 2005).

The effects of DUB phosphorylation events are not limited to apparent direct changes in enzymatic activity. Cycling-dependent kinase 1 (Cdk1) phosphorylates Ub C-terminal hydrolase 1 (USP1) at S313, a modification that is required for the interactions of USP1 with

USP1-associated factor (UAF), which in turn stimulates the catalytic activity of USP1 (Villamil *et al.*, 2012). Ub C-terminal hydrolase 10 (USP10) is phosphorylated by protein kinase ataxia telangiectasia mutated (ATM) on T42 and S337 and this modification was associated with nuclear translocation and stabilization of USP10 (Yuan *et al.*, 2010). Phosphorylation of S680 of USP8 by 14-3-3ε also regulates its subcellular localization, being essential for its maintenance in the cytosol (Ballif *et al.*, 2006). Finally, phosphorylation of Ub C-terminal hydrolase 25 (USP25) by spleen tyrosine kinase (SYK) decreases the level of the DUB, through proteasomal-independent mechanisms (Cholay *et al.*, 2010).

Perhaps ironically, though not surprisingly, DUBs and other enzymes involved in Ub signaling are themselves targets for ubiquitination (Weissman *et al.*, 2011). Polyubiquitination of certain DUBs is admitted to regulate their turnover by inducing degradation, as has been demonstrated for Ub C-terminal hydrolase 7 (USP7) (Boutell *et al.*, 2005). Interestingly, in some cases polyubiquitination has been shown to be mediated by the E3 ligases with which DUBs normally interact (Reyes-Turcu *et al.*, 2009): this occurs with Ub C-terminal hydrolase 4 (USP4) and Rho52, an E3 enzyme (Wada and Kamitani, 2006), and has been also suggested to happen between atx3 and many of its interacting E3 ligases (CHIP, E4B, gp78, MITOL and possibly parkin, as explained above). However, the dependence of proteasomal degradation on modification by polyUb is disputed in both DUBs (Berke *et al.*, 2005; Matsumoto *et al.*, 2004; Miller *et al.*, 2004; Todi *et al.*, 2007; Wada and Kamitani, 2006). Other DUBs shown to be polyubiquitinated but to which no outcome of this PTM has been ascribed include Ub C-terminal hydrolase 36 (USP36) and Ub C-terminal hydrolase (DUB-1) (Kim *et al.*, 2005; Lee *et al.*, 2008). Interestingly, monoubiquitination of other DUBs has been reported to affect their proteolytic activity. UCHL1 is monoubiquitinated at several lysine residues in close proximity to its active site and this modification appears to hinder its activity by inhibiting interaction with potential ubiquitinated substrates (Meray and Lansbury, 2007). USP25 is monoubiquitinated at K99, a modification that has been hypothesized to increases its enzymatic activity, by interplaying with sumoylation at the same lysine residue (conjugation of SUMO), which has been described to decrease activity by reducing the interaction with polyUb chains (Denuc *et al.*, 2009; Meulmeester *et al.*, 2008).

Modulation of polyglutamine toxicity by post-translational modifications

Proteins associated with the development of neurodegenerative diseases have been frequently reported to be targeted by PTMs, which have sometimes been implicated in modulating the toxic properties of the proteins and the deleterious changes they cause. As pointed throughout, the regions flanking the repeat sequences of polyQ-containing proteins are admitted to influence the toxicity pathways resulting from expansion. These regions are possibly targeted by PTMs, either as part of normal regulatory mechanisms or as a result of aberrations produced by the pathogenic mutation; whichever the case, the outcomes of these modifications may have implications in polyQ diseases pathogenesis (Gatchel and Zoghbi,

2005; Takahashi *et al.*, 2010). Modification of polyQ-containing proteins may be either neurotoxic, when they contribute to toxicity-associated mechanisms such as aggregation, proteolytic cleavage (itself a PTM) and aberrant interactions, or neuroprotective, in cases where the PTMs lead to degradation of the pathogenic proteins (Pennuto *et al.*, 2009). There are many concrete examples of PTMs that influence aspects of polyQ-induced toxicity, with reports focusing frequently on ubiquitination, sumoylation, palmitoylation, acetylation and, specially, phosphorylation (Bauer and Nukina, 2009; Ehrnhoefer *et al.*, 2011; La Spada and Taylor, 2010; Pennuto *et al.*, 2009). The following subsections will address the current data regarding phosphorylation of polyQ-containing proteins and the effects of this PTM on disease-related mechanisms (Table II).

A. Phosphorylation of huntingtin

Huntingtin (htt), the protein involved in HD, is known to be modified by phosphorylation in many different residues and it has been extensively demonstrated that this modifications influences the toxic outcomes caused by polyQ expansion of htt (Ehrnhoefer *et al.*, 2011). Overall, the modifications that have been so far characterized indicate that phosphate-conjugation plays a protective role in HD-related events. Htt is a large protein that has been functionally related to diverse cellular pathways including axonal transport, transcription and signaling, possibly functioning as a scaffolding protein (Gatchel and Zoghbi, 2005; Williams and Paulson, 2008). Notably, due to its large size, studies frequently utilize htt truncated forms instead of the full-length protein.

Activation of Akt, shown to phosphorylate S421 *in vitro*, was initially described to decrease inclusion formation and cell death in striatal neuron cultures expressing an expanded htt N-terminal fragment (the striatum is harshly affected in HD) (Humbert *et al.*, 2002). Later, another kinase – serum/glucocorticoid regulated kinase (SGK) – was also shown to target S421 and to protect striatal neurons against expanded htt-induced cell death (Rangone *et al.*, 2004). Inhibition of calcineurin, a phosphatase demonstrated to dephosphorylate S421 *in vitro* and in cells, was also reported to prevent death of HD cell culture models (Pardo *et al.*, 2006). Important evidence for the protective role of S421 phosphorylation *in vivo* was obtained with lentiviral rat models of HD expressing a fragment of expanded htt in the striatum, in which mimicking phosphorylation of S421 by mutation of this residue to an aspartate decreased the neuronal loss elicited by the pathogenic protein fragment (Pardo *et al.*, 2006). Mechanistically, the protective effects of S421 phosphorylation may be related to htt role in axonal transport: in cultures of rat cortical neurons, expanded htt hinders the axonal transport of vesicles, but mimicking phosphorylation of S421 restores transport to the levels observed with non-expanded htt (Colin *et al.*, 2008; Zala *et al.*, 2008). Phosphorylation of S421 was also shown to reduce caspase 6-mediated cleavage of expanded htt and its nuclear localization, two events recognized to be deleterious in HD (Warby *et al.*, 2009). Recent results further suggested that phosphorylation of S421 may be influenced by excitotoxic events: the levels of S421

Table II: Phosphorylation of polyQ disease-causing proteins

Disease name	Protein product	Phosphorylation sites	Kinases	Described Effects
HD	huntingtin	S13	IKK	Reduces cleavage, aggregation and cytotoxicity and increases turnover
		S16	n.d.	
		S412	Akt, SGK	Reduces cleavage, inclusion formation, nuclear localization and cytotoxicity and rescues axonal transport
		S434	Cdk5	Reduces cleavage, aggregation and cytotoxicity
		S531	n.d.	Reduces cleavage and cytotoxicity
		S1181 S1201	Cdk5	Reduces cytotoxicity
		T3	n.d.	Increases aggregation and reduces cytotoxicity
DRLPA	atrophin-1	S734	JNK	n.d.
SBMA	androgen receptor	S215 S792	Akt	Reduces ligand binding, nuclear translocation, transcriptional activity, aggregation and cytoxicity, and increases turnover
		S426	n.d.	Increases toxicity
		S516	MAPK	Increases cleavage and cytotoxicity
		S651	n.d.	Promotes nuclear exportation
SCA1	ataxin-1	S776	Akt	Reduces turnover and increases inclusion formation and cytotoxicity
MJD/ SCA3	ataxin-3	S236 S340 S352	CK2	Increases nuclear transport and transcriptional repression activity
		S256	GSK3β	Reduces aggregation

The table summarizes the information presented in the text and is based on the studies thereby cited. Cytotoxicity variously includes cell death and demise described in cell cultures or neurodegeneration evaluated in animal models

Abbreviations: HD, Huntington's disease; DRPLA, dentatorubral-pallidoluysian atrophy; SBMA, spinal and bulbar muscular atrophy; SCA, spinocerebellar ataxia, MJD, Machado-Joseph disease; n.d., none described; IKK; IκB kinase; SGK, serum/glucocorticoid regulated kinase; Cdk5, cyclin-dependent kinase 5; JNK, c-Jun N-terminal kinase; MAPK, mitogen-activated protein-kinase; CK2, casein kinase 2; glycogen synthase kinase 3β (GSK3β).

phosphorylation decrease in YAC HD model mice-derived neurons upon excitotoxic NMDAR stimulation, reportedly through the action of PP1 and PP2A phosphatases (Metzler *et al.*, 2010). The decrease in phosphorylation was associated with neuronal loss but, importantly, blockade of these phosphatases blocked NMDA-induced cell death (Metzler *et al.*, 2010).

Cyclin-dependent kinase 5 (Cdk5) phosphorylates htt at S434 (Luo *et al.*, 2005), S1181 and S1201 (Anne *et al.*, 2007), *in vitro* and in cells, and these PTMs were also related to decreased toxicity. In neural cell models, phosphorylation of S434 decreased aggregation and cell death, an effect that was associated with a decreased propensity to caspase-mediated

cleavage (Luo *et al.*, 2005). Phosphorylation of S1181 and S1201 was demonstrated to be stimulated by DNA damage, and inhibiting their modification by mutating alanine residues rends the non-expanded htt toxic, leading to cell death of rat striatal neurons similar to what is elicited by expanded htt (Anne *et al.*, 2007). Contrarily, mutating both S1181 and S1201 of expanded htt to negatively charged aspartate residues decreases toxicity.

T3 of htt was reported to be phosphorylated in mouse brain and an hht fragment containing phosphomimetic T3D was reported to lead to stronger aggregation in both cell cultures and *in vivo*, in neurons from transgenic *Drosophila* larvae (Aiken *et al.*, 2009). Curiously, although the non-phosphorylatable T3A form decreases aggregation, both mutants were shown to reduced neurodegeneration and lethality in this model, indicating that the T3 residue probably has an intrinsic property leading to toxicity, that decreases upon mutation to either alanine or aspartate. It was suggested that, given the differences in aggregation between the two T3 mutants, different rescue mechanisms may be at work. It is possible that, in accordance with current opinions, the microscopic aggregates observed in this study do not correspond to the toxic species (Aiken *et al.*, 2009).

Overexpression of IKK in striatal precursor cells leads to the phosphorylation of S13 and S16 of a htt fragment, though *in vitro* assays indicate that the IKK-catalyzed phosphorylation is only direct in the case of S13 (Thompson *et al.*, 2009). Importantly, phosphorylation of S13 was further confirmed to target endogenous htt. In transfected cells, increased phosphorylation at S13 and S16 was associated with decreased levels of the htt fragment and, interestingly, phosphomimicking of both residues or overexpression of IKK decreased polyubiquitination and sumoylation at nearby lysine residues and increased degradation of the htt fragment by the proteasome and the lysosome. Contrastingly, htt fragments with expanded glutamines, which were shown to present reduced levels of S13 and S16 phosphorylation, had a tendency to accumulate in cells, possibly due to decreased clearing (Thompson *et al.*, 2009). *In vitro*, the phosphomimetic mutants of similar fragments containing 37 glutamines (the threshold of HD risk) showed decreased tendency to aggregate, comparing to non-mutated fragments and non-phosphorylatable mutants (Gu *et al.*, 2009; Mishra *et al.*, 2012). Importantly, in a transgenic mouse model expressing full-length expanded htt, the disease phenotype is largely preserved when S13 and S16 are mutated to alanines, but is rescued by mutation to aspartate (phosphomimetic mutant). The disease signs of the alanine-mutated model include htt aggregation, selective neurodegeneration (cortex and striatum; the cerebellum is spared) and motor as well as psychiatric-like deficits (Gu *et al.*, 2009). Counter-intuitively, taking into account these possible protective roles of S13 and S16, phosphomimicking of both residues increases nuclear localization in transfected cortical neuronal cultured (Thompson *et al.*, 2009) and, in particular, phosphorylation of S16 has recently been associated with nuclear accumulation of N-terminal fragments (Havel *et al.*, 2011).

A mass spectrometry (MS) analysis of full-length htt expressed in cell lines identified three additional htt phosphorylational sites – S2076, S2653 and S2657 – along with a monophosphorylated peptide to which an individual phosphorylation site could not be

mapped; phosphorylation can target either S533, S535 or S356 (Schilling *et al.*, 2006). This amino acids lie on a proteolytic susceptibility domain of htt and S536 in particular has been identified as a site for calpain cleavage (Gafni *et al.*, 2004). Mutating this residue to aspartate, but not the other two, reduced the cleavage of C-terminally truncated expanded htt and the toxicity associated with expression of this protein, in a cell line (Schilling *et al.*, 2006).

Important insights into the relevance of phosphorylation defects in HD derive also from the analysis of kinases in the brain of HD patients and animal models. Cdk5 purified from the brains of a HD mouse model displays a reduced activity (Luo *et al.*, 2005) and, in HD patients brain, Akt is more prone to suffer caspase-mediated proteolytic cleavage, as detected in the cerebellum, cortex and, specially, in the striatum (Humbert *et al.*, 2002). Contrastingly, however, the levels of SGK are increased in HD patients' brain, which nonetheless supports a role for this kinase in HD-related mechanisms (Rangone *et al.*, 2004).

Finally, there is some important evidence for a correlation between the patterns of these protective phosphorylation events and the cell selectivity of HD: generally speaking, reports demonstrate that phosphorylation is often reduced in cell types known to be specially sensitive to expanded htt toxicity. The levels of phosphorylated T3 of a htt fragment are reduced in transfected striatal precursor cells when compared to non-neuronal cell lines, and phosphorylation decreases even more upon polyQ expansion of that htt fragment. Interestingly, this last difference is only observed in rat striatal precursor cells but not in non-neuronal cell lines (Aiken *et al.*, 2009). In HD mouse models, the levels of T3 phosphorylation are specially decreased in the striatum, when compared to the cortex (Aiken *et al.*, 2009). In a HD cell culture model, phosphorylation of expanded htt at S421 is decreased when compared to wild-type cell lines (Pardo *et al.*, 2006) and the same was observed for transfected cell lines expressing expanded or non-expanded truncated htt and for YAC transgenic mice (Warby *et al.*, 2005). S421 is phosphorylated under physiological conditions in both human and wild-type mouse brain, but, in the last case, it was further observed that the phosphorylation levels in the three particular brain regions analyzed varied: it was higher in the cerebellum, less in the cortex and least in the striatum (Ehrnhoefer *et al.*, 2011; Warby *et al.*, 2005). This correlates with the neurodegeneration pattern observed in HD (Warby *et al.*, 2005). Interestingly, stimulation of NMDARs in the striatum of YAC HD model mice decreases the levels of S421 phosphorylation relatively to wild-type animals (Metzler *et al.*, 2010), indicating that excitoxic stimuli may increase neuronal susceptibility by decreasing the protective effect of S421 phosphorylation.

B. Phosphorylation of other polyglutamine disease-causing proteins

The androgen receptor (AR) is a testosterone-associated steroid hormone receptor that is widely studied because of its involvement in prostate cancer, though it is also related to another disease, SBMA, which is caused when the polyQ region of this protein is expanded (Williams and Paulson, 2008). A large number of phosphorylation sites has been mapped in AR:

S16, S83, S96, S215, S258, S310, S426, S516, S651, S792, Y223, Y267, Y307, Y346, Y357, Y362/363, Y393, Y534, Y551 and Y915 (Gioeli *et al.*, 2006; Guo *et al.*, 2006; Palazzolo *et al.*, 2007; Pennuto *et al.*, 2009). The phosphorylation of some of these residues has been associated with the functions of AR; for instance, S651 phosphorylation is induced by stress kinase signaling and was shown to modulate AR transcriptional activity, by increasing its nuclear exportation (Gioeli *et al.*, 2006). Interestingly, serine phosphorylation of AR, irrespective of particular serine residues, increases with larger glutamine repeats (LaFevre-Bernt and Ellerby, 2003), but particular phosphorylation events appear to be either protective or deleterious, depending on the phosphorylation site. In cell lines, blockade of S516 phosphorylation, which is catalyzed by a mitogen-activated protein-kinase (MAPK), abrogates polyQ-expanded AR-derived cell death and formation of caspase-3-derived cleavage products, which have been implicated in the toxicity mechanisms of SBMA (LaFevre-Bernt and Ellerby, 2003). Preventing S426 and S516 phosphorylation also reduces toxicity of the polyQ-expanded AR, but turns the non-expanded AR toxic (Funderburk *et al.*, 2009). Phosphorylation of S215 and S792 was suggested to be mediated by Akt and to be associated with a reduction in expanded AR ligand binding, ligand-dependent nuclear translocation, transcriptional activation and citotoxicity, in cell lines (Palazzolo *et al.*, 2007). This phosphorylation event was further demonstrated to reduce expanded AR aggregation and increase its degradation by the UPP in cultured cells, and Akt activation was shown to ameliorate the disease phenotype of a SBMA mouse model (Palazzolo *et al.*, 2009).

Atrophin-1 is a protein involved in transcription regulation and is causatively related to the development of DRPLA (Bauer and Nukina, 2009). S734 of atrophin-1 is phosphorylated by the c-Jun N-terminal kinase (JNK), but the affinity of this enzyme decreases when the polyQ region of atrophin-1 is expanded. This alteration was suggested to delay neuronal pro-survival pathways (Okamura-Oho *et al.*, 2003).

Ataxin-1 (atx1) causes SCA1 and its function has been also associated with transcription regulation. Phosphorylation of S776 has been reported to play a critical role in the pathogenesis of this SCA1, considering that mutating this residue to alanine renders expanded atx1 unable to form aggregates in a cell line and, remarkably, transgenic mice expressing this mutated form in Purkinje cells displayed a considerably milder disease phenotype, when compared to animals expressing non-mutated expanded atx1 (Emamian *et al.*, 2003). The ameliorated characteristics included less inclusion number, less degeneration of Purkinje cells, and increased motor performance. Akt-mediated phosphorylation, which was shown to target S776, leads to the binding of expanded atx1 and the 14-3-3 protein *in vitro* (Chen *et al.*, 2003b). This interaction is considered to be very relevant for pathogenesis: in cell lines, cotransfection of 14-3-3 was shown to stabilize expanded atx1 and increase inclusion formation; in transgenic *Drosophila*, 14-3-3 co-expression increased neurodegeneration caused by expanded atx1 (Chen *et al.*, 2003b).

Post-translational modifications of ataxin-3

As explained before, DUBs are frequently observed to display a low enzymatic activity *in vitro*, and atx3 is no exception (Chow *et al.*, 2004a; Komander *et al.*, 2009). Thus, it is predicted that atx3 activity, and consequently the biologic function of this protein, may be regulated by PTMs, either directly or by interfering with important interactions with other proteins (Almeida *et al.*, 2013; Reyes-Turcu *et al.*, 2009). Furthermore, it is also possible that other properties of atx3, such as subcellular localization and turnover, both possibly relevant for its physiological role and for the pathogenesis of MJD, may be as well regulated by these kinds of mechanisms. The differential regulation of atx3 subcellular localization by PTMs and other mechanisms in different cells may explain the diversity in intracellular distribution observed both in cell lines and human brain cells (Trottier *et al.*, 1998). Finally, attending to the effects of phosphorylation on the toxicity mechanisms caused by other polyQ-containing proteins, it is plausible to admit that PTMs of atx3 conceivably interfere with the pathways linking polyQ-expansion of atx3 to the disease outcomes in MJD, either leading to protection or aggravating the deleterious effect of the pathogenic protein. The fact that the understanding of regulation of atx3 by PTMs may simultaneously elucidate about its biological function and the pathogenic mechanisms of MJD justifies the interest of scientific research in this area.

Atx3 is currently known to be targeted by different PTM mechanisms. As exposed above when dealing with the turnover and degradation of atx3, polyubiquitination has been described to target this protein, though there is controversy whether it leads to degradation by the proteasome; this may not be true, at least in some cases (Berke *et al.*, 2005; Jana and Nukina, 2004; Matsumoto *et al.*, 2004; Todi *et al.*, 2007; Tsai *et al.*, 2003). One study demonstrated that the expanded protein is more stable than its non-expanded counterpart and that it is degraded by the proteasome less efficiently; this would be expected to contribute to the accumulation of the pathogenic protein and to the persistence of its toxic effects (Matsumoto *et al.*, 2004). However, increased ubiquitination did not correlate with increased degradation, i.e., the two forms were ubiquitinated to similar extents. Thus, the differences observed may be due to an inefficient proteasomal recognition and degradation due to the expanded polyQ tract (Matsumoto *et al.*, 2004). Nevertheless, it appears that there is not much consensus on the increased stability of the expanded form and, in effect, another study reported that both normal and expanded forms of atx3 are degraded with the same efficiency by the proteasome and that there is no inhibition of the proteasome by soluble expanded atx3 (Berke *et al.*, 2005).

Recent reports demonstrated that atx3 is also monoubiquitinated in cells (including neural cells), and that this modification increases its DUB activity independent of potential cofactors or interactors, *in vitro* (Todi *et al.*, 2009). K117 of the JD, located in the vicinity of the catalytic site, is the preferentially ubiquitinated lysine residue (Figure 9) both *in vitro* and in cells (modification of other lysines was less frequently detected), and ubiquitination of this residue alone is sufficient for the observed activity enhancement (Todi *et al.*, 2010).

Interestingly, though the UIMs are important in determining cleaving preferences, the increase in activity by monoubiquitination occurs independently from the functionality of these motifs (Todi *et al.*, 2010; Todi *et al.*, 2009). However, when UIM1 and UIM2 are not functional, monoubiquitinated atx3 inverts its preferences, cleaving K48-linked chains more efficiently than K63-linked ones (Todi *et al.*, 2010; Todi *et al.*, 2009). Furthermore, availability of K117 for ubiquitination increases atx3 ability to promote aggresome formation, which is dependent on its DUB activity (Todi *et al.*, 2010). Taking into consideration that several proteotoxic stressors enhanced atx3 ubiquitination (mono- and polyubiquitination), authors have suggested that the upregulation of atx3 activity by ubiquitination may serve as a positive feedback mechanism in response to proteotoxic stress (Todi *et al.*, 2009). In transgenic *Drosophila*, coexpression of atx3 and isolated polyQ sequences reduces degeneration caused by the toxic repeated sequences, through an undisclosed process that was nonetheless unrelated to a decrease in toxic polyQ sequence stability (Tsou *et al.*, 2013). It was further demonstrated that contrary to atx3 where all lysine residues had been mutated, atx3 with only one lysine residue at position 117 – which was shown to be ubiquitinated in *Drosophila* as well – was sufficient to produce this effect (Tsou *et al.*, 2013). These results strongly suggest an important role for K177 ubiquitination on the *in vivo* function of atx3. Importantly, ubiquitination of atx3 is not targeted by its own DUB activity in *trans*, arguing against the possibility that atx3 regulates its own activity by regulating its ubiquitination status (Todi *et al.*, 2007).

Through biochemical analysis of the phosphoamino acids present on ^{32}P-orthophosphate-radiolabled samples of atx3, Mueller and collaborators (2009) showed that atx3 is phosphorylated on serine residues. In fact, several serine phosphorylation sites have been mapped, all of them located in the UIMs: S236, in the first UIM, S256 and 260/261 (it is not clear which of the adjacent serine residues is phosphorylated), located on the second UIM, and S340 and 352 of the third UIM (Figure 9) (Fei *et al.*, 2007; Mueller *et al.*, 2009). Importantly, there are already some clues to the possible biological relevance of these modifications. The study by Mueller and collaborators (2009) showed that stimulating phosphorylation of serine residues 236, or 340 and 352 simultaneously, by mutating these amino acids to aspartate, leads to an increased nuclear localization in cells lines, admitted to be important for aggregation and toxicity of the expanded form, and enhances repression of atx3-regulated transcription in gene reporter assays of MMP2 expression (Mueller *et al.*, 2009). Curiously the increased nuclear localization of atx3 occurs independently from the described NLS pathway, at least for S340 and S352 (Macedo-Ribeiro *et al.*, 2009; Mueller *et al.*, 2009). Additionally, a phosphomimetic mutant of residues 340 and 352 also increased the stability and half-life of atx3 (Mueller *et al.*, 2009). CK2 was shown to interact with atx3 and to phosphorylate its UIM-containing C-terminal region (Mueller *et al.*, 2009; Tao *et al.*, 2008) and pharmacological inhibition of this kinase not only reduced the amount of nuclear atx3 and activated atx3-regulated gene transcription, but also decreased NI formation, indicating that CK2-dependent phosphorylation regulates these properties, admittedly by interference with the phosphorylated state of atx3 (Mueller *et al.*, 2009). Considering what was discussed about the conditioning role of the nuclear localization and decreased turnover of atx3 in the deleterious

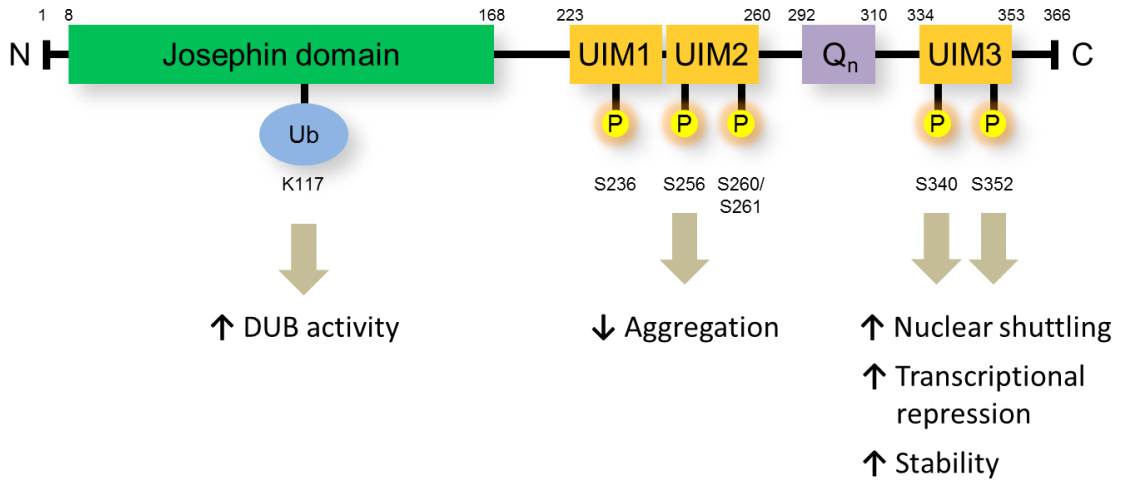

Figure 9: Mapping and effects of atx3 PTMs. Apart from being polyubiquitinated, atx3 has been shown to be monoubiquitinated at K117, a PTM that was demonstrated to increase its DUB enzymatic activity. Five serine residues present in the UIMs have also been described to be phosphorylated: S236, S256, S260/S261, S340 and S352. Hindering S256 phosphorylation was shown to increase aggregation of polyQ-expanded atx3, suggesting that this modification may be protective against aggregation. Mimicking phosphorylation of residues S340 and S352 was shown to increase atx3 nuclear shuttling and atx3-mediated repression of transcription and to increase the stability of the protein. Mimicking S236 elicited analogous effects on nuclear transport and transcriptional repression (not represented). The figure uses the same domain annotations as figure 3, except for the region C-terminally of UIM2; those annotations are based on what is mentioned by the authors describing the phosphorylation sites on UIM3 (Mueller et al., 2009), using an atx3 sequence with 19 glutamine repeats (the protein sequence corresponds to Uniprot human atx3 isoform 2 - code P54252-2).

mechanisms of MJD, a phosphorylation-mediated increase in stability and nuclear localization conceivably interferes with protein aggregation and toxicity (Bichelmeier *et al.*, 2007; Breuer *et al.*, 2010). Phosphorylation of serines 236, 340 and 352 may participate in the nuclear translocation of expanded atx3 and, in the nucleus, the phosphorylated protein may lead to aberrant atx3-regulated gene expression (Evert *et al.*, 2006a; Mueller *et al.*, 2009). The increased stability may contribute to increased aggregation and NI formation. In fact, C-terminal-containing fragments of atx3 showed an increase of NI formation when serines 340 and 352 were mutated to mimic phosphorylation (Mueller *et al.*, 2009).

Fei and coworkers (2007) reported that S256 is phosphorylated *in vitro* by glycogen synthase kinase 3β (GSK3β), but observed a decreased phosphorylation of the expanded form of the protein. Contrary to the observations indicating a possible nefarious effect for atx3 phosphorylation, these authors observed that preventing phosphorylation of S256 by mutating this residue to alanine enhanced the aggregation of an expanded form of atx3. These results indicate that there may be some relation between the phosphorylated state of S256 and the formation of the toxic protein aggregates. It is not surprising that the effects of phosphorylation may differ according to the particular residues that are modified.

A recent study suggested that a serine residue of the JD may be important in atx3 responses to proteotoxic stress (Reina *et al.*, 2010). Under normal conditions, nuclear localization of atx3 is determined by its NLS and by CK2-dependent phosphorylation, but it was

reported that proteotoxic stimuli such as heat shock and oxidative stress overrides those signals and increase atx3 nuclear localization independently (Antony *et al.*, 2009; Macedo-Ribeiro *et al.*, 2009; Mueller *et al.*, 2009; Reina *et al.*, 2010). Two different regions seem important for this transport: the JD, namely S111, and the C-terminal region comprising the polyQ sequence and the rest of the C-terminal (but not the UIMs). Considering that S111 was a putative target for phosphorylation, the authors of this study mutated S111 to an alanine residue and observed that heat shock no longer induced an increase in atx3 nuclear localization; mutation to an aspartate, however, was not sufficient for localization in the nucleus, but responded normally to heat shock (Reina *et al.*, 2010). Although these results suggest that modification of S111 may be important in regulating the behavior of atx3 after stress stimuli, phosphorylation at S111, or at any other residue of the JD, remains undescribed.

1.8 Objectives

The toxicity derived from the pathogenic expansion of polyQ-containing proteins is usually attributed to changes in biologic function, subcellular localization, molecular interactions and aggregation of the proteins carrying the pathogenic mutation, but it is extensively recognized that the regions outside the polyQ tract are crucial in determining toxicity. Phosphorylation is a reversible post-translational mechanism known to regulate diverse protein properties, and it has been frequently described to target disease-related proteins outside their repeat sequence and to influence the deleterious alterations the polyQ expansion causes. The mechanisms involved in MJD and the cellular role of atx3 are still not clearly understood, but comprehending how this protein is regulated by phosphorylation, and how this modification affects atx3 when the protein is expanded, is due to yield relevant contributions. Alterations caused by phosphorylation may increase our understanding of how atx3 behaves in a cell, but may also help uncover important points of regulation that interfere with toxicity mechanisms.

In a previous approach to the study of atx3 phosphorylation, we identified a novel phosphorylation site of the protein through MS, that was localized in the catalytic JD – serine 12 (Matos, 2009). The current work aims at characterizing this modification, both in terms of the outcomes it might have regarding atx3 activity as a DUB, and in respect to the way S12 phosphorylation might alter aggregation of expanded atx3 and the neurodegeneration it causes. With these objectives, we moved to confirm that atx3 is phosphorylated in neuronal cells and determine the effects of this modification on atx3 DUB enzymatic activity *in vitro*, using phosphomimetic mutants of atx3. The effects of S12 phosphorylation in the context of expanded atx3-induced toxicity were analyzed by observing how different forms of atx3 generated by mutation of S12 affected relevant morphological characteristics of cultured neurons. Finally, the outcomes of those mutations were further evaluated *in vivo*, using a well described lentiviral rat model of MJD with striatal pathology.

The current study is the first to characterize the phosphorylation of an amino acid residue of atx3 present in the catalytic domain of the protein. Additionally, it is also the first to investigate the effects of atx3 phosphorylation specifically in neuronal cells and in *in vivo* animal models of MJD.

Chapter 2

Materials and Methods

Chapter 2 – Materials and Methods

Expression plasmids

Eukaryotic expression pEFGP-C1 plasmids encoding human atx3 variant MJD1a (NCBI accession number: AAB33571.1) with 28 glutamines (GFP-atx3 28Q) or 84 glutamines (GFP-atx3 28Q) fused with the GFP in the N-terminal was a kind gift from Dr. Henry Paulson, University of Iowa (Iowa City, IA USA; plasmids described in Chai *et al.*, 1999b). Bacterial expression pDEST17 plasmid encoding hexahistidine (6His)-tagged human atx3 variant MJD1-1 (NCBI accession number: NP_004984.2) with 13 glutamines (6His-atx3) has been previously described by our group (Gales *et al.*, 2005). Site-directed mutagenesis was used as described elsewhere (Scarff *et al.*, 2013) to introduce a cleavage site for the recombinant tobacco etch virus (TEV) protease between the open reading frame and the N-terminal sequence coding for the 6His tag (6His-TEVg-atx3). Eukaryotic expression plasmid SIN-W-PGK encoding human atx3 variant MJD1a with 72 glutamines and a N-terminal Myc tag (Myc-atx3 72Q) and plasmid SIN-CW-PGK-nls-LacZ-LTR-TRE encoding an universal short hairpin (shRNA) targeting human and rat atx3 (shRNA-atx3) were a kind gift from Dr. Luís Pereira de Almeida, University of Coimbra (Coimbra, Portugal; plasmids described in Alves *et al.*, 2008b and Alves *et al.*, 2010, respectively; shRNA-atx3 is thereby designated as shAtaxUNIV), as were the constructs used in the viral production (pCMVDR-8.92, pMD.G and pRSV-Rev). Site-directed mutagenesis was used to mutate serine 12 of atx3 encoded in the expression plasmids to aspartate or alanine, as described below.

Site-directed mutagenesis

Mutagenesis was performed using the QuickChange Site-Directed Mutagenesis Kit (Stratagene, Cambridge, UK) or the QuikChange II XL Site-Directed Mutagenesis Kit (Agilent Technologies, Santa Clara, CA, USA), in accordance to the procedure suggested by the manufacturers. Phosphomimetic atx3 S12D mutants, with S12 substituted by aspartate, were generated using primers atx31_1n_S12D_fo (5'-CAC GAG AAA CAA GAA GGC GAC CTT TGT GCT

CAA CAT TGC CTG-3') and atx31_1n_S12D_re (5'-CAG GCA ATG TTG AGC ACA AAG GTC GCC TTC TTG TTT CTC GTG-3'). Phospho-null atx3 S12A mutants, where S12 was exchanged for alanine, were produced employing primers atx31_1n_S12A_fo (5'-CAC GAG AAA CAA GAA GGC GCA CTT TGT GCT CAA CAT TGC CTG-3') and atx31_1n_S12A_re (5'-CAG GCA ATG TTG AGC ACA AAG TGC GCC TTC TTG TTT CTC GTG-3'). Primers were acquired from Eurofins MWG Operon, as part of Fisher Scientific (Loures, Portugal).

Mutation of the expression plasmids was confirmed after automatic DNA sequencing performed by STAB VIDA (Setúbal, Portugal).

Antibodies

The details of the antibodies used in Western blot, immunocytochemistry and immunohistochemistry are summarized in Table III.

Mass spectrometry

MS analysis of GFP-atx3 directed at the detection of phosphorylation sites was performed in GFP-atx3 samples prepared from transiently transfected human embryonic kidney (HEK) 293FT cells, after purification by immunoprecipitation and SDS-polyacrylamide gel electrophoresis (PAGE). The following procedures have been previously described (Matos, 2009), but are hereby reproduced. Attending to the particularities in cell culture and transfection used in the preparation of the samples subjected to the MS analysis, these techniques are also described in this section, separately from the other cell culture and transfection methods used in the present work, for the sake of comprehensibility.

HEK 293FT cells were grown in Dulbecco's Modified Eagle's Medium (DMEM), supplemented with 10% (v/v) fetal bovine serum (FBS), 0,1 mM non-essential amino acids (NEAA), 6 mM L-glutamine, 1mM sodium pyruvate (in Minimum Essential Medium – MEM) and 500 µg/ml geneticin, and maintained at 37 °C, in a humidified atmosphere containing 5 % CO_2. One day prior to transfection, fully confluent HEK 293FT cells were diluted 1:6 and then seeded onto 10 cm diameter culture plates. After 24 h of growth, transfection was carried out using Lipofectamine® Transfection Reagent (Invitrogen Life Technologies, Barcelone, Spain) with a modified version of the manufacturer's protocol, as follows: after substituting the culture medium for 6,4 ml Opti-MEM supplemented with 10 % FBS, lipid-DNA complexes obtained by mixing 10 µg of DNA plasmid with 6 µl of Lipofectamine reagent in 800 ml Opti-MEM were added to each cell plate; after overnight incubation under normal growth conditions, transfection medium was replaced for normal HEK 293FT cell medium and expression was left to occur for 24 h of cell growth. Some HEK 293FT cell cultures were subjected to chemical stimulation directed at enhancing phosphorylation with 20 nM okadaic acid (OA) for 16 h (Dorval and Fraser, 2006), 5 mM sodium orthovanadate (SOV) for 30 min (Martin *et al.*, 2006)

Table III: Antibodies used in Western blots, immunocytochemistry and immunohistochemistry

	Antibody	Species (and clonality)	Dilution	Incubation conditions	Manufacturer
Western blot					
primary antibodies	anti-atx3 (clone 1H9)	mouse (mono.)	1:1.000	1-2h, RT or ON, 4 °C	Millipore (Billerica, MA, USA)
	anti-Patx3	rabbit (poly.)	1.1.000 or 1:20	1h, RT or ON, 4 °C	Eurogentec (Seraing, Belgium; details below)
	anti-actin (β)	mouse (mono.)	1:5.000	1-2h, RT	Sigma-Aldrich (St. Louis MO, USA)
	anti-Ub	rabbit (poly.)	1:1.000	1-2h, RT	Dako (Glostrup, Denmark)
	anti-GFP	mouse (mono.)	1:1.000	1-2h, RT	Roche Applied Science (Penzberg, Germany)
secondary antibodies (ALP-conjugated)	anti-mouse IgG	donkey (poly.)	1:10.000	1h, RT	Jackson Immunoresearch (West Grove, PA, USA)
	anti-rabbit IgG	donkey (poly.)	1:10.000	1h, RT	Jackson Immunoresearch (West Grove, PA, USA)
Immunocytochemistry					
primary antibodies	anti-PSD-95	mouse (mono.)	1:200	ON, 4 °C	Affinity BioReagents (Golden, CO, USA)
	anti-VGLUT1	guinea pig (poly.)	1:100.000	ON, 4 °C	Millipore (Billerica, MA, USA)
secondary antibodies	Alexa Fluor® 568 anti-mouse IgG	goat (poly.)	1:500	45 min, RT	Invitrogen (Carlsbad, CA, USA)
	Alexa Fluor® 647 anti-guinea pig IgG	goat (poly)	1:500	45 min, RT	Molecular Probes (Eugene, OR, USA)
Immunohystochemistry					
primary antibodies	anti-atx3	mouse (mono.)	1:4.000	ON, 4 °C	Millipore (Billerica, MA, USA)
	anti-DARPP-32	rabbit (poly.)	1:5.000	ON, 4 °C	Chemicom (Waterdown, ON, Canada)
secondary antibodies (biotinylated)	anti-mouse IgG	goat (poly.)	1:200	2h, RT	Vector Laboratories (Burlingame, CA, USA)
	anti-rabbit IgG	goat (poly.)	1:200	2h, RT	Vector Laboratories (Burlingame, CA, USA)

Abbreviations: ALP, alkaline phosphatase; atx3, ataxin-3; Patx3, ataxin-3 phosphorylated at serine 12; Ub, ubiquitin; GFP, green fluorescent protein; IgG, immunoglobulin G; PSD-95, postsynaptic density protein 95; VGLUT1, vesicular glutamate transporter subtype 1; DARPP-32, dopamine- and cyclic AMP-regulated phosphoprotein of 32 kDa; mono., monoclonal; poly. polyclonal; RT, room temperature; ON, overnight.

or 200 nM phorbol 12-myristate 13-acetate (PMA) for 20 min (following the recommendations from the manufacturer; for others details on these compounds see Chapter 2 and Table IV). These treatments were carried out before cell harvesting, at 37 °C.

HEK 293FT cell extracts were prepared after briefly washing cultures with cold phosphate buffer saline (PBS; 137 mM NaCl, 2,7 KCl, 1,8 mM K_2PO_4, 10 mM $Na_2HPO_4 \cdot H_2O$, pH 7,4), by adding of 600 µl of immunoprecipitation buffer (IPB; 20 mM Tris pH 7,0, 100 mM NaCl, 2 mM EDTA, 2 mM EGTA, 50 mM NaF, 1 mM Na_3VO_4) supplemented with 1 % Triton X-100, 1 µM OA and protease inhibitors (1 mM dithiothreitol – DTT, 0,1 mM phenylmethanesulphonyl fluoride (PMSF), 10 µg/ml chymostatin, pepstatin, antipain and leupeptin – CLAP) and scraping on ice. After being sonicated on a probe sonicator for 1 min, lysates were cleared of their insoluble fraction by centrifugation (13.200 x g, 10 min, 4 °C) and protein concentration was assessed by the bicinchoninic acid (BCA) method using the BCA protein kit (Thermo Scientific, Rockford, IL, USA) according to the recommendations of the manufacturer. One mg of protein from each extract (diluted to 1 mg/ml, with the same buffer) was pre-cleared by incubation with 50 µl of a slurry of Protein A Sepharose beads (1:1 in IPB) for 1 h, followed by riddance of the beads by centrifugation (13.200 x g, 5 min). Samples were then incubated overnight with 3 µg of anti-GFP antibody and precipitation of the immunocomplexes was performed by incubation with 100 µl of the Protein A Sepharose slurry for 2 h 30 min. The beads were then washed by centrifugation (13.200 x g, 1 min), 2 times with IPB plus 1 % Triton X-100, 3 times with IPB containing 500 mM NaCl and 1 % Triton X-100 and 2 times with IPB. The above procedures were all carried out at 4°C. Elution was finally achieved by adding 50 µl of 2x concentrated SDS-PAGE sample buffer (125 mM Tris pH 6,8, 100 mM glycine, 40 % glycerol, 4 % SDS, 200 mM DTT, 0,01 % bromophenol blue) to the beads, boiling at 95 °C for 5 min and spinning with centrifugal filters (13.000xg, 5 min). 3 samples of each extract were subjected to this immunoprecipitation procedure, but collectively eluted in sequence by adding 2x concentrated SDS-PAGE sample buffer to the beads of one samples, boiling, spinning, adding the resulting eluent to another sample's beads and starting the procedure again.

The triple immunoprecipitants (~100-150µl) were alkylated by incubation with 1% (v/v) acrylamide for 20 min, at room temperature, and their protein content was separated by SDS-PAGE in 7,5% polyacrylamide gels using the PROTEAN® II xi system (100 µl of each was loaded into the gel). Gel fixation and staining were performed simultaneously by incubation with 45 % (v/v) methanol, 10 % (v/v) acetic acid, 0,25 % (w/v) Coomassie brilliant blue R for 8 min, and followed by destaining with 25% methanol, 5% acetic acid. In order to minimize possible contaminations with keratin every material contacting with the gel was washed with 1% SDS and mQ water. Polyacrilamide gel bands containing GFP-atx3 were excised using a clean scalpel, covered in mQ water and frozen.

Online liquid chromatography (LC) followed by ion spray MS (LC-ES-MS) analysis of the bands of interest was performed by the Proteomics Center at Children's Hospital Boston (Boston, MA, USA). Gel-contained protein samples were subjected to an in-gel digestion with 12,5 ng/µl sequencing-grade trypsin (Promega, Madison, USA) in 100 mM ammonium bicarbonate, overnight, at 37 °C, after which the resulting peptides were extracted with 100

mM ammonium bicarbonate and acetonitrile and lyophilized. Samples were resuspended in 5% acetonitrile, 5% formic acid and then directly injected into a LC/MS system encompassing a micro-autosampler, a Survey high performance LC (HPLC) pump and a Proteome X (LTQ) mass spectrometer (all acquired from Thermo Finnigan, San Jose, CA, USA). The LC system featured a reversed phase column, packed in-house using C18 Magic packing material (3 mm, 200 Å; Michrom Bioresources, Auburn, CA, USA), and PicoTip Emitters (New Objective, Woburn, USA). In the LC/MS system, peptides were eluted with 0,1 % formic acid in acetronitrile, using a 30 min linear gradient of 8 % to 34 % acetonitrile, and then applied to the mass spectrometer by electrospray ionization. MS spectra were acquired by the Proteome X (LTQ) mass spectrometer in a data-dependent fashion, with the 6 top abundant species being selected for automated fragmentation. Phosphorylated peptides were detected by the characteristic mass shift of 80 or 98 m/z that corresponds to the neutral loss of a phosphate group. When the fragmentation of a MS spectrum resulted in an immediate neutral loss mimicking this mass shift in the MS2 (MS/MS), then a MS3 (MS/MS/MS) fragmentation was performed on the resulting MS2 peak. The mass spectrometric data obtained was searched against the human international protein index database (IPI human 336) using the protein identification software Mascot (version 2.2.04; Matrix Sciences, London, UK) according to the appropriate search criteria necessary for the detection of phosphorylation. Spectra sequence identified by Mascot to be phosphorylated were validated manually to guarantee proper recognition of phosphorylated amino acid position and to access overall quality of the data obtained.

Generation of the phospho-specific antibody

Custom production of the phospho-specific anti-Patx3 antibody was carried out by Eurogentec (Seraing, Belgium). A atx3 peptide containing amino acids 8-20 and a phosphate group conjugated to S12 – KQEG-S(PO_3H_2)-LCAQHCLN – was synthesized and coupled with the highly immunogenic (Berzofsky and Berkower, 1993) keyhole limpet hemocyanin (KLH) protein carrier. This antigen was used for the immunization of two rabbits, the animals were bled and the responsiveness of serums was tested by Elisa. Phospho-specific antibody purification was performed on the serum of the best responding animal through a series of affinity chromatography steps involving two columns: the first containing the modified peptide and the second containing the unmodified peptide. The first chromatography captured antibodies against both the phosphorylated and non-phosphorylated peptide, while the flow-through of the second chromatography was specific only against the peptide containing the modified serine. The antibody was provided in PBS 0,1 % BSA (bovine serum albumin), 0,01 % thimerosal, and kept at –20 °C after adding 1 volume of glycerol and aliquoting.

Mammalian cell line culture and transfection

Two cell lines were used in the experiments presented in this study: the fibroblast-like COS-7 cell line derived from African green monkey kidney and the HeLa cell line, derived from human cervical cancer. Both were cultured in DMEM pH 7,2, supplemented with 44 mM $NaCO_3$, 10 % (v/v) FBS and 1 % (v/v) penicillin-streptomycin. Cells were maintained in 75 cm^2 flasks according to standard procedures, in an incubator at 37 °C, with a humidified atmosphere containing 5 % CO_2.

One day prior to transfection, fully confluent cells were diluted and seeded onto either 100 mm diameter culture plates (1:6) or 6 well culture plates (1:5-6), depending on the experiment. After 18-24 h of growth, cells were transiently transfected using the Lipofectamine® Transfection Reagent (Life Technologies, a part of Thermo Fisher Scientific, Waltham, MA, USA), according to the manufacturer's indications. Cells cultured in 6 well plates were transfected with 2 µg of plasmid DNA and 12,5 µl of transfection reagent, while for cells in 100 mm dishes 10 µg of DNA and 25 µl of reagent were used instead. Expression was left to occur for 24-48 h before extracts were prepared.

Primary cortical neuron culture

Cortices of Wistar rat embryos with 18 days were dissected and treated for 15 min, at 37 °C, with 0,06 % (w/v) trypsin in calcium- and magnesium-free Hank's balanced salt solution (HBSS; 5,36 mM KCl, 0,44 mM KH_2PO_4, 137 mM NaCl, 4,16 mM $NaHCO_3$, 0,34 mM $Na_2HPO_4{\cdot}2H_2O$, 5 mM glucose, 1 mM sodium pyruvate, 10 mM 4-(2-hydroxyethyl)-1-piperazineethanesulfonic acid (HEPES) and 0,001 % (w/v) phenol red). Tissue was washed 6 times with HBSS and cells were finally resuspended in neuronal plating medium (MEM supplemented with 10 % (v/v) horse serum, 0,6 (w/v) % glucose and 1 mM sodium pyruvate) and passed through a 0,2 µm filter.

Cells were then seeded in high, medium or low density, according to the experimental objectives. For high-density cultures, cells were seeded onto 6 well culture plates coated with poly-D-lysine (0,1 mg/ml), to a density of 9 x 10^5 cells/well. Medium-density cultures were prepared in poly-D-lysine-coated 15 mm coverslips, by plating 2,5 x 10^5 cells/well onto coverslip-containing 12 well culture plates. For both types, 2-4 h after platting medium was substituted by Neurobasal medium supplemented with 2 % (v/v) SM1, 0,5 mM glutamine and 0,12 mg/ml gentamycin. In the case of the low-density cultures (Banker cultures), cells were plated on poly-D-lysine-coated 18 mm coverslips, in 60 mm culture plates, to a density of 3,25 x 10^5 cells/plate. After 2-3 h, coverslips were turned over an astroglial feeder layer (grown in MEM supplemented with 10 % (v/v) horse serum, 0,6 % (w/v) glucose and 1 % (v/v) penicillin-streptomycin), kept apart by wax dots, and maintained in Neurobasal medium supplemented with SM1.

After 3 days *in vitro* (DIV), cultures were treated with 5 µM cytosine arabinoside in order to prevent the overgrowth of glial cells. High- and medium-density cultures were fed once a week, by replacing 1/3 of the culture medium with fresh medium. Low-density cultures were fed twice a week with 1 ml of fresh medium. Cortical neuron cultures were kept in an incubator at 37 °C, with a humidified atmosphere containing 5 % CO_2, up to 15 DIV.

Transfection of cortical neurons

Expression plasmids were transfected into 9-10 DIV cortical neurons by a calcium phosphate transfection procedure adapted from a previously described protocol (Jiang *et al.*, 2004). In order to generate DNA complexes, 2,5 M $CaCl_2$ in 10 mM HEPES was added drop-wise to the DNA solution, for a final concentration of 250 mM $CaCl_2$. The resulting solution was added to an equal volume of HEPES-buffered transfection solution (274 mM NaCl, 10 mM KCl, 1,4 mM Na_2HPO_4, 11 mM dextrose and 42 mM HEPES, pH 7,2) and the mixture was then stirred and incubated at room temperature (RT) for 30 min in order for the complexes to form.

Before adding the complexes, conditioned medium of high- or medium- density cultures was reserved except for ~1/3 of the volume, to which kynurenic acid was added to a final concentration of 2 mM, in order to block the ionotropic glutamate receptors. In the case of the low-density cultures, the coverslips were transferred to 12 well culture plates containing conditioned medium with kynurenic acid. The DNA complexes were added drop-wise to each well (10 µg of DNA for high-density and 4 µg for medium- and low-density cultures) and cells were incubated for 1,5 h. After that, transfection medium was substituted by fresh culture medium containing 2 mM kynurenic acid and slightly acidified with HCl (~5 mM), in order to destroy the DNA complexes. After a 15 min incubation, medium of high- and medium-density cultures was substituted by the reserved conditioned medium and the coverslips of low-density cultures were moved back into the astroglial feeder layer-containing plate.

Expression was left to occur for a maximum of 5 DIV under normal cell culture incubation conditions.

Chemical stimuli

In some experiments, transfected COS-7 cells were subjected to chemical stimulation with particular compounds aimed at enhancing phosphorylation through activation of kinases or inhibition of phosphatases: 20 nM OA for 16 h (Dorval and Fraser, 2006), 5 mM SOV for 30 min (Martin *et al.*, 2006), 200 nM PMA for 20 min (following the recommendations of the producer), 10 µM forskolin (FSK) for 20 min (Gomes *et al.*, 2004) or 300 nM staurosporine (STS) for 3 h (Lobo *et al.*, 2011). In other experiments using COS-7 cells, HeLa cells, or cortical neurons, enhancement of endogenous phosphorylation was achieved by treatment with a homemade cocktail of phosphatase inhibitors consisting of 0,5-10 µM OA, 5 mM Na_3VO_4 and 5

mM NaF, for 45-60 min. All concentrations are final and were selected attending to the manufacturer's instructions and standard procedures. Treatments were carried out under regular culture conditions in the period of incubation before cell harvesting.

OA and STS were acquired from Calbiochem, as part of Merck KGaA (Darmstadt, Germany), and SOV was acquired from Calbiochem as part of Merck Millipore (Billerica, MA, USA), PMA from Biomol, as part of Enzo Life Sciences (Lausen Switzerland), FSK from Tocris Bioscience (Bristol, UK), and NaF from Merck (Darmstadt, Germany).

Table IV: Compounds used to interfere with phosphatase or kinase activity

Compound	Effect on phosphorylation (according to manufacturers' indications)
Okadaic acid (OA)	Inhibits PP1 and PP2A
Sodium orthovanadate (SOV – Na_3VO_4)	Inhibits tyrosine and alkaline phosphatases
Sodium fluoride (NaF)	Inhibits a wide spectrum of serine/threonine and acidic phosphatases
Staurosporine (STS)	Inhibits a wide spectrum of protein kinases, including PKA, PKC and CaMK
Phorbol 12-myristate 13-acetate (PMA)	Stimulates PKC
Forskolin (FSK)	Stimulates PKA

Other abbreviations: PP1, protein phosphatase 1; PP2A, protein phosphatase 2A; PKA, protein kinase A; PKC, protein kinase C; CaMK, calcium/calmodulin-dependent protein kinase.

Bacterial expression and purification of recombinant proteins

Escherichia coli BL21(DE3)-SI cells were transformed with the pDEST17 plasmids encoding 6His-atx3 or 6His-TEVg-atx3 (WT and S12D forms) through heat shock. Cells were grown at 37 °C in NaCl-free Lysogeny Broth (LB; 10 % (w/v) triptone, 5% (w/v) yeast extract) with 100 µg/l ampicillin and 0,2 % (w/v) glucose until the optical density (absorbance at 600 nm) reached 0,4-0,8, at which point expression was induced through addition of NaCl to a final concentration of 300 mM. Expression was left to occur for 3 h, at 30 °C. The cells were then collected by centrifugation (10.500 x g, 20 min, 4 °C) and resuspended in imidazole buffer (20 mM sodium phosphate buffer pH 7,5, 0,5 M NaCl and 10 mM imidazole) containing 50 mg/l lysozyme and conserved at –20 °C.

Before purification, serine protease inhibitor PMSF was added to a final concentration of 1 mM and cell extracts were digested with 5 µg/ml DNAse I, in the presence of 10 mM $MgCl_2$, for 1 h, in ice, after which the samples were cleared of their insoluble fraction by centrifugation (17.400 x g, 40 min, 4 °C). The resulting supernatant was applied to a 5 ml

HisTrap HP column (Amersham Biosciences, Carnaxide, Portugal) and eluted by rise of the imidazole concentration to 250 mM imidazole. Atx3-containing fractions were pooled and loaded into a Hiprep 26/60 Sephacryl S-200 High Resolution column (GE Healthcare, Carnaxide, Portugal) equilibrated in buffer A (20 mM HEPES pH 7,5, 200 mM NaCl, 1 mM DTT, 1 mM EDTA, 5 % (v/v) glycerol). Elution was carried out at 4 °C with a flow rate of 0,5 ml/min and resulting fractions were analyzed by SDS-PAGE followed by Page blue staining and analytic size-exclusion chromatography in a Superose 12 10/300 GL column (GE Healthcare, Carnaxide, Portugal). The purest fractions were pooled and concentrated on Vivaspin15 centrifugal concentrators (cutoff of 10 kDa, Vivascience, Sartorius). Afterwards, samples were immediately frozen in liquid nitrogen and stored at –80 °C. Protein concentration was assessed by measurement of the absorbance at 280 nm using extinction coefficients of 36,160 $M^{-1}{\cdot}cm^{-1}$ and 31,400 $M^{-1}{\cdot}cm^{-1}$, for 6His-atx3 and 6His-TEVg-atx3, respectively.

Production of lentiviral vectors

Lentiviral vectors encoding human full-length expanded atx3 (WT and mutants S12D and S12A) or shRNA-atx3 were produced in HEK 293T cells using the four-plasmid system described by de Almeida and collaborators (de Almeida *et al.*, 2002). HEK 293T cells (cultured as described previously for the COS-7 and HeLa cells) were plated into 100 mm dishes in a density of 4 x 10^6 cells/dish and subjected the following day to transient calcium phosphate transfection. DNA complexes were formed by mixing 0,5 M $CaCl_2$ with the DNA constructs (for each plate: 13 µg of the pCMVDR-8.92 packaging construct, 3,75 µg of pMD2G, 3 µg of pRSV-Rev and 13 g of SIN-W-PGK-ATX3 72Q WT, S12D or S12A or shAtaxUNIV), to a final concentration of 0,25 M $CaCl_2$. The solution was stirringly mixed with an equal volume of HEPES-buffered solution (280 mM NaCl, 1,5 mM Na_2HPO_4, 100 mM HEPES, pH 7,1) and 1 ml of DNA complexes was added to each dish. Cells were incubated at 37 °C, in a humidified atmosphere containing 3 % CO_2, for 6h, after which transfection media was replaced with fresh culture.

After 48 h of culture incubation at 37 °C, 5 % CO_2, the supernatants were collected, filtered (0,45 µm Stericup® Filter Unit, Merck Millipore, Billerica, MA, USA), concentrated by ultracentrifugation (90 m, 19.000 x g, 4 °C) and resuspended in 1% (w/v) BSA PBS. When the viral particles were aimed at animal striatal injections, this was followed by another ultracentrifugation step before final resuspension in the same solution. The content level of batches was assessed by p24 antigen ELISA (Retrotek HIV-1 p24 Antigen ELISA, Zepto Metrix Corporation, Buffalo, NY, USA) and stocks were stored at –80 °C.

Infection of cortical neurons – ataxin-3 silencing

High-density cortical neuron cultures with 8 DIV were infected with lentiviral particles encoding shRNA-atx3. On the day prior to infection, neurons were fed by removing 500 µl of culture medium and adding 750 µl of fresh medium. On the occasion of the infection, the conditioned medium from each culture well was reserved except for 1 ml, to which hexadimethrine bromide was added to a final concentration of 8 µg/ml. Viral particles were administered at a ratio of 1 ng of p24 antigen/10^5 cells. The following day, infection medium was substituted by the reserved conditioned medium and 1 ml of fresh Neurobasal medium, supplemented with SM1. Expression was left to occur for 6 days under normal culture conditions.

Preparation of cell extracts

Cell cultures were briefly washed with cold PBS (137 mM NaCl, 2,7 KCl, 1,8 mM K_2PO_4, 10 mM $Na_2HPO_4{\cdot}H_2O$, pH 7,4) and extracts were prepared by adding radioimmunoprecipitation (RIPA) buffer (50 mM Tris, 150 mM NaCl, 5 mM EGTA, 1 % (v/v) Triton X-100, 0,5 % (w/v) sodium deoxycholate, 0,1 % (w/v) SDS, pH 7,5; or, alternatively, 10 mM Tris-HCl pH 7,2, 150 mM NaCl, 5 mM EDTA, 0,1 % (v/v) Triton X-100, 1 % (w/v) sodium deoxycholate, 0,1 % (w/v) SDS) supplemented with protease inhibitors (10 µg/ml CLAP, 1 mM DTT and 0,1 mM PMSF) and scraping cells on ice. Buffer volume depended on culture size: 100-200 µl/well for 6 well plates and 500 µl for 100 mm dishes. Depending on the objectives, the RIPA buffer would be also supplemented with phosphatase inhibitors 5 mM NaF, 2 mM Na_3VO_4 and 1 µM OA or, alternatively, a commercial cocktail of phosphatase inhibitors (Roche Applied Science, Penzberg, Germany). Some extracts from COS-7 cells were prepared in the same way, but using instead immunoprecipitation buffer (IPB; 20 mM Tris-HCl pH 7,0, 100 mM NaCl, 2 mM EDTA, 2 mM EGTA, 50 mM NaF and 1 mM Na_3VO_4) supplemented with 1 % (v/v) Triton X-100, 1 µM AO and protease inhibitors.

After scraping, cells were briefly sonicated with a probe sonicator for 1 min and total protein concentration was determined by the BCA method using the Pierce® BCA Protein assay kit as recommended by the manufacturer (Thermo Scientific, Rockford, USA). Cell extracts were kept frozen at –20 or –80 °C.

Lambda phosphatase reaction

COS-7 cell extracts prepared with RIPA buffer without phosphatase inhibitors were diluted to a concentration of 2,5 µg/µl and incubated with lambda phosphatase (New England

Biolabs, Ipswich, MA, USA) for 2 h, at 30 °C, under the buffering conditions suggested by the manufacturer. A total of 800 units of enzyme were used to digest 200 µg of protein. Reaction was stopped by adding 5x sample concentrated buffer (composition below) to the reaction mix. In these experiments, cell extracts that were not incubated with lambda phosphatase were prepared in RIPA buffer supplemented with a commercial cocktail of phosphatase inhibitors (Roche Applied Science; Penzberg, Germany).

SDS-PAGE and Western blot

Samples destined for SDS-PAGE were denatured by adding 2x (125 mM or 250 mM Tris-HCl pH 6,8, 20 % (v/v) glycerol, 4 % (w/v) SDS, 200 mM DTT and ~0,01 % (w/v) bromophenol blue) or 5x concentrated sample buffer (625 mM Tris-HCl pH 6,8, 50 % (v/v) glycerol, 10 % (w/v) SDS, 500 mM DTT and ~0,01% (w/v) bromophenol blue) and heating them for 5 min at 95 °C. Depending on the experiment, 35-150 µg of total protein were subjected to electrophoresis, keeping the same protein amount for every lane in any particular experiment, except otherwise noted. Samples were loaded into 4 % (w/v) bis-acrylamide stacking gels (156 mM Tris-HCl pH 6,5 with 0,2 % (w/v) SDS or 125 mM Tris-HCl pH 6,8 with 0,1 % (w/v) SDS) and separated in 7,5, 10, 12,5 or 15 % (w/v) running gels (500 mM Tris-HCl pH 8,8 with 0,2 % (w/v) SDS or 375 mM Tris-HCl pH 8,8 with 0,2 % (w/v) SDS), depending on the intended degree of molecular weight separation. Running was carried out in Mini-PROTEAN® 3 Electrophoresis Cell systems or Mini-PROTEAN® Tetra Cell systems (Bio-Rad, Amadora, Portugal), according to standard proceedings. After the desired separation was achieved, proteins were electrotransfered overnight (40 V) into polyvinylidene difluoride (PVDF) membranes (Merck Millipore, Billerica, MA, USA), in a Trans-Blot® Electrophoretic Cell (Bio-Rad, Amadora, Portugal) system, at 4 °C. One of three molecular weight standards was separated along with the samples: the Precision Plus Portein™ All Blue Standard (Bio-Rad, Amadora, Portugal), the EZ-Run™ Pre-Stained *Rec* Protein Ladder (Fisher BioReagents, Loures, Portugal) or the NZYColour Protein Marker II (NZYTech, Lisboa, Portugal).

Membranes were blocked for 1-2 h with Tris-buffered saline (20 mM Tris and 137 mM NaCl, pH 7,6) containing 0,1 % (v/v) Tween 20 (TBS-T) and 5 % (w/v) low-fat dry milk. Incubation with the primary antibodies, diluted in 0,5 % (w/v) low-fat dry milk TBS-T, was carried out for 1-2 h at RT, or overnight at 4 °C (details are presented in the Antibodies section above). Membranes were washed with 0,5 % (w/v) low-fat dry milk TBS-T (3 times, 10 min each) and then incubated with the appropriate alkaline phosphatase-conjugated secondary antibodies diluted in the same solution. After a final wash, membranes were developed using Enhanced Chemifluorescence substrate (ECF; GE Healthcare, Carnaxide, Portugal) and scanning was performed using a Storm 860 Gel and Blot Imaging System (Amersham Biosciences, Buckinghamshire, UK) or a VersaDoc Imaging System Model 3000 (Bio-Rad, Amadora, Portugal). In the case of the anti-Patx3 antibody, 5 % (w/v) low-fat dry milk TBS-T was used in every step, except for the last washing step, which used milk-free TBS-T instead.

When antibody reprobing was intended, membranes were incubated with 40 % (v/v) methanol for 30-45 min and stripped with 0,2 mM NaOH for 15 min, before blocking again and labelling with antibodies as described above.

Densitometric analysis of Western blot protein bands was performed using ImageJ (National Institute of Health, USA).

Protein structure analysis, sequence alignment and molecular weight estimation

JD and UIM1-UIM2 tertiary structures were obtained from the Research Collaboratory for Structural Bioinformatics (RCSB) Protein Data Bank (PDB; identification codes: 1YZB, 2JRI and 2KLZ) and structural analysis and modelling was performed using the PyMOL Molecular Graphics System software (DeLano Scientific, San Carlos, USA).

Amino acid sequences of atx3, atx3L, Josephin-1 and Josephin-2 were obtained from the NCBI (USA) or UniProt (UniProt, 2014) databases. Sequence alignment was performed with the Crustal Omega online tool from the European Molecular Biology Laboratory – European Bioinformatics Institute (EMBL-EBI; Hinxton, UK) and prepared with ESPript 3.0 (Robert and Gouet, 2014). Details of the sequences used in the alignment are given in the respective figure. Molecular weight estimation was performed with the Protein Molecular Weight Calculator online tool from Science Gateway, using the reference amino acid sequences of human, mouse and rat atx3 obtained from UniProt (codes P54252, Q9CVD2 and O35815, respectively).

Activity assays with Ub-AMC

Bacterially expressed 6His-atx3 or 6His-TEVg-atx3 (WT and S12D forms) was incubated with 0,5 µM Ub-C-terminal 7-amino-4-methylcoumarin (Ub-AMC; Boston Biochem, Cambridge, MA, USA), in the presence of Ub-AMC assay buffer (20 mM HEPES pH 7,5, 5 % (v/v) glycerol and 1 mM EDTA), 0,1 mg/ml BSA and 10 mM DTT, in 96 well plates. Reaction was started by addition of atx3 to the reaction mixture, for a final concentration of 0,2 µM, and left to occur at 30 °C in a SpectraMax Gemini EM Fluorescence Microplate Reader (Molecular Devices, Sunnyvale, CA, USA). Product formation was continually assessed by fluorescence recording (excitation – 380 nm; emission – 460 nm), for a maximum of 40 min. Three independent experiments were performed for both 6His-atx3 and 6His-TEVg-atx3, each including 2-4 replicates.

For each replicate, initial reaction velocity was calculated as the slope of the trend line traced based on the fluorescence values (relative fluorescence units – RFU) of the first 2 min of reaction, after subtraction of the value of the negative control (buffer and Ub-AMC only, with an additional 0,2 M BSA). The obtained velocity values were normalized to the mean WT velocity of the respective experiment.

Activity assays with polyUb chains

Bacterially expressed 6His-atx3 (WT and S12D forms) was incubated with 250 nM K48- or K63-linked chains (Boston Biochem, Cambridge, MA, USA) of 6 Ub monomers, after mixing (~75 % of final reaction volume) with 50 mM HEPES, 0,5 mM EDTA, 0,1 µg/ml ovalbumin and 1 mM DTT. Reaction was started by addition of atx3 for a final concentration of 100 nM and left to occur for 20 h, at 37 °C. Samples (10 µl) were taken from the reaction mixture at different time points (0, 2, 5 and 20 h) and immediately denatured by adding 2x concentrated sample buffer. Formation of lower-molecular weight Ub species was assessed by Western blot.

Active deubiquitinase-labelling assays with Ub-VS

Extracts from COS-7 cells (cultured in 6 well culture plates and transiently transfected with GFP-atx3 constructs) were prepared as above, but using instead 170 µl of Ub-vinylsulfone (Ub-VS) reaction buffer (50 mM Tris-HCl pH 7,4, 250 mM sucrose and 5 mM $MgCl_2$), supplemented with 1 mM ATP, 1 mM DTT and 1 µM OA, and frozen at –20 °C. On the occasion of the assays, cells were thawed, centrifuged at 16.100 x g, 4 °C, for 10 min, and Ub-VS (HAUbVS; Enzo Life Sciences, Farmingdale, NY, USA) was added to the suitable volume of soluble supernatants, for a final concentration of 12, 24 or 45 ng/µl Ub-VS. Binding was left to occur for varying time periods, up to a maximum of 90 min, at RT. Samples (10 or 20 µl) were collected at varying time points and immediately denatured by addition of 2x concentrated sample buffer and heating for 5 min at 95 °C. Molecular size deviation caused by conjugation of GFP-atx3 to Ub-VS was analyzed by Western blot.

Immunocytochemistry and fluorescence microscopy

Transfected cortical neurons with 14-15 DIV (or 12-13 DIV, in the case of the aggregation experiments) were fixed with 4 % paraformaldehyde / 4 % sucrose (w/v) in PBS for 15 min at RT and permeabilized for 5 min at 4 °C with 0,25 % (v/v) Triton X-100 in PBS. Unspecific binding sites were blocked by incubation with 10 % (w/v) BSA in PBS, for 30 min at 37 °C. Neurons were then incubated overnight at 4 °C with the primary antibodies diluted in PBS containing 3 % (w/v) BSA (antibody details are provided in the Antibodies section above), and then washed with PBS (6 times, 10 min each). After incubation with the secondary antibodies diluted in 3 % (w/v) BSA PBS for 45 min at 37 °C, coverslips were washed again and finally mounted using fluorescent mounting medium (Dako, Glostrup, Denmark).

Quantification of GFP-atx3 aggregate-containing neurons (medium-density cultures) was performed by manually scanning coverlips and observing the GFP fluorescence with a Zeiss Axiovert 200M microscope (Carl Zeiss AG, Oberkochen, Germany) using a 63x oil objective (Plan-Apochromat, 1,4 numeric amplitude).

Images of GFP-atx3-expressing neurons used for the Sholl analysis (low-density cultures) were acquired using a Zeiss Axiovert 200M microscope and a 20x objective (LD-PlanNeofluar, 0,4 numeric amplitude). Tracing of the cell body and dendrites was drawn based on the GFP signal, using the Neurolucida software. Sholl analysis with 10 µm distant circles centered in the cell body was performed with the Neurolucida Explorer software (both from MBF Bioscience, Williston, VT, USA).

Synapse observation and imaging was performed with a Zeiss Cell Observer microscope (Carl Zeiss AG, Oberkochen, Germany) with a 63x oil objective (Plan-Apochromat, 1,4 numeric amplitude), after randomly selecting dendritic tracts (minimum 10 µm) in GFP-atx3-expressing neurons (low-density cultures). Image analysis was performed using the Fiji software (Schindelin *et al.*, 2012), for quantification of synaptic puncta intensity, area and number, from manually thresholded images. Instances of colocalization of pre and postsynaptic markers were quantified as functional synapses.

For each individual experiment, cells were cultured and immunocytochemically processed on the same occasion and images were acquired with the same settings. Sholl analysis and quantification of aggregates and puncta were performed blindly to condition.

Generation of the lentiviral rat model

Adult male Wistar rats with ~200 g (Charles River Laboratories, Wilmington, MA, USA) were stereotaxically injected for delivery of lentiviral vectors to the striatum, following the procedure described by (Alves *et al.*, 2008b). Prior to injection, viral stocks were thawed on ice and resuspended by vortexing. Animals were anesthetized by intraperitonial injection of a mixture of 75 mg/kg ketamine and 10 mg/kg xylazine, positioned on an appropriate stereotaxic frame and surgically prepared for injection. For each rat, one injection was performed in each hemisphere: lentiviral particles enconding SIN-W-PGK-ATX3 72Q WT were injected in the left hemisphere and particles encoding SIN-W-PGK-ATX3 72Q S12D or S12A were injected in the right one. The coordinates used (with bregma as reference) were: 0,5 mm rostral to bregma, 3,0 mm lateral to midline and 5 mm ventral from the skull surface, with the mouth bar set at 0,0 mm. A total of 400.000 ng of p24 antigen were administered in each hemisphere (2 µl, 0,2 µl/min) using a 10 µl Hamilton syringe (Bonaduz, GR, Switzerland) and an automatic injector (Stoelting Co., Wood Dale, IL, USA). The syringe needle was left in place for 5 min after injection, to allow diffusion and minimize backflow, before removing it and suturing the animals' skin.

Animals were housed in a temperature-controlled room and maintained on a 12 h ligh/dark cycle. Food and water were supplied *ad libitum* and proceedings were executed in accordance with European Union Directive 2010/63/EW.

Histological processing

Four weeks after injection, animals were terminally anesthetized with 80 mg/kg sodium pentobarbital (intraperitonially) and transcardially perfused with 4 % (w/v) paraformaldehyde in PBS, pH ~7. Whole brains were removed and incubated for ~48 h in 20 % (w/v) sucrose PBS. Tissue was then frozen at –80 °C and 25 µm coronal sections of the striatal region were cut using a cryostat-microtome (Leica CM3050S, Leica Microsystems Nussloch GmbH, Nussloch, Germany). Slices were stored at 4 °C, free-floating in 0,02 % (w/v) sodium azide PBS inside 48 well plates, until further use.

Immunohistochemistry

Immunohistochemical labelling was started by inhibiting endogenous peroxidase activity by incubating sections with 0,1 % (v/v) phenylhydrazine in PBS, for 30 min at 37 °C. Slices were washed with PBS (3 times, 5, 5 and 10 min, respectively) and then blocked by incubation with 10 % (v/v) normal goat serum, diluted in 0,1 % (v/v) Triton X-100 PBS, for 1-2 h, at RT. Labelling with the primary antibody, diluted in blocking solution, was performed overnight, at 4 °C (details are provided in the Antibodies section), and followed by another washing step with PBS (3 times, 5, 10 and 10 min, respectively). The suitable biotinylated secondary antibody, diluted in blocking solution, was incubated at RT for 2h, after which slices were washed as before. Signal was developed by incubating slices with the VECTASTAIN Elite Avidin-Biotin-Peroxidase Kit at RT, for 30-40 min, followed by washing with PBS and incubation with the 3,3´-diaminobenzidine Peroxidase Substrate Kit. Both kits were acquired from Vector Laboratories (Burlingame, CA, USA) and used according with the manufacturer's instructions. Sections were finally mounted, dehydrated using a sequence of 75, 96, 100 % (v/v) ethanol and xylene, and coverslipped with the Eukitt mounting medium (O. Kindler GmbH & CO., Freiburg, Germany). For the slices of one animal where abnormal immunoreactivity of the anti-atx3 was observed, immunohistochemical processing was performed using the Mouse on Mouse Basic Kit instead, following the instructions of the supplier (Vector Laboratories).

Striatal slices were analyzed and imaged with a Zeiss Axiovert 200M microscope, at 5x (Fluar, 0,25 numeric amplitude) and 20x magnifications (LD-PlanNeofluar, 0,4 numeric amplitude). Composite images of complete aggregate-containing or dopamine- and cyclic AMP-regulated phosphoprotein of 32 kDa (DARPP-32)-depleted regions were automatically acquired using the MozaiX function of the AxioVision software.

Quantitative analysis of immunohistochemistry images

Quantification of atx3-positive aggregates and determination of the area of the DARPP-32 depletion was made in 7-11 slices for each animal, spread over the anterior-posterior extent of the striatum and separated by 175 μm (25 μm x 7 slices).

Counting of atx3-positive aggregates was performed on 20x-magnified images of each hemisphere using ImageJ. After manually thresholding images so that the recognizable atx3-positive accumulations were included in the examination, particles larger than 3 μm^2 were automatically analyzed and counted (scale – 2 pixel/μm; Alves *et al.*, 2008a). These methods were performed blindly to hemisphere side. Estimative calculation of the total number of aggregates in the entire striatum was achieved by multiplying the number of aggregates in each section by 8, since each slice quantified was 7 sections apart from each other, and adding all values. When comparing the quantity of aggregates between the two hemispheres, two percentages were calculated for each animal brain, representing the total number of aggregates in one hemisphere as a ratio of the total number of aggregates in the two hemispheres.

Determination of the area of the DARPP-32-depleted regions in the two hemispheres of each slice was performed on 5x-magnified images, using ImageJ to manually define the regions with decreased antibody reactivity and quantify their area (scale – 0,5 pixel/μm). This analysis was performed blindly to hemisphere side. Total depleted volume was estimated by multiplying the area by 200 μm – the total thickness of 8 slices – and adding all values (Alves *et al.*, 2008a). When comparing the volume of the DARPP-32-depleted region between the two hemispheres, two percentages were calculated for each animal brain, representing the total volume in one hemisphere as a ratio of the sum of the volumes from the two hemispheres.

Statistical analysis

Statistical analysis was performed using the GraphPad Prism 5 software (GraphPad Software, La Jolla, CA, USA). Comparison between two conditions was performed with the Student's t-test when the values of both samples presented a Gaussian distribution or with the Mann-Whitney test in the cases were values did not pass normality tests. Multiple comparisons were performed with two-way analysis of variance (ANOVA), followed by Bonferroni post-hoc tests.

Chapter 3

Phosphorylation of serine 12 of ataxin-3: validation and functional consequences

Chapter 3 – Phosphorylation of serine 12 of ataxin-3: validation and functional consequences

3.1 Introduction – Detection of serine 12 as a phosphorylation site of ataxin-3 by mass spectrometry

The present study sprouted from a previously performed MS analysis of atx3, directed at the detection of novel phosphorylation sites (Matos, 2009). MS techniques are customarily utilized in studies that aim at mapping phosphorylated amino acids (Dephoure *et al.*, 2013; Macek *et al.*, 2009) and have already been successfully employed in the examining of phosphorylation of polyQ-containing proteins such as htt and the AR (Aiken *et al.*, 2009; Gioeli *et al.*, 2006; Guo *et al.*, 2006; Schilling *et al.*, 2006). MS directed at protein mapping starts by a proteolytic digestion of the purified protein of interest, yielding peptides that are then chromatographically separated, ionized and analyzed by a mass spectrometer. Tandem MS allows the measuring of the mass-to-charge (m/z) ratio and intensity of the intact peptides (generating a MS1 spectrum), at the same time subjecting those peptides to a gas-phase fragmentation and consequent generation of fragment ions that are also detected by the spectrometer (MS/MS or MS2 spectrum) (Macek *et al.*, 2009). Algorithmic treatment of the data collected in the spectra allows the identification and sequencing of peptides through sequence database matching (Dephoure *et al.*, 2013). MS can be used to detect and map PTMs and several possible approaches exist for the analysis of phosphorylated peptides. Conjugation of a phosphate group (HPO_3) to a peptide causes an increase in mass of 80 Da and the detection of this mass shift in fragment ions allows the identification of phosphorylation sites (Witze *et al.*, 2007). Additionally, during fragmentation, phosphorylated peptides often lose phosphate as a neutral species; a *neutral loss* that generates fragments with a mass decreased by –80 (HPO_3) or –98 Da (H_3PO_4), which can be further isolated, fragmented and analyzed by the mass spectrometer (MS/MS/MS or MS3 spectrum). Treatment of the obtained spectra also allows the mapping of phosphorylation sites (Witze *et al.*, 2007). These methods are based on the detection of positive fragment ions, but detection of negatively charged reporter ions can also inform about phosphorylation. Proton removal during ionization of peptides containing

phosphorylated residues may yield phosphate-derived precursor ions (PO_3^-) of –79 Da that are indicative of the presence of phosphorylated peptides, whose identity can be then determined by positive ion MS2 (Macek *et al.*, 2009; Witze *et al.*, 2007).

In order to identify phosphorylated amino acids of atx3 that would be possibly relevant for the functionality of the human protein, the samples subjected to MS consisted of GFP-tagged human atx3 with 28Q (isoform MJD1a), transiently expressed in the human HEK 293FT cell line. In order to enhance phosphorylation, cells were treated with the protein kinase C (PKC) stimulator phorbol 12-myristate 13-acetate (PMA), or with sodium orthovanadate (SOV) or okadaic acid (OA), two protein phosphatase inhibitors (Table IV in Chapter 2). GFP-atx3 28Q was purified by immunoprecipitation with an anti-GFP antibody and by posterior electrophoretic separation in polyacrylamide gel (Figure 10A); the bands corresponding to the full-length fusion protein were excised and subjected to a tryptic digestion, and the resulting GFP-atx3 28Q-derived peptides were separated by reverse-phase HPLC and directly electrosprayed into the mass spectrometer. The analysis performed was directed at detecting neutral losses of phosphate and obtain the MS3 spectra of the corresponding peptidic fragment product. This analysis would allow the detection and sequencing of phosphorylated peptides derived from human atx3.

The mass spectrometric examination of the GFP-atx3 28Q sample obtained from OA-stimulated cells revealed the presence of one phosphorylated peptide: Q9-EG-pS12-LCAQHCLNNLLQGEYFSPVELSSIAHQLDEEE-R45 (Figure 10B). Importantly, it identified for the first time serine 12 of atx3 as a phosphorylated amino acid residue. The fact that S12 was detected to be phosphorylated in HEK 293FT cells, under no pharmacological stimulus except for the inhibition of endogenous phosphatases, indicates that this modification happens normally under the cell culture conditions used and suggests that S12 phosphorylation may be biologically relevant for human cells. The MS analysis did not yield any other phosphorylation sites in this or in the other GFP-atx3 28Q samples, but given the stochastic nature of the MS detection techniques and the variable results they yield, this observation cannot rule out the possible phosphorylation of other atx3 amino acid residues, such as the ones previously described (Fei *et al.*, 2007; Mueller *et al.*, 2009).

3.2 Detection of phosphorylated ataxin-3 in cell lines and neurons

Generation of the phospho-specific antibody anti-Patx3

Mass spectrometric detection of phosphorylated S12 in GFP-atx3 samples obtained from transfected cells is a strong indication that atx3 is normally phosphorylated at that site, under standard culture conditions. Nonetheless, given the originality of this observation, it would be important to confirm the modification using other techniques. The selection of such techniques could also be of radical significance in directing forthcoming experimental approaches aiming at understanding the biologic relevance of S12 phosphorylation. Production

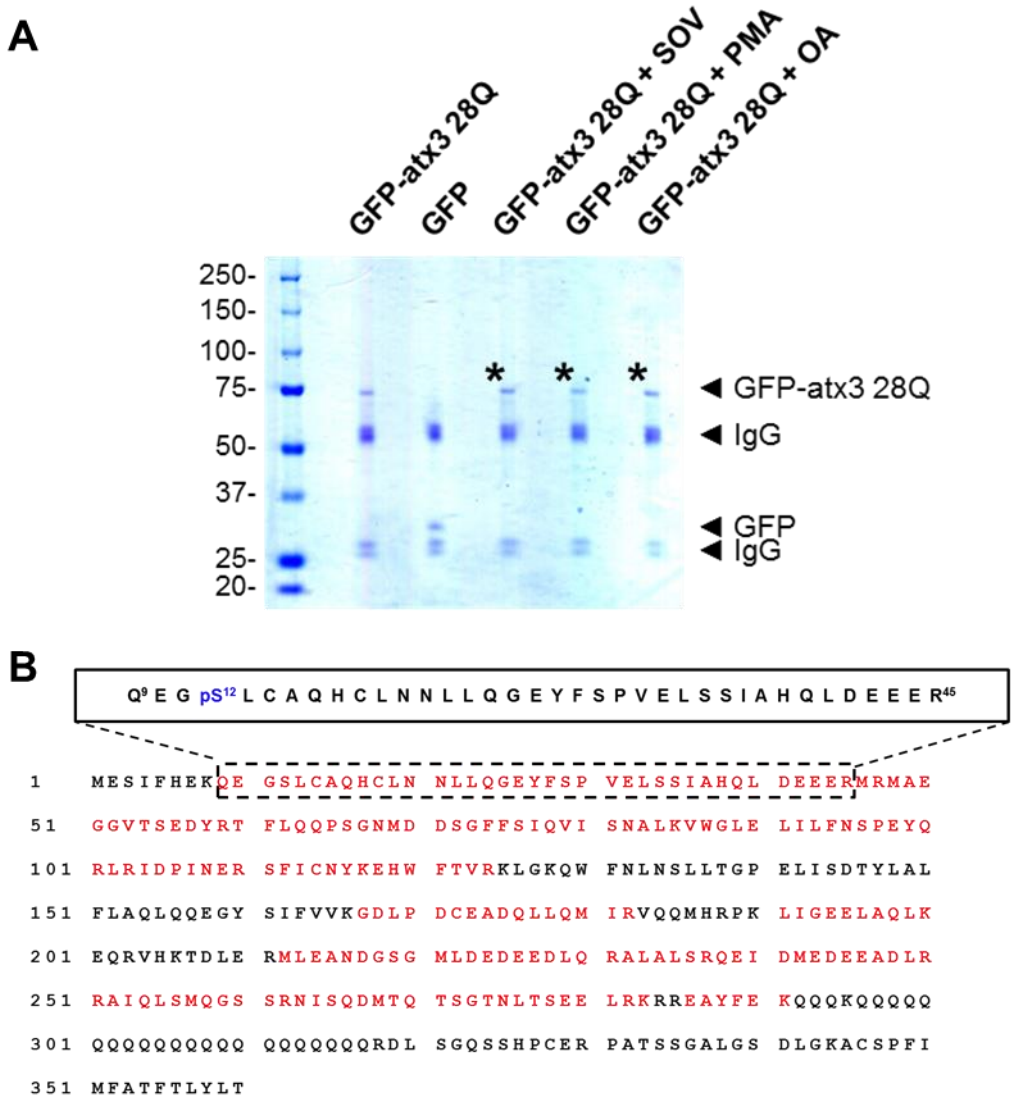

Figure 10: MS detection of S12 as a phosphorylation site of atx3. ***A*** HEK 293FT cells were transiently transfected with GFP-atx3 28Q and expression was left to occur for 24 h, during which time period cells were stimulated with phorbol 12-myristate 13-acetate (PMA), sodium orthovanadate (SOV) or okadaic acid (OA). GFP-atx3 28Q was then purified by immunoprecipitation using a monoclonal anti-GFP antibody and SDS-PAGE and the resulting gel was stained with Coomassie blue. Asterisk (*) represents GFP-atx3 28Q bands (~75kDa) subjected to posterior tryptic digestion and MS analysis. Bands of ~50 kDa and ~25 kDa are admitted to correspond to the heavy and light chains of the antibody (IgG). ***B*** LC-ES-MS detected one phosphorylated peptide in the protein sample prepared after OA stimulation and mapped the phosphorylation site to S12. Human atx3 isoform MJD1a amino acid sequence (NCBI accession number: AAB33571.1) is represented with the peptides covered by the MS analysis colored in red

of an antibody that specifically detects the phosphorylated S12 residue of atx3 presented itself as a promising approach, considering that such a tool would allow not only the confirmation of the results of the MS analysis by detecting atx3 phosphorylation at S12 in transfected mammalian cell lines, but would also permit expansion on that observation.

Generation of the antibody recognizing atx3 phosphorylated at S12 (anti-Patx3) was ordered to Eurogentec (Seraing, Belgium), a company specialized in manufacturing antibodies recognizing proteins with modified amino acid residues. The antibody was raised in rabbits, immunized against a peptide containing phosphorylated S12 and designed by the company based on atx3 amino acid sequence: KQEG-S(PO_3H_2)-LCAQHCLN (Figure 11). The peptide shares no significant homology with any other human, African green monkey, rat or mouse proteins, according to Basic Local Alignment Search Tool (BLAST) analysis (NCBI, USA). This fact decreased the probability of eventual unspecific reactivity with other targets. The generated polyclonal antibodies were purified so that only the fraction specifically recognizing the phosphorylated atx3 peptide was provided.

Detection of serine 12 phosphorylation with the anti-Patx3 antibody

The first approach to employ the anti-Patx3 phospho-specific antibody in confirming atx3 phosphorylation in mammalian cells was to probe extracts of COS-7 cells transfected with GFP-atx3 28Q by Western blot. Usage of GFP, a high molecular weight tag (27 kDa), would allow the distinction between the overexpressed GFP-atx3 and the possibly phosphorylated endogenous atx3 in these cells. Recombinant 6His-TEVg-atx3 produced in *Escherichia coli* was concurrently analyzed as a negative control, since it is widely accepted that the phosphorylation mechanisms of eukaryotes are not conserved (or are only poorly conserved and limited) in prokaryotes (Huang *et al.*, 2012; Macek *et al.*, 2009).

Western blot analysis of the COS-7 cell samples transfected with GFP-atx3 28Q revealed two discrete bands, with a difference of molecular weight of about 25 KDa (Figure 12A). This difference in size is similar to the difference between endogenous atx3 and GFP-atx3, leading to the assumption that the higher-weight band revealed by the anti-Patx3 corresponds to GFP-atx3 (~65 kDa) and the lower one to endogenous atx3 (~40 kDa). Furthermore, the higher band is not present in non-transfected cells, corroborating the idea that it corresponds to GFP-atx3. The absence of any band in the lane corresponding to the bacteria-derived protein indicated that the immunoreactivity observed is directed at phosphorylated species.

Along with COS-7 cells transfected and incubated under regular conditions, samples from transfected cells stimulated with compounds aimed at increasing protein phosphorylation levels were also analyzed by Western blot (Figure 12A). Two of these compounds – phosphatase inhibitors OA and SOV – were used with the objective of causing a general increase of phosphorylated species, so as to strengthen the phosphorylation signal. The other two compounds are activators of specific kinases: forskolin (FSK) activates protein kinase A (PKA), while PMA activates PKC. A possible increase in the phosphorylated atx3 signal elicited by one of them could be indicative of the involvement of the respective kinase in the pathways responsible for phosphorylating S12 of atx3. However, none of the stimuli was able to visibly increase the amount of phosphorylated GFP-atx3 or endogenous atx3, in COS-7 cells.

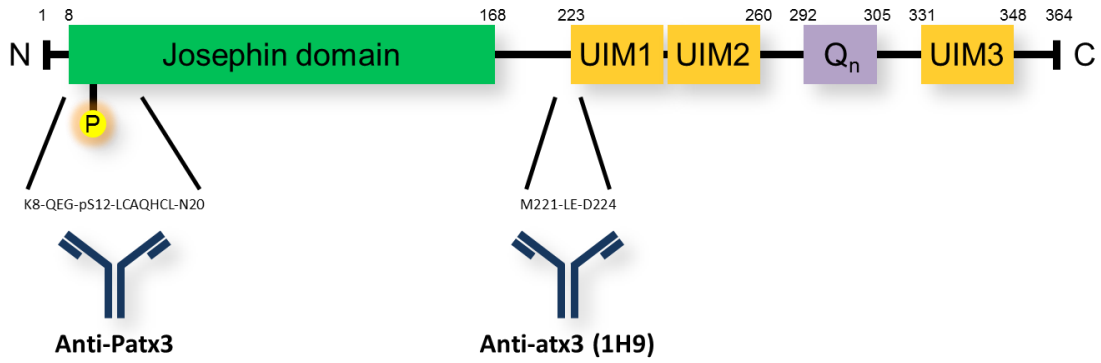

Figure 11: Amino acid sequences recognized by the antibodies used to detect atx3. The commercial mouse monoclonal antibody (clone 1H9) used to detect total atx3 recognizes an epitope localized in the vicinity of UIM1. The polyclonal phospho-specific antibody generated in this study was raised by immunizing rabbits of a peptide containing phosphorylated S12. The figure uses the same domain annotations as figure 3.

Western blot analysis of cells expressing expanded GFP-atx3 84Q also revealed two bands, admittedly corresponding to the overexpressed GFP-atx3 and the endogenous protein (Figure 12B). The 10 kDa molecular weight difference between GFP-atx3 28Q and GFP-atx3 84Q (~75 kDa) is in agreement with what is expected due to the difference in the number of glutamine residues. GFP-atx3 mutants where S12 had been substituted by an aspartate residue were also transfected into COS-7 and analyzed through the same procedures (Figure 12A and 12B). This kind of mutation is commonly used to mimic phosphorylation of serine residues, as will be discussed in section 3.4. In agreement with what has been observed for phospho-specific antibodies targeting other phosphoproteins (Li *et al.*, 2010), the phosphomimetic mutant of atx3 was recognized by the anti-Patx3.

The relative difference in molecular sizes explained above, along with the absence of higher weight bands in the non-transfected cell samples, serves as good proof that the phospho-specific antibody detects atx3. However, the sizes of the species revealed by the anti-Patx3 antibody are lower than what is expected for GFP-atx3 28Q and 84Q and endogenous atx3. Reprobing with the anti-atx3 antibody revealed bands of higher molecular weight: a ~75 kDa band for GFP-atx3 28Q and a ~47 kDa band corresponding to endogenous atx3 (Figure 12A). Nonetheless, given the evidence presented above, the bands observed with the anti-Patx3 are admittedly atx3- and GFP-atx3-derived products. The discrepancies may be explained by the fact that the anti-Patx3 antibody is detecting only fragments of GFP-atx3 and endogenous atx3. Proteolytic cleavage of atx3 has been repeatedly studied and reports by several authors have described a variety of cleavage products, deriving from endogenous atx3 (Berke *et al.*, 2004) as well as from transfected expanded and non-expanded atx3, including in COS-7 cells (Pozzi *et al.*, 2008) (see section 3.4). The fact that only the putative fragments are detected as being phosphorylated would however indicate that either atx3 is phosphorylated at S12 only after being cleaved into the products of the observed sizes, or that phosphorylation at S12 leads to cleavage.

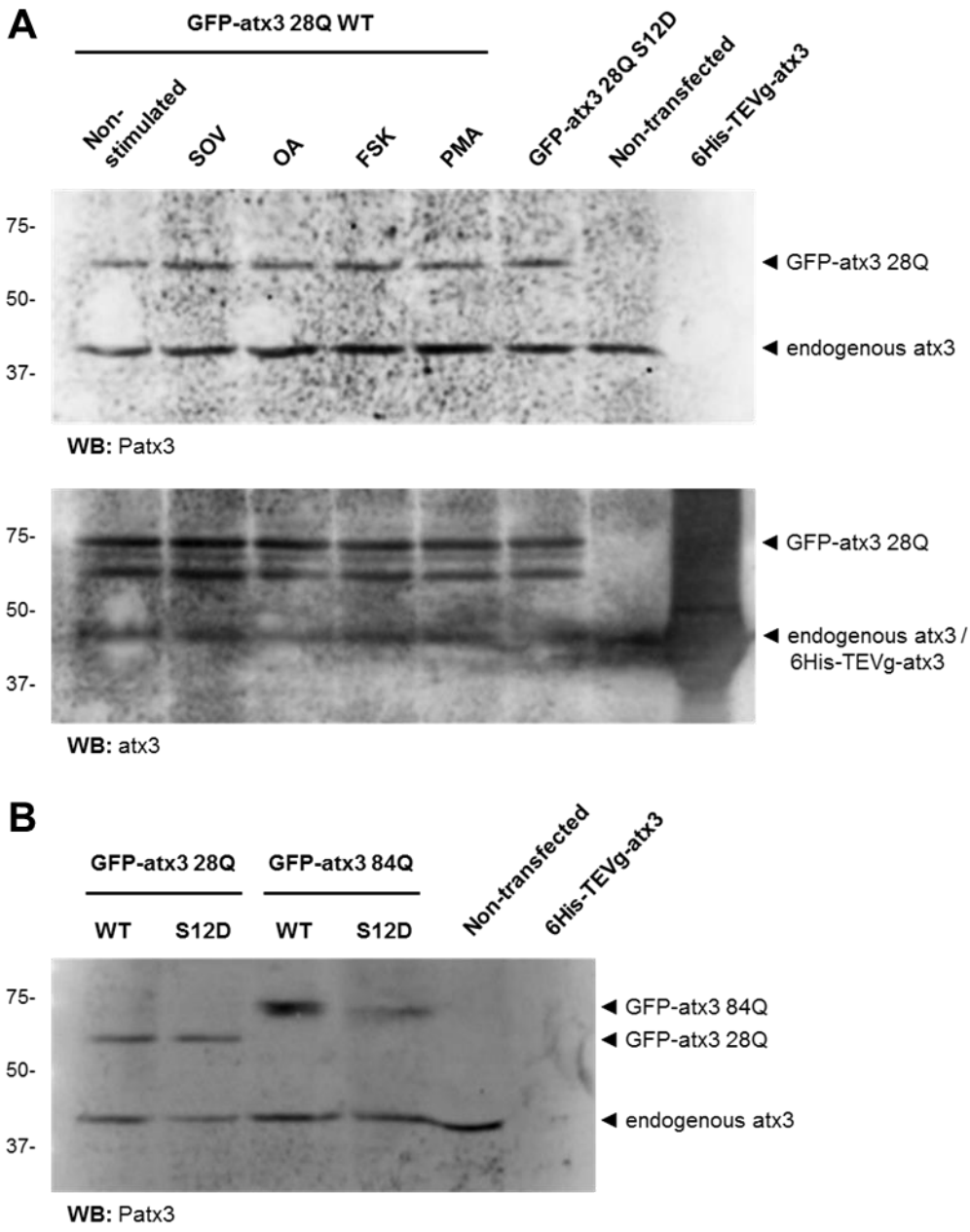

Figure 12: Phospho-specific anti-Patx3 antibody detects GFP-atx3 28Q and endogenous atx3-derived species in COS-7 cells. ***A*** COS-7 cells were transiently transfected with GFP-atx3 and stimulated with SOV (5 mM, 30 min), OA (20 mM, 16 h), FSK (10 µM, 20 min) or PMA (200 mM, 20 min) in order to enhance protein phosphorylation. Western blot analysis with the anti-Patx3 antibody, directed at the detection of phosphorylated S12 of atx3, revealed two protein bands: one corresponding to GFP-atx3 28Q (~65 kDa) and the other to endogenous COS-7 atx3 (~40 kDa). None of the chemical stimuli increased the signal revealed by the anti-Patx3. Non-transfected cells yielded just one band corresponding to endogenous atx3, and no protein band was detected in purified recombinant 6His-TEVg-atx3, produced in *E. coli*. Reprobing with the commercial anti-atx3 1H9 antibody labelled proteins of higher molecular weight, indicating that the species observed with the anti-Patx3 probably correspond to atx3-derived fragments (GFP-atx3 28Q: ~75 kDa; endogenous atx3 and 6His-TEVg-atx3: ~48 kDa). ***B*** In samples expressing GFP-atx3 84Q, the anti-Patx3 detected a higher molecular weight band corresponding to an expanded protein-derived fragment (~75 kDa). The phospho-specific antibody also detected species derived from phosphomimetic mutants GFP-atx3 28Q S12D and GFP-atx3 84Q S12D. COS-7 cell extracts were prepared in the presence of phosphatase inhibitors. 35 µg of each COS-7 sample and 30 µg of purified 6His-TEVg-atx3 were analyzed in these experiments.

Confirming phosphorylation – Lambda phosphatase experiments

In following Western blot experiments the bands revealed by the anti-Patx3 antibody in COS-7 cells presented a different profile, with the band of highest intensity migrating at ~35 kDa. In order to confirm the identity of that band as a phosphorylated species, cell extracts from non-transfected cells were prepared without any phosphatase inhibitors, and digested with lambda phosphatase, an enzyme able to remove phosphate groups from serine and other amino acid residues (Zhuo *et al.*, 1993). Reaction with lambda phosphatase led to the disappearance of the observed band, confirming that it in fact corresponds to a phosphorylated protein (Figure 13A). Another band, fainter and of lower molecular weight (~30 kDa), also disappeared with the treatment. Stimulation with staurosporine (STS), a broad-spectrum inhibitor of protein kinases, had no effect in the observed bands.

In another experiment, COS-7 cells were treated with a cocktail of phosphatase inhibitors (AO, SOV and sodium fluoride – NaF) and the anti-Patx3 immunoreactivity was compared in extracts from treated and control cells, the latter prepared in the absence of any phosphatase inhibitors (Figure 13B). Similarly to what was observed when using the lambda phosphatase assay, this procedure yielded two protein bands of high intensity in the phosphatase inhibitors-treated COS-7 cells, which were absent in non-stimulated samples. Experiments with HeLa cell extracts also yielded two bands of similar sizes – that were diminished or absent in the non-stimulated samples (Figure 13C).

Confirming ataxin-3 detection – Ataxin-3 silencing strategies

The phospho-specific antibody against phosphorylated S12 atx3 apparently labels an atx3 fragment. If this molecular tool reliably detects the levels of endogenous S12-atx3 phosphorylation in different experimental conditions, it is very useful for the future characterization of the importance of this PTM. No protein band in the Western blots labelled with anti-atx3 antibody corresponds clearly to the bands observed with the phospho-specific antibody, but the antibody against total atx3 used in this study targets an epitope (M221-LD-E224; Goti *et al.*, 2004) in the vicinity of UIM1 sequence, and may therefore be unable to detect N-terminal atx-3 fragments that are detected by the anti-Patx3 antibody (Figure 11). Nevertheless, to validate the specificity of the phospho-specific antibody, it is necessary to confirm that the fragments observed do in fact result from atx3.

In order to clarify the identity of the lower molecular weight species detected by the anti-Patx3 antibody we used an atx3 knockdown strategy employing shRNAs. In these experiments, rat primary cortical neuron cultures were used instead of the above cell lines, for two reasons. First, significantly knocking down atx3 in cell lines proved difficult, probably because the continuous cell division assures a continuous production of cells that didn't take the shRNAs. Secondly, considering that MJD only affects neurons, it would be important to expand on the observations made in cell lines and definitely prove that atx3 S12

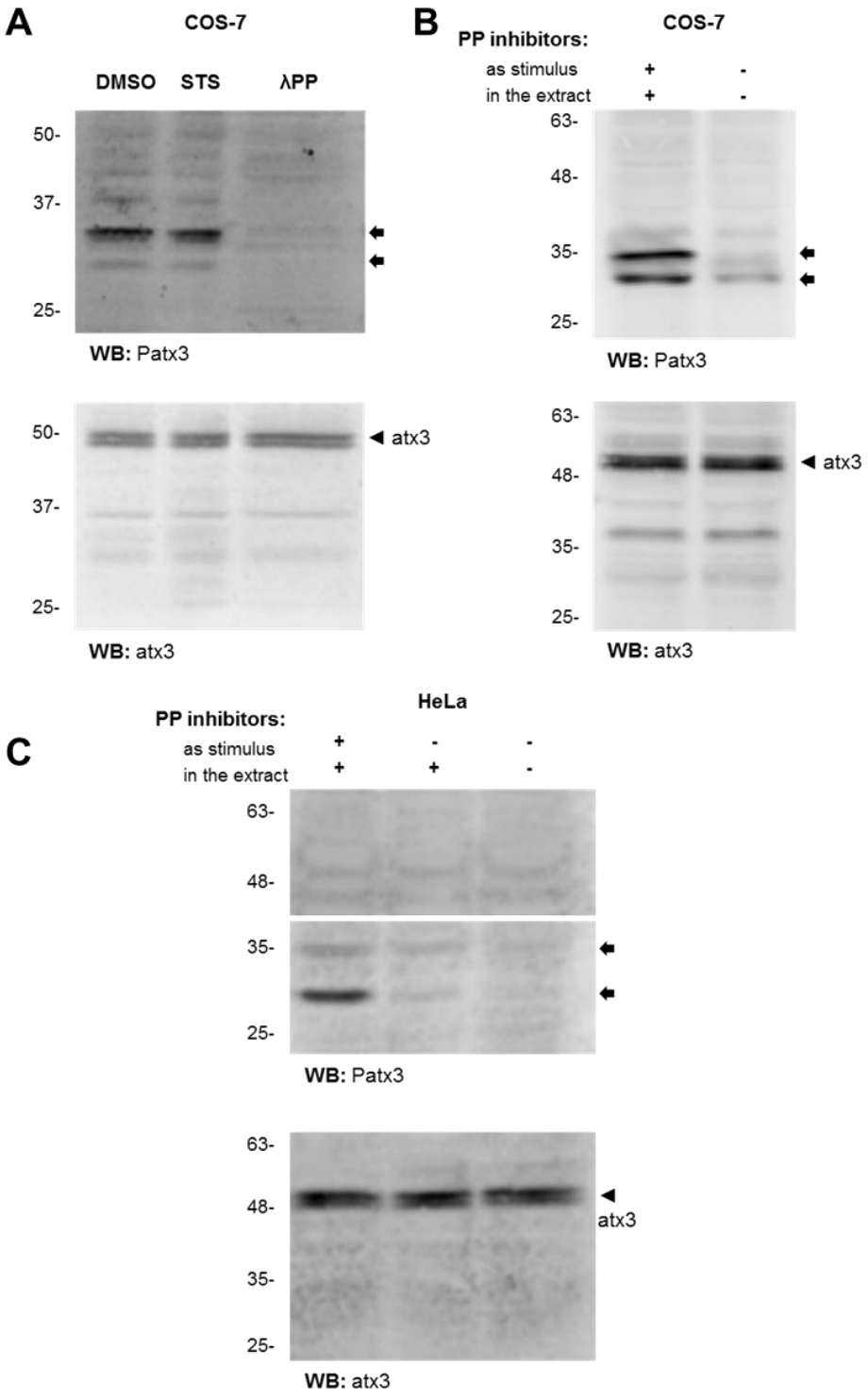

Figure 13: Anti-Patx3 detects phosphorylated protein species. ***A*** COS-7 cells were either stimulated with STS (300 nM, 3h) or incubated with lambda phosphatase (λPP) after extract preparation, and then analyzed by Western blot with the anti-Patx3 antibody. Only the extracts from control cells (treated with STS vehicle dimethyl sulfoxide – DMSO) and from STS-treated cells were prepared in the presence of phosphatase (PP) inhibitors. The two bands revealed by the anti-Patx3 antibody (~30 and ~35 kDa, indicated by arrows) were absent from the extracts digested with lambda phosphatase, confirming that they correspond to phosphorylated species. ***B*** Both in COS-7 and ***C*** HeLa cells, stimulus with a cocktail of phosphatase (PP) inhibitors (1 or 10 µM OA in HeLa and COS-7 respectively, 5 mM SOV, 5mM NaF, 45-60 min) and preparation of cell extracts in the presence of PP inhibitors revealed similar bands, that were absent or diminished in the non-stimulated cells prepared without PP inhibitors.

phosphorylation occurs in that cell type. The shRNAs (shRNA-atx3), generated and characterized by Alves and coworkers (2010) were delivered through lentiviral vectors and the infected neurons were stimulated as above and analyzed by Western blot with the anti-Patx3 antibody. The bands detected by the antibody are absent from the cells where atx3 was silenced, confirming their identity as endogenous atx3-derived species (Figure 14). Their size is lower than that of the bands observed in the cell line samples, but it should be noted that the endogenous rat atx3 has a lower molecular weight (~43 kDa) than the protein from the cell lines (~48 kDa) (Berke *et al.*, 2004).

Taken together, the above observations are strong proof that the antibody is detecting phosphorylated species derived from atx3. It is therefore safe to assume that S12 of atx3 – or of proteolysis-derived atx3 products – is phosphorylated in mammalian cell lines (including human-derived cells) and, importantly, in neurons.

3.3 Ataxin-3 structure analysis and functional predictions

Having identified S12 of atx3 as a phosphorylation site, we focused on investigating what are the possible functional consequences of this PTM. Phosphorylation is a highly dynamic cellular mechanism capable of modulating different properties of a protein, including enzymatic activity, intermolecular interactions, turnover and subcellular localization. In the case of atx3, modification of S12 could assumably regulate at least a part of them.

A first analysis of atx3 amino acid sequence and domain structure reveals that S12 localizes in the JD (amino acids 8-168; Almeida *et al.*, 2013), the catalytic domain of atx3 positioned at the N-terminal part of the protein (Figure 15C). Observing the tertiary NMR structure of the JD of atx3 (Nicastro *et al.*, 2005; PDB code: 1YZB), it is noticeable that S12 localizes on the surface of this domain and is consequently accessible for phosphate conjugation (excluding the still undisclosed contribution of the C-terminal tail to atx3 tertiary structure). Importantly, S12 is in close proximity to the cysteine residue of the catalytic site, C14, but is also in the vicinity of the other amino acids of the catalytic triad, H119 and N134, and nearby Q9, another amino acid important for the enzymatic activity (Figure 15A and B). S12 is located in the joint region between the globular catalytic subdomain and the flexible helical hairpin predicted to play a role in enzymatic target recognition (Komander *et al.*, 2009; Nicastro *et al.*, 2009). According to the NMR structure data describing the Ub-binding sites present at the surface of the JD, S12 is localized in close proximity to the region where the C-terminus of the Ub molecule interacting with the catalytic cleft (site 1) is positioned upon binding (Figure 15D and E) (Nicastro *et al.*, 2009, PDB code: 2JRI).

Considering the proximity of S12 to elements related to atx3 enzymatic activity, it is logical to speculate that phosphorylation at this residue could affect atx3 DUB activity. Conjugation of a phosphate group to S12 might affect the conformation of the surrounding amino acids, as a consequence of its volume and/or negative charge. Changes in the conformation of the active site amino acids or alterations that could affect substrate binding

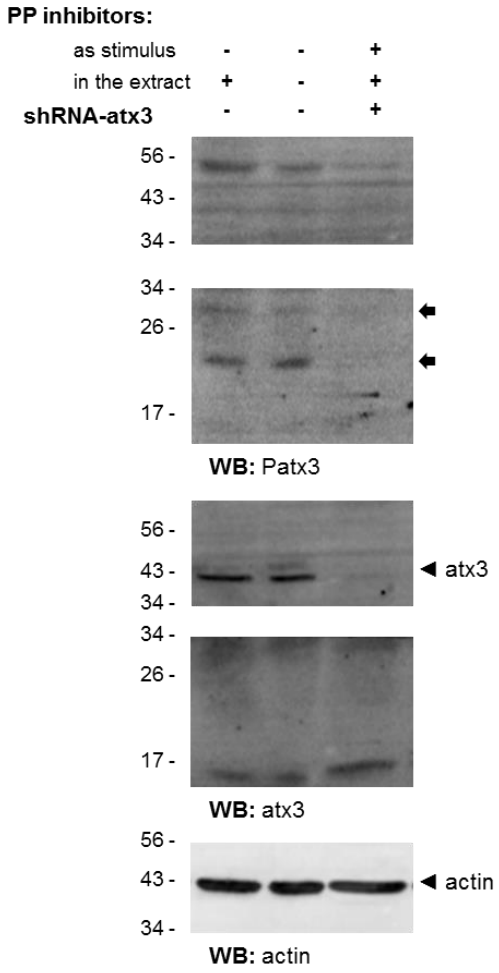

Figure 14: Anti-Patx3 detects N-terminal fragments of atx3 in rat cortical neurons. Extracts from 14 DIV mice cortical neuron cultures were prepared with or without PP inhibitors and analyzed by Western blot. Probing with the anti-atx3, which targets an epitope in the vicinity of UIM1, revealed one band corresponding to endogenous rat atx3 (~43 kDa), while the anti-Patx3 antibody, directed at the N-terminal part of the atx3 antibody, revealed two bands of lower molecular weight (~25 and ~30 kDa, indicated by arrows). Neurons infected at 8 DIV with lentiviral particles encoding shRNAs targeting atx3, stimulated with a cocktail of PP phosphatase inhibitors (0,5 µM OA, 5 mM SOV, 5mM NaF, 45-60 min) and sampled in the presence of PP inhibitors yielded no similar bands. Actin was labelled as a loading control.

might result in changes in the proteolytic activity (Huang *et al.*, 2012; Hunter, 2007; Renatus and Farady, 2012; Tarrant and Cole, 2009). Importantly, a previously described PTM of atx3 – ubiquitination at K117, localized in the JD, in the proximity of the catalytic site – was shown to increase its DUB activity (Todi *et al.*, 2010).

Other evidence suggesting the importance of the amino acid at position 12 in the context of the catalytic activity of the JD may be inferred from the analysis of other JD-containing proteins (Amerik and Hochstrasser, 2004; Komander *et al.*, 2009; Reyes-Turcu *et al.*, 2009; Tzvetkov and Breuer, 2007). Comparing the amino acid sequences from atx3 homologs in humans and other vertebrates with that of the Josephin-1 and -2 (which are mainly constituted by the JD), it is interesting to note that, at the position corresponding to S12, Josephin-1 and -2 have a negatively charged residue – glutamate (Figure 16). On the other

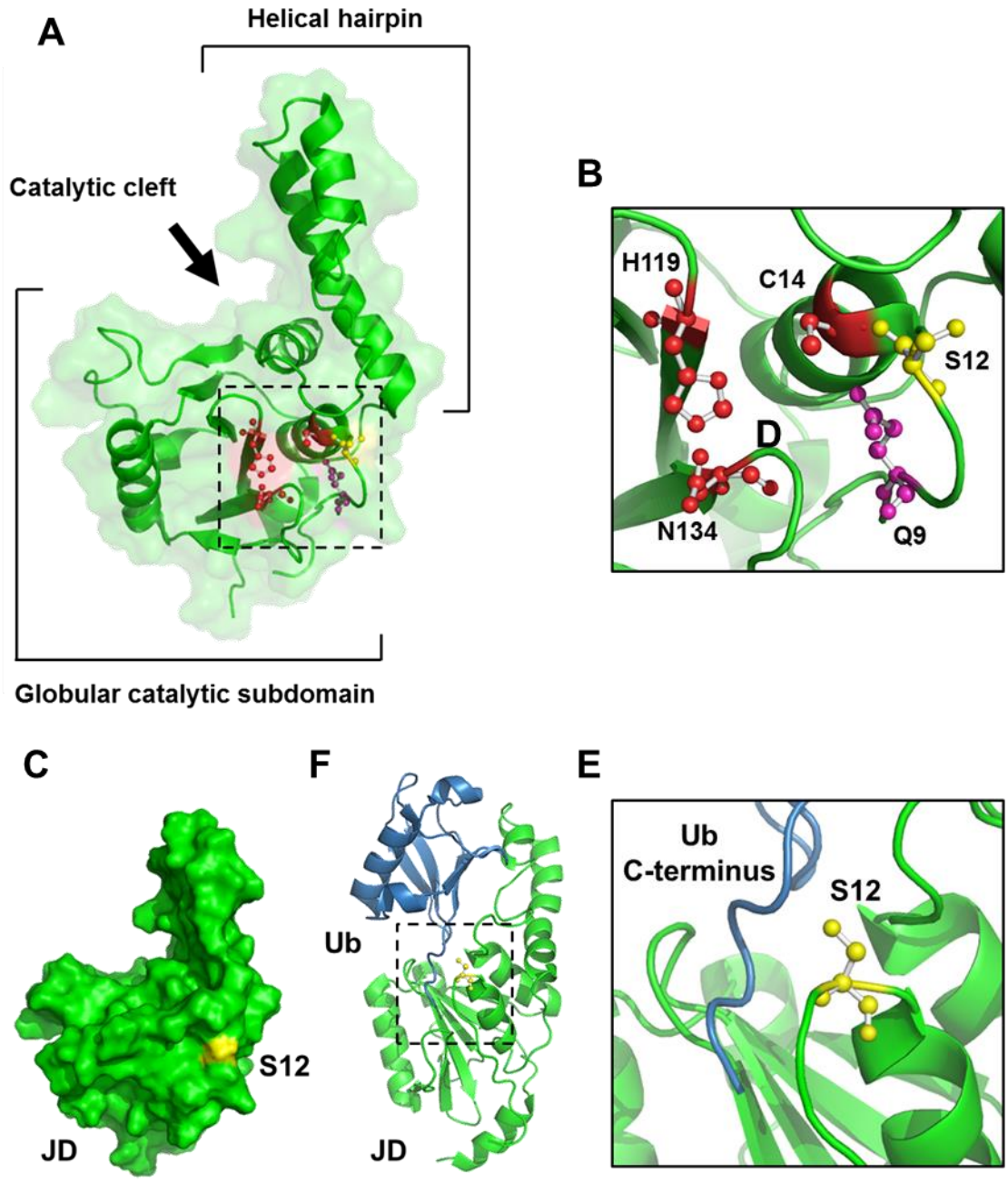

Figure 15: S12 is localized in the catalytic domain of atx3. ***A*** S12 (in yellow) is localized in the joint region between the two subdomains of the JD, ***B*** in close proximity to the amino acids of the catalytic triad and to glutamine 9 (PDB code: 1YZB). **C** S12 is accessible at the surface of the isolated JD. ***D, E*** Binding of a Ub molecule to the Ub-binding site 1 of the JD positions the C-terminal region of Ub close to S12 (PDB code: 2JRI).

hand, the human atx3L, which shares a high degree of homology with atx3, has an aromatic phenylalanine at that position. The activity of the JDs isolated from human atx3, atx3L protein, Josephin-1 and Josephin-2 has been shown to be markedly different, when tested against several different Ub model substrates, *in vitro* (Weeks *et al.*, 2011). The variations observed may be attributed to other sequence or structural differences between the protein JDs, but it

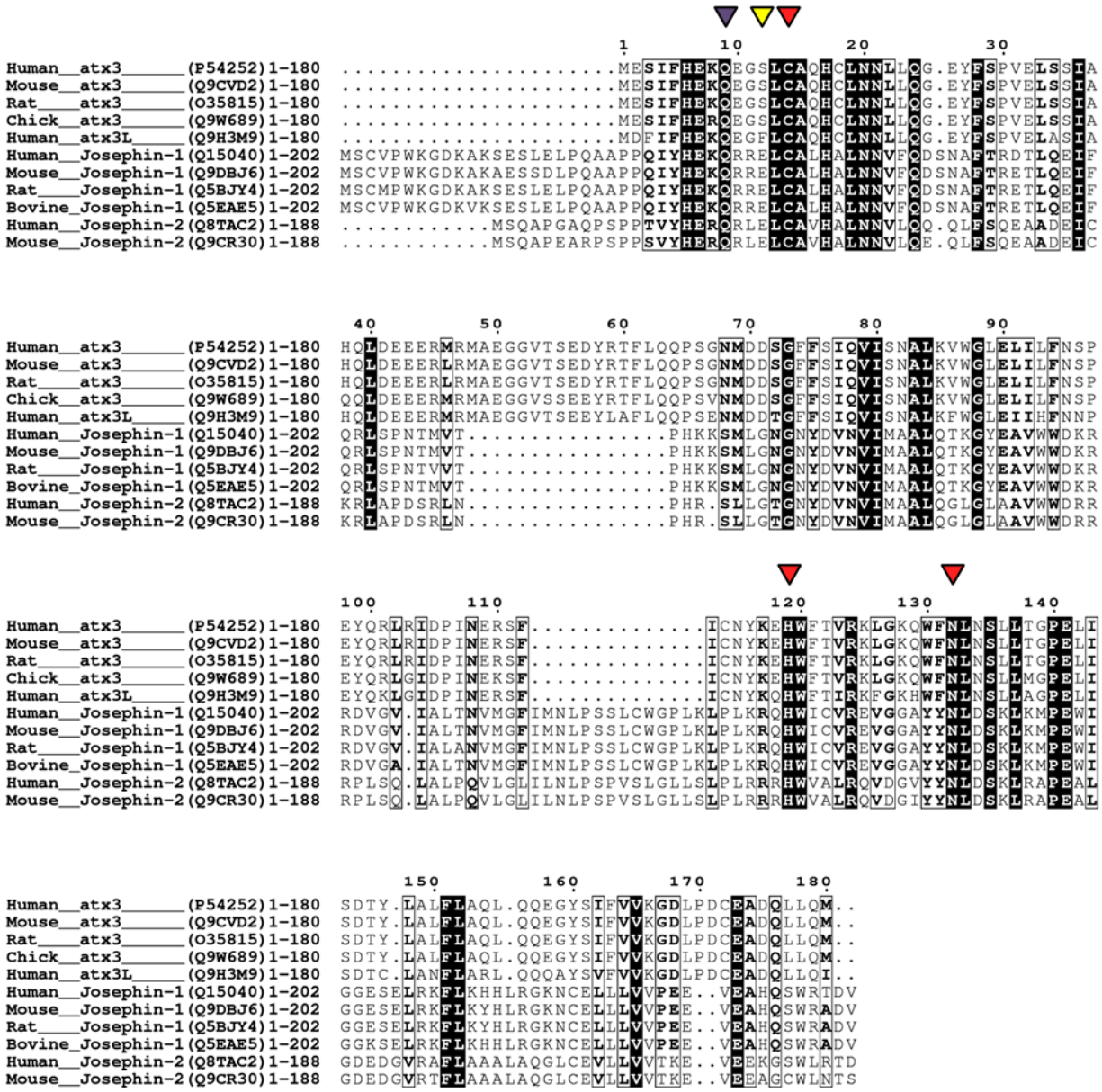

Figure 16: S12 is conserved in vertebrate atx3 but is substituted by a phenylalanine residue in atx3L and by a glutamate residue in Josephin-1 and -2. The figure represents the alignment of the JD of several vertebrate Josephin DUBs: human, mouse, rat and chick atx3; human atx3L; human, mouse, rat and bovine Josephin-1; and human and mouse Josephin-2. Protein sequences were obtained from the Uniprot database (codes are represented in brackets). Alignment was performed with Crustal Omega and prepared with ESPript 3.0, using the first 180 residues of atx3 and atx3L and the whole sequence of Josephin-1 and -2. Strictly conserved residues are represented by white letters in a black background and highly similar residues (global score: 0,7) by bold letters in framed columns. Arrowheads point the conserved residues of the catalytic triad (red), points the conserved glutamine residue next to the catalytic site (purple) and the position of S12 in atx3 (yellow).

is possible that the residue occupying the position of S12 plays an important role.

Notably, the crystal structure of the complex formed by Ub and the atx3L JD revealed that F12, along with other aromatic amino acids, forms an hydrophobic enclosure around the active center, through which the C-terminus of the Ub molecule threads (Weeks *et al.*, 2011). The position also appears to be suitable for interaction with the lysine side chain forming the

isopeptide bond. In fact, it has been reported that mutation of the S12 of the atx3 JD to a phenylalanine increases proteolysis of Ub substrates, consistent with the proposed relevance of this residue in determining activity. It is possible that a negative charge at amino acid position 12 will possibly introduce steric hindrance leading to a rearrangement of the helical hairpin, which is essential for the correct positioning of the R74 of the Ub substrate and maintenance of the active site structure (Weeks *et al.*, 2011).

Taking all these indications into consideration, we investigated the effect S12 phosphorylation has on atx3 enzymatic activity.

3.4 Generation of ataxin-3 phosphomutants

Taking into account that phosphorylation is a reversible, highly dynamic, modification, it is believed that, at any given time point in a cell, only a fraction of the population of a particular protein is phosphorylated (Seo and Lee, 2004). A common strategy used to study the behavior and effects of a phosphoprotein is to constitutively mimic the conjugation of the phosphate groups, by substituting some or all phosphorylatable residues of the protein with acidic amino acids (Mueller *et al.*, 2009; Pearlman *et al.*, 2011; Thorsness and Koshland, 1987). Serines are usually mutated to aspartate residues, though sometimes glutamate is used instead. The reason for this is that conjugation of a phosphate group to the hydroxyl moiety of a serine increases the volume of its side chain and renders it negatively charged; aspartate shows relative chemical similarity to phosphoserine, mimicking both features to some degree (Figure 17). The biochemical and biological behavior of these phosphomimetic mutants is admitted to replicate (to some extent) that of the original protein, as if it was continuously phosphorylated (Dephoure *et al.*, 2013; Pearlman *et al.*, 2011; Tarrant and Cole, 2009).

Simultaneously, experiments commonly include another kind of mutant of the phosphorylation site(s) – the phospho-null, or phospho-dead, mutants. These mutants mimic proteins so as to resemble them in a permanent non-phosphorylated state. In the case of phosphorylated serines, this is achieved by substituting them with alanine residues, since the two amino acids have comparable characteristics, but alanine lacks the hydroxyl group with which the phosphate conjugates (Dephoure *et al.*, 2013; Mueller *et al.*, 2009; Pearlman *et al.*, 2011; Tarrant and Cole, 2009).

Phosphomimetic and phospho-null mutants of the atx3 constructs used in the present study were generated through site-directed mutagenesis, by substituting S12 with an aspartate (S12D) or an alanine residue (S12A), respectively. These mutants were used throughout the several experiments aiming at understanding the functional effect of S12 phosphorylation, except for the experiments employing atx3 purified from *E. coli*, since the non-mutated protein is considered non-phosphorylated (as explained in section 3.2). Importantly, in this study the non-mutated protein is designated as wild-type (WT), regardless of glutamine sequence size; WT thus describes the presence of serine at position 12 and not the absence of polyQ expansion, as is the case of other works.

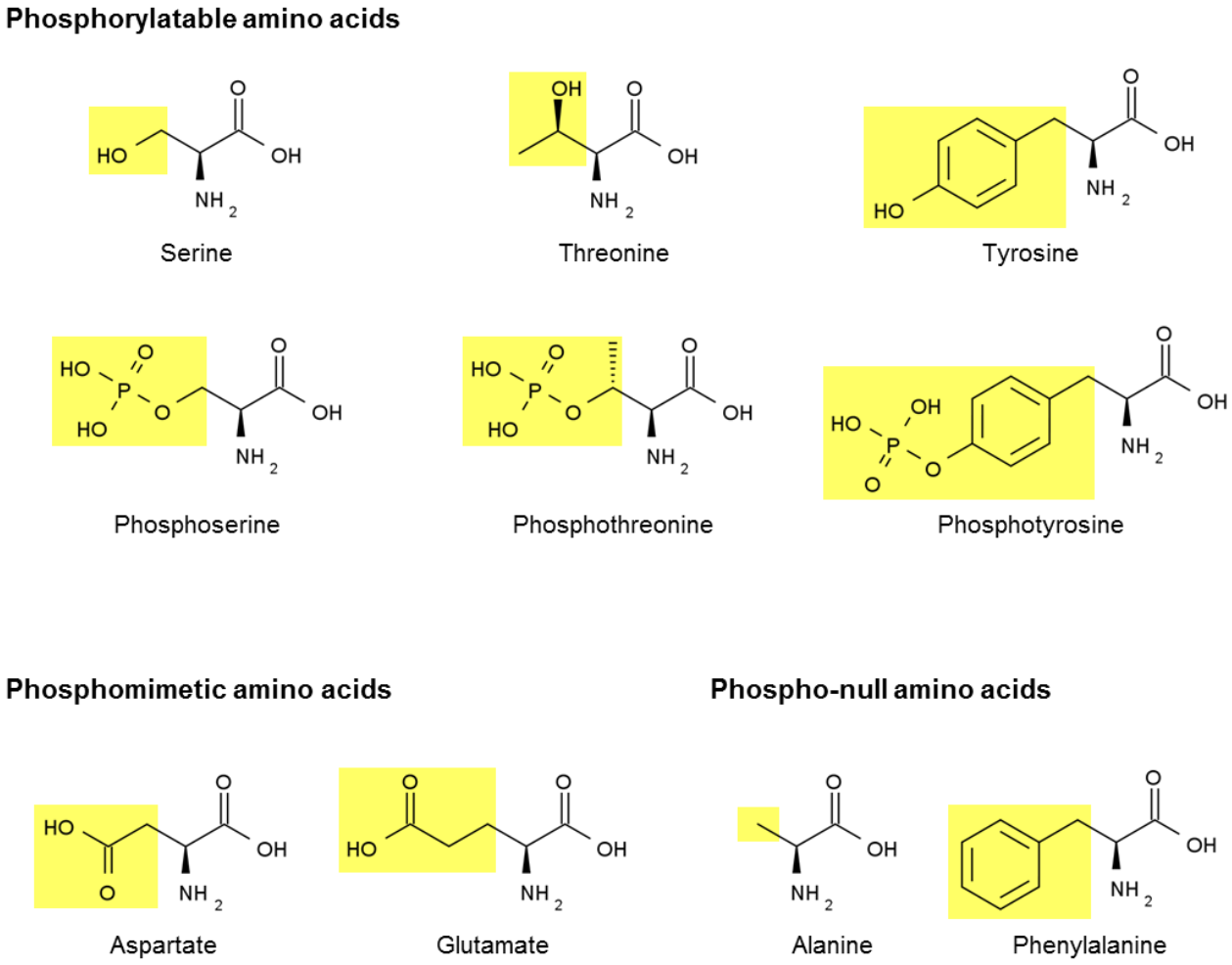

Figure 17: Chemical structures of phospho-accepting amino acids and of amino acids used to model phosphorylation states. Eukaryotic proteins possess three amino acids with hydroxyl group-containing side chains able to conjugate with phosphate. Mimicking constitutive phosphorylation is commonly attempted by substituting them, through point mutations, with negatively charged acidic amino acids – aspartate or glutamate. Abrogating the ability to conjugate with phosphate is achieved by replacing the amino acids with alanine (or phenylalanine, in some studies of tyrosine phosphorylation). Amino acids are represented with neutralized charges and side chains are highlighted by yellow boxes.

3.5 Ataxin-3 phosphorylation at serine 12 affects its proteolytic activity

In vitro activity assays with Ub-AMC

One method of studying atx3 proteolytic activity is to perform *in vitro* assays using Ub-containing model substrates, by subjecting them to digestion with purified atx3 (Burnett *et al.*, 2003; Harris *et al.*, 2010; Weeks *et al.*, 2011). Ub-AMC is a compound commonly used when studying DUB activity and has already been used in studies with atx3 (Burnett *et al.*, 2003; Harris *et al.*, 2010; Love *et al.*, 2007). Being a fluorogenic substrate, product formation

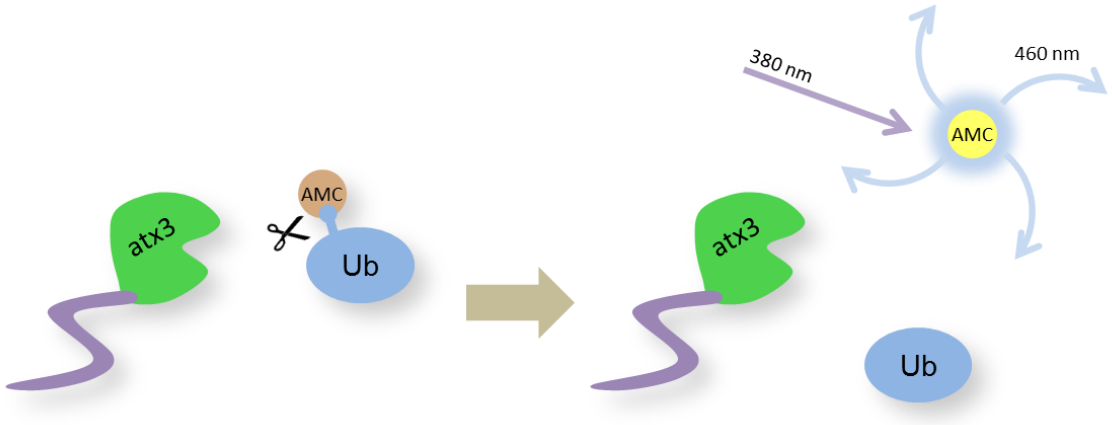

Figure 18: DUB activity assays with Ub-AMC. Ub-AMC is a fluorogenic model substrate which yields AMC upon proteolytic cleavage by DUBs. Recording the fluorescence emitted by AMC upon excitation (excitation – 380 nm; emission – 460 nm) allows a time-dependent assessment of product formation. The schematic representation uses atx3 as an example.

resulting from cleavage can be assessed by continuously recording the fluorescence emitted by the AMC that is yielded during the reaction (Figure 18). This allows for a continuous and sensitive detection of product formation and consequent evaluation of DUB activity.

With the objective of determining possible differences in DUB activity resulting from atx3 phosphorylation at S12, recombinant 6His-atx3 WT and 6His-atx3 S12D were produced in *E. coli* and purified in accordance to the procedure described by Gales and coworkers (2005). Recombinant atx3 forms were incubated with Ub-AMC and fluorescence emitted by the AMC fluorophore was measured throughout the course of the reaction. Observation of the respective reaction curves reveals that the cleavage rate is higher for non-phosphorylated 6His-atx3 WT, comparing to the phosphomimetic 6His-atx3 S12D (Figure 19A). Moreover, the initial reaction velocity, measured as the rate of product formation in the first 2 min (the period while direct proportionality holds) significantly decreases to 43,6 ± 4,7 % (standard error of the mean – SEM) of the initial velocity of the reaction catalyzed by 6His-atx3 WT, when S12 is mutated (Figure 19B). Similar results were obtained with samples of atx3 containing a different tag and prepared independently – 6His-TEVg-atx3 WT and S12D (Figure 19C).

As explained above, the proximity of S12 to the catalytic site strongly suggested that phosphorylation of this residue would affect atx3 enzymatic activity. The observations made with the Ub-AMC reaction support this idea, indicating that the phosphomimetic mutant of atx3 is less effective at the cleavage of a monoUb substrate than the non-phosphorylated protein.

In vitro activity assays with polyUb chains

Previous studies have shown that atx3 enzymatic activity *in vitro* is weak against polyUb substrates with few (less than 4) monomers, leading to the idea that atx3 biological

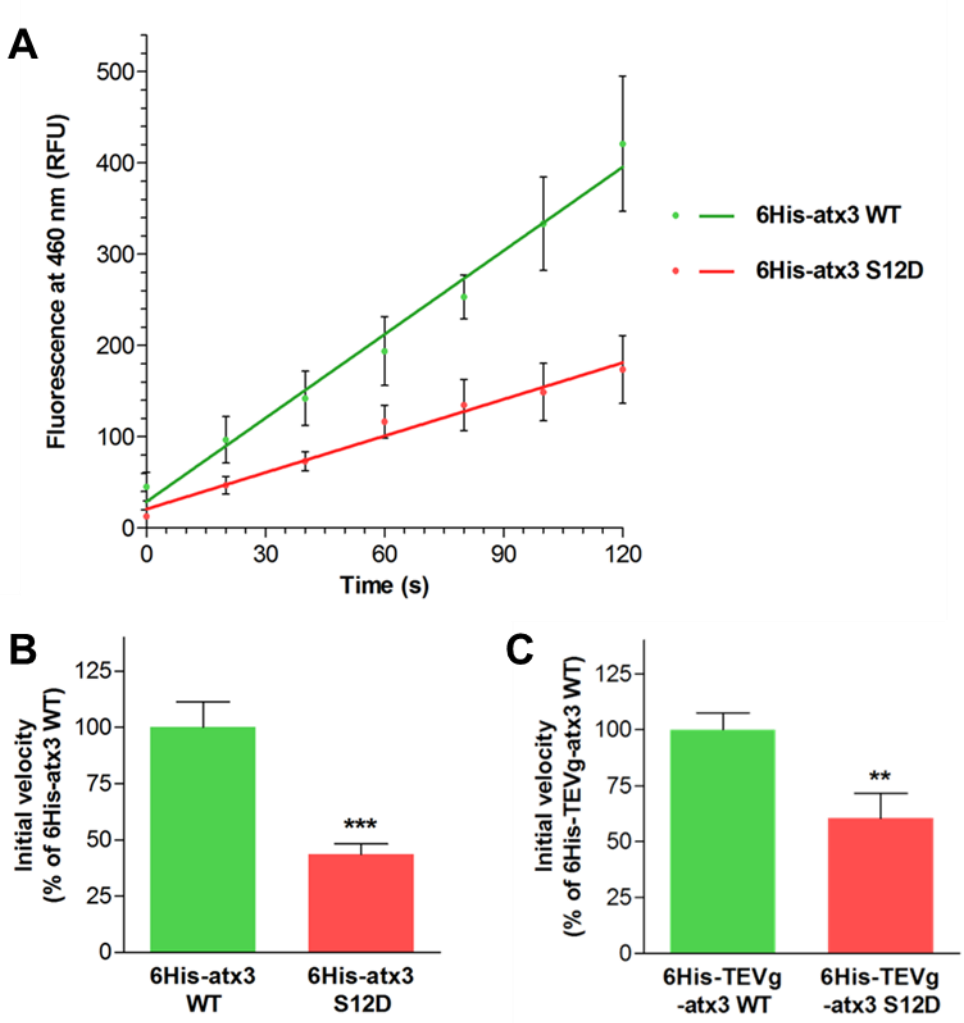

Figure 19: Mimicking atx3 phosphorylation at S12 decreases enzymatic activity against Ub-AMC. ***A*** Purified 6His-atx3 WT and 6His-atx3 S12D produced in *E. coli* were incubated (30 °C, for a maximum of 40 min) with Ub-AMC (0,5 µM) and product formation was assessed by measuring the fluorescence emission at 460 nm, during 380 nm excitation. Throughout the reaction, 6His-atx3 S12D shows a decreased enzymatic activity against Ub-AMC, comparing to 6His-atx3 WT. The reaction curve of initial product formation (0-120 s) is illustrated by one representative experiment; dots correspond to mean ± SEM fluorescence values (relative fluorescence units - RFU) of technical replicates (n = 3), after subtraction of the value of the negative control (buffer and Ub-AMC only, which showed no fluorescence increase during the assay). ***B*** The initial reaction velocity of 6His-atx3 S12D is decreased (to 43,6 ± 4,7 %) in relation to 6His-atx3 WT. Bars represent mean ± SEM of initial velocity values (RFU/min) of the replicates (n = 8) of 3 independent experiments, each of them normalized to the mean value of 6His-atx3 WT in the respective experiment. Student's t-test: *** - P< 0,001. ***C*** Cleavage of Ub-AMC by 6His-TEVg-atx3 S12D is also reduced (initial velocity of 60,5 ± 11,1 %) in comparison to 6His-TEVg-atx3 WT (n = 10 replicates, from in 3 independent experiments). Student's t-test: ** - P < 0,01.

function is more linked to polyUb chain editing than to complete disassembly of chains and yielding of Ub monomers (Burnett and Pittman, 2005; Kuhlbrodt *et al.*, 2011; Matos *et al.*, 2011; Winborn *et al.*, 2008). For this reason, comparing to Ub-AMC, polyUb chains may be better substitutes for the actual, yet unknown, biologic substrate(s) of atx3, in *in vitro* activity assays. In these experiments, product formation is assessed through sampling of the reaction mix at different time points, followed by Western blot analysis directed at the detection of Ub

species. Proteolytic cleavage leads to the formation of lower molecular weight species, corresponding to polyUb chains of decreased number of monomers.

In order to evaluate the possible differences in the cleavage of polyUb chains between non-phosphorylated atx3 and the phosphomimetic mutant, recombinant 6His-atx3 was incubated with either K48- or K63-linked polyUb chains of 6 monomers and samples were obtained at different time points, for a total period of 20 h. For both types of polyUb chains, throughout the course of the experiment 6His-atx3 S12D led to a decreased formation of lower molecular weight Ub species, comparing to 6His-atx3 WT (Figure 20). This was observed for both K48- and K63-linked polyUb chains, though the difference is more prominent in the reaction with the K63-linked chains. In fact, both 6His-atx3 WT and 6His-atx3 S12D are less effective at cleaving K48-linked chains than chains of K63 linkage, an observation that is in accordance with the atx3 cleavage preferences described by other authors (Harris *et al.*, 2010; Weeks *et al.*, 2011; Winborn *et al.*, 2008).

These results demonstrate that the presence of a negatively charged aspartate at position 12 decreases the ability of atx3 to cleave polyUb chains of different linkage types. Taken together, these *in vitro* activity assays strongly suggest that atx3 phosphorylation at S12 decreases its DUB activity. Observing that this effect extends to the cleavage of polyUb chains is of particular interest, taking into account that K48- and K63-linked chains play many cellular roles and are thus regarded as physiologically relevant (Weeks *et al.*, 2011; Winborn *et al.*, 2008).

It is worthy of note that, throughout the course of the reaction, the levels of 6His-atx3 decrease, and that this effect is much more noticeable with the WT protein. Nonetheless, far from contradicting the assumptions made, this observation gives further significance to the explained differences in cleavage efficiency. Yet, it would be important to understand this decrease in atx3 levels during an *in vitro* assay. Mauri and collaborators (2006) have described that purified atx3 is subjected to slow autolytic fragmentation *in vitro*, a process that is mediated by the cysteine residue of the active site (Pozzi *et al.*, 2008). The “ability” of 6His-atx3 S12D to better maintain its levels through the 20 h period of incubation could be explained as resulting from lesser autolytic cleavage activity by this mutant. This could serve as another testimony of the decrease on atx3 enzymatic activity that results from the interference the negatively charged amino acid has on the active site. Another explanation for the decrease on 6His-atx3 levels would be the occurrence of atx3 aggregation *in vitro*. Non-expanded atx3 has repeatedly been shown to aggregate in *vitro* (Chow *et al.*, 2004a; Ellisdon *et al.*, 2007; Gales *et al.*, 2005; Saunders and Bottomley, 2009) and it could be the case that, in these long-lasting activity assays, 6His-atx3 forms aggregates leading to a decrease in the levels of its soluble monomeric form. This would imply that 6His-atx3 S12D has a lesser tendency to aggregate than 6His-atx3 WT, under the conditions of this activity assay. The current experiment does not allow for any definite conclusions whatsoever, as no atx3 bands other than the ones expected for the full-length monomeric form were observed.

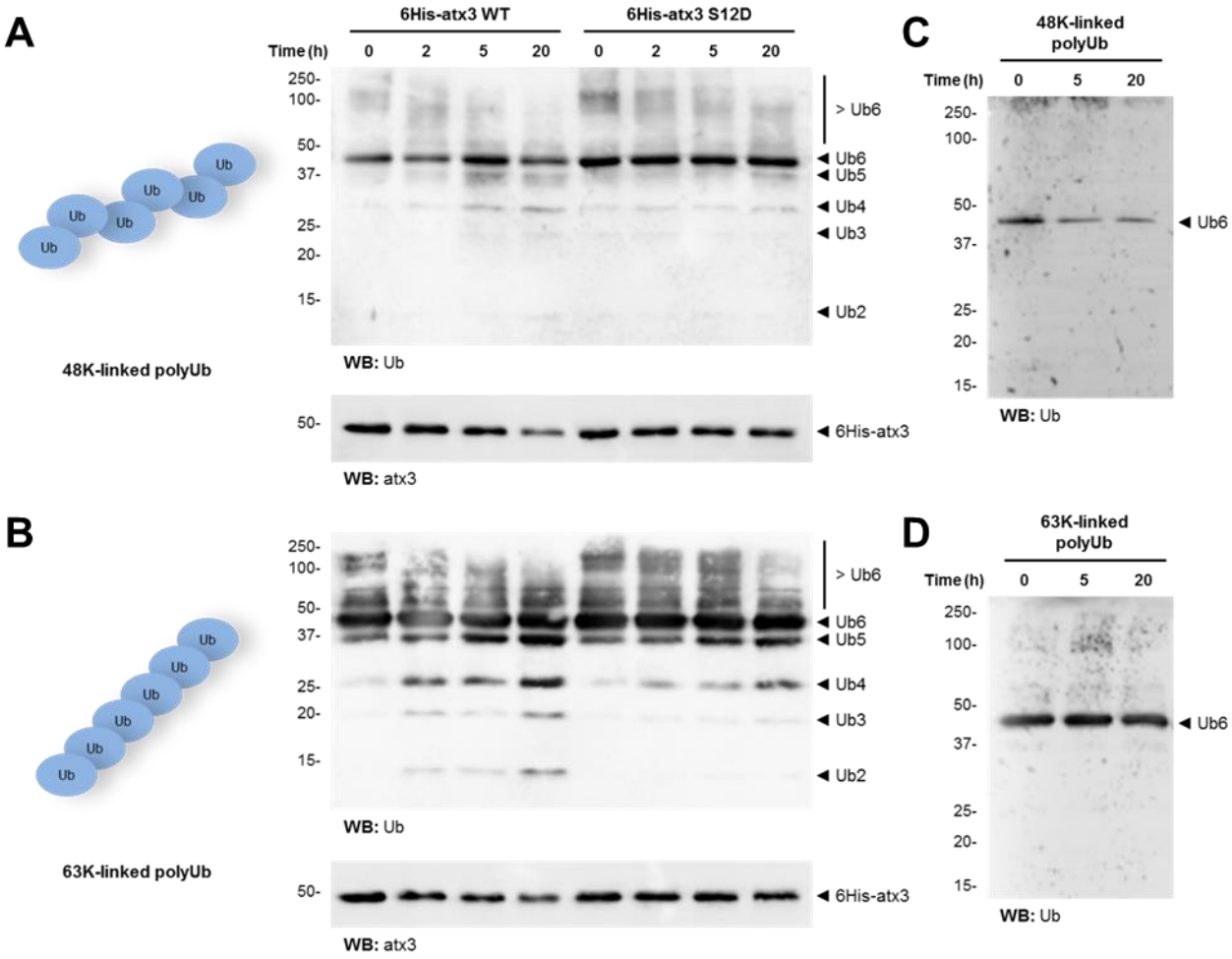

Figure 20: Mimicking atx3 phosphorylation at S12 decreases enzymatic activity against polyUb chains. Purified 6His-atx3 WT and 6His-atx3 S12D produced in *E. coli* were incubated (37 °C) with ***A*** K48- or ***B*** K63-linked polyUb chains of six monomers (6Ub) and samples were collected at different time points (0, 2, 5 and 20 h) and analyzed by Western blot with an anti-Ub antibody, in order to assess product formation. Through the course of the reaction, cleavage of polyUb chains by 6His-atx3 leads to the formation of lower molecular weight Ub species, composed of a smaller number of monomers (Ub2-5). 6His-atx3 S12D elicits less polyUb cleavage than 6His-atx3 WT, against chains of either linkage type. The accompanying schematic representation of hexameric polyUb chains illustrates the fact that K63-linked chains are admitted to adopt a more extended conformation than chains of K48-linkage. ***C, D*** PolyUb chains incubated in the absence of 6His-atx3 showed no apparent degradation during the 20 h period of the reaction.

Ub-VS binding assays

The assays described strongly indicate that mimicking phosphorylation at S12 of atx3 results in a decrease of its DUB activity. It would be relevant to determine if the same happened not only *in vitro*, but also in a cellular context. Still, testing that is problematic, mainly because it is difficult to isolate the contribution of atx3 DUB activity from that of other, possibly more efficient, DUBs (Chow *et al.*, 2004b).

Labelling Ub in cell lysates prepared from HeLa cell cultures by Western blot renders a protein smear corresponding to the several ubiquitinated proteins present in the cells (Figure

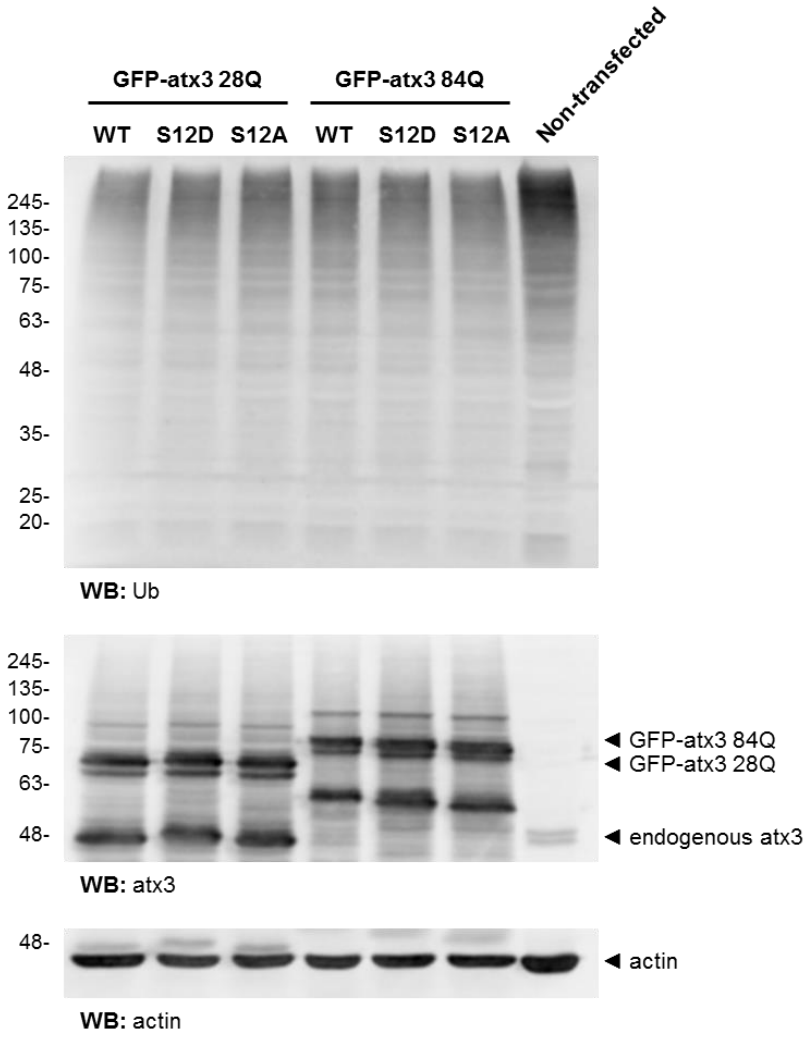

Figure 21: Phosphomutation of S12 does not alter the profile of ubiquitinated proteins in cells overexpressing atx3. HeLa cells were transfected with WT and phosphomutants S12D and S12A of both GFP-atx3 28Q and GFP-atx3 84Q and analyzed by Western blot with an anti-Ub antibody, in order to detect ubiquitinated proteins. Overexpression of atx3 leads to a decrease in intensity of the smear corresponding to the several ubiquitinated proteins present in HeLa cell lysates, having non-transfected cells as reference. The deubiquitination caused by GFP-atx3 expression occurs irrespectively of particular S12 mutations or polyQ length, considering that no blunt differences are observed between the samples of cells transfected with different GFP-atx3 forms. Atx3 was labelled as a control for the transfection procedure and actin as a loading control for the Western blot.

21). Cells transfected with GFP-atx3 constructs clearly show a decrease of ubiquitinated species, admittedly due to the deubiquitination elicited by the overexpressed protein. However, there is no apparent difference in the ubiquitinated species profiles between the WT forms and the phosphomutants of GFP-atx3 with 28 or 84Q. There are several DUBs in eukaryotic cells – approximately 79 are expressed in human cells (Komander *et al.*, 2009; Nijman *et al.*, 2005) – and, consequently, it is not surprising that the relative contribution of atx3 for overall cell deubiquitination is relatively modest and indistinguishable between the several mutants used in this study. For the same reason, simple incubation of cell lysates with model substrates such as those described above was not expected to be any more informative.

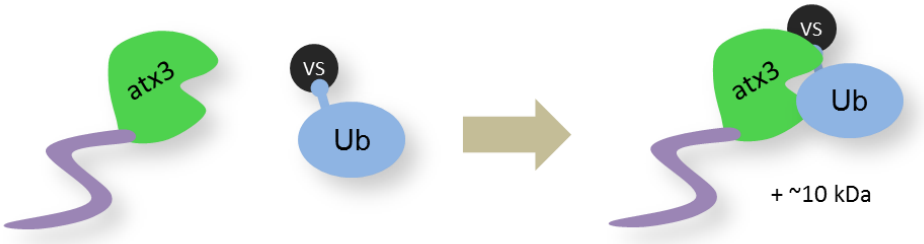

Figure 22: Labelling DUBs with Ub-VS. Ub-VS conjugates with the cysteine residue of the active site of DUBs, forming adducts. These adducts can be detected by Western blot, through the characteristic molecular weight shift the conjugation of Ub-VS causes (~+10 kDa). The schematic representation uses atx3 as an example.

Ub-VS is a potent inhibitor of many cysteine protease DUBs, binding irreversibly to the cysteine residue of the catalytic site and forming covalently conjugated adducts (Figure 22) (Borodovsky *et al.*, 2001; Reyes-Turcu *et al.*, 2009; Wilkinson *et al.*, 2005). It has been repeatedly used to derivatize and consequently label several DUBs, including Josephin-1 and -2, and such conjugation occurs only when DUBs are active (Borodovsky *et al.*, 2001; Seki *et al.*, 2013). Since this compound has been used to successfully label DUBs in crude cell extracts (Borodovsky *et al.*, 2001; Wilkinson *et al.*, 2005), we tried the analyze whether Ub-VS conjugated with atx3 expressed in mammalian cell lines and check if there was any difference in conjugation resulting from mutation of S12. The benefit of this approach is that it allows the study of the behavior of atx3 independently of other DUBs.

Initially, we characterized the time-dependent formation of complexes between Ub-VS and either non-expanded or expanded atx3. In order to do that, cell extracts prepared from COS-7 cells transfected with GFP-atx3 28Q WT or GFP-atx3 84Q WT were incubated with Ub-VS for a total period of 90 min. Protein samples were recovered at different time points and analyzed by Western blot. Conjugation of Ub-VS to GFP-atx3 leads to the appearance of higher molecular weight bands, corresponding to the resulting adducts (Figure 23A). Their intensity increases with time, as opposed to that of the bands of the non-conjugated GFP-atx3. Non-expanded and expanded GFP-atx3 show no apparent differences in their efficiency to conjugate with Ub-VS throughout the assay, binding almost the totality of the inhibitor at the end of the reaction period (Figure 23B).

Based on these results, we decided to simplify the assays with the S12 phosphomutants by analyzing the samples at just two different time points: 10 min, a period of rapid increment in Ub-VS conjugation, and 45 min, at which time the maximum level of conjugation was almost reached. Comparing the GFP-positive Western blot profile of the samples transfected with GFP-atx3 WT, S12D and S12A (28Q) and incubated with Ub-VS, no differences in conjugation with the inhibitor were detected (Figure 24). Conjugation of Ub-VS to GFP-atx3 28Q thus appears to be independent from the substitution of S12 to aspartate or alanine. These results indicate that the fraction of GFP-atx3 28Q that is active is equivalent independently of mutation to a phosphomimetic or a phospho-null form. Importantly, this should not be taken to mean that the enzymatic activity of the different forms is similar, as this

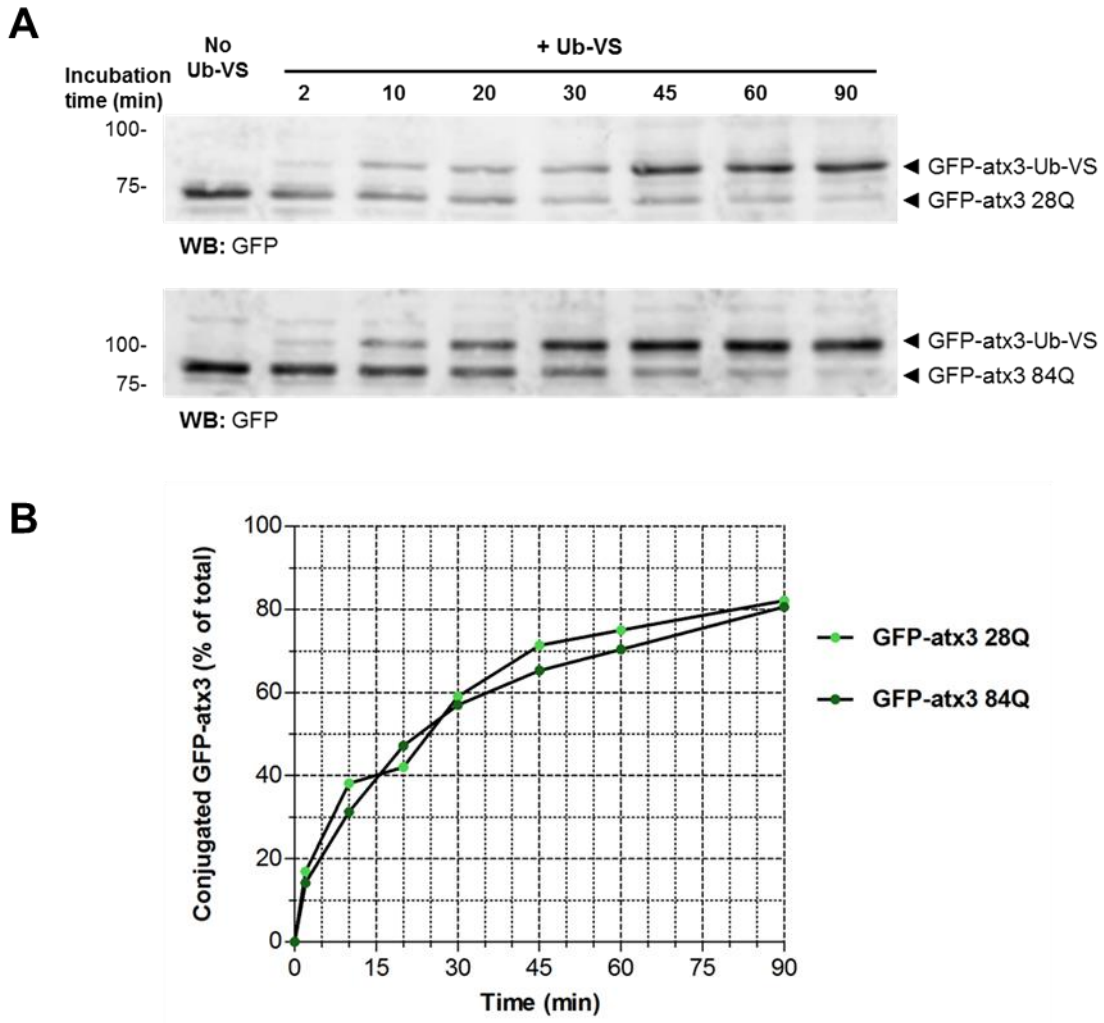

Figure 23: Conjugation of Ub-VS to atx3 occurs in a time-dependent manner. ***A*** COS-7 cells were transfected with GFP-atx3 28Q or GFP-atx3 84Q, lysated and incubated (RT) with Ub-VS. Samples were collected at different time points and analyzed by Western blot with an anti-GFP antibody, so as to detect GFP-atx3 and the adducts formed by Ub-VS conjugation. Through the course of incubation, there was an increase in intensity of the higher molecular weight species that correspond to the adducts (GFP-atx3-Ub-VS). ***B*** Western blot bands were densitometrically analyzed and the amount of conjugated GFP-atx3 at each time point was calculated as the percentage of the intensity of the GFP-atx3-Ub-VS bands relatively to the intensity of these and the unconjugated GFP-atx3 bands combined. The curve illustrates the time-dependent increase of Ub-VS conjugation to GFP-atx3, starting from a rapid increase in the first minutes of the reaction (2-15 min) but beginning to stabilize after ~45 min. The maximum amount of conjugation obtained was around 80 %. No apparent differences in Ub-VS conjugation exist between GFP-atx3 28Q and GFP-atx3 84Q.

assay does not provide information concerning the actual efficiency of the cleavage promoted by the active site. In fact, studies made with other DUBs show that efficiency of Ub-VS conjugation does not necessarily correlate with efficient proteolytic cleavage (Borodovsky *et al.*, 2001): otubain-1 is unable to bind Ub-VS but cleaves K48-linked chains *in vitro* (Wang *et al.*, 2009) and Ub C-terminal hydrolase 2 (USP2) is less sensitive to Ub-VS than Ub C-terminal hydrolase 36 (USP21), but cleaves Ub-AMC with more efficiency (Rivkin *et al.*, 2013).

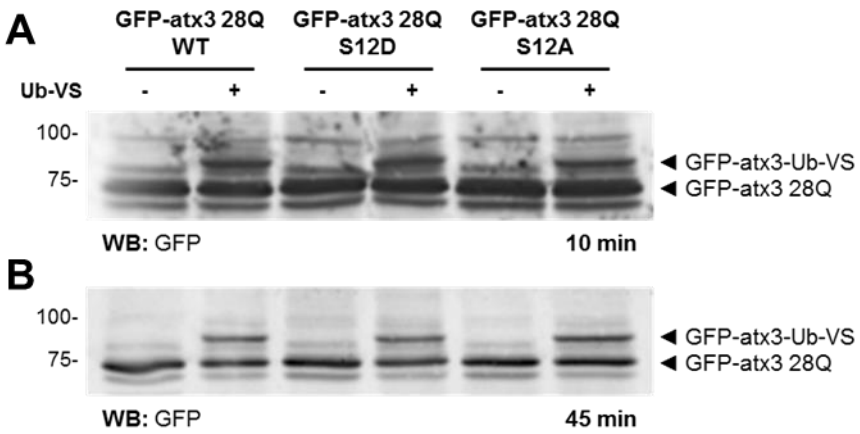

Figure 24: Phosphomutation of S12 does not alter atx3 conjugation to Ub-VS. COS-7 cells were transfected with WT or phosphomutated (S12D or S12A) forms of GFP-atx3 28Q, lysated and incubated (RT) with Ub-VS, for either ***A*** 10 min or ***B*** 45 min. Western blot analysis of the samples revealed that, for both incubation times, the amount of GFP-atx3 28Q that conjugated with Ub-VS (GFP-atx3-Ub-VS) is not affected by mutation of S12 residue.

These results suggest that mutation of S12 does not affect the binding of an Ub derivative to the catalytic site, which indicates that the mutations of that residue do not bluntly affect the conformation of the active site of the GFP-atx3 phosphomutants expressed in cells. Attending to the observations made *in vitro*, this could indicate that phosphorylation of S12 does not alter the binding of Ub substrates to C14, but affects the effectiveness of substrate cleavage. However, the experiments performed cannot rule out the possibility that the binding of the actual biologic Ub substrates differs between the non-phosphorylated and the phosphorylated forms. Atx3 is known to show a preference for binding and cleaving polyUb chains, thus limiting the conclusions made with a monoUb derivative (Burnett *et al.*, 2003; Mao *et al.*, 2005; Winborn *et al.*, 2008).

Chapter 4

Phosphorylation of serine 12 of ataxin-3: consequences for polyglutamine-induced toxicity

Chapter 4 – Phosphorylation of serine 12 of ataxin-3: consequences for polyglutamine-induced toxicity

4.1 Ataxin-3 phosphorylation at serine 12 prevents the decrease in neuronal dendritic length caused by polyglutamine expansion

Phosphorylation of S12 was predicted to affect atx3 DUB activity based on the close disposition of this amino acid residue to the catalytic site. The results obtained with the phosphomimetic S12D mutant support this hypothesis. However, it would be important and very relevant to test whether phosphorylation of S12 also affects events related to expanded atx3 toxicity, such as cellular alterations with possible deleterious effects and aggregate formation. Interference with the phosphorylation state of the protein may prove beneficial in terms of disease progression and severity.

With the objective of characterizing the effect of S12 phosphorylation on expanded atx3-induced toxicity, primary cultures of rat cortical neurons were favored over cell lines, because it is believed that the cell toxicity mechanisms caused by polyQ-expansion depend greatly on cell type and, in MJD, only neurons are targeted (Rüb *et al.*, 2013; Takahashi *et al.*, 2010; Yamada *et al.*, 2001; Zoghbi and Orr, 2000). Accordingly, any conclusions regarding toxicity events that were based in experiments utilizing fibroblast-like cell lines would be limited. Though MJD is chiefly described as a disease affecting the cerebellum and the brainstem, increasing evidence has implicated the cerebral cortex in the pathogenic mechanisms, contrary to the early idea that this region was mainly spared in MJD (Alves *et al.*, 2008b; Pedroso *et al.*, 2013; Rüb *et al.*, 2013; Yamada *et al.*, 2001). Authors have described reduced glucose metabolism (Soong *et al.*, 1997; Taniwaki *et al.*, 1997) and atrophy in the cortex of MJD patients' brain (D'Abreu *et al.*, 2012; Lopes *et al.*, 2013; Murata *et al.*, 1998), as well as the presence of polyQ NIs (Ishikawa *et al.*, 2002; Yamada *et al.*, 2001).

It is pertinent to investigate whether S12 phosphorylation of atx3 interferes with neuromorphological changes resulting from polyQ expansion of the protein. In MJD, many different neurodegeneration parameters have been studied in both patients and animal models, including neuronal marker depletion, cell death and brain region atrophy. One

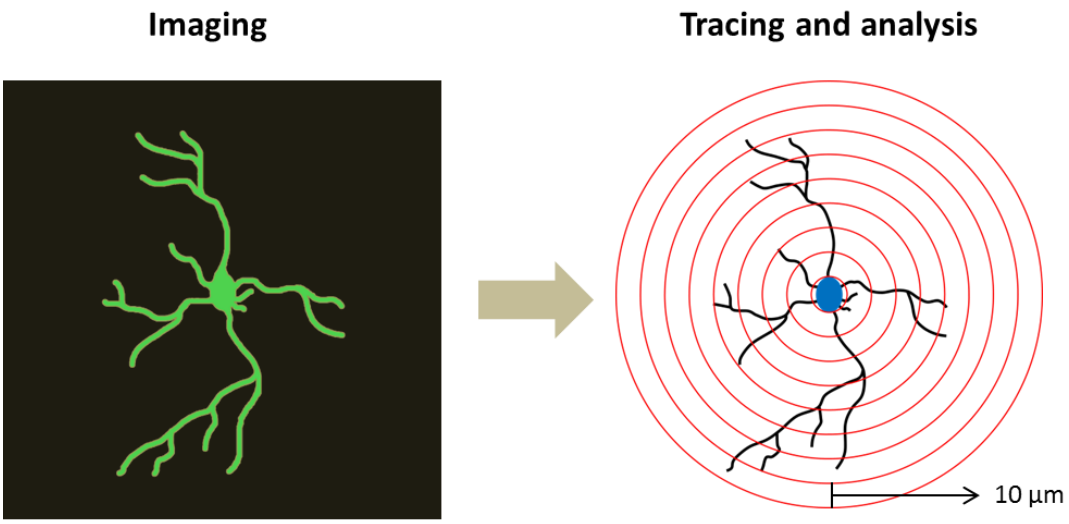

Figure 25: Analysis of dendritic morphology. Imaging cultured neurons labeled with an appropriate fluorophore and virtually tracing their cell bodies and neurites allows the computational analysis of several morphological parameters. The total length of dendritic tracts can be determined by summing the length of each individual dendritic tract (represented in black). Sholl analysis consists in determining the number of times de dendritic tracts intersect equidistant circles (in red) centered on the cell body (in blue), thus allowing the appreciation of dendritic arborization. The current study used circles distancing 10 µm from each other.

possible output of cell toxicity in cortical neuron cultures is the observation of neuritic degeneration, i. e., the loss of neuronal projections, such as dendrites. One important factor that can be analyzed when comparing the dendritic morphology of neurons is the total length of dendrites, expressed as the sum of the length of all the dendritic tracts of a cell. Quantitative analysis of the complexity of dendritic arborization of an imaged neuron may be achieved through Sholl analysis, a technique whereby equidistant circles of increasing radius centered on the cell body are drawn and the number of intersections with dendrites is determined (Figure 25). The resulting values are a function of both the number and length of dendrites – an increased number of intersections corresponds to a larger number of dendritic projections, at any given distance from the cell body.

First, in order to determine if expanded GFP-atx3 in fact affects the dendritic structure of cortical neurons, cells transfected with GFP-atx3 28Q and GFP-atx3 84Q were imaged through fluorescence microscopy (Figure 26A). Following the tracing of the respective cell bodies and dendrites, the total length of dendritic tracts was compared between neurons expressing the two constructs. GFP-atx3 84Q-expressing neurons had a lesser total extension of dendrites, in line with the idea that polyQ expansion of atx3 leads to dendritic loss (Figure 26B). Sholl analysis of the neuronal tracing in each condition was then performed in order to determine the number of crossings with circles distancing 10 µm from each other. Observation of the resulting curves revealed that neurons expressing GFP-atx3 84Q WT have a withered dendritic tree, with significantly less dendrites reaching 80 to 160 µm from the cell body (Figure 26C). Furthermore, contrary to neurons transfected with GFP-atx3 28Q WT, GFP-atx3 84Q WT-expressing cells have no dendrites reaching more than 170 µm from the cell body.

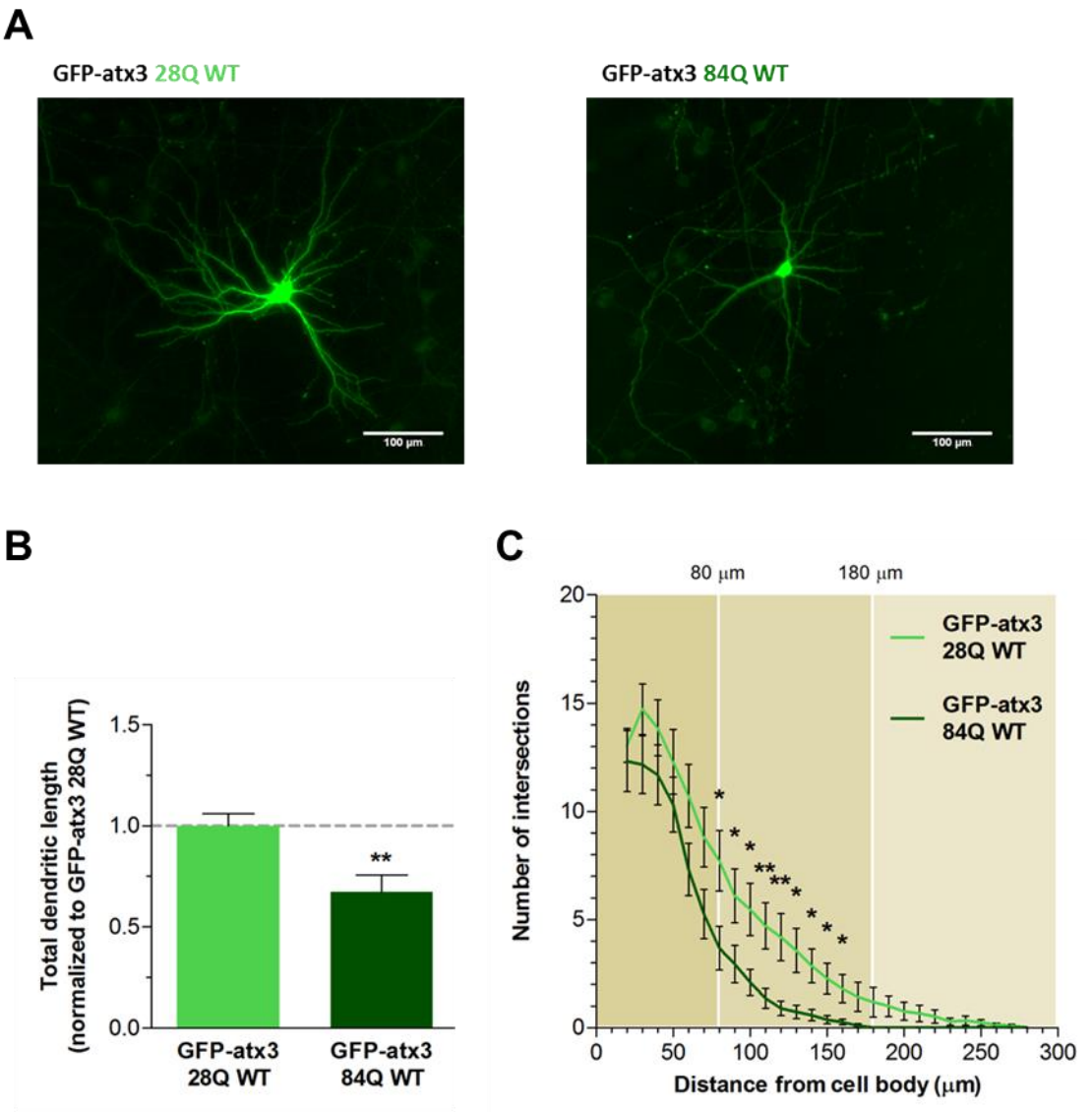

Figure 26: Pathogenic polyglutamine expansion of GFP-atx3 leads to dendrite tract loss and contraction in cortical neurons. ***A*** Cultured rat cortical neurons with 9-10 DIV were transfected with GFP-atx3 28Q WT or GFP-atx3 84Q WT, fixed 5 days later and imaged in the fluorescence microscope. Representative images of each condition are shown. ***B*** Neurons expressing GFP-atx3 84Q WT have a reduced total dendritic length, expressed by the sum of the length of all dendritic tracts in each particular neuron analyzed. Bars represent total dendritic length (mean ± SEM) of the neurons analyzed in each condition (n = 19-21, from two independent experiments), normalized to the mean total dendritic length of neurons transfected with GFP-atx3 28Q WT in each independent experiment. Values were compared using the student's t-test: ** - P < 0,01. ***C*** Sholl analysis demonstrates a decrease of dendrites reaching more than 80 µm from the cell body. The curves represent the number of intersections (mean ± SEM, n = 19-21 neurons in each condition, from two independent experiments) as function of the distance from the cell body. Differences are statistically significative in the region distancing between 80 and 160 µm from the cell body. GFP-atx3 84Q WT-expressing neurons have no dendrites reaching 180 µm. The number of crossing at each distance was compared using the student's t-test: * - P < 0,05; ** - P < 0,01.

This indicates that, in the cultured rat cortical neurons used in this study, expression of GFP-atx3 with an expanded glutamine tract causes dendritic loss or shrinkage.

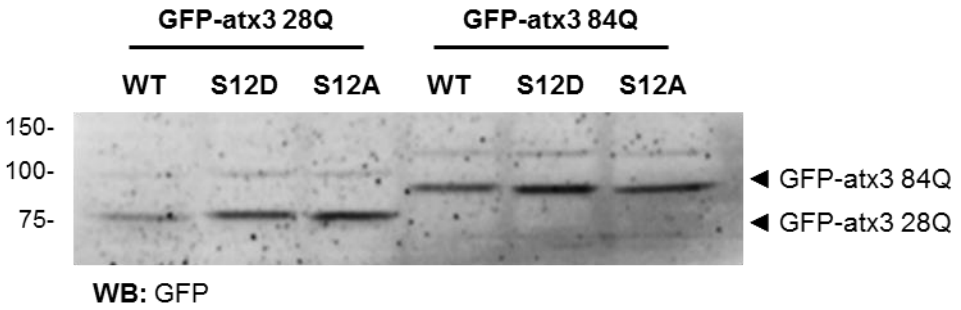

Figure 27: Transfection of rat cortical neurons with GFP-atx3 phosphomutants. Cultured rat cortical neurons with 9-10 DIV were transfected with GFP-atx3 28Q WT, GFP-atx3 84Q WT or the respective S12D or S12A mutants and 5 days later whole cell lysates were analyzed by Western blot with an anti-GFP antibody. The differences in electrophoretic movement between GFP-atx3 28Q and GFP-atx3 84Q reflect the differences in molecular size resulting from the distinct number of glutamine residues.

Previous studies using neurons from transgenic *Drosophila* larvae have detected dendritic abnormalities resulting from expanded atx3 expression (Lee *et al.*, 2011), and a severe impairment of dendritic arborization was also recently described to occur in the Purkinje cells of a MJD mouse model (Konno *et al.*, 2014). The experiments using the MJD mouse model were performed in symptomatic animals expressing only a truncated fragment of polyQ-expanded atx3 (known to be more toxic that the full-length protein; Goti *et al.*, 2004; Warrick *et al.*, 1998; Yoshizawa *et al.*, 2000) and comparison was made with wild-type littermates. The current results constitute the first evidence that expanded atx3 causes an observable dendritic loss/shrinkage in transfected mammalian neuron cultures, namely in neurons isolated from the cortex, and represent compelling evidence that full-length atx3 causes dendritic loss or shortening as a consequence of polyQ expansion, in mammalian neurons. These changes in the dendritic arborization may represent one pathologic mechanism by which expanded atx3 disrupts neuronal structure and, consequently, function, without (or before) inducing cell death.

In order to investigate if S12 phosphorylation affects the dendritic shrinkage caused by GFP-atx3 84Q WT expression, cortical neurons were transfected with GFP-atx3 84Q S12D or S12A (Figure 27) and total dendritic length was analyzed as above. The phospho-null mutant of GFP-atx3 84Q exhibited similar effects to those of GFP-atx3 84Q WT but, interestingly, neurons expressing GFP-atx3 84Q S12D had a significantly higher total dendritic length, showing no differences relative to the total dendritic length of cells expressing GFP-atx3 28Q WT Figure 28A and B). Surprisingly, GFP-atx3 28Q S12A displayed an increased toxicity comparing to the other non-expanded forms, leading to a decreased total length of dendrites. These results suggest that phosphorylation of S12 protects against dendritic tract loss and that compromise of this modification is enough to cause a loss of dendritic tracts.

Dendritic arborization was also evaluated by Sholl analysis, as above. Comparing the curves obtained when analyzing the neurons transfected with GFP-atx3 84Q WT or its phosphomutants, no striking differences were detected in the dendritic profile, namely in the region distancing more than 80 µm from the cell body (Figure 29A and B). However, the

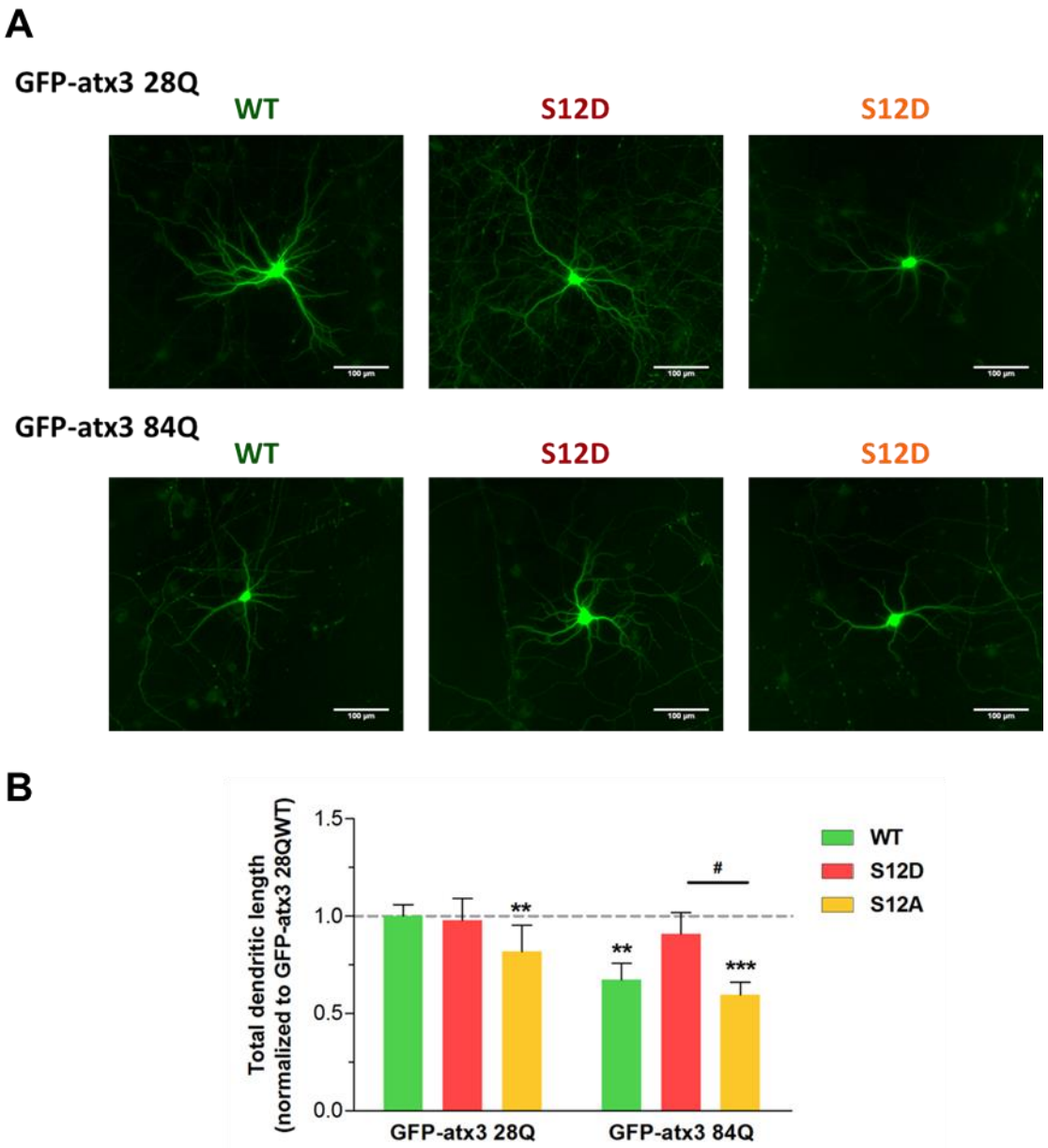

Figure 28: Mimicking phosphorylation at S12 rescues dendritic tract loss caused by expanded atx3 expression. ***A*** Cultured rat cortical neurons with 9-10 DIV were transfected with GFP-atx3 28Q WT, GFP-atx3 84Q WT or the respective S12D or S12A mutants, fixed 5 days later and imaged in the fluorescence microscope. Representative images if neurons transfected with the phosphomutants are shown. ***B*** Transfection with GFP-atx3 84Q S12D elicits no differences comparing to the GFP-atx3 28Q WT control. Similarly to GFP-atx3 84Q WT, expression of phospho-null GFP-atx3 84Q S12A causes a reduction of total dendritic length. Bars represent total dendritic length (mean ± SEM) of the neurons analyzed in each condition (n = 16-21, from two independent experiments), normalized to the mean total dendritic length of neurons transfected with GFP-atx3 28Q WT in each independent experiment. The Mann-Whitney test was used to compare each condition with cells transfected with GFP-atx3 28Q WT: ** - $P < 0,01$; *** - $P < 0,01$. Comparison between other pairs of conditions was performed by two-way ANOVA, followed by Bonferroni post-hoc test: # - $P < 0,05$.

phosphomimetic mutant displays a slight tendency for having a larger number of dendrites at almost every distance, while the phospho-null mutant shows the opposite behavior, even producing a statistically significant decrease in the number of dendrites at 50 µm. Considering

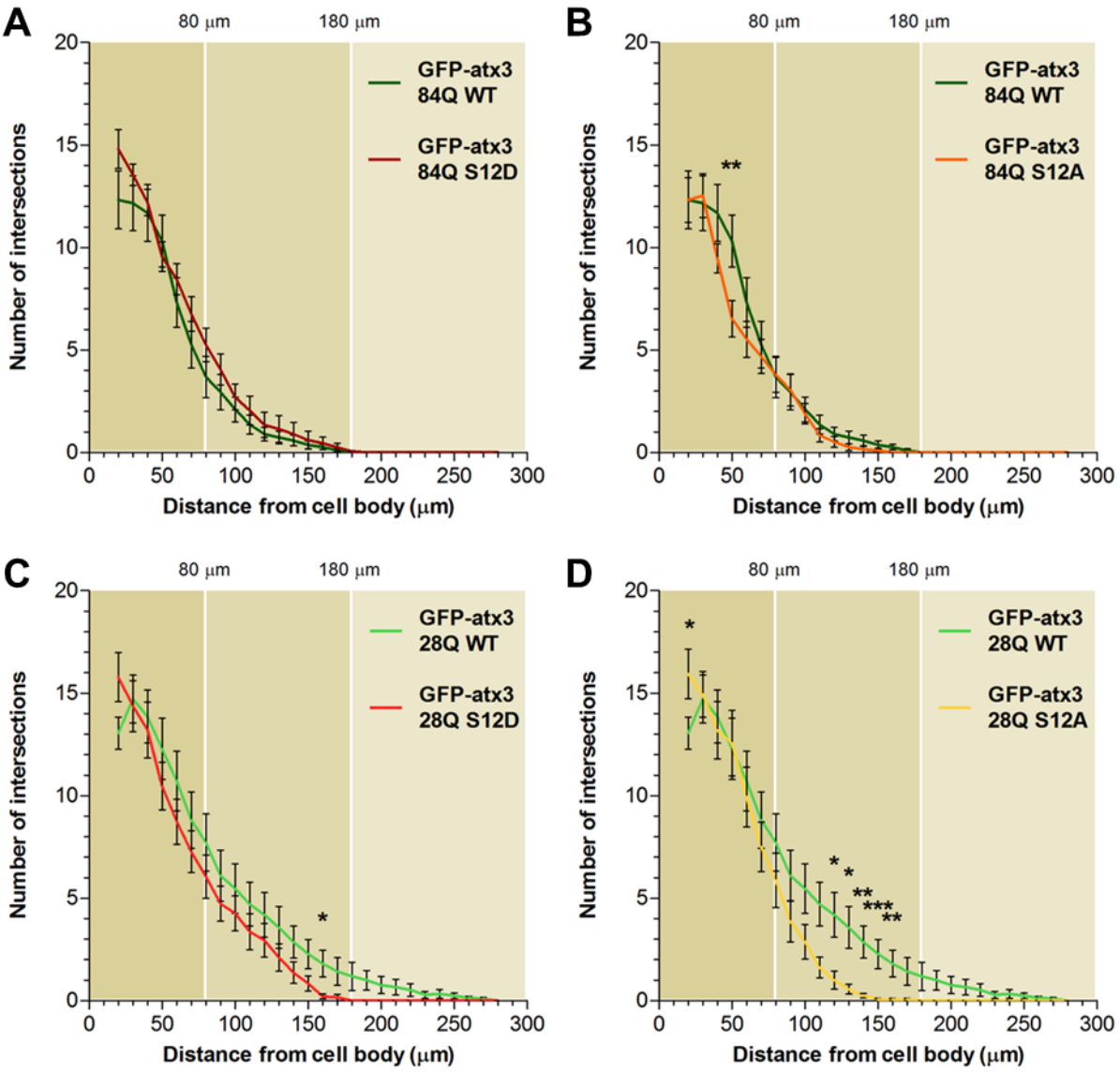

Figure 29: Mutating S12 does not hinder the dendritic shrinkage caused by expanded atx3 expression. Cultured rat cortical neurons transfected with GFP-atx3 28Q WT, GFP-atx3 84Q WT or the respective S12D or S12A mutants were imaged in the fluorescence microscope and subjected to Sholl analysis. ***A*** Mimicking S12 phosphorylation in GFP-atx3 84Q WT does not elicit striking differences regarding the way dendrites project from the cell body, though neurons transfected with GFP-atx3 84Q S12D tend to have more dendrites reaching every distance analyzed, albeit without statistical significance. ***B*** The phospho-null mutant of GFP-atx3 84Q WT shows the contrary tendency, which reaches statistical significance in the number of crossings at 50 µm. ***C, D*** The two phosphomutants of GFP-atx3 28Q display a tendency for decreasing the amount of dendrites reaching bigger distances from the cell body, limited in the case of GFP-atx3 28Q S12D, but expressive in the case of GFP-atx3 28Q S12A (especially in the region distancing between 120 and 160 µm from the cell body). The curves represent the number of intersections (mean ± SEM, n = 16-21 neurons in each condition, from two independent experiments) as function of the distance from the cell body. The number of crossing at each distance was compared between each condition pair using the Mann-Whitney test: * - P < 0,05; ** - P < 0,01; *** - P < 0,01.

the results obtained in the analysis of the total dendritic length, phosphorylation at S12 may not counter the hampered dispersal of dendrites caused by polyQ expansion, but hinders the

actual deletion of dendritic tracts. This effect is possibly expressed by the tendentially increased number of interceptions detected in the Sholl analysis, when comparing GFP-atx3 S12D with its WT counterpart.

Comparison between the dendritic complexity of neurons expressing GFP-atx3 28Q WT or its S12D and S12A forms revealed some propensity for lesser arborization in the neurons transfected with the phosphomutants (Figure 29C and D). In fact, the only neurons presenting dendrites at 190 µm from the cell body or at longer distances were the ones transfected with GFP-atx3 28Q WT. While the effect is very mild in the case of GFP-atx3 28Q S12D, neurons transfected with GFP-atx3 28Q S12A showed a noticeably shrunken dendritic tree starting at 120 µm from the cell body. It can be assumed that the phosphomutants of non-expanded GFP-atx3, and especially GFP-atx3 28Q S12A, may have some associated toxicity, as had been hinted by the total dendritic length results.

Taken together, the exploration of the two factors considered in the current analysis of dendritic morphology – total dendritic length decrease and dendritic shrinkage, as inferred from the Sholl Analysis curve – suggests that phosphorylation of S12 may be implicated in the mechanisms linking atx3 to dendritic degeneration. GFP-atx3 28Q S12D shows no significant evidence of inducing dendritic demise, comparing to GFP-atx3 28Q WT; on the other hand, GFP-atx3 28Q S12A leads to a visible loss of dendritic dispersal and to a diminished length of dendrites, revealing an increased neuronal toxicity by this non-phosphorylatable form. PolyQ expansion causes a noticeable shrinkage of the dendritic tree in the neurons transfected with any of the GFP-atx3 84Q constructs, but only the WT and S12A forms lead to an actual decrease of the total dendritic length. The dendrites of neurons transfected with GFP-atx3 84Q S12D have a total length comparable to that of the neurons transfected with GFP-28Q WT, suggesting that phosphorylation of S12 may have a protective role against this particular aspect of dendritic degeneration. All these differences caused by phosphomutation of atx3 indicate that, in a cellular context, S12 phosphorylation of expanded atx3 may hinder the actual loss of dendrites, leading to a more contracted dendritic tree, while provoking no decrease in the actual length of dendritic tracts.

4.2 Ataxin-3 phosphorylation at serine 12 prevents excitatory synapse loss triggered by polyglutamine expansion

Having observed relevant effects of the phosphomimetic form of GFP-atx3 84Q in protecting against decreased dendritic length, we tested whether the S12 phosphomutations affect subtler characteristics of neuronal morphology, of no lesser biologic or pathogenic relevance. Recently, investigation of proteinopathic neurodegenerative diseases has frequently been moving its focus from the study of neuronal death mechanisms to the characterization of the possible functional changes the pathogenic proteins cause in neurons. It is believed that changes in neuronal functions may precede – or even cause – the actual loss of neurons, and that some disease symptoms may arise from this type of defects. For this

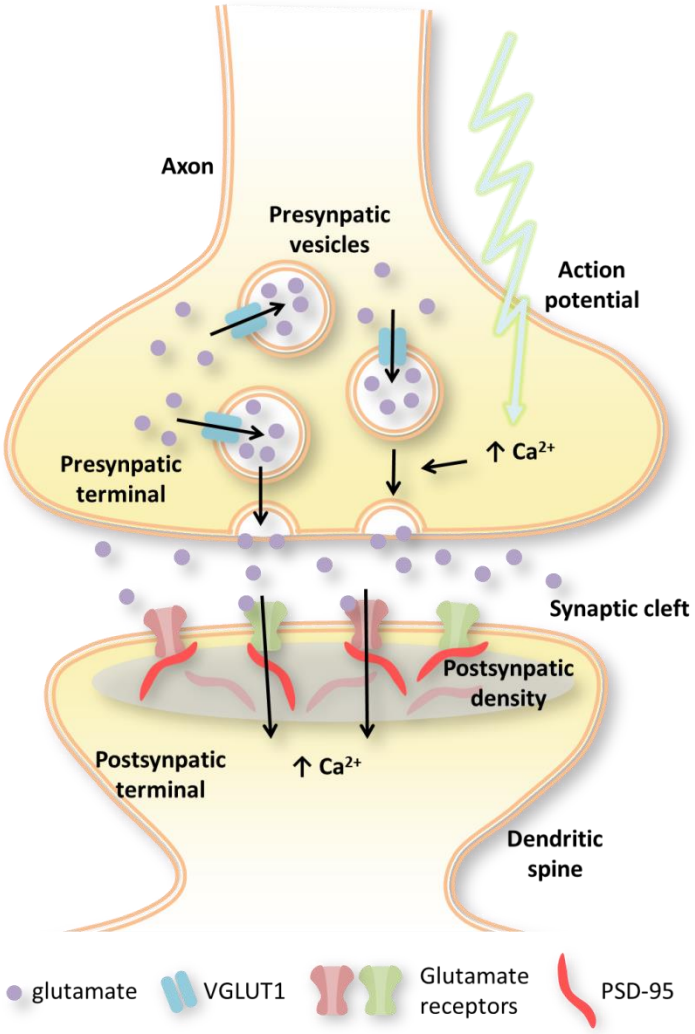

Figure 30: The glutamatergic synapse. In the presynaptic terminal, glutamate is accumulated in presynaptic vesicles through the action of transporter protein such as VGLUT1. Depolarization of the presynaptic membrane caused by an incoming action potential leads to the entry of calcium ions and the consequent rise in intracellular calcium concentration, activating cellular pathways that cause the vesicles to fuse with the plasma membrane. The neurotransmitter is released in the synaptic cleft, diffuses and binds to extracellular regions of glutamate receptors present in the postsynaptic membrane, leading to their activation and thus contributing to the depolarization of the post-synaptic neuron. Glutamate receptors are anchored to the underlying post-synaptic density, a protein-rich structure of the dendritic spine that contains the scaffolding protein PSD-95 with which glutamate receptors interact directly or indirectly.

reason, it is essential to evaluate if toxic proteins such as expanded polyQ-containing ones cause neuronal changes with functional relevance.

Neurons of the rat cortex establish functional synapses when cultured under the conditions used in this study (Louros *et al.*, 2014). It is important to determine if expression of atx3 with a pathogenic expansion affects their ability to establish and/or maintain synaptic connections, and then evaluate the eventual differences caused by phosphomutation of S12. This could serve not only as a measure of the health of the neurons, but also of the possible

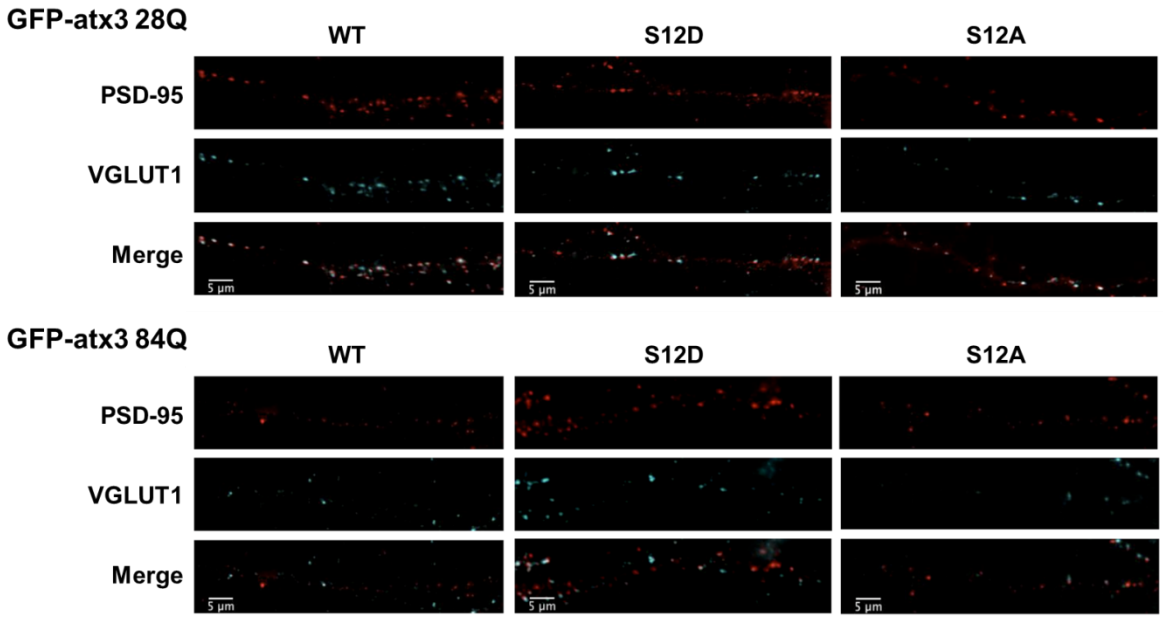

Figure 31: Effects of S12 phosphomutation on glutamatergic synapse markers of cortical neurons transfected with GFP-atx3. Low-density rat cortical neuron cultures with 9-10 DIV were transfected with GFP-atx3 28Q WT, GFP-atx3 84Q WT or the respective S12D or S12A mutants and fixed 5 days later. Glutamatergic synapse markers VGLUT1 (pre-synaptic) and PSD-95 (post-synaptic) were immunocytochemically labeled and dendritic tracts of GFP-atx3-expressing neurons were imaged. The figure shows representative dendritic sections evidencing VGLUT1 and PSD-95-positive puncta and the respective colocalization (merge).

compromise of their function, since synapses are the structures responsible for transmitting signals between neurons.

Glutamate is the most prevalent excitatory neurotransmitter in the vertebrate brain. In the human and rat cortices, the majority of neurons are glutamatergic (DeFelipe, 2011), establishing synapses that use this amino acid as a means to propagate the nervous impulses to the dendrites of contacting neurons. In this type of neurons, glutamate is accumulated inside synaptic vesicles at the presynaptic region of an axon and, upon depolarization of the plasma membrane caused by the arrival of an action potential, Ca^{2+} enters the cell and leads to the fusion of those vesicles with the presynaptic membrane (Figure 30). Glutamate is thus secreted into the synaptic cleft, diffuses and eventually binds to its receptors at the postsynaptic membrane, contributing to the depolarization of the postsynaptic neuron (Popoli *et al.*, 2012).

We started by investigating if expression of GFP-atx3 84Q WT had a detectable effect in the number of glutamatergic synapses present in cultured rat cortical neurons, comparing to GFP-atx3 28Q WT. Immunocytochemical visualization of glutamatergic synapses can be achieved through the labeling of pre- and postsynaptic protein markers. The vesicular glutamate transporter subtype 1 (VGLUT1) is a protein associated with glutamate-accumulating synaptic vesicles, playing a role in the transport and consequent packaging of this neurotransmitter (Popoli *et al.*, 2012). Being specifically localized in glutamate-releasing

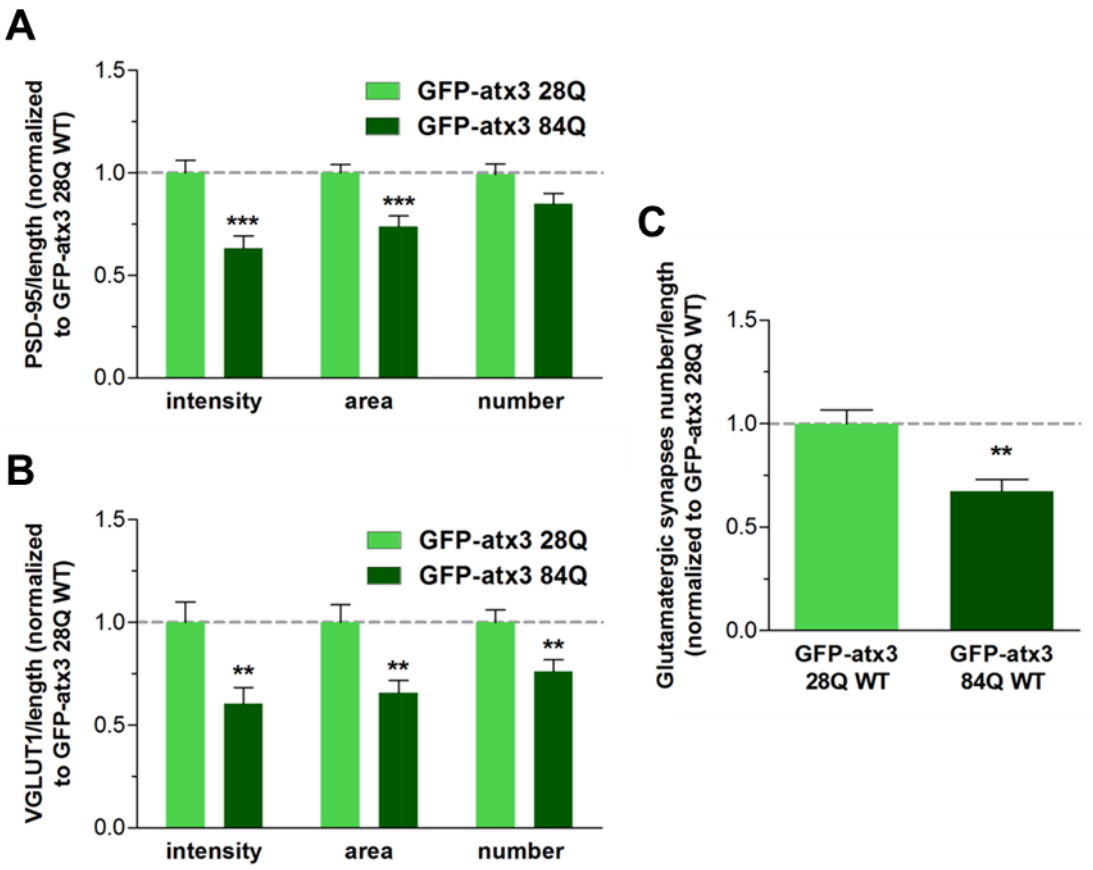

Figure 32: Polyglutamine expansion of GFP-atx3 causes a loss of functional glutamatergic synapses in cortical neurons. Comparing to GFP-atx3 28Q WT, expression of GFP-atx3 84Q WT in cultured cortical neurons causes a decrease in the intensity and area of ***A*** PSD-95 and ***B*** VGLUT1 puncta. The number of VGLUT1-positive accumulations also decreases significantly compared to control. ***C*** The number of functional glutamatergic synapses, defined as the instances of colocalization between the two synaptic markers, decreases in neurons transfected with GFP-atx3 84Q WT, comparing to cells expressing GFP-atx3 28Q WT. In every graph bars represent mean ± SEM of the values per dendritic section length (n = 30-32 neurons in each condition, from three independent experiments), normalized to the mean value of GFP-atx3 28Q WT in the respective experiment. Comparison between the two conditions used the Mann-Whitney test: ** - P < 0,01; ; *** - P < 0,001.

terminals, VGLUT1 was used as a presynaptic marker. In the postsynaptic region of excitatory synapses, neurotransmitter receptors are clustered in protein-rich structures named postsynaptic densities (PSDs), comprised also of many proteins of the cytoskeleton, proteins acting in signal transduction and scaffolding proteins. PDS-95 is a scaffolding protein enriched in the PSD of glutamatergic synapses (Hunt *et al.*, 1996; Kim and Sheng, 2004), therefore serving as a reliable postsynaptic marker.

Fluorescence microscopy observation of rat cortical neuron cultures labelled with anti-PSD-95 and anti-VGLUT1 antibodies reveals a punctuate signal, as expected of synaptic proteins, which are enriched in these discrete cell structures (Figure 30). Comparing to neurons transfected with GFP-atx3 28Q WT, neurons expressing its expanded counterpart show a remarkable decrease in the intensity and area of the PSD-95-positive puncta, indicative of a possible interference of the polyQ-expanded protein with the accumulation of this

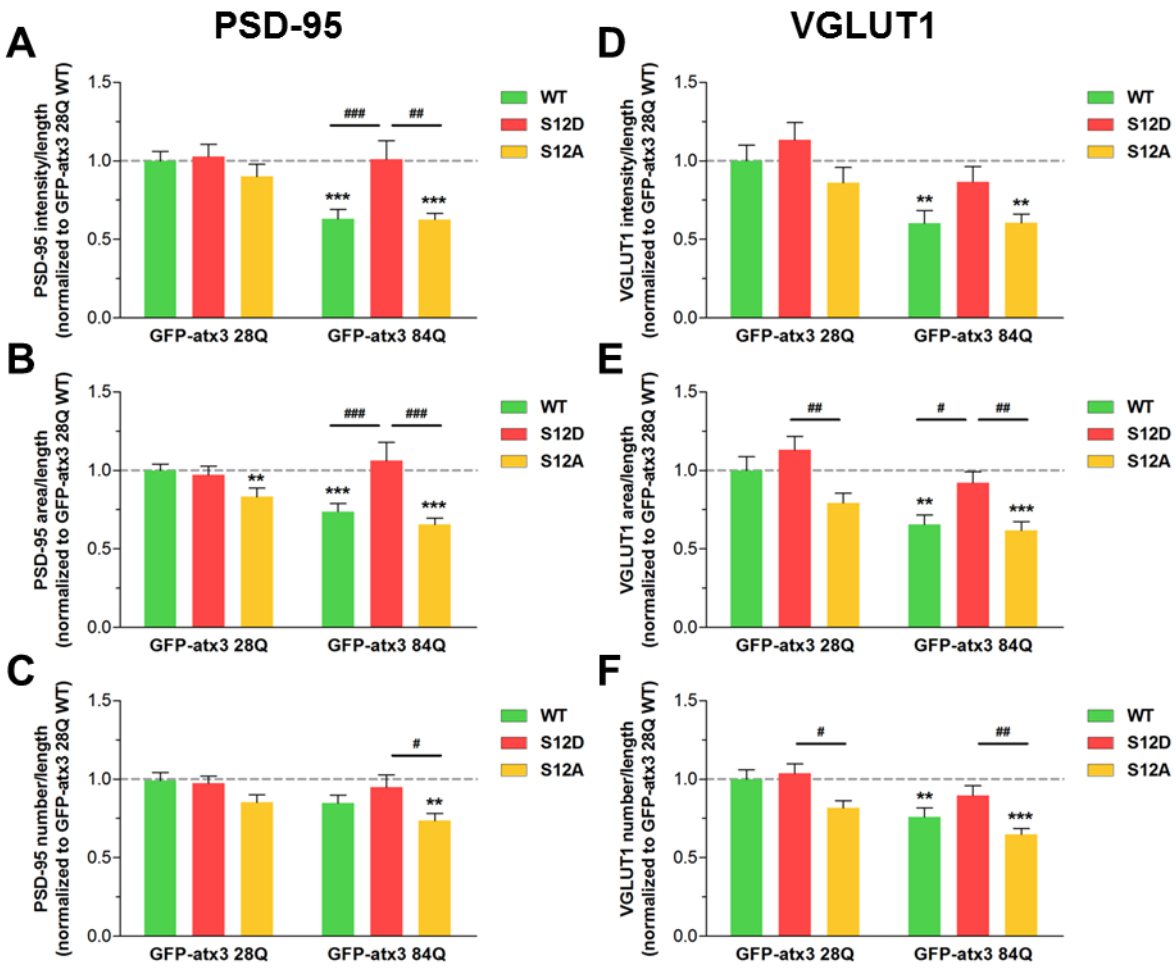

Figure 33: Mimicking S12 phosphorylation hinders the loss of glutamatergic synapse markers in cortical neurons expressing expanded GFP-atx3. Expression of GFP-atx3 84Q S12D does not leads to any decrease in the intensity, area or number of ***A-C*** PSD-95 or ***D-F*** VGLUT1 synaptic puncta in cultured cortical neurons, comparing to what is observed with GFP-atx3 28Q WT. Transfection with phospho-null GFP-atx3 84Q S12A causes a decrease similar to what is elicited by GFP-atx3 84Q WT expression.. In every graph bars represent mean ± SEM of the values per dendritic section length (n = 24-32 neurons in each condition, from three independent experiments), normalized to the mean value of GFP-atx3 28Q WT in the respective experiment. The Mann-Whitney test was used to compare each condition with cells transfected with GFP-atx3 28Q WT: ** - P < 0,01; *** - P < 0,01. Comparison between other pairs of conditions was performed by two-way ANOVA, followed by Bonferroni post-hoc test: # - P < 0,05; ## - P < 0,01; ### - P < 0,001.

scaffold protein in postsynaptic terminals (Figure 31 and 32A). Analysis of the VGLUT1-positive puncta in the same experimental conditions also revealed a decrease in the intensity, area and number of puncta arising from GFP-atx3 84Q WT expression and representing a possible influence over the presynaptic terminals contacting with the dendrites of the GFP-atx3-expressing neurons (Figure 31 and 32B). More important than the labelling of each marker by itself, in this type of preparations, instances of colocalization between VGLUT1 and PSD-95 puncta are an expression of the close localization between the pre- and postsynaptic terminals,

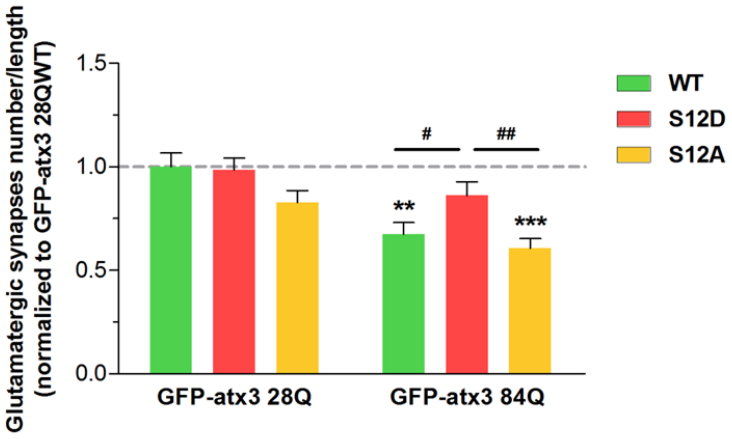

Figure 34: Mimicking S12 phosphorylation hinders the loss of functional glutamatergic synapsis in cortical neurons expressing expanded GFP-atx3. The number of functional glutamatergic synapses, defined as the instances of colocalization between the two synaptic markers – PSD-95 and VGLUT1 –, does not decrease in neurons transfected with GFP-atx3 84Q S12D, comparing to cells expressing GFP-atx3 28Q WT. Expression of phopho-null GFP-atx3 84Q S12A causes a decrease similar to what is obtained by transfection with GFP-atx3 84Q WT. Bars represent mean ± SEM of the number of functional synapses per dendritic section length (n = 24-32 neurons in each condition, from three independent experiments), normalized to the mean value of GFP-atx3 28Q WT in the respective experiment. The Mann-Whitney test was used to compare each condition with cells transfected with GFP-atx3 28Q WT: ** - $P < 0,01$; *** - $P < 0,01$. Comparison between other pairs of conditions was performed by two-way ANOVA, followed by Bonferroni post-hoc test: # - $P < 0,05$; ## - $P < 0,01$.

admittedly representing the presence of functional glutamatergic synapses. Expression of GFP-atx3 84Q WT in cortical neurons leads to a significant decrease in the number of glutamatergic synapses, measured by the number of colocalizing VGLUT1 and PSD-95 puncta (Figure 31 and 32C).

All these observations constitute important and original evidence concerning the toxic effects of expanded atx3 in cortical neurons. When expanded, atx3 leads to a decrease in the signal of two synaptic markers and in the number of functional glutamatergic synapses, two events that may be indicative not only of relevant particularities of cell demise, but that could also be linked to possible nefarious effects in neuronal transmission. The results support the idea of an involvement of synaptic dysfunction in the toxic mechanisms elicited by polyQ-expanded atx3.

The effects of S12 phosphorylation in the observed changes caused by GFP-atx3 84Q expression were once more addressed by comparison between the behavior of the GFP-atx3 WT forms and their phosphomutants (Figure 31). GFP-atx3 84Q S12A, the non-phosphorylatable from, causes similar effects to the ones observed for GFP-atx3 84Q WT (Figure 33A-F and 34). Comparing to GFP-atx3 28Q WT, the S12A expanded form leads to a decrease in the intensity, area and number of puncta of both PSD-95 and VGLUT1, and also to a reduced number of functional synapses. Contrastingly, GFP-atx3 S12D does not cause any significant decrease in any of these parameters. In fact, overall the phosphomimetic mutation reverts the effects provoked by GFP-atx3 84Q WT, leading to higher levels of synaptic marker labelling and, importantly, to a number of glutamatergic synapses similar to that observed in

neurons transfected with non-expanded atx3. Similarly to what was observed with the experiments described above, the effect of GFP-atx3 28Q S12D is not different from that of GFP-atx3 28Q WT, but the S12A mutant of the non-expanded form repeatedly shows a slight tendency for the reduction of all the synaptic parameters analyzed.

The differential effects caused by mutation of S12 hint to the fact that phosphorylation of this amino acid residue may play a role in protecting against the mechanisms by which expanded atx3 leads to the observed synaptic dysfunction of cultured cortical neurons. Phosphorylation of S12 appears to be important for the maintenance of the number of functional glutamatergic synapses in cells expressing expanded atx3, suggesting that this PTM constitutes a protective mechanism against the synaptotoxicity of the expanded protein. The biological importance of atx3 as a synaptic regulator has not been explored, but may possibly be related to an as of yet undisclosed function of this DUB.

4.3 Ataxin-3 phosphorylation at serine 12 affects its aggregation in cortical neurons

Given the recognized role of aggregation in the toxicity pathways involved in polyQ expansion diseases, we moved on to test whether the S12 phosphomutations affect atx3 tendency to aggregate. The other reports concerning atx3 phosphorylation described five phosphorylation sites, distributed among the 3 UIMs, the regions of atx3 described to be responsible for the selectivity in the interaction with PolyUb chains (Burnett *et al.*, 2003; Fei *et al.*, 2007; Mao *et al.*, 2005; Mueller *et al.*, 2009; Schmitt *et al.*, 2007; Winborn *et al.*, 2008). In cultured cells, modification of three of those sites to aspartate – S236, S340 and S352 – was described to increase the nuclear localization of atx3, an important step leading to aggregation and toxicity of the expanded protein (Bichelmeier *et al.*, 2007; Macedo-Ribeiro *et al.*, 2009; Matos *et al.*, 2011). Mimicking phosphorylation of residues S340 and S352 also increased the stability and half-life of atx3 in cells. Pharmacological inhibition of CK2, an enzyme described as being able to phosphorylate the UIM-containing C-terminal region of atx3, reduced the amount of nuclear atx3 and decreased NI formation, possibly as a result of the two effects described above (Bichelmeier *et al.*, 2007; Breuer *et al.*, 2010; Mueller *et al.*, 2009). Contrastingly, other authors described that preventing phosphorylation of S256 through a phospho-null mutation to alanine enhanced its ability to aggregate in cells (Fei *et al.*, 2007). These observations demonstrate that interference with phosphorylation sites of atx3 may affect its tendency to aggregate, though the actual effect – increase or decrease of aggregation – differs depending on the phosphorylation sites in question, and possibly on the experimental setting. It thus seemed pertinent to investigate whether phosphorylation of S12 has an effect on the aggregation of atx3.

It has been repeatedly demonstrated that the atx3 JD is, by itself, prone to self-assemble *in vitro*, playing a role in the early conformational changes leading to full-length atx3

aggregation and modulating the aggregation of both expanded and non-expanded atx3 (Ellisdon *et al.*, 2006; Gales *et al.*, 2005; Masino *et al.*, 2011; Masino *et al.*, 2004; Saunders and Bottomley, 2009). Conceivably, changes caused by PTMs of the JD, such as phosphorylation at S12, could affect the dynamics of atx3 aggregation. As explained before (section 3.3), according to the NMR structure of the complex formed between atx3 JD and two Ub moieties (Nicastro *et al.*, 2009; PDB code: 2JRI), S12 is in close proximity to the C-terminal part of the Ub molecule that binds at site 1, which is localized in the cleft formed between the helical hairpin and the globular subunit (Figure 15D and E). Interestingly, the two Ub binding sites identified overlap with the regions described as taking part in JD self-assembly (Masino *et al.*, 2011; Nicastro *et al.*, 2009). It has been hypothesized that atx3 aggregation is dependent upon the molecular interactions it establishes and, *in vitro*, association of the JD with Ub protects against aggregation (Fiumara *et al.*, 2010; Masino *et al.*, 2011; Song *et al.*, 2010). It is therefore plausible that phosphorylation at S12 may affect the interactions mediated by the Ub binding sites of the JD, thus influencing atx3 aggregation. The studies of atx3 phosphorylation mentioned above serve as testimony to the fact that interference with regions interacting with Ub – the UIMs – affects aggregation of the protein.

In order to evaluate aggregation we again preferred the neuronal culture model over cell lines, considering that aggregation is possibly linked to neuron-specific toxicity. Cortical neurons were transfected with GFP-tagged WT or phosphomutated forms of atx3 with 28Q or 84Q, and the GFP fluorescent signal was visualized through fluorescence microscopy. Both non-expanded and polyQ-expanded atx3 formed noticeable aggregates in cortical neurons, but that was not the case for every cell, with many presenting a diffuse GFP-atx3 signal spread over the whole neuron. Distribution of the aggregates varied between cells, being found chiefly in the nucleus but sometimes also in the cytoplasm, or in both regions; in some rare cases, aggregates were also observed in neurites. Nevertheless, no evident association was established between any of the GFP-atx3 forms and the cellular localization of the corresponding aggregates. The shape of the GFP-atx3 aggregates observed was generally spherical or ovoid, but their size varied between cells (Figure 35A). Some cells presented just minute accumulations of GFP-atx3, nonetheless considered as aggregates, whereas, in the other extreme of the spectrum, other cells exhibited sizeable lumps of GFP-positive signal, forming a structure akin to a net of aggregated GFP-atx3. The number of aggregates also varied markedly, but there was no obvious relationship between aggregate size and/or number and any of the GFP-atx3 forms that were transfected. The great diversity in aggregate sizes, along with the large number of aggregates in some of the cells and the fact that they distributed three-dimensionally, turned the simple quantification of the number of aggregates unfeasible.

Objective comparison between the aggregation profiles generated by the different GFP-atx3 forms was achieved through the determination of the number of cells that presented aggregates, in the context of the overall population of transfected cells. Cells were counted as having GFP-atx3 aggregation when they presented at least one noticeable instance of GFP-positive accumulation, regardless of size; cells displaying only diffuse GFP signal were counted

as having no aggregates (Figure 35A). Aggregation of GFP-atx3 in cortical neuron cultures was thus expressed as the fraction of cells with aggregates, normalized to the values obtained with transfection with GFP-atx3 84Q WT, in each experiment.

PolyQ expansion of atx3 is known to be the triggering factor for pathogenesis in MJD and has been repeatedly described to be the cause of abnormal aggregation of polyQ sequence-containing proteins (as discussed in section 1.5). In agreement with this premise, non-expanded GFP-atx3 28Q WT displays a profoundly decreased tendency to aggregate, when compared to the GFP-atx3 84Q WT (Figure 35B). As mentioned above, in this cortical neuron-based assay even the non-expanded WT form with 28 glutamine residues formed detectable aggregates, but results indicate that the 84 glutamine-containing WT protein aggregates more. This observation serves as validation to this aggregation experiments, seeing as it reflects the acknowledged association between the tendency to aggregate and the length of the polyQ sequence.

Comparing aggregation between neurons transfected with GFP-atx3 84Q WT or its phosphomutants S12D and S12A, it is possible to detect a significant decrease in the fraction of neurons with aggregates, caused by the phospho-null mutation of S12 to alanine (Figure 35B). GFP-atx3 84Q has a serine residue at position 12, available for phosphorylation by the cell kinases, but alanine is not a subject for this PTM. This could indicate that, when polyQ-expanded atx3 is not phosphorylated, its tendency to form detectable aggregates is diminished. However, the phosphomimetic S12D mutant of GFP-atx3 84Q displayed a similar behavior, although the tendential decrease does not reach statistical significance. This suggests that phosphorylation of expanded atx3 at S12 decreases its tendency to aggregate and that the non-phosphorylated S12 plays a role in the aggregation pathway.

Aggregation of GFP-atx3 28Q S12D is lower than what is observed for GFP-atx3 84Q WT, but GFP-atx3 S12A appears to lead to higher levels of aggregation than its WT and S12D counterparts. Considering that both phosphomutants of expanded atx3 apparently lead to reduced aggregation, the effect of actual S12 phosphorylation of the pathogenic protein remains indefinite, though blockade of this modification elicited the most evident decrease in the tendency of GFP-atx3 84Q to form aggregates in cultured cortical neurons. However, hindering phosphorylation of GFP-atx3 28Q appears to have the opposite effect, increasing the amount of cells with aggregates. These observations suggest that the availability of S12 is an important factor influencing this toxicity hallmark, in neurons. In a biological context, the modifications caused by phosphorylation of S12 are very likely to influence whatever aggregation mechanisms are mediated by this amino acid residue. Importantly, this toxic outcome has parallels with the effects of GFP-atx3 S12A on neuronal morphology.

Finally, it is important to refer that, in cultures transfected with GFP-atx3 84Q WT but contrary to the cells expressing other constructs, it was not uncommon to find cells containing vast numbers of large aggregates that were not scored because of their unhealthy appearance (Figure 35A). In other words, many neurons appeared to have died as a result of GFP-atx3 84Q WT transfection (but not GFP-atx3 84Q S12D or S12A), possibly through mechanisms involving aggregation. Consequently, the number of GFP-atx3 84Q WT-transfected cells displaying

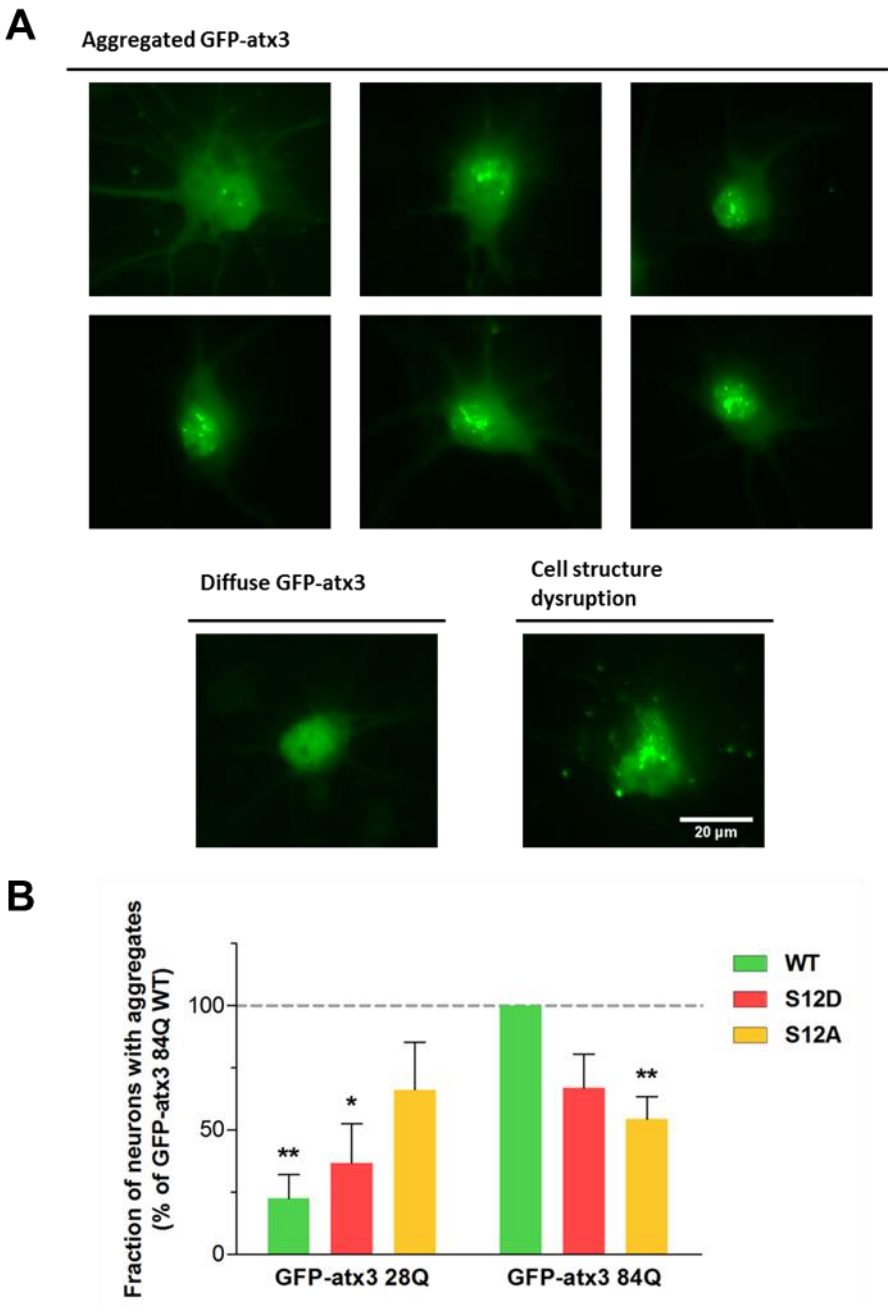

Figure 35: Mutating S12 decreases the fraction of transfected cortical neurons with GFP-atx3 84Q aggregates. ***A*** Cultured rat cortical neurons with DIV 9-10 were transfected with GFP-atx3 28Q WT, GFP-atx3 84Q WT or the respective S12D or S12A mutants, fixed 3 days later and observed in the fluorescence microscope. The number of cells with GFP-atx3 aggregates was counted versus the number of cells presenting only diffuse GFP-atx3 signal. The fluorescence microscopy images provided focus the cells bodies of neurons transfected with GFP-atx3 84Q and illustrate the diversity in number and size of the aggregates obtained with this experimental model. GFP-positive neurons displaying a compromised structure were excluded from the counting. ***B*** Mutation of S12 of GFP-atx3 84Q decreases the fraction of cells with aggregates comparing to what is elicited by GFP-atx3 84Q. The decrease reaches statistical significance with the phospho-null GFP-atx3 84Q S12A. Bars represent the fraction of neurons with aggregates (mean ± SEM, 25-59 neurons were counted in each condition in n = 4 independently prepared cultures), expressed as a percentage of GFP-atx3 84Q WT. Statistical analysis comparing the values of each sample with 100 % used the one sample t-test: * - $P < 0,05$; ** - $P < 0,01$.

aggregates may be underestimated; if that is the case, the differences observed in the percentage of cells showing aggregates between the expanded GFP-atx3 84Q and the phosphomutants-transfected cells should be even more marked. This serves as a testimony of the great toxicity elicited by GFP-atx3 84Q WT, when compared with its phosphomutants and the non-expanded constructs.

4.4 Phosphomutation of serine 12 reduces aggregation and neurodegeneration in a lentiviral rat model of MJD

The above experiments characterize the effects of the phosphomimetic and phospho-null mutations of S12 in several toxicity-related events caused by expression of expanded atx3 in cortical neurons. Considering the relevant differences that were detected in dendritic arborization, synapse number and aggregation, it was appropriate to further investigate similar effects in other, more complex, MJD-modeling systems. Accordingly, we explored the possible changes caused by S12 phosphorylation on the pathogenic events occurring in an animal model of MJD.

Since 1996 (Ikeda and Dikic, 2008), researchers have employed many different animal models to the study of MJD. Models have been generated in *Caenorhabditis elegans* (Christie *et al.*, 2014; Teixeira-Castro *et al.*, 2011), *Drosophila* (Warrick *et al.*, 2005; Warrick *et al.*, 1998), mice (transgenic models are reviewed in Colomer Gould, 2012; Nóbrega *et al.*, 2013) and rat (Alves *et al.*, 2008b), through the transgenic expression of either full-length human expanded atx3 or a C-terminal fragment containing the polyQ sequence (Matos *et al.*, 2011). The available mammal models vary significantly in terms of the particular construct and isoform used to generate them, the expression system employed, the number of glutamines of the polyQ tract and the levels and distribution of the translated protein product (Colomer Gould, 2012; Matos *et al.*, 2011). Nonetheless, overall they replicate many features with parallels in the human disease, including inclusion formation in some regions of the CNS, neurodegeneration (expressed as cell loss, morphological abnormalities or atrophy) and motor symptoms, though varying in several particular aspects.

Using MJD animal models to evaluate the possible consequences of S12 phosphomutation of expanded atx3 required appropriate means to compare their effect with that of its non-mutated counterpart. For this reason, the lentiviral rat model with striatal pathology described by Alves and coworkers (2008a, 2008b, 2010) presented itself as an advantageous experimental tool. The striatum has been increasingly implicated in MJD pathogenesis, with reports describing decreased glucose metabolism (Taniwaki *et al.*, 1997), impaired dopaminergic transmission (Wullner *et al.*, 2005; Yen *et al.*, 2002) and the presence of NIs (Alves *et al.*, 2008b) in the striatum of patients. The rat model is generated by direct delivery of viral particles encoding Myc-tagged full-length atx3 with 72 glutamines (isoform 1a) to the striatum of adult animals by stereotaxic injection, leading to a much localized expression of the transgene. Contrary to the expression of the correspondent non-expanded construct

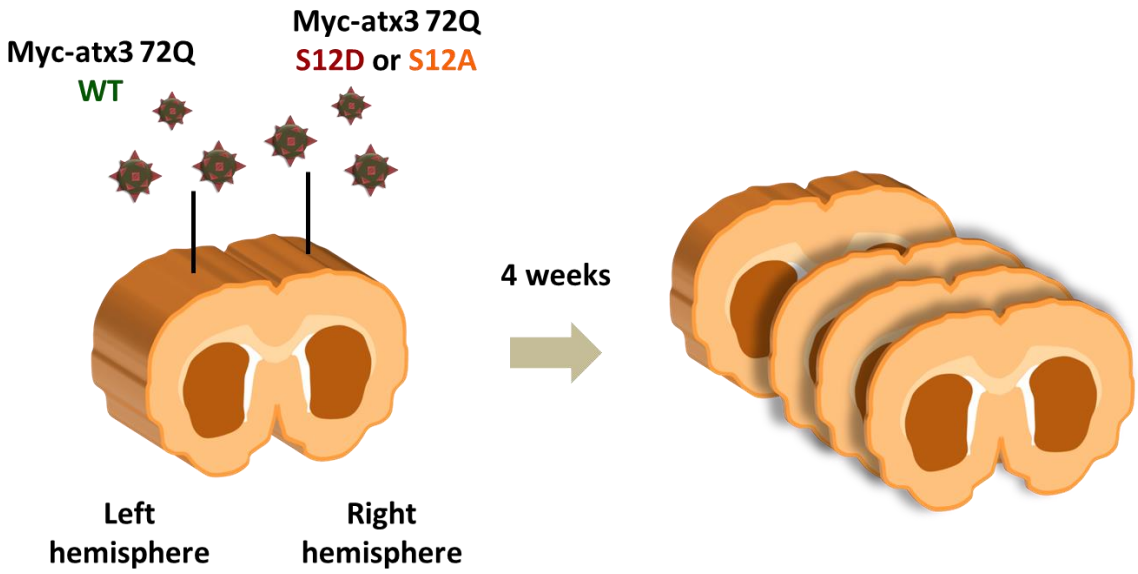

Figure 36: Strategy used to generate the lentiviral MJD rat model with striatal pathology and determine the outcome of atx3 S12 phosphomutations. Myc-atx3 72Q-encoding lentiviral particles were delivered billaterally into rat striata by stereotaxic injection. The left hemisphere striatum was injected with Myc-atx3 72Q WT and the right hemisphere with one of its respective phosphomutants: S12D or S12A. Four weeks after injection striatal slices were prepared and immunohistochemically analyzed in order to evaluate the Myc-atx3 72Q-derived lesions.

(27Q), transduction with Myc-atx3 72Q leads to the formation of NIs and to neuronal loss, conveyed by the observation of cell death features and the depletion of neuronal markers (Alves *et al.*, 2008b). Because viral vectors encoding different proteins can be injected into the striatal region of each of the brain's hemispheres, comparison between the effects of two forms of expanded atx3 – one of which may be a phosphomutant – can be performed in the tissue of the same animal, increasing the significance of the observed differences. A very similar approach has been used to assess differences in neuronal death caused by phosphorylation of htt at S421 (Pardo *et al.*, 2006). Another advantage of this model, when compared with transgenic animals, is that expression of the phosphomutants starts only at the adult phase. Phosphomutants of a protein mimic phosphorylation states in a constitutive way, whereas actual phosphorylation is assumed to be dynamic and reversible. Expression of the phosphomutated atx3 in a transgenic animal could implicate developmental effects that are not within the scope of the current study, as the objective is to study effects of phosphorylation in neurodegenerative features, such as those of the lentiviral rat model.

Experiments were planned so as to compare the toxic effects of Myc-atx3 72Q WT with those of each of its S12 phosphomutants – phosphomimetic Myc-atx3 72Q S12D and non-phosphorylatable Myc-atx3 72Q S12A. Accordingly, for every animal, lentiviral particles encoding Myc-atx3 72Q WT were stereotaxically injected into the striatum of one of the brain's hemispheres (left), while the striatum of the contralateral hemisphere (right) was injected with particles encoding either Myc-atx3 72Q S12D or Myc-atx3 72Q S12A (Figure 36). Animals were sacrificed 4 weeks after injection, and coronal brain slices of the whole striatal region were immunohistochemically processed and analyzed.

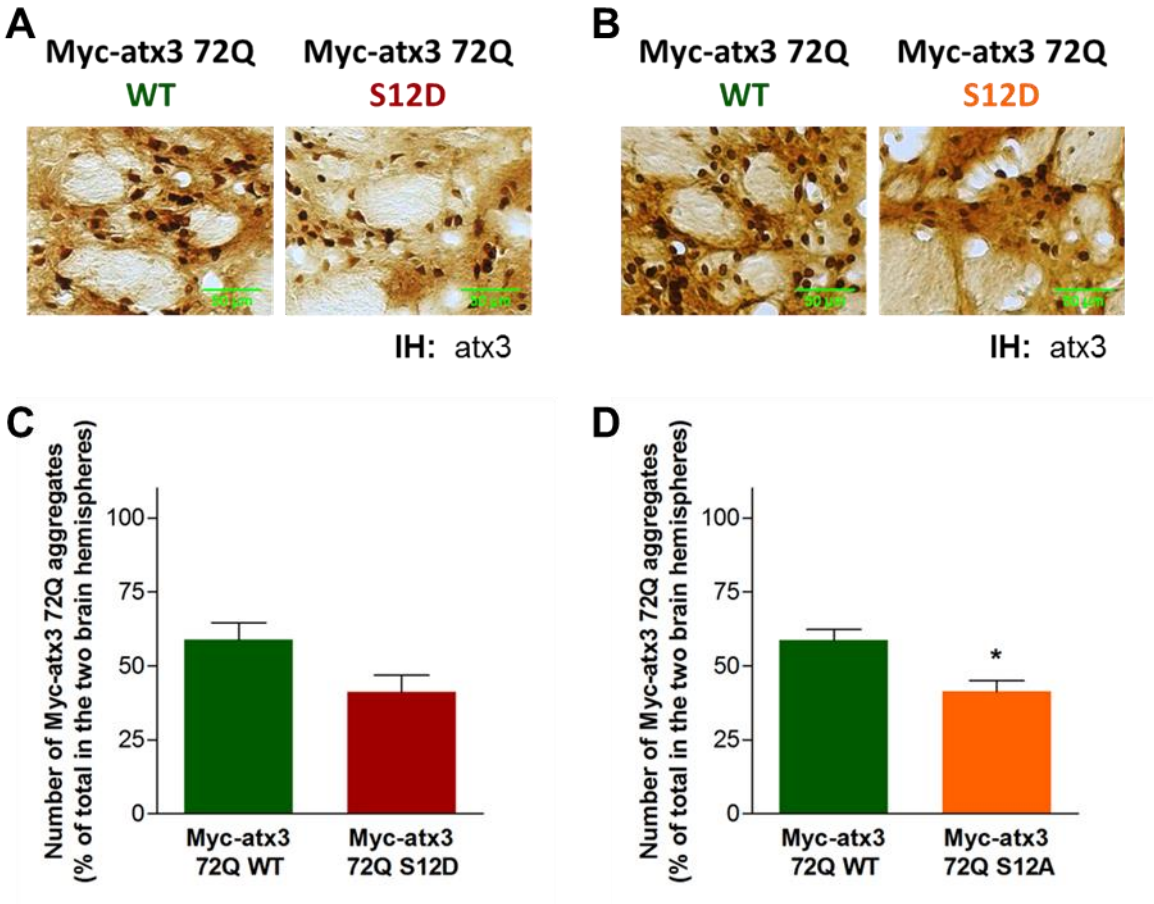

Figure 37: Mutating S12 reduces the amount of atx3 aggregates in the striatum of a lentiviral MJD rat model. ***A, B*** Striatal slices of lentiviral MJD rat models were immunohistochemically probed with an anti-atx3 antibody and imaged in the optical microscope in order to detect Myc-atx3 72Q accumulations. Representative images of the peroxidase staining of striatal sections displaying aggregates are shown for each bilateral injection condition (Myc-atx3 72Q WT:Myc-atx3 72Q S12D or Myc-atx3 72Q WT:Myc-atx3 72Q S12A). ***C, D*** Comparing to the hemisphere expressing Myc-atx3 72Q WT, both phosphomutants lead to a tendential decrease in the number of aggregates in the striatum. The decrease is statistically significant in the case of the phospho-null mutant. Bars represent the number of atx3-positive accumulation in each hemisphere (mean ± SEM; n = 4 animals injected with Myc-atx3 72Q WT:Myc-atx3 72Q S12D; n = 6 animals injected with Myc-atx3 72Q S12A), as a percentage of the total number of aggregates in the two hemispheres. Estimation of the number of aggregates in the whole striatum of each hemisphere was based on the quantification of 7-12 equidistant striatal slices. Counting of the number of aggregates in each slice was performed in mosaics of images comprising the whole region with striatal aggregates. Statistical analysis used the Mann-Whitney test: * - $P < 0,05$.

In order to evaluate and compare the formation of aggregates elicited by each of Myc-atx3 72Q forms, slices were labelled with an anti-atx3 antibody and the regions of the striatum demonstrating atx3 aggregation were imaged and quantified (Alves *et al.*, 2008a; Nascimento-Ferreira *et al.*, 2011). Anti-atx3 antibody labelling was considered to correspond to instances of aggregation whenever a strong and compact signal was observed. Transduction of the rat striatum with any of Myc-atx3 72Q forms led to the formation of detectable aggregates, in agreement with what has been described for this animal model (Figure 37A and B). However, mutation of S12 to alanine significantly decreased the amount of aggregates formed,

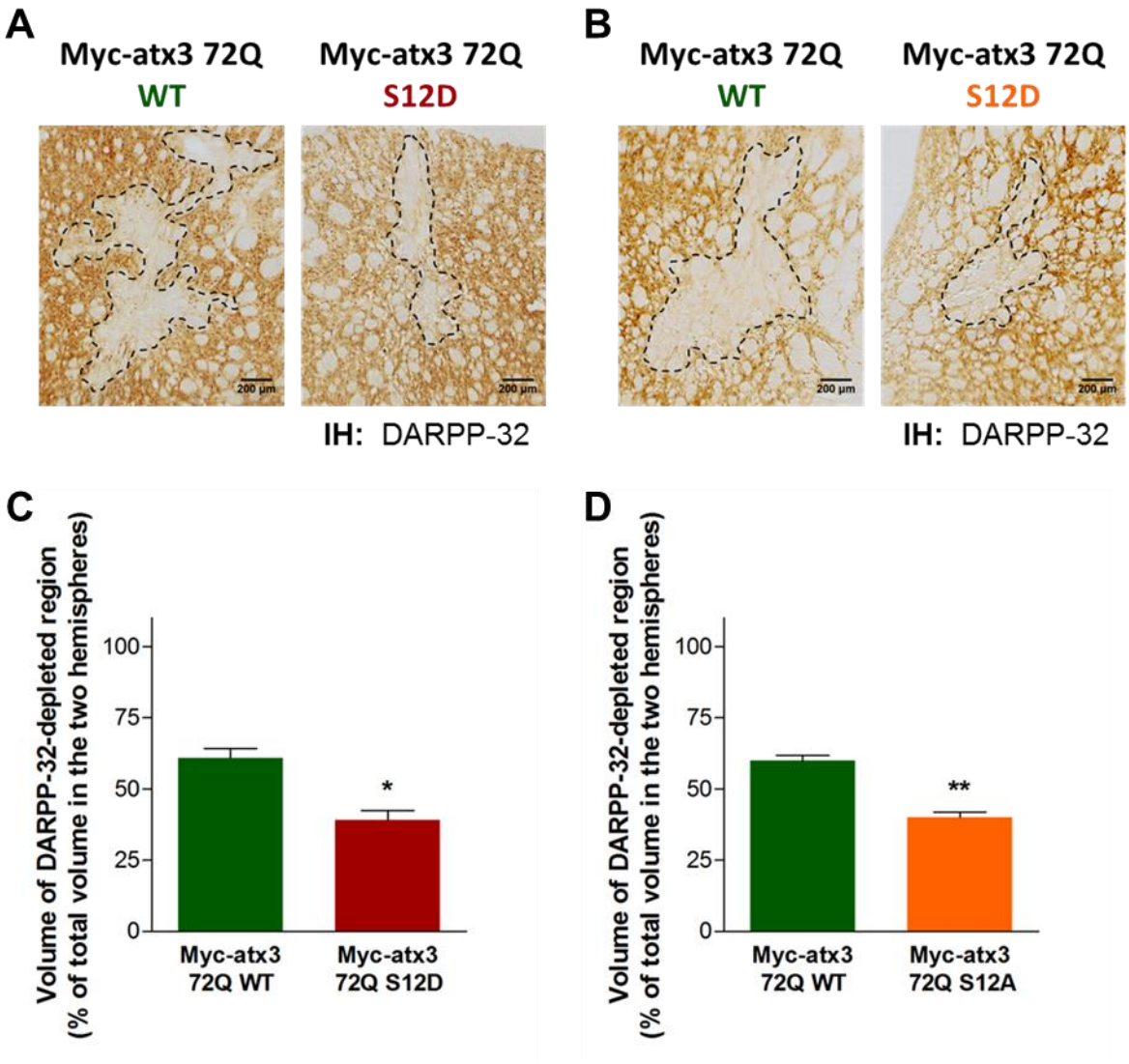

Figure 38: Mutating S12 of atx3 reduces the lesion induced by expanded atx3 injection in a striatum of a lentiviral MJD rat model. ***A, B*** Striatal slices of lentiviral MJD rat models were immunohistochemically probed with an anti-DARPP-32 antibody and imaged in the optical microscope. Representative images of the peroxidase staining of striatal sections evidencing DARPP-32 immunoreactivity loss (limited by the interrupted line) are shown for each bilateral injection condition (Myc-atx3 72Q WT:Myc-atx3 72Q S12D or Myc-atx3 72Q WT:Myc-atx3 72Q S12A). ***C, D*** Comparing to the hemisphere expressing Myc-atx3 72Q WT, both phosphomutants lead to a statistically significant decrease in the volume of the region displaying DARPP-32 immunoreactivity depletion. Bars represent the volume of the DARPP-32-depleted region in each hemisphere (mean ± SEM; n = 4 animals injected with Myc-atx3 72Q WT:Myc-atx3 72Q S12D; n = 5 animals injected with Myc-atx3 72Q WT:Myc-atx3 72Q S12A), as a percentage of the total volume in the two hemispheres. The whole volume of the DARPP-32-depleted region was estimated based on the area of DARPP-32 depletion in 7-11 equidistant striatal slices. Statistical analysis used the Mann-Whitney test: * - $P < 0,05$; ** - $P < 0,01$.

comparing to Myc-atx3 72Q WT (Figure 37D). The phosphomimetic S12D mutant showed the same tendency, though without statistical significance (Figure 37C). Phosphomutation of S12 is consequently admitted to be able to decrease the propensity of expanded atx3 to form aggregates.

Examination of the severity of neurodegeneration caused by each Myc-atx3 72Q form was performed by labelling the slices with an antibody detecting a neuronal marker: dopamine- and cyclic AMP-regulated phosphoprotein of 32 kDa (DARPP-32). This protein is associated with dopaminergic transmission both structurally and functionally, being enriched in neurons receiving dopaminergic inputs and playing a role in the regulation of dopamine-mediated neurotransmission (Fienberg *et al.*, 1998; Ouimet *et al.*, 1984). Because DARPP-32 is found in the cytosol and is highly enriched in the striatum (Blom *et al.*, 2013; Fienberg *et al.*, 1998), depletion arising from Myc-atx3 72Q WT expression in this region is interpreted as resulting from the degeneration of striatal neurons (Alves *et al.*, 2008a; Nascimento-Ferreira *et al.*, 2011; Pardo *et al.*, 2006). Expression of Myc-atx3 72Q WT, S12D or S12A led to a localized loss of anti-DARPP-32 antibody immunoreactivity, compatible with the toxicity expected of atx3 with a pathogenic polyQ expansion (Figure 38A and B). Nonetheless, the volume of the DARPP-32-depleted region was significantly reduced in the case of the injections with the phosphomutants, comparing to Myc-atx3 72Q WT (Figure 38C and D). These observations indicate that mutations of S12 of atx3 to alanine or aspartate decrease the degree of neurodegeneration caused by expression of the expanded protein.

Previous studies with this lentiviral MJD rat model show that treatments targeting atx3 toxicity (protein silencing or autophagy activation) reduce both the amount of atx3 aggregates and the extent of degeneration (Alves *et al.*, 2008a; Alves *et al.*, 2010; Alves *et al.*, 2008b; Nascimento-Ferreira *et al.*, 2011). Accordingly, the two events are interpreted as being different expressions of expanded atx3 toxicity, regardless of whether the aggregates are actually harmful by themselves or in fact result from cellular mechanisms targeting other deleterious species. Our results indicate that the Myc-atx3 72Q phosphomutants are less toxic than the WT expanded protein with a serine at site 12, giving rise to smaller amounts of aggregates and to less severe neuronal marker depletion in the striatum. Such markedly similar behaviors between the two phosphomutants, with parallels in the aggregation experiments performed in cortical neurons, is somewhat unexpected and hard to interpret in terms of the actual effect of protein phosphorylation. Regardless, the observations made in this MJD animal model strongly suggest that changes targeting S12 may constitute an importantly mechanism modulating the toxicity of expanded atx3, with possible protective outcomes.

Chapter 5

Final considerations

Chapter 5

Chapter 5 – Final considerations

5.1 General discussion

The current study aimed at characterizing a novel PTM of atx3 – phosphorylation of S12, a residue localized in the catalytic domain of the protein. Utilizing a phospho-specific antibody specifically targeting phosphorylated S12, we were able to detect phosphorylated species in mammalian cell lines, which were confirmed to correspond to atx3-derived fragments in rat neurons. The results indicate that S12 of atx3 is phosphorylated in human cells but the observations made in rat neurons are of special relevance, considering that MJD specifically affects neuronal cells in human patients.

Having observed that S12 is localized in the vicinity of the catalytic site amino acids and is especially close to C14, we predicted that phosphorylation of that residue could affect the proteolytic activity of atx3. Using model substrates usually employed in the study of the enzymatic activity of atx3 and other DUBs, we observed that when S12 is mutated to aspartate in order to mimic the phosphorylated state, the activity of the protein decreases, *in vitro*. The results obtained thus suggest that phosphorylation of S12 decreases the DUB activity of atx3. The observation that this decrease is also detected when atx3 reacts with polyUb chains is of particular physiologic relevance, considering that atx3 is believed to target polyubiquitinated proteins *in vivo*.

The analysis of the possible influence of S12 phosphorylation on the toxicity of atx3 carrying a pathogenic expansion of glutamine residues was performed in cultured neurons, which have been very rarely used in MJD studies, despite their relevance in comparison to the more widely used cell lines. Transfection of cortical neurons with expanded GFP-tagged atx3 resulted in less arborized dendritic trees and in a decreased amount of functional glutamatergic synapses, in comparison to neurons transfected with non-expanded GFP-atx3. Remarkably, non-phosphorylatable expanded GFP-atx3 elicited similar effects, but the phosphomimetic mutant limited the loss of total length of dendrites and the decrease of functional synapse number. The contrasting effects of different phosphomutants of S12 suggest that the phosphorylation of this amino acid residue influences specific morphological (and possibly functional) outcomes of expanded atx3 toxicity. Atx3 aggregation is recognized

to constitute an important aspect of expanded atx3 toxicity and transfection of rat cortical eurons with GFP- atx3 leads to the formation of GFP-positive aggregates. While expression of expanded atx3 led to a higher amount of cells with aggregates than the non-expanded protein, hindering phosphorylation of S12 by mutation of this residue to alanine decreased the fraction of cells containing atx3 aggregates, indicating that interfering with S12 phosphorylation may be important in mediating atx3 aggregation mechanisms.

Finally, we explored the effect of the S12 mutants of atx3 in the disease-related characteristics of a MJD lentiviral rat model with striatal pathology. Injection of lentiviral particles encoding expanded atx3 into the rat striatum leads to the formation of atx3-positive aggregation bodies and to a localized loss of neuronal markers, reflecting demise of striatal neurons. Mutation of S12 to aspartate or alanine decreases the number of aggregates formed and the extent of neuronal loss, suggesting a protective effect that may be modulated in a natural context by the phosphorylation of S12 of atx3.

The following segments will elaborate on these considerations and suggest additional explanations for the results obtained.

Phosphorylation of ataxin-3 fragments

The mass spectrometric detection of S12 phosphorylation used a protein sample of GFP-atx3, immunoprecipitated from HEK 293FT cells with an anti-GFP antibody, targeting the N-terminally localized tag. The electrophoretic separation that followed allowed the separation of the protein species contained in the immunoprecipitants, which, attending to the Coomassie blue staining, consisted uniquely of full-length GFP-atx3 and IgG chains. Since the band that was later excised and analyzed by MS presented a molecular weight consistent with what was expected and routinely obtained with full-length GFP-atx3 28Q (~75 kDa), it is admitted that, in HEK 293FT cells, full-length atx3 is phosphorylated at S12.

However, the phospho-specific anti-Patx3 antibody that was produced so as to specifically recognize phosphorylation of atx3 at S12 did not recognize the full-length protein, labelling only protein species of lower molecular weight than what was expected for endogenous and GFP-tagged atx3. The lambda phosphatase assays and the experiments with phosphatase inhibitors stimuli indicate that the protein products labelled by the anti-Patx3 correspond to phosphorylated protein, while the shRNA silencing of atx3 in cortical neurons confirms that the observed species derive from atx3. Therefore, it is possible to conclude that the anti-Patx3 labelled only atx3-derived fragments.

Considering that the anti-Patx3 antibody targets the N-terminal region of atx3, the fragments must include N-terminal parts of the protein. As exposed in section 1.4, over the years different authors have reported the observation of atx3-derived fragments of variable molecular size, deriving from different regions. Fragments have been detected in diverse types of cell cultures, resulting from endogenous or transfected atx3, in transgenic animal models and in patients' brain tissue (Goti *et al.*, 2004). Particularly, in COS-7 cells, endogenous atx3

was shown to generate a caspase-derived fragment of about 28 kDa that was labelled by the anti-atx3 antibody (Berke *et al.*, 2004). In the same cell line, Pozzi and coworkers (2008) described two fragments derived from transfected non-expanded (6 glutamines) murine atx3, which were immunoreactive to an antibody directed at a N-terminal tag: one fragment with 37 and the other with 42 kDa. Upon digestion with calpain, human atx3 expressed in HEK 293FT cells yields a ~30 kDa fragment that is labelled with the anti-atx3 1H9 antibody, nonetheless described as an N-terminal fragment, seeing as polyQ sequence length does not alter the molecular size of the fragment that is produced (Hübener *et al.*, 2013). Simões and collaborators (2012) detected a ~26 kDa fragment of human atx3 containing the N-terminus of the protein, that also arises independently from polyQ repeat length and that was also labelled by the monoclonal anti-atx3 antibody.

In our study, the endogenous atx3-derived fragments labelled by the anti-Patx3 antibody in COS-7 and HeLa cells had an apparent molecular weight of 30 and 35 kDa (and 40 kDa, in the first experiment described). The fragments detected in rat cortical neuron migrated at an apparent molecular size of 30 and 22 kDa. It is possible that these fragments correspond to the atx3-derived species described by other authors, but it is challenging to try to make any definite correspondence, in part because of the uncertainty in the molecular weight estimation based on the molecular weight standards used in Western blot techniques. Furthermore, comparison with fragments yielded by overexpressed atx3 presents additional sources of variability, since different studies employ different atx3 forms, derived from different animal species, fused with diverse tags and with varying glutamine lengths. Studies delving into the formation of atx3 fragments also employ different sampling techniques and frequently different kinds of procedures that direct the activity of proteolytic enzymes; it is not surprising that the observed fragments are consequently diverse. Nonetheless, the observation of N-terminal fragments by other authors supports the plausibility of the detection of N-terminal fragments with the anti-Patx3 antibody we generated.

The endogenous atx3 fragments described in COS-7 cells (28 kDa; Berke *et al.*, 2004) and mouse (30 kDa; Hübener *et al.*, 2013) and the polyQ size-independent N-terminal fragments derived from human atx3 (Simões *et al.*, 2012) are all labelled by the commercial 1H9 anti-atx3 antibody, which binds a region in the vicinity of UIM1 (amino acids 221-224, localized in the C-terminal tail of atx3). However, in our Western blot experiments, the anti-atx3 antibody does not label any protein species that clearly correspond to the fragments labelled by the phospho-specific antibody (but the anti-Patx3 signal disappears when atx3 is silenced in neurons, proving the specificity of the immunoreactivity). This could mean that the fragments we observe result from cleavage occurring N-terminally of amino acids 221-224. Hübener and coworkers (2011; 2013) have suggested that the 30 kDa fragment they observed derived from cleavage at position 260 and, in fact, a protein fragment composed by the first 259 amino acids of atx3 (which include the JD, UIM1 and part of UIM2) was calculated to have a molecular size of ~30 kDa, for both mouse and human atx3. Though we observed a fragment with this molecular size in COS-7 and HeLa cells and in cortical neurons, it would not be expected that they included the amino-acids 221-224. Estimation of the molecular weight of a

fragment formed by the 220 first amino acids of human, rat and mouse atx3 (the length between the N-terminus of atx3 and the N-terminus of anti-atx3 epitope) using the same calculation tools (Protein Molecular Weight Calculator – Science Gateway) yields a value of ~25 kD, which is compatible with the smaller (and most evident) fragment we observed in neuronal cultures. If the remaining fragments we detected in our analyses in fact contain the 221-224 amino acid epitope, in could be the case that the anti-atx3 is not detecting them because they are rare species, when compared to full-length endogenous atx3; the stronger immunoreactivity derived from a higher proportion of full-length atx3 could mask the fragments, and then render them undetectable in our experiments. In COS-7 cells, the anti-atx3 antibody reveals several faint bands with lower molecular weight than the full-length protein that could possibly correspond to the fragments.

In part, results actually suggest that some of the fragments may contain the polyQ sequence and, by extension, amino acids 221-224. Only this explains why the phospho-specific antibody detected fragments of GFP-atx3 28Q and GFP-atx3 84Q that differed in molecular size, when the only difference between these two atx3 forms is the length of the polyQ region. Interestingly, the estimated molecular size of a fragment containing the amino acids of atx3 comprised between the N-terminus and the end of the polyQ sequence is ~35 kDa for the human protein (with 13Q) and ~34 kDa for both mouse (6Q) and rat (5Q) atx3; this matches the size of one of the endogenous atx3-derived fragments detected in COS-7 and HeLa cells. The molecular weight of atx3 varies depending on the number of repeated glutamines, and the differences in electrophoretic movement detected between atx3 of different mammalian species are largely attributed to differences in polyQ sequence length (Berke *et al.*, 2004). In our study, atx3 from COS-7 and HeLa cells lines displays about 50 kDa, while rat atx3 migrates at about 43 kDa, meaning that atx3 from the cell lines shall have a larger number of glutamines. The higher molecular weight of the fragments produced in the cell lines could result from the fact that the endogenous protein is larger, and this would support the idea that at least the fragment with ~35 kDa contains the polyQ sequence. Independently of the C-terminal topology of the fragments observed, it is important to stress the point that our results indicate that they include the N-terminal part of atx3.

Having detected phosphorylation at S12 in full-length atx3 through MS, it is somewhat puzzling to observe that the phospho-specific antibody only recognizes fragments of atx3. One simple explanation would be that, contrary to HEK 239FT cells, in COS-7 cells phosphorylation of S12 targets only atx3 fragments. However, if we would consider that phosphorylation occurs similarly in both cell lines and in the other cells used in this study as well, another explanation would be that, although the full-length protein is phosphorylated at S12, the fraction of modified protein is low, compared to the fraction of fragments that are phosphorylated; the anti-Patx3 antibody would yield a stronger signal when labelling the fragments, ultimately masking the full-length protein signal. This possibility raises the hypothesis that phosphorylation at S12 may be intimately linked to the proteolytic events generating the fragments we detected. Either atx3 is preferentially phosphorylated at S12 upon cleavage, or phosphorylation of this residue eventually leads to proteolytic cleavage of atx3; the two

hypotheses would help explain why the antibody only detected fragments as being phosphorylated. Considering that even endogenous atx3 is known – and here further demonstrated – to yield cleavage product, these events could have possible ties with atx3 function. In fact, increasing evidence demonstrates that there is frequent interplay between phosphorylation events and proteolytic cleavage (Renatus and Farady, 2012).

One study exploring phosphorylation of htt at S13 employed a phospho-specific antibody that also labelled htt fragments derived from the endogenous protein (Thompson *et al.*, 2009). Interestingly – and with parallels with our own observations – in some experiments with cultured cells the antibody did not detect full-length endogenous htt (or gave only a very faint sign) unless IKK (the kinase responsible for the modification) was overexpressed or pharmacologically stimulated. At the same time, however, phosphorylated htt fragments could be detected. Taking also into account that IKK activation leads to proteolysis of htt (Khoshnan *et al.*, 2009), it was suggested that phosphorylation of htt could mediate the cleavage of this protein (Thompson *et al.*, 2009).

Phosphorylation of serine 12 and atx3 deubiquitinase activity

Analysis of the tertiary structure of the JD and the localization of S12 close to the catalytic site led to the prediction that modification of this residue by phosphorylation could affect the enzymatic activity of atx3. The in *vitro assays* performed with the S12D phosphomimetic mutant of atx3 confirmed this assumption, suggesting that phosphorylation at S12 reduces the enzymatic activity of the protein. In addition, the results obtained when incubating the protein with polyUb chains indicate that the modification does not alter the preference of atx3 for chains of particular linkage type, considering that the decrease in product formation was observed for both K48- and K63-linked chains. These results, along with the fact that mutating S12 to aspartate or alanine does not alter Ub-VS binding to the C14, suggest that phosphorylation may thus produce a decrease in the efficiency of ataxin-3 for cleaving isopeptide bonds formed by Ub.

Structural studies show that, contrary to several other DUBs, atx3 is synthetized in an active form and substrate binding does not conduct to major structural rearrangements (Nicastro *et al.*, 2009; Nicastro *et al.*, 2005). The fact that purified atx3 displays DUB activity *in vitro* is in agreement with this idea. The effects we observe when mutating S12 to aspartate can either result from alterations in conformation, possibly of the amino acids of the catalytic site, or derive from changes in the interaction with the Ub substrates. Phosphorylation is generally believed to mediate activity changes through this type of modifications. It is tempting to assume that, given the localization of S12 in the JD, conjugation of a phosphate group could alter, even if only subtly, the conformation of the amino acids of the active site, hindering the proteolysis mechanism they catalyze. Todi and coworkers (2010), who observed an increase in atx3 DUB activity when atx3 is ubiquitinated at K177 (a residue localized in the surface of the JD that is opposite to the catalytic cleft), suggest that the changes they observe

could be due to an increased exposure of the catalytic site or to an altered position of the catalytic residues and consequent changes in isopeptide bond attack.

Interestingly, however, observations with many proteases suggest that changes in activity caused by phosphorylation frequently involve alterations in substrate binding, rather than modifications of the catalytic residues (Renatus and Farady, 2012). Weeks and coworkers (2011) suggested that changes in the efficiency of atx3 activity by mutation of S12 (in their study to phenylalanine) could result from an alteration of atx3 affinity for Ub. The same authors postulated that S12 of atx3 is appropriately positioned to interact with the side chain of the lysine residue forming the isopeptide bond, and if this is true, the negative charge of aspartate – and admittedly of a phosphorylated serine – could cause changes in that interaction. Phosphorylation of DUBA at S177 activates the enzyme, but the modification was shown to not interact with the active site amino acids; instead, it was suggested to stabilize the structural core of the enzyme and the phosphorylated serine was demonstrated to be able to directly interact with the C-terminal region of Ub (Huang *et al.*, 2012). Though DUBA is catalytically inactive when non-phosphorylated and requires interaction with the Ub to acquire a catalytically competent conformation, this example demonstrates that phosphorylation targeting residues able to interact with Ub C-terminus may mediate changes in DUB activity. Phosphorylation of caspase-6 at S257 or substitution of this residue to aspartate has been shown to inactivate proteolysis by this enzyme (Velazquez-Delgado and Hardy, 2012). Structural studies of the phosphomimetic mutant suggested that the steric bulk introduced by phosphorylation causes structural alterations that, while having limited impact on the catalytic residues, deform the substrate recognition site (Renatus and Farady, 2012; Velazquez-Delgado and Hardy, 2012). These results support the idea that the reduced DUB activity we observe with the phosphomimetic atx3 mutant may derive from changes in Ub interaction.

Whether S12 phosphorylation affects the conformation of the active site amino acids or the interaction of the JD with Ub, apparently it does not alter binding of Ub to C14 of atx3, attending to the Ub-VS assays performed. It may thus decrease atx3 enzymatic activity by hindering the following steps of isopeptide bond cleavage, either by affecting the dynamics of the interaction of the amino acids playing a role in cleavage, or by altering the binding and positioning of Ub at other levels. S12 is localized close to the JD Ub-binding site 1, whose integrity is essential for Ub substrate cleavage; the presence of a negative charge may alter the docking of Ub and the way Ub is positioned. Additionally, S12 position may influence the mobility of the helical hairpin of the JD, which has been shown to undergo conformational changes when binding Ub and to interact with this protein (Nicastro *et al.*, 2009; Weeks *et al.*, 2011). The helical hairpin has been suggested to be implicated in determining the specificity of the JD and in stabilizing substrates (Nicastro *et al.*, 2009; Nicastro *et al.*, 2005).

The biological significance of the activity decrease we observe remains to be further investigated. The comparative activity of DUBs, and in particular of DUBs of the Josephin family, is markedly different depending on the substrate that is used; for instance, while the JD of Josephin-2 is better at cleaving Ub-AMC and K63-linked polyUb chains than atx3 JD, it shows less activity than atx3 JD against 48-linked chains (Weeks *et al.*, 2011). More than illustrating

how closely-related proteins show different substrate preferences, these observation demonstrate that the conclusions regarding DUB activity are always dependent on the substrates that are used. Our results strongly indicate that phosphorylation causes a decrease in activity, but in order to truly comprehend the functional outcomes of these changes in activity, it would be important to determine how phosphorylation affected deubiquitination of particular endogenous proteins. These ubiquitinated substrates remain, however, illusive, and it is thus hard to predict any cellular changes resulting from atx3 decreased activity. Mutation of C14 to an alanine renders atx3 inactive and leads to the accumulation of ubiquitinated proteins of various molecular sizes (Berke *et al.*, 2005). It would be expected that the decrease in activity caused by phosphorylation of S12 also contributes to a lesser deubiquitination of the ubiquitinated substrates of atx3. We could not detect any clear difference between the ubiquitinated protein profile after transfecting HeLa cells with GFP-atx3 or its S12D phosphomutants, but it is admissible that such procedure is not sufficient to observe marked differences. For example, the accumulation of polyubiquitinated proteins upon C14A mutation that Berke and coworkers (2005) observed in Western blots resulted from experiments that made also use of the overexpression of Ub. The accumulation of endogenous Ub signal was only reported in immunocytochemistry experiments. Ideally, the effects of atx3 S12 phosphorylation would be evaluated in the ubiquitination profile of a particular protein known to be endogenously deubiquitinated by atx3, but candidates are still scant; possibly the E3 ligases known to interact with atx3 (CHIP and parkin) would be important starting points (Todi *et al.*, 2010; Winborn *et al.*, 2008).

A decreased of deubiquitination of atx3 substrates may have diverse cellular consequences, considering the versatility of Ub signals. Phosphorylation of S12 may modulate the turnover of designated proteins degraded through the UPP or the ERAD, interfere with transcription regulation or affect any other cellular function with which atx3 is involved through its Ub chain editing activity. Particularly, complete inactivation of atx3 DUB activity by the C14A mutation was reported to stabilize ERAD substrates (Wang *et al.*, 2006) and to decrease atx3-mediated transcriptional repression (Evert *et al.*, 2006a). It could be argued that, according to our results with the phosphomutants using Ub-AMC, S12 phosphorylation only decreases the enzymatic activity by ~40-60 % and so the cellular outcomes of this activity change would be limited. However, ubiquitination is a very dynamic process, and a particular Ub signal is the result of a complex interplay between ubiquitination and deubiquitination, possibly involving different cycles of Ub conjugation and removal (Marfany and Denuc, 2008; Nguyen *et al.*, 2014; Zhang *et al.*, 2013). Even discrete changes in the rate of atx3 activity could have a significant impact on the formation of Ub signals and the time different Ub arrangements dwell in particular proteins. Furthermore, considering that DUBs may act at different points of the pathways using Ub signals and admitting that there exists a subset of substrates that are preferentially deubiquitinated by atx3, even a slight activity decrease may elicit downstream alterations that critically affect the functioning of particular cellular systems. Finally, taking into account that the enzymatic activity of atx3 is normally low *in vitro* possibly as a result from the fact that the substrates used do not appropriately reflect the endogenous

substrates of atx3, it is possible that phosphorylation of atx3 produces effects on the deubiquitination of physiological substrates that are different than the ones we observe with the Ub models: the decrease in activity might even be more pronounced, or maybe phosphorylation affects the preference for particular ubiquitinated substrates. Whatever the case, phosphorylation at S12 of atx3 may constitute a regulation point of different cellular pathways, by interfering with ubiquitination and with the downstream interpretation of Ub signals.

The comparison between the amino acid sequences of the four DUBs of the Josephin family raises an interesting hypothesis regarding the evolutionary importance of S12 phosphorylation. The residue at the position equivalent to S12 is a negatively charged glutamate, for Josephin-1 and Josephin-2, and an aromatic phenylalanine, in atx3L. According to the observation made by Weeks and collaborators (2011) using the isolated JDs of these proteins, regardless of the model substrate used (Ub-AMC, Ub-6His, K48-linked polyUb chains or K63-linked polyUb chains), the enzymatic activity of atx3 is higher than that of Josephin-1, and lower than the activity of atx3L (as detailed above, however, the comparison between the activity of atx3 JD and Josephin-2 JD is not so straightforward). The same authors reported that mutation of S12 to phenylalanine increases atx3 activity, while the current study demonstrates that mutation to a negatively charged aspartate decreases it. Though atx3L, and specially Josephin-1, display many other differences besides the residue at that particular position, it is possible that it plays a part in determining cleavage efficiency. It is thus conceivable that, in the case of atx3, evolution favored the maintenance of an amino acid – serine – that can be reversibly turned negative or neutral as a result of upstream regulatory pathways. Results from a recent study employing comparative genomics (Pearlman *et al.*, 2011) suggest that this evolutionary "trick", whereby phosphorylation sites arise from aspartate or glutamate residues, is highly likely to have occurred in some phosphorylated proteins (5% of the sites analyzed).

Ataxin-3 in the cerebral cortex

The current work represents the first effort at exploring the effects of atx3 phosphorylation in MJD-related toxicity events using neuronal cells and *in vivo* animal models. This approach frankly increases the relevance of the results obtained, considering that MJD specifically targets neuronal cells. Nonetheless, the preference for cortical neuron cultures is possibly not as obvious, since the cerebral cortex is commonly believed to be spared in MJD. This idea is nowadays, questionable. As explained in section 4.1, studies have shown that the cortex of MJD patients is sometimes atrophic (D'Abreu *et al.*, 2012; Lopes *et al.*, 2013; Murata *et al.*, 1998). Classically, however, studies have failed to detect changes in the cortex, and even when polyQ-containing inclusions have been observed (Ishikawa *et al.*, 2002; Yamada *et al.*, 2001), this fact has been related to the concept that inclusion do not play a part in the toxicity mechanisms. Alves and coworkers (2008b) have observed that the injection of lentiviral vectors encoding expanded atx3 into the rat cortex leads to inclusion formation, but to no

detectable loss of neurons. Regardless of the questionable importance of the visible inclusions in the pathogenesis mechanisms, they serve as disease markers. Though the cortical neurons are not frequently found to visibly degenerate, it is possible that they are dysfunctional in MJD; the presence of inclusions may reflect this dysfunction, even if it is not causatively involved (Schöls *et al.*, 2004). Purkinje cells, which are also usually considered to be spared by expanded atx3-induced degeneration, have been shown to be dysfunctional in a symptomatic animal model with ubiquitous atx3 expression (Shakkottai *et al.*, 2011). The cortex of MJD patients has been described to display impaired glucose metabolism (Soong *et al.*, 1997; Taniwaki *et al.*, 1997), which may be indicative of dysfunction, and including in presymptomatic disease gene carriers, demonstrating that early functional changes may precede the harsher compromise of neuronal structure (Soong and Liu, 1998). Furthermore, Rüb and collaborators (2013) recently postulated that the pathophysiologic involvement of the cerebellothalamocortical motor loop in MJD involves Betz pyramidal cells of the primary motor cortex. Remarkably, atx3 has been described to be highly expressed in the cortex; in the human brain, expression of atx3 is higher in the cortex than in the cerebellum (Trottier *et al.*, 1998). Additionally, in the motor cortex, atx3 is specially enriched in pyramidal neurons, the most abundant neuronal subtype of the cortex. These observations support the idea that atx3 function may be particularly important in the cortex.

Assuming that the polyQ expansion of atx3 is deleterious for cortical neurons in MJD patients, even when no visible neuronal loss is registered, the current study represents an important first insight into the mechanisms of neuronal dysfunction that may be at work. We observed that expression of expanded atx3 reduces the branching and the total extension of dendrites, and decreases the number of functional glutamatergic synapses. In the brain, similar changes might have a negative impact in the establishment/maintenance of the neuronal network, possibly leading to dysfunction. It is worthy to contemplate the possibility that these putative disease outcomes are not limited to the cortex, and take part in the neurodegeneration-related changes occurring in other regions of the brain, such as the cerebellum, the pons or the striatum. These neuron-specific alterations may help explain why neurons are specifically targeted in MJD.

The changes in neuronal structure caused by expanded atx3 expression can result from different effects. First, as atx3 has been related to transcriptional regulation and cytoskeletal organization, changes caused by polyQ expansion could affect the expression and correct organization of proteins responsible for the development and maintenance of neurites. In *C. elegans*, knocking out atx3 was shown to alter the expression of diverse genes related to cell structure, mobility and development (Rodrigues *et al.*, 2007). In HeLa cells, silencing atx3 disorganizes the cytoskeleton, even without changing the levels of tubulin, actin or vimentin, and decreases the levels of cell adhesion molecules (Rodrigues *et al.*, 2010). The effects we observe in relation to the synaptic marker accumulations can also be explained by changes in transcription and in cytoskeletal structure. Chou and collaborators (2008) have shown a decrease in the genetic expression of several synaptic proteins in the cerebellum of transgenic mice. One of the genes whose expression was affected was VGLUT2, though no changes were

reported regarding the actual protein levels. The role of the cytoskeleton in formation and maintaining of synapses is also critical, considering that synaptic proteins are usually organized in cytoskeletal specializations such as the PSDs and that the contact between pre- and postsynaptic terminal is mediated by proteins that are intrinsically associated with the cytoskeleton. In our experiments, VGLUT1 was labelled in presynaptic regions, in neurons that were not expressing GFP-atx3; the observed effects may be due to alterations in the regulation of contact proteins that alter the establishment of neuronal contacts. The phenotype caused by expanded atx3 expression could also be underlined by alterations in protein quality control systems caused by expansion of atx3: an increased degradation of important players may have an impact in both dendrite development and maintenance and in synapse structure and functionality. Furthermore, the synaptic defects may also be caused by impaired delivery of protein to the synapse, either through possible blockade of protein transport along neurites caused by atx3 aggregation, or by alterations in protein sorting resulting from atx3 function in the ERAD and/or in the editing of K63-linked polyUb chains. Recently, in transfected cell lines, the JD of Josephin-1 was found to associate with the plasma membrane and to affect its dynamics (Seki *et al.*, 2013). The protein was further observed to enhance endocytosis in an activity-dependent manner, supporting the idea that DUBs of the Josephin family may regulate the levels of proteins expressed at the plasma membrane.

The aggregation of expanded atx3 may be responsible for the dysfunctionality of the protein upon expansion, possibly by abrogating physiological interactions that are important for normal functions or by mediating deleterious interactions that sequester proteins from the systems with which they are normally involved. This setup could explain effects at the different levels such as transcriptional regulation, cytoskeletal organization, intracellular transport and degradation. This is not to say that the visible aggregates we detect are the actual toxic species, considering that it is commonly believed that small oligomeric species are the ones linking aggregation to toxicity (Takahashi *et al.*, 2010). Moreover, is also plausible that even monomeric expanded atx3 mediates some of these possible pathogenic pathways.

PolyQ-expansion and phosphorylation of serine 12 as determinants of neuronal morphology

The results we obtained suggest that the alterations in dendritic morphology and in synapse number may not just be due to polyQ toxicity mechanisms, but be instead (or at least partially) related to a possible function of atx3 in maintaining dendrites and synapses. Throughout the experiments characterizing the morphology of transfected cortical neurons, the phospho-null mutant of non-expanded atx3 leads to a tendential impairment of the structures analyzed. Cells transfected with phosphomimetic non-expanded atx3 however, are similar to the cells transfected with WT non-expanded atx3. One possible explanation for these results is that atx3 function is important in the development and/or maintenance of dendritic projections and synapses, but this function is dependent on the phosphorylation state of S12:

the WT, with serine at position 12, can be phosphorylated, and thus acts similarly to the phosphomimetic S12D mutant; conversely, non-phosphorylatable atx3 S12A does not elicit the same effects, resulting in less dendrites and a decreased number of synapses. The effects observed were not always statistically significative, but the repeated tendency in different types of analyses is nonetheless striking. Another possible hint into the fact that the morphological phenotype produced by polyQ expansion is related to atx3 function is that it can be partially prevented by mimicking phosphorylation.

If S12 phosphorylation is important in some atx3-mediated regulation of cell structure, then why does polyQ-expanded atx3 with serine at position 12 elicit the same phenotype as the phospho-null mutant? If the protein can be phosphorylated, it would be expected to behave as the phosphomimetic mutant of the expanded form. It is interesting to notice that while the effects of non-expanded WT atx3 are similar to those of its S12D mutant, the effects of the WT expanded form are more comparable to those of its S12A mutant. This could mean that polyQ expansion of atx3 hinders its phosphorylation, thus affecting the possible mechanisms responsible for the maintenance of neuronal structure. Mimicking phosphorylation in the expanded protein, however, reverts the defects. It is still unknown how the C-terminal tail of atx3 is organized is relation to the JD, but it is possible that, when the polyQ region is expanded, the C-terminal tail blocks accessibility to S12, hindering its phosphorylation. The results obtained are insufficient to support this hypothesis, but it is a possibility worthy of further investigation.

The effects of S12 phosphorylation may be a result of its effect on atx3 DUB activity, which we demonstrated to be decreased *in vitro*. In accordance to what was stated above, we would expect that, in cortical neurons, non-expanded WT atx3 and its S12D would be less active than the S12A form, allowing the maintenance of Ub signals that are important for the pathways regulating the maintenance of dendrites and synapses. In the expanded forms we tested, the activity of S12D atx3 would be maintained low, but would increase in the WT – if in fact the polyQ expansion hindered phosphorylation – to levels similar to those of S12A, thus explaining the similar phenotype. It is interesting to note that, when the DUB activity is completely inhibited in non-expanded atx3, the impact in atx3-mediated transcriptional regulation is rather modest; however, when the protein is expanded, that inhibition is sufficient to counter the aberrant expression caused by expanded atx3 (Evert *et al.*, 2006a). If in fact polyQ expansion of atx3 would hinder the phosphorylation of this protein, it could represent the loss of an endogenous mechanism responsible for keeping atx3 activity in check, leading to transcriptional aberration. The changes in activity caused by S12 phosphorylation may nonetheless be related to the other possible mechanisms mentioned in the previous section. PSD-95 is known to be degraded by the proteasome as a consequence of polyubiquitination (Colledge *et al.*, 2003); given the role proposed for atx3 as an editor of atypical polyUb chains, the increased activity of non-phosphorylated atx3 could enhance editing of mixed linkage polyUb chains bound to PSD-95, yielding pure K48 that could target it for degradation, thus reducing its levels.

Another possibility that cannot be excluded is the conceivable interference of S12 phosphorylation with atx3 properties other than its enzymatic activity. S12 may mediate protein-protein contacts that occur specifically when the residue is phosphorylated, and these functional interactions are possibly responsible for the development and/or maintenance of dendrites and synapses. Consequently, the changes observed when S12 is mutated to alanine could be due to alterations of the way atx3 binds to its protein partners, leading to deleterious effects. The effects of WT expanded atx3 could again be explained by a hindered phosphorylation: when the protein is not expanded it is phosphorylated normally and is thus able to interact regularly, but when expanded phosphorylation is hindered and so are the interactions atx3 establishes. S12 phosphorylation may interfere with the binding of known molecular partners of atx3, especially the ones that interact directly with the JD, such as NEDD8 (Ferro *et al.*, 2007), tubulin (Mazzucchelli *et al.*, 2009), HHR23A/B (Nicastro *et al.*, 2005) and parkin (Durcan *et al.*, 2012; Durcan *et al.*, 2011). Changes in the interaction between atx3 and tubulin might produce effects in the organization of the cytoskeleton or in intracellular protein transport. Interference with HHR23A/B could be related to changes in protein degradation, while atx3 interaction with parkin and the E2s that participate in parkin ubiquitination could affect the generation of ubiquitination signals. In none of the others DUBs whose enzymatic activity was described to be diminished by phosphorylation, the modified residue is localized next to the catalytic site; interestingly the phosphorylated residue in CYLD – S418 – is localized in the region admitted to regulate the interaction with its endogenous substrate TARF2, exemplifying how the modification of a residue in a region mediating the interactions can affect deubiquitination of a physiologic ubiquitinated substrate (Riley *et al.*, 2013). Finally, an interactomics study of several proteins involved in hereditary ataxias suggested that atx3 may interact with protein interacting with C kinase (PICK1), which is involved in the organization of membrane proteins, such as glutamate receptors and ion channels (Lim *et al.*, 2006). This type of interaction may impart changes at the level of the synaptic expression of proteins. Interestingly, silencing of PICK in *Drosophila* expressing a truncated form of expanded atx3 has been shown to have a protective effect, preventing the degeneration caused by the polyQ-expanded fragment (McHurk 2012). Ubiquilin-1, demonstrated to interact with atx3 (albeit through undisclosed mechanisms), is known to directly interact with GABARs, interfere with their assembly in the endoplasmic reticulum and to mediate their insertion in the plasma membrane (Saliba *et al.*, 2008). Indeed, it would be relevant to test whether expanded atx3 affects inhibitory synapses, and whether phosphorylation of S12 is implicated.

Phosphorylation of serine 12 as a protector against expanded ataxin-3-induced toxicity

In the biological setting of a cell, atx3 always has a serine at site 12. According to our results, this serine residue is a target for phosphorylation, and considering that this PTM is reversible and dynamic, it is assumed that only a fraction of the total population of atx3 is

actually phosphorylated at any given time point. Phosphomimetic S12D atx3 mimics the protein in a permanent phosphorylated state, as if 100% of the atx3 population was phosphorylated at all time, while the phospho-null S12A atx3 cannot be phosphorylated at any moment. The behavior of WT atx3 would be expected to be something in between that of the two phosphomutants: if the cellular population of WT atx3 is highly phosphorylated, it would be expectable that its behavior would be close to that of the S12D mutant; conversely, its behavior would be more similar to that of the S12A, if the population of phosphorylated atx3 was limited. This appears to be the case in our experiments exploring dendritic morphology and synapse number, even suggesting that expanded atx3 may by less phosphorylated than the non-expanded form, considering that the effects of the transfection with expanded atx3 are more similar to those of its phospho-null mutant. Considering the impairment of dendritic morphology and loss of synapses a result of a toxic action of atx3 elicited by polyQ expansion, results support the idea that S12 phosphorylation has a protective effect.

However, contrary to the notion that the behavior of the naturally-occurring protein lies somewhere between that of its phospho-null and phosphomimetic mutants, the analysis of the fraction of cells with GFP-atx3 aggregates in cortical neuron cultures and the results with the lentiviral rat model indicate that, independently of the actual amino acid residue into which serine is mutated, the toxicity of expanded atx3 diminishes. In both cases, aggregates are clearly a mark of toxicity: in cortical neurons, the percentage of cells with aggregates is significantly higher in cells expressing GFP-atx3 84Q, when compared to cells transfected with GFP-atx3 28Q; in the lentiviral rat model, not only do we and others observe that an increased number of aggregates is associated with larger depletion of a neuronal marker (Alves *et al.*, 2008a; Nascimento-Ferreira *et al.*, 2011), but the authors of the model also demonstrate that expression of non-expanded atx3 does not lead to the aggregation elicited by expanded atx3 expression (Alves *et al.*, 2008b). While the phospho-null mutation is the only to significantly decrease aggregation of expanded atx3 (although the phosphomimetic mutant shows a clear trend to reduced aggregation), in the neuronal cultures and animal model, both mutants present a reduced neuronal toxicity in the striatum, as observed by the lesser depletion of DARPP-32.

Seeing things from a different angle, it could be argued that the presence of an unchanged S12 may be a factor leading to toxicity; the phosphorylation of S12, as a biologic mechanism actually turning it into a different chemical entity, could have an effect in "turning it off". In a cellular context, S1S of expanded atx3 may contribute to pathways turning the protein more toxic, like misfolding, cleavage, or aggregation, through mechanisms involving its lateral chain. Phosphorylation would alter the serine's side chain, limiting those toxic functions, in accordance to what is observed for the phosphomimetic mutant. According to this hypothesis, the alanine at position 12 in the phospho-null mutant would not be able to participate in the toxic pathways involving S12, because of the differences between the two amino acids (namely their side chains). This would explain the similar behaviors between the two phosphomutants.

One way to conciliate the opposing effects of the mutants in the neuromorphology experiments with their similar effect regarding toxicity is that, although the toxicity-related characteristics (aggregation and DARPP-32 depletion) we analyzed are mediated by a non-phosphorylated serine, the "morphological effects" are indeed a functional consequence of phosphorylation, and so the alanine mutant does not produce them, contrary to the mutant to aspartate. When describing the effects htt phosphorylation at T3, Aiken and coworkers (2009) encountered apparent discrepancies with parallels with our observations. Though the phosphomimetic mutant of T3 led to increased aggregation of an htt fragment in striatal precursor cells and in a *Drosophila* model, the respective phospho-null mutant decreased aggregation. However, both mutations were neuroprotective in the animal model, reducing lethality and neurodegeneration. This led the authors to suggest two explanations: either there was another modification of T3, such as glycosylation, that could be responsible for the toxicity of the expanded htt fragment, or T3 displays an "intrinsic property" that leads to toxicity (Aiken *et al.*, 2009). The rescue they observed when mutating T3 could be due to distinct mechanisms mediated by each mutation, seeing as the mutation to aspartate (which elicited the greatest neurodegeneration rescue) increases aggregation, while the mutation to alanine reduces it. Interestingly, it was also determined that increased number of glutamines correlate with decreased phosphorylation of T3. In the case of the phosphorylation of S12, we suggest that both the S12D and the S12A mutations may interfere with the putative toxic mechanism mediated by S12, hindering aggregation and cell loss. However, phosphorylation, as observed by the behavior of the phosphomimetic mutant, contributes to other functional pathways with which atx3 may be involved and that are admittedly important in maintaining neuronal function, such as the maintenance of dendrites and functional synapses. These effects may be mediated by the reduced DUB activity of the phosphorylated protein, or by the putative interaction it influences.

Intriguingly, on par with the tendency of the S12A mutant of non-expanded atx3 to decrease synaptic markers and dendritic arborization and length in cortical neurons, results indicate that the protein has an increased tendency to aggregate as well. Possibly S12 not only mediates toxicity when the protein is expanded, by is also important in keeping atx3 in a non-toxic state when the protein is not expanded. A hypothesis that would explain why the two phosphomutants appear to be protective against expanded atx3-induced toxicity, while the phospho-null mutant of the non-expanded protein appears to be itself toxic, could make use of the growing concept that aberrant interactions underlie the toxicity of pathogenic polyQ-containing protein (Williams and Paulson, 2008). S12 of atx3 may be critical for the mediation of important protein-protein interactions established by atx3, in part by its ability to be phosphorylated and modulate interactions in that state. That would explain why the phosphomimetic mutant displays a similar behavior to that of the WT protein; in the phospho-null mutant, S12 is not there to be phosphorylated or to mediate conceivable interactions that depend on its non-phosphorylated state. When atx3 is expanded, it interacts aberrantly: with other atx3 molecules, leading to aggregation; with physiological molecular partners, leading to abnormalities in its normal cellular functions; or with new partners with which atx3 interacts

only when expanded, possibly capturing important elements of cellular systems that thus become dysfunctional. Possibly some physiologic interactions are actually abrogated, similarly leading to impairment of atx3 normal functions. An alanine at position 12 may inhibit some of the aberrant interactions, eliciting the protective effect observed and reducing aggregation. An aspartate at that position could rescue a subset of the normal interactions, thus producing a protective effect, albeit not as strong. Interestingly, the maintenance of functional interactions with Ub has been shown to be protective against atx3 aggregation (Masino *et al.*, 2011). Considering the possibility that the similar outcomes of the two mutations are the result of a similar "net" interference with molecular interactions, it is also worthy to note that the detection of analogous functional effects elicited by a phosphomimetic and a phospho-null mutant of a particular phosphorylation site have been observed with other proteins; for example, in the collapsing response mediator protein-2 (CRMP-2), both phosphomutants of S522 elicited similar outcomes in a downstream calcium channel, decreasing calcium influx (Brittain *et al.*, 2012). The effects of S12 in the dendritic morphology would be specific of interactions mediated by the phosphoserine, and are thus only replicated by the aspartate mutant.

Lastly, an additional comment must be added regarding the usage of phosphomimetic mutants to study the behavior of phosphorylated proteins. Mutation of phosphorylatable residues to negatively charged residues is a widespread strategy employed to mimic constitutively phosphorylated amino acids, as explained in section 3.4 and repeatedly exemplified in section 1.7. Nonetheless, there are limitations to their usage, and examples where they fail to mimic a phosphorylated state. For example, the triggering of the enzymatic activity of DUBA by S177 phosphorylation could not be replicated by substituting S177 with an aspartate or a glutamate residue (Huang *et al.*, 2012). The limitations of phosphomimetic mutants may be explained by several factors. First, mutations to alanine or glutamate constitutively introduce a negative charge on the protein that, in spite of representing a great experimental advantage, is in contradiction with the reversible nature of phosphorylation. Proteins are phosphorylated after being synthetized and acquiring the correct folding, and consequently the extemporaneous negative charge may interfere with the folding of the protein. Additionally, phosphoamino acids are not completely similar to any natural amino acid: the negative charge introduced by an aspartate or a glutamate residue (–1) is not the same as that of a phosphorylated residue (–1,5 or –2), at physiologic pH, and the size of the ionic shell produced by a conjugated phosphate is also different (Dephoure *et al.*, 2013; Hunter, 2012; Pearlman *et al.*, 2011). Thus, phosphomimetic amino acids may not be able to replicate particular molecular interactions. It has been suggested that substituting a single phosphorylatable amino acid with two neighboring acidic amino acids may produce better phosphomimetics. In our study, it is difficult to ascertain how well our phosphomutants replicate the phosphorylated state of atx3. The phospho-specific antibody was able to recognize the phosphomimetic mutants, suggesting that their denatured structure is sufficiently similar to that of the phosphoserine-containing peptide that was used to produce and purify the anti-Patx3 antibody. The fact that they produce effects that are markedly

distinct from the WT protein indicates that our mutations were successful in producing changes in the properties of the protein, that possibly reflect those of phosphorylated atx3.

Many of the hypotheses raised by the results obtained in this study require additional testing and further delving into the consequences of phosphorylation of S12 of atx3. The drawing of a clearer picture of the effects of this PTM entails the exploration of the structural effects of phosphate conjugation to S12, the investigation of possible effects in protein properties other than activity and a more particularized analysis of the cellular systems involved in the changes observed. Nonetheless, the current results indicate that interference with the native state of S12 decreases the toxicity of atx3. In a natural context, a way to interfere with S12 would be by phosphorylating this residue. Considering the effects of the phosphomimetic mutant in the rescue of the morphology of the dendritic tree, the number of synapses and the depletion of DARPP-32-positive signal, we suggest that phosphorylation of atx3 may be protective against the toxicity of expanded atx3.

5.2 Future perspectives

A better characterization of the effects of S12 phosphorylation will benefit from additional experiments aimed at unveiling factors that relate the levels of phosphorylated atx3 with MJD pathogenesis. The phospho-specific antibody that we produced will be useful in detecting phosphorylation in MJD animal models or in MJD patients' brain, allowing the comparison between the S12 phosphorylation state between disease and healthy conditions. This could help determine if atx3 polyQ expansion affects phosphorylation and possibly confirm some of the hypotheses presented above. Furthermore, it will be very important to determine if atx3 phosphorylation levels correlate with the regional vulnerability in MJD. If S12 phosphorylation is protective against atx3 toxicity, lower levels of phosphorylation in particular brain regions could be related to the toxicity outcomes observed.

Mutating S12 to aspartate elicited a significant effect in atx3 DUB activating, leading to reduction of the cleavage of Ub substrates. The current study used atx3 WT produced in *E. coli* as the non-phosphorylated control, but considering that other effects were analyzed also through the lens of the phospho-null mutant to alanine, it will be important to check if the same mutant, produced and purified under the same conditions, affects the DUB activity of atx3 in any way. We predict the cleavage efficiency of the S12A mutant will be similar to that of atx3 WT or possibly higher, attending to the effects produced when S12 is mutated to phenylalanine (Weeks *et al.*, 2011). Moreover, phosphorylation of S12 may affect other properties of atx3, such as its subcellular localization (including nuclear shuttling), its turnover, and, importantly, its molecular interactions. A better comprehension of the biologic importance of this PTM will require the characterization of the effect of phosphorylation on these parameters. Comparison between atx3 WT and its S12 phosphomutants may be informative, and it will also be substantial to observe the possible differences that arise in the presence polyQ expansion. Preliminary studies applying nuclear fractionation protocols to

transfected cells lines yielded no definitive conclusions regarding the enrichment of any atx3 form in the nucleus, but it could be important to make a similar characterization in neurons. Our microscopic observations showed no visible effect of the mutants in atx3 subcellular localization, but a biochemical characterization is possibly bound to express tendencies more objectively. Experiments employing fluorescence recovery after photobleaching (FRAP) performed in transfected COS-7 cells revealed no striking differences in the mobility of GFP-atx3 between the WT protein and the respective phosphomutants, but further investigation will be necessary to appreciate this property. The interference of the phosphomutants in atx3 interactions or turnover are yet to be investigated. Additionally, it will be important to use other strategies to evaluate the aggregation of the phosphomutants. *In vitro* studies (Gales *et al.*, 2005) could be helpful in appreciating the intrinsic tendency of the proteins to aggregate, in the absence of other cellular players that may possibly influence this process. Furthermore, it will be important to determine if the different phosphomutations, apart from affecting the number of cells that present aggregation, also produce alterations in the number, size and subscellular localization of aggregates, that could not be evaluated in the current study. For this task, it will crucial to analyze the aggregates three-dimensionally, so that their volume, shape and localization can be correctly appreciated.

Understanding the mechanisms underlying the morphological changes that expanded atx3 causes in cortical neurons may yield significant contributions to the comprehension of the pathogenesis of MJD. The alterations we observed may possibly lead to neuronal dysfunction, representing toxicity mechanisms that have not been appropriately contemplated so far. Importantly, the analysis of dendritic morphology and synaptic number and structure could also be performed in cells derived from other brain regions such as the cerebellum, possibly derived from MJD animal models, thus excluding the need for transfection. It will be important to determine if the changes caused by expanded atx3 and the countering effect of S12 phosphorylation are due to an action at the level of transcription regulation, secretory pathway regulation and sorting, axonal transport, membrane trafficking or protein degradation, and what are the molecular targets of these actions.

The current results are not sufficient to ascertain if the effects in neurons are a consequence of the activity changes produced by phosphomutation. Considering that the phosphomimetic mutant decreases atx3 enzymatic activity, it would be interesting to test the effect of the expression of the inactive C14A mutant, using atx3 with polyQ tracts of different length. Admittedly, complete abrogation of DUB activity may produce different effects than a decrease in the rate of cleavage, but these studies could elucidate if the phenotypes we observe are linked with atx3 DUB activity or other properties that are also regulated by S12 phosphorylation.

A promising approach to further explore the effects of S12 phosphorylation *in vivo*, possibly beyond the influence on aggregate formation and neuronal depletion, could make use of transgenic animals expressing atx3 with S12 mutated to aspartate. In this respect, it would be interesting to utilize a recently developed strategy for generating knock-in mouse models expressing human expanded atx3 (Figiel *et al.*, 2014). Expression of expanded atx3 S12D using

Table V: Kinases putatively responsible for phosphorylation of S12 of atx3

Kinase		Score
Protein kinase A	PKA	0,57
DNA-dependent protein kinase	DNA PK	0,48
Cell division cycle 2 kinase	Cdc2	0,46
Glycogen synthase kinase 3	GSK3	0,46
Calcium/calmodulin-dependent protein kinase 2	CaMK2	0,42
Casein kinase 1	CK1	0,38
Casein kinase 2	CK2	0,35
Protein kinase C	PKC	0,32
Ribosomal s6 kinase	RSK	0,28
p38 mitogen-activated protein kinase	p38MAPK	0,28
Protein kinase ataxia-telangiectasia mutated	ATM	0,26
Protein kinase G	PKG	0,26
Cyclin-dependent kinase 5	Cdk5	0,14
Protein kinase B	PKB	0,08

Prediction was made with NetPhosk 1.0 (Blom *et al.*, 2004) using the amino acid sequence of human atx3 isoform MJD1a (NCBI accession number: AAB33571.1). Score values (0,00-1,00) define how well the amino acid sequence containing the phosphate-accepting residue conforms with the sequence preferences determined for each kinase

the same approach could yield enlightening outputs in terms of the outcomes of phosphorylation in behavioral phenotypes and other MJD neurodegenerative features. Cell culture models derived from these mice could help understand the molecular mechanisms and cellular pathways with which S12 phosphorylation interferes.

Finally, unveiling the kinase (or kinases) that mediates S12 phosphorylation will be decisive for the future outcomes of the study of this PTM. One way to tackle this issue would be to employ *in vitro* phosphorylation assays, using purified atx3 and particular kinases that could putatively target S12. The selection of these kinases can be made based on the comparison between their preferred consensus sequences and the amino acid sequence in which S12 is inserted (Table V). Detection of phosphorylation could make use of radiolabelled phosphate and the determination of phosphate conjugation specifically to S12 could be achieved by comparing the results obtained between atx3 WT and atx3 with a mutated S12. Alternatively, detection of S12 phosphorylation could also take advantage of the phospho-specific antibody generated. Knowing the enzyme(s) that could be involved in S12 phosphorylation *in vitro* would then help design additional experimental approaches. Modifying the activity of kinases (either through pharmacological stimuli of by regulating the levels of the enzymes) and comparing the effects produced on atx3 properties could allow the evaluation of the effects of S12 phosphorylation without the need to nelly on phosphomimetic mutants. Modulating the phosphorylation state of atx3 by interfering with the kinases involved could also allow the analysis of the effects in neuronal cultures derived from MJD models.

Importantly, in some experiments with a phospho-specific antibody recognizing phosphorylated 421 of htt, satisfactory detection of the htt could only be achieved after stimulating or overexpressing Akt, which is one the kinases responsible for that modification (Humbert 2002). It is possible that a similar approach will help detect phosphorylation of full-length atx3 in the culture models used in our study.

5.3 Conclusion

The current study demonstrated that S12 of atx3 is phosphorylated in mammalian cell lines and in cultured cortical neurons, where it chiefly targets atx3-derived fragments. Importantly, this is the first study to show that atx3 is phosphorylated in neuronal cells, suggesting that phosphorylation of S12 may participate in regulatory mechanisms occurring in neurons. The presence of a phosphomimetic aspartate at position 12 was shown to decrease atx3 DUB activity, a change that may interfere with the pathways with which atx3 is functionally involved.

A morphological analysis of neurons expressing polyQ-expanded atx3 suggested that the pathogenic pathways involved in MJD may include neuronal dysfunction derived from an impaired establishment of neuronal networks, resulting from poor dendritic arborization and loss of functional synapses. These changes are possibly related to yet undescribed pathogenic alterations that occur in the cortex of MJD patients even without significative neuronal loss, but may take place in neurons from other brain regions as well, representing a wither neuronal-specific mechanism of cellular dysfunction. The cortical cell model generated in this study may be useful in evaluating the impact of different factors putatively affecting atx3 toxicity in neurons. Importantly, mimicking phosphorylation of expanded atx3 reverts the phenotype observed, indicating that this novel PTM mediates a protective mechanism against the neuromorphological alterations. In lentiviral rat MJD models with striatal pathology, mutations of S12 also decreased neuronal toxicity, indicating that interference with S12 *in vivo*, such as that resulting from phosphorylation, is a possible means of modulating the toxicity of expanded atx3.

Further studies will be necessary to determine if S12 phosphorylation is a promising target for therapeutic strategies aiming at MJD treatment.

References

Aiken, C.T., Steffan, J.S., Guerrero, C.M., Khashwji, H., Lukacsovich, T., Simmons, D., Purcell, J.M., Menhaji, K., Zhu, Y.Z., Green, K., Laferla, F., Huang, L., Thompson, L.M., Marsh, J.L., 2009. Phosphorylation of threonine 3: implications for Huntingtin aggregation and neurotoxicity. *J Biol Chem* 284**,** 29427-29436.

Albrecht, M., Golatta, M., Wullner, U., Lengauer, T., 2004. Structural and functional analysis of ataxin-2 and ataxin-3. *Eur J Biochem* 271**,** 3155-3170.

Albrecht, M., Hoffmann, D., Evert, B.O., Schmitt, I., Wullner, U., Lengauer, T., 2003. Structural modeling of ataxin-3 reveals distant homology to adaptins. *Proteins* 50**,** 355-370.

Almeida, B., Fernandes, S., Abreu, I.A., Macedo-Ribeiro, S., 2013. Trinucleotide repeats: a structural perspective. *Frontiers in neurology* 4**,** 76.

Alves, S., Nascimento-Ferreira, I., Auregan, G., Hassig, R., Dufour, N., Brouillet, E., Pedroso de Lima, M.C., Hantraye, P., Pereira de Almeida, L., Deglon, N., 2008a. Allele-specific RNA silencing of mutant ataxin-3 mediates neuroprotection in a rat model of Machado-Joseph disease. *PLoS One* 3**,** e3341.

Alves, S., Nascimento-Ferreira, I., Dufour, N., Hassig, R., Auregan, G., Nobrega, C., Brouillet, E., Hantraye, P., Pedroso de Lima, M.C., Deglon, N., de Almeida, L.P., 2010. Silencing ataxin-3 mitigates degeneration in a rat model of Machado-Joseph disease: no role for wild-type ataxin-3? *Hum Mol Genet* 19**,** 2380-2394.

Alves, S., Regulier, E., Nascimento-Ferreira, I., Hassig, R., Dufour, N., Koeppen, A., Carvalho, A.L., Simoes, S., de Lima, M.C., Brouillet, E., Gould, V.C., Deglon, N., de Almeida, L.P., 2008b. Striatal and nigral pathology in a lentiviral rat model of Machado-Joseph disease. *Hum Mol Genet* 17**,** 2071-2083.

Amerik, A.Y., Hochstrasser, M., 2004. Mechanism and function of deubiquitinating enzymes. *Biochim Biophys Acta* 1695**,** 189-207.

Amm, I., Sommer, T., Wolf, D.H., 2014. Protein quality control and elimination of protein waste: the role of the ubiquitin-proteasome system. *Biochim Biophys Acta* 1843**,** 182-196.

Anne, S.L., Saudou, F., Humbert, S., 2007. Phosphorylation of huntingtin by cyclin-dependent kinase 5 is induced by DNA damage and regulates wild-type and mutant huntingtin toxicity in neurons. *J Neurosci* 27**,** 7318-7328.

Antony, P.M., Mantele, S., Mollenkopf, P., Boy, J., Kehlenbach, R.H., Riess, O., Schmidt, T., 2009. Identification and functional dissection of localization signals within ataxin-3. *Neurobiol Dis* 36**,** 280-292.

Araujo, J., Breuer, P., Dieringer, S., Krauss, S., Dorn, S., Zimmermann, K., Pfeifer, A., Klockgether, T., Wuellner, U., Evert, B.O., 2011. FOXO4-dependent upregulation of superoxide dismutase-2 in response to oxidative stress is impaired in spinocerebellar ataxia type 3. *Hum Mol Genet* 20**,** 2928-2941.

Arrasate, M., Mitra, S., Schweitzer, E.S., Segal, M.R., Finkbeiner, S., 2004. Inclusion body formation reduces levels of mutant huntingtin and the risk of neuronal death. *Nature* 431**,** 805-810.

Ballif, B.A., Cao, Z., Schwartz, D., Carraway, K.L., 3rd, Gygi, S.P., 2006. Identification of 14-3-3epsilon substrates from embryonic murine brain. *Journal of proteome research* 5**,** 2372-2379.

Bauer, P.O., Nukina, N., 2009. The pathogenic mechanisms of polyglutamine diseases and current therapeutic strategies. *J Neurochem* 110**,** 1737-1765.

Baylies, M.K., Michelson, A.M., 2001. Invertebrate myogenesis: looking back to the future of muscle development. *Curr Opin Genet Dev* 11**,** 431-439.

Berke, S.J., Chai, Y., Marrs, G.L., Wen, H., Paulson, H.L., 2005. Defining the role of ubiquitin-interacting motifs in the polyglutamine disease protein, ataxin-3. *J Biol Chem* 280**,** 32026-32034.

Berke, S.J., Schmied, F.A., Brunt, E.R., Ellerby, L.M., Paulson, H.L., 2004. Caspase-mediated proteolysis of the polyglutamine disease protein ataxin-3. *J Neurochem* 89**,** 908-918.

Berzofsky, J.A., Berkower, I.J. 1993. Immunogenicity and Antigen Structure. In: *Fundamental Immunology*. pp. 235-282. Ed. W.E. Paul. Raven Press: New York.

Bettencourt, C., Fialho, R.N., Santos, C., Montiel, R., Bruges-Armas, J., Maciel, P., Lima, M., 2008. Segregation distortion of wild-type alleles at the Machado-Joseph disease locus: a study in normal families from the Azores islands (Portugal). *J Hum Genet* 53**,** 333-339.

Bettencourt, C., Lima, M., 2011. Machado-Joseph Disease: from first descriptions to new perspectives. *Orphanet journal of rare diseases* 6**,** 35.

Bettencourt, C., Santos, C., Montiel, R., Costa Mdo, C., Cruz-Morales, P., Santos, L.R., Simoes, N., Kay, T., Vasconcelos, J., Maciel, P., Lima, M., 2009. Increased transcript diversity: novel splicing variants of Machado-Joseph disease gene (ATXN3). *Neurogenetics* 11**,** 193-202.

Bevivino, A.E., Loll, P.J., 2001. An expanded glutamine repeat destabilizes native ataxin-3 structure and mediates formation of parallel beta -fibrils. *Proc Natl Acad Sci U S A* 98**,** 11955-11960.

Bichelmeier, U., Schmidt, T., Hubener, J., Boy, J., Ruttiger, L., Habig, K., Poths, S., Bonin, M., Knipper, M., Schmidt, W.J., Wilbertz, J., Wolburg, H., Laccone, F., Riess, O., 2007. Nuclear localization of ataxin-3 is required for the manifestation of symptoms in SCA3: in vivo evidence. *J Neurosci* 27**,** 7418-7428.

Blom, H., Ronnlund, D., Scott, L., Westin, L., Widengren, J., Aperia, A., Brismar, H., 2013. Spatial distribution of DARPP-32 in dendritic spines. *PLoS One* 8**,** e75155.

Blom, N., Sicheritz-Ponten, T., Gupta, R., Gammeltoft, S., Brunak, S., 2004. Prediction of post-translational glycosylation and phosphorylation of proteins from the amino acid sequence. *Proteomics* 4**,** 1633-1649.

Boeddrich, A., Gaumer, S., Haacke, A., Tzvetkov, N., Albrecht, M., Evert, B.O., Muller, E.C., Lurz, R., Breuer, P., Schugardt, N., Plassmann, S., Xu, K., Warrick, J.M., Suopanki, J., Wullner, U., Frank, R., Hartl, U.F., Bonini, N.M., Wanker, E.E., 2006. An arginine/lysine-rich motif is crucial for VCP/p97-mediated modulation of ataxin-3 fibrillogenesis. *EMBO J* 25**,** 1547-1558.

Borodovsky, A., Kessler, B.M., Casagrande, R., Overkleeft, H.S., Wilkinson, K.D., Ploegh, H.L., 2001. A novel active site-directed probe specific for deubiquitylating enzymes reveals proteasome association of USP14. *EMBO J* 20**,** 5187-5196.

Boutell, C., Canning, M., Orr, A., Everett, R.D., 2005. Reciprocal activities between herpes simplex virus type 1 regulatory protein ICP0, a ubiquitin E3 ligase, and ubiquitin-specific protease USP7. *Journal of virology* 79**,** 12342-12354.

Boy, J., Schmidt, T., Wolburg, H., Mack, A., Nuber, S., Bottcher, M., Schmitt, I., Holzmann, C., Zimmermann, F., Servadio, A., Riess, O., 2009. Reversibility of symptoms in a conditional mouse model of spinocerebellar ataxia type 3. *Hum Mol Genet* 18**,** 4282-4295.

Bredesen, D.E., Rao, R.V., Mehlen, P., 2006. Cell death in the nervous system. *Nature* 443**,** 796-802.

Breuer, P., Haacke, A., Evert, B.O., Wullner, U., 2010. Nuclear aggregation of polyglutamine-expanded ataxin-3: fragments escape the cytoplasmic quality control. *J Biol Chem* 285**,** 6532-6537.

Brittain, J.M., Wang, Y., Eruvwetere, O., Khanna, R., 2012. Cdk5-mediated phosphorylation of CRMP-2 enhances its interaction with CaV2.2. *FEBS Lett* 586**,** 3813-3818.

Bryson-Richardson, R.J., Currie, P.D., 2008. The genetics of vertebrate myogenesis. *Nat Rev Genet* 9**,** 632-646.

Burk, K., Globas, C., Bosch, S., Klockgether, T., Zuhlke, C., Daum, I., Dichgans, J., 2003. Cognitive deficits in spinocerebellar ataxia type 1, 2, and 3. *Journal of neurology* 250**,** 207-211.

Burnett, B., Li, F., Pittman, R.N., 2003. The polyglutamine neurodegenerative protein ataxin-3 binds polyubiquitylated proteins and has ubiquitin protease activity. *Hum Mol Genet* 12**,** 3195-3205.

Burnett, B.G., Pittman, R.N., 2005. The polyglutamine neurodegenerative protein ataxin 3 regulates aggresome formation. *Proc Natl Acad Sci U S A* 102**,** 4330-4335.

Campbell, D.S., Holt, C.E., 2001. Chemotropic responses of retinal growth cones mediated by rapid local protein synthesis and degradation. *Neuron* 32**,** 1013-1026.

Cancel, G., Gourfinkel-An, I., Stevanin, G., Didierjean, O., Abbas, N., Hirsch, E., Agid, Y., Brice, A., 1998. Somatic mosaicism of the CAG repeat expansion in spinocerebellar ataxia type 3/Machado-Joseph disease. *Human mutation* 11**,** 23-27.

Cartier, A.E., Djakovic, S.N., Salehi, A., Wilson, S.M., Masliah, E., Patrick, G.N., 2009. Regulation of synaptic structure by ubiquitin C-terminal hydrolase L1. *J Neurosci* 29**,** 7857-7868.

Carvalho, D.R., La Rocque-Ferreira, A., Rizzo, I.M., Imamura, E.U., Speck-Martins, C.E., 2008. Homozygosity enhances severity in spinocerebellar ataxia type 3. *Pediatric neurology* 38**,** 296-299.

Cemal, C.K., Carroll, C.J., Lawrence, L., Lowrie, M.B., Ruddle, P., Al-Mahdawi, S., King, R.H., Pook, M.A., Huxley, C., Chamberlain, S., 2002. YAC transgenic mice carrying pathological alleles of the MJD1 locus exhibit a mild and slowly progressive cerebellar deficit. *Hum Mol Genet* 11**,** 1075-1094.

Chai, Y., Berke, S.S., Cohen, R.E., Paulson, H.L., 2004. Poly-ubiquitin binding by the polyglutamine disease protein ataxin-3 links its normal function to protein surveillance pathways. *J Biol Chem* 279**,** 3605-3611.

Chai, Y., Koppenhafer, S.L., Bonini, N.M., Paulson, H.L., 1999a. Analysis of the role of heat shock protein (Hsp) molecular chaperones in polyglutamine disease. *J Neurosci* 19**,** 10338-10347.

Chai, Y., Koppenhafer, S.L., Shoesmith, S.J., Perez, M.K., Paulson, H.L., 1999b. Evidence for proteasome involvement in polyglutamine disease: localization to nuclear inclusions in SCA3/MJD and suppression of polyglutamine aggregation in vitro. *Hum Mol Genet* 8**,** 673-682.

Chai, Y., Shao, J., Miller, V.M., Williams, A., Paulson, H.L., 2002. Live-cell imaging reveals divergent intracellular dynamics of polyglutamine disease proteins and supports a sequestration model of pathogenesis. *Proc Natl Acad Sci U S A* 99**,** 9310-9315.

Chen, F., Sugiura, Y., Myers, K.G., Liu, Y., Lin, W., 2010. Ubiquitin carboxyl-terminal hydrolase L1 is required for maintaining the structure and function of the neuromuscular junction. *Proc Natl Acad Sci U S A* 107**,** 1636-1641.

Chen, H., Polo, S., Di Fiore, P.P., De Camilli, P.V., 2003a. Rapid Ca2+-dependent decrease of protein ubiquitination at synapses. *Proc Natl Acad Sci U S A* 100**,** 14908-14913.

Chen, H.K., Fernandez-Funez, P., Acevedo, S.F., Lam, Y.C., Kaytor, M.D., Fernandez, M.H., Aitken, A., Skoulakis, E.M., Orr, H.T., Botas, J., Zoghbi, H.Y., 2003b. Interaction of Akt-phosphorylated ataxin-1 with 14-3-3 mediates neurodegeneration in spinocerebellar ataxia type 1. *Cell* 113**,** 457-468.

Chen, P.C., Qin, L.N., Li, X.M., Walters, B.J., Wilson, J.A., Mei, L., Wilson, S.M., 2009. The proteasome-associated deubiquitinating enzyme Usp14 is essential for the maintenance of synaptic ubiquitin levels and the development of neuromuscular junctions. *J Neurosci* 29**,** 10909-10919.

Chen, S., Berthelier, V., Hamilton, J.B., O'Nuallain, B., Wetzel, R., 2002. Amyloid-like features of polyglutamine aggregates and their assembly kinetics. *Biochemistry* 41**,** 7391-7399.

Chen, X., Tang, T.S., Tu, H., Nelson, O., Pook, M., Hammer, R., Nukina, N., Bezprozvanny, I., 2008. Deranged calcium signaling and neurodegeneration in spinocerebellar ataxia type 3. *J Neurosci* 28**,** 12713-12724.

Cholay, M., Reverdy, C., Benarous, R., Colland, F., Daviet, L., 2010. Functional interaction between the ubiquitin-specific protease 25 and the SYK tyrosine kinase. *Experimental cell research* 316**,** 667-675.

Chou, A.H., Chen, S.Y., Yeh, T.H., Weng, Y.H., Wang, H.L., 2011. HDAC inhibitor sodium butyrate reverses transcriptional downregulation and ameliorates ataxic symptoms in a transgenic mouse model of SCA3. *Neurobiol Dis* 41**,** 481-488.

Chou, A.H., Yeh, T.H., Kuo, Y.L., Kao, Y.C., Jou, M.J., Hsu, C.Y., Tsai, S.R., Kakizuka, A., Wang, H.L., 2006. Polyglutamine-expanded ataxin-3 activates mitochondrial apoptotic pathway by upregulating Bax and downregulating Bcl-xL. *Neurobiol Dis* 21**,** 333-345.

Chou, A.H., Yeh, T.H., Ouyang, P., Chen, Y.L., Chen, S.Y., Wang, H.L., 2008. Polyglutamine-expanded ataxin-3 causes cerebellar dysfunction of SCA3 transgenic mice by inducing transcriptional dysregulation. *Neurobiol Dis* 31**,** 89-101.

Chow, M.K., Ellisdon, A.M., Cabrita, L.D., Bottomley, S.P., 2004a. Polyglutamine expansion in ataxin-3 does not affect protein stability: implications for misfolding and disease. *J Biol Chem* 279**,** 47643-47651.

Chow, M.K., Mackay, J.P., Whisstock, J.C., Scanlon, M.J., Bottomley, S.P., 2004b. Structural and functional analysis of the Josephin domain of the polyglutamine protein ataxin-3. *Biochem Biophys Res Commun* 322**,** 387-394.

Chow, M.K., Paulson, H.L., Bottomley, S.P., 2004c. Destabilization of a non-pathological variant of ataxin-3 results in fibrillogenesis via a partially folded intermediate: a model for misfolding in polyglutamine disease. *J Mol Biol* 335**,** 333-341.

Christie, N.T., Lee, A.L., Fay, H.G., Gray, A.A., Kikis, E.A., 2014. Novel polyglutamine model uncouples proteotoxicity from aging. *PLoS One* 9**,** e96835.

Clague, M.J., Urbe, S., 2006. Endocytosis: the DUB version. *Trends in cell biology* 16**,** 551-559.

Cohen, P., 2002. The origins of protein phosphorylation. *Nat Cell Biol* 4**,** E127-130.

Colin, E., Zala, D., Liot, G., Rangone, H., Borrell-Pages, M., Li, X.J., Saudou, F., Humbert, S., 2008. Huntingtin phosphorylation acts as a molecular switch for anterograde/retrograde transport in neurons. *EMBO J* 27**,** 2124-2134.

Colledge, M., Snyder, E.M., Crozier, R.A., Soderling, J.A., Jin, Y., Langeberg, L.K., Lu, H., Bear, M.F., Scott, J.D., 2003. Ubiquitination regulates PSD-95 degradation and AMPA receptor surface expression. *Neuron* 40**,** 595-607.

Colomer Gould, V.F., 2012. Mouse models of spinocerebellar ataxia type 3 (Machado-Joseph disease). *Neurotherapeutics : the journal of the American Society for Experimental NeuroTherapeutics* 9**,** 285-296.

Costa, M.C., Gomes-da-Silva, J., Miranda, C.J., Sequeiros, J., Santos, M.M., Maciel, P., 2004. Genomic structure, promoter activity, and developmental expression of the mouse homologue of the Machado-Joseph disease (MJD) gene. *Genomics* 84**,** 361-373.

Coutinho, P., Ruano, L., Loureiro, J.L., Cruz, V.T., Barros, J., Tuna, A., Barbot, C., Guimaraes, J., Alonso, I., Silveira, I., Sequeiros, J., Marques Neves, J., Serrano, P., Silva, M.C., 2013. Hereditary ataxia and spastic paraplegia in Portugal: a population-based prevalence study. *JAMA neurology* 70**,** 746-755.

Crimmins, S., Jin, Y., Wheeler, C., Huffman, A.K., Chapman, C., Dobrunz, L.E., Levey, A., Roth, K.A., Wilson, J.A., Wilson, S.M., 2006. Transgenic rescue of ataxia mice with neuronal-specific expression of ubiquitin-specific protease 14. *J Neurosci* 26**,** 11423-11431.

Cummings, C.J., Zoghbi, H.Y., 2000. Fourteen and counting: unraveling trinucleotide repeat diseases. *Hum Mol Genet* 9**,** 909-916.

D'Abreu, A., Franca, M.C., Jr., Yasuda, C.L., Campos, B.A., Lopes-Cendes, I., Cendes, F., 2012. Neocortical atrophy in Machado-Joseph disease: a longitudinal neuroimaging study. *Journal of neuroimaging : official journal of the American Society of Neuroimaging* 22**,** 285-291.

de Almeida, L.P., Ross, C.A., Zala, D., Aebischer, P., Deglon, N., 2002. Lentiviral-mediated delivery of mutant huntingtin in the striatum of rats induces a selective neuropathology modulated by polyglutamine repeat size, huntingtin expression levels, and protein length. *J Neurosci* 22**,** 3473-3483.

DeFelipe, J., 2011. The evolution of the brain, the human nature of cortical circuits, and intellectual creativity. *Frontiers in neuroanatomy* 5**,** 29.

Demuro, A., Mina, E., Kayed, R., Milton, S.C., Parker, I., Glabe, C.G., 2005. Calcium dysregulation and membrane disruption as a ubiquitous neurotoxic mechanism of soluble amyloid oligomers. *J Biol Chem* 280**,** 17294-17300.

Denuc, A., Bosch-Comas, A., Gonzalez-Duarte, R., Marfany, G., 2009. The UBA-UIM domains of the USP25 regulate the enzyme ubiquitination state and modulate substrate recognition. *PLoS One* 4**,** e5571.

Dephoure, N., Gould, K.L., Gygi, S.P., Kellogg, D.R., 2013. Mapping and analysis of phosphorylation sites: a quick guide for cell biologists. *Molecular biology of the cell* 24**,** 535-542.

DiAntonio, A., Haghighi, A.P., Portman, S.L., Lee, J.D., Amaranto, A.M., Goodman, C.S., 2001. Ubiquitination-dependent mechanisms regulate synaptic growth and function. *Nature* 412**,** 449-452.

do Carmo Costa, M., Bajanca, F., Rodrigues, A.J., Tome, R.J., Corthals, G., Macedo-Ribeiro, S., Paulson, H.L., Logarinho, E., Maciel, P., 2010. Ataxin-3 plays a role in mouse myogenic differentiation through regulation of integrin subunit levels. *PLoS One* 5**,** e11728.

Donaldson, K.M., Li, W., Ching, K.A., Batalov, S., Tsai, C.C., Joazeiro, C.A., 2003. Ubiquitin-mediated sequestration of normal cellular proteins into polyglutamine aggregates. *Proc Natl Acad Sci U S A* 100**,** 8892-8897.

Dorval, V., Fraser, P.E., 2006. Small ubiquitin-like modifier (SUMO) modification of natively unfolded proteins tau and alpha-synuclein. *J Biol Chem* 281**,** 9919-9924.

Doss-Pepe, E.W., Stenroos, E.S., Johnson, W.G., Madura, K., 2003. Ataxin-3 interactions with rad23 and valosin-containing protein and its associations with ubiquitin chains and the proteasome are consistent with a role in ubiquitin-mediated proteolysis. *Mol Cell Biol* 23**,** 6469-6483.

Durcan, T.M., Fon, E.A., 2013. Ataxin-3 and its e3 partners: implications for machado-joseph disease. *Frontiers in neurology* 4**,** 46.

Durcan, T.M., Kontogiannea, M., Bedard, N., Wing, S.S., Fon, E.A., 2012. Ataxin-3 deubiquitination is coupled to Parkin ubiquitination via E2 ubiquitin-conjugating enzyme. *J Biol Chem* 287**,** 531-541.

Durcan, T.M., Kontogiannea, M., Thorarinsdottir, T., Fallon, L., Williams, A.J., Djarmati, A., Fantaneanu, T., Paulson, H.L., Fon, E.A., 2011. The Machado-Joseph disease-associated mutant form of ataxin-3 regulates parkin ubiquitination and stability. *Hum Mol Genet* 20**,** 141-154.

Durr, A., 2010. Autosomal dominant cerebellar ataxias: polyglutamine expansions and beyond. *Lancet Neurol* 9**,** 885-894.

Edelmann, M.J., Kramer, H.B., Altun, M., Kessler, B.M., 2010. Post-translational modification of the deubiquitinating enzyme otubain 1 modulates active RhoA levels and susceptibility to Yersinia invasion. *FEBS J* 277**,** 2515-2530.

Ehrnhoefer, D.E., Sutton, L., Hayden, M.R., 2011. Small changes, big impact: posttranslational modifications and function of huntingtin in Huntington disease. *The Neuroscientist : a review journal bringing neurobiology, neurology and psychiatry* 17**,** 475-492.

Eletr, Z.M., Wilkinson, K.D., 2014. Regulation of proteolysis by human deubiquitinating enzymes. *Biochim Biophys Acta* 1843**,** 114-128.

Ellisdon, A.M., Pearce, M.C., Bottomley, S.P., 2007. Mechanisms of ataxin-3 misfolding and fibril formation: kinetic analysis of a disease-associated polyglutamine protein. *J Mol Biol* 368**,** 595-605.

Ellisdon, A.M., Thomas, B., Bottomley, S.P., 2006. The two-stage pathway of ataxin-3 fibrillogenesis involves a polyglutamine-independent step. *J Biol Chem* 281**,** 16888-16896.

Emamian, E.S., Kaytor, M.D., Duvick, L.A., Zu, T., Tousey, S.K., Zoghbi, H.Y., Clark, H.B., Orr, H.T., 2003. Serine 776 of ataxin-1 is critical for polyglutamine-induced disease in SCA1 transgenic mice. *Neuron* 38**,** 375-387.

Evers, M.M., Toonen, L.J., van Roon-Mom, W.M., 2014. Ataxin-3 protein and RNA toxicity in spinocerebellar ataxia type 3: current insights and emerging therapeutic strategies. *Molecular neurobiology* 49**,** 1513-1531.

Evert, B.O., Araujo, J., Vieira-Saecker, A.M., de Vos, R.A., Harendza, S., Klockgether, T., Wullner, U., 2006a. Ataxin-3 represses transcription via chromatin binding, interaction with histone deacetylase 3, and histone deacetylation. *J Neurosci* 26**,** 11474-11486.

Evert, B.O., Schelhaas, J., Fleischer, H., de Vos, R.A., Brunt, E.R., Stenzel, W., Klockgether, T., Wullner, U., 2006b. Neuronal intranuclear inclusions, dysregulation of cytokine expression and cell death in spinocerebellar ataxia type 3. *Clin Neuropathol* 25**,** 272-281.

Evert, B.O., Vogt, I.R., Kindermann, C., Ozimek, L., de Vos, R.A., Brunt, E.R., Schmitt, I., Klockgether, T., Wullner, U., 2001. Inflammatory genes are upregulated in expanded

ataxin-3-expressing cell lines and spinocerebellar ataxia type 3 brains. *J Neurosci* 21**,** 5389-5396.

Evert, B.O., Vogt, I.R., Vieira-Saecker, A.M., Ozimek, L., de Vos, R.A., Brunt, E.R., Klockgether, T., Wullner, U., 2003. Gene expression profiling in ataxin-3 expressing cell lines reveals distinct effects of normal and mutant ataxin-3. *J Neuropathol Exp Neurol* 62**,** 1006-1018.

Fan, M.M., Raymond, L.A., 2007. N-methyl-D-aspartate (NMDA) receptor function and excitotoxicity in Huntington's disease. *Prog Neurobiol* 81**,** 272-293.

Fang, S., Weissman, A.M., 2004. A field guide to ubiquitylation. *Cellular and molecular life sciences : CMLS* 61**,** 1546-1561.

Fei, E., Jia, N., Zhang, T., Ma, X., Wang, H., Liu, C., Zhang, W., Ding, L., Nukina, N., Wang, G., 2007. Phosphorylation of ataxin-3 by glycogen synthase kinase 3beta at serine 256 regulates the aggregation of ataxin-3. *Biochem Biophys Res Commun* 357**,** 487-492.

Ferrigno, P., Silver, P.A., 2000. Polyglutamine expansions: proteolysis, chaperones, and the dangers of promiscuity. *Neuron* 26**,** 9-12.

Ferro, A., Carvalho, A.L., Teixeira-Castro, A., Almeida, C., Tome, R.J., Cortes, L., Rodrigues, A.J., Logarinho, E., Sequeiros, J., Macedo-Ribeiro, S., Maciel, P., 2007. NEDD8: a new ataxin-3 interactor. *Biochim Biophys Acta* 1773**,** 1619-1627.

Fienberg, A.A., Hiroi, N., Mermelstein, P.G., Song, W., Snyder, G.L., Nishi, A., Cheramy, A., O'Callaghan, J.P., Miller, D.B., Cole, D.G., Corbett, R., Haile, C.N., Cooper, D.C., Onn, S.P., Grace, A.A., Ouimet, C.C., White, F.J., Hyman, S.E., Surmeier, D.J., Girault, J., Nestler, E.J., Greengard, P., 1998. DARPP-32: regulator of the efficacy of dopaminergic neurotransmission. *Science* 281**,** 838-842.

Figiel, M., Switonski, P.M., Krzyzosiak, W.J. (2014) Humanized ataxin-3 knock-in mouse recapitulates the genetic features and SCA3/MJD pathogenesis of neurons and glia. In: *9th FENS Forum of Neuroscience*: Milan, Italy.

Fiumara, F., Fioriti, L., Kandel, E.R., Hendrickson, W.A., 2010. Essential role of coiled coils for aggregation and activity of Q/N-rich prions and PolyQ proteins. *Cell* 143**,** 1121-1135.

Fujigasaki, H., Uchihara, T., Koyano, S., Iwabuchi, K., Yagishita, S., Makifuchi, T., Nakamura, A., Ishida, K., Toru, S., Hirai, S., Ishikawa, K., Tanabe, T., Mizusawa, H., 2000. Ataxin-3 is translocated into the nucleus for the formation of intranuclear inclusions in normal and Machado-Joseph disease brains. *Exp Neurol* 165**,** 248-256.

Fujigasaki, H., Uchihara, T., Takahashi, J., Matsushita, H., Nakamura, A., Koyano, S., Iwabuchi, K., Hirai, S., Mizusawa, H., 2001. Preferential recruitment of ataxin-3 independent of expanded polyglutamine: an immunohistochemical study on Marinesco bodies. *J Neurol Neurosurg Psychiatry* 71**,** 518-520.

Funderburk, S.F., Shatkina, L., Mink, S., Weis, Q., Weg-Remers, S., Cato, A.C., 2009. Specific N-terminal mutations in the human androgen receptor induce cytotoxicity. *Neurobiology of aging* 30**,** 1851-1864.

Gafni, J., Hermel, E., Young, J.E., Wellington, C.L., Hayden, M.R., Ellerby, L.M., 2004. Inhibition of calpain cleavage of huntingtin reduces toxicity: accumulation of calpain/caspase fragments in the nucleus. *J Biol Chem* 279**,** 20211-20220.

Gales, L., Cortes, L., Almeida, C., Melo, C.V., Costa, M.C., Maciel, P., Clarke, D.T., Damas, A.M., Macedo-Ribeiro, S., 2005. Towards a structural understanding of the fibrillization pathway in Machado-Joseph's disease: trapping early oligomers of non-expanded ataxin-3. *J Mol Biol* 353**,** 642-654.

Gaspar, C., Lopes-Cendes, I., Hayes, S., Goto, J., Arvidsson, K., Dias, A., Silveira, I., Maciel, P., Coutinho, P., Lima, M., Zhou, Y.X., Soong, B.W., Watanabe, M., Giunti, P., Stevanin, G., Riess, O., Sasaki, H., Hsieh, M., Nicholson, G.A., Brunt, E., Higgins, J.J., Lauritzen, M., Tranebjaerg, L., Volpini, V., Wood, N., Ranum, L., Tsuji, S., Brice, A., Sequeiros, J., Rouleau, G.A., 2001. Ancestral origins of the Machado-Joseph disease mutation: a worldwide haplotype study. *Am J Hum Genet* 68**,** 523-528.

Gatchel, J.R., Zoghbi, H.Y., 2005. Diseases of unstable repeat expansion: mechanisms and common principles. *Nat Rev Genet* 6**,** 743-755.

Gioeli, D., Black, B.E., Gordon, V., Spencer, A., Kesler, C.T., Eblen, S.T., Paschal, B.M., Weber, M.J., 2006. Stress kinase signaling regulates androgen receptor phosphorylation, transcription, and localization. *Molecular endocrinology* 20**,** 503-515.

Goellner, G.M., Rechsteiner, M., 2003. Are Huntington's and polyglutamine-based ataxias proteasome storage diseases? *Int J Biochem Cell Biol* 35**,** 562-571.

Gomes, A.R., Cunha, P., Nuriya, M., Faro, C.J., Huganir, R.L., Pires, E.V., Carvalho, A.L., Duarte, C.B., 2004. Metabotropic glutamate and dopamine receptors co-regulate AMPA receptor activity through PKA in cultured chick retinal neurones: effect on GluR4 phosphorylation and surface expression. *J Neurochem* 90**,** 673-682.

Goti, D., Katzen, S.M., Mez, J., Kurtis, N., Kiluk, J., Ben-Haiem, L., Jenkins, N.A., Copeland, N.G., Kakizuka, A., Sharp, A.H., Ross, C.A., Mouton, P.R., Colomer, V., 2004. A mutant ataxin-3 putative-cleavage fragment in brains of Machado-Joseph disease patients and transgenic mice is cytotoxic above a critical concentration. *J Neurosci* 24**,** 10266-10279.

Goto, J., Watanabe, M., Ichikawa, Y., Yee, S.B., Ihara, N., Endo, K., Igarashi, S., Takiyama, Y., Gaspar, C., Maciel, P., Tsuji, S., Rouleau, G.A., Kanazawa, I., 1997. Machado-Joseph disease gene products carrying different carboxyl termini. *Neurosci Res* 28**,** 373-377.

Gu, X., Greiner, E.R., Mishra, R., Kodali, R., Osmand, A., Finkbeiner, S., Steffan, J.S., Thompson, L.M., Wetzel, R., Yang, X.W., 2009. Serines 13 and 16 are critical determinants of full-length human mutant huntingtin induced disease pathogenesis in HD mice. *Neuron* 64**,** 828-840.

Gunawardena, S., Her, L.S., Brusch, R.G., Laymon, R.A., Niesman, I.R., Gordesky-Gold, B., Sintasath, L., Bonini, N.M., Goldstein, L.S., 2003. Disruption of axonal transport by loss of huntingtin or expression of pathogenic polyQ proteins in Drosophila. *Neuron* 40**,** 25-40.

Guo, Z., Dai, B., Jiang, T., Xu, K., Xie, Y., Kim, O., Nesheiwat, I., Kong, X., Melamed, J., Handratta, V.D., Njar, V.C., Brodie, A.M., Yu, L.R., Veenstra, T.D., Chen, H., Qiu, Y., 2006.

Regulation of androgen receptor activity by tyrosine phosphorylation. *Cancer cell* 10**,** 309-319.

Haacke, A., Broadley, S.A., Boteva, R., Tzvetkov, N., Hartl, F.U., Breuer, P., 2006. Proteolytic cleavage of polyglutamine-expanded ataxin-3 is critical for aggregation and sequestration of non-expanded ataxin-3. *Hum Mol Genet* 15**,** 555-568.

Haacke, A., Hartl, F.U., Breuer, P., 2007. Calpain inhibition is sufficient to suppress aggregation of polyglutamine-expanded ataxin-3. *J Biol Chem* 282**,** 18851-18856.

Hamilton, A.M., Zito, K., 2013. Breaking it down: the ubiquitin proteasome system in neuronal morphogenesis. *Neural plasticity* 2013**,** 196848.

Hands, S., Sinadinos, C., Wyttenbach, A., 2008. Polyglutamine gene function and dysfunction in the ageing brain. *Biochim Biophys Acta* 1779**,** 507-521.

Harris, G.M., Dodelzon, K., Gong, L., Gonzalez-Alegre, P., Paulson, H.L., 2010. Splice isoforms of the polyglutamine disease protein ataxin-3 exhibit similar enzymatic yet different aggregation properties. *PLoS One* 5**,** e13695.

Havel, L.S., Wang, C.E., Wade, B., Huang, B., Li, S., Li, X.J., 2011. Preferential accumulation of N-terminal mutant huntingtin in the nuclei of striatal neurons is regulated by phosphorylation. *Hum Mol Genet* 20**,** 1424-1437.

Hayashi, M., Kobayashi, K., Furuta, H., 2003. Immunohistochemical study of neuronal intranuclear and cytoplasmic inclusions in Machado-Joseph disease. *Psychiatry and clinical neurosciences* 57**,** 205-213.

Hegde, A.N., Inokuchi, K., Pei, W., Casadio, A., Ghirardi, M., Chain, D.G., Martin, K.C., Kandel, E.R., Schwartz, J.H., 1997. Ubiquitin C-terminal hydrolase is an immediate-early gene essential for long-term facilitation in Aplysia. *Cell* 89**,** 115-126.

Heir, R., Ablasou, C., Dumontier, E., Elliott, M., Fagotto-Kaufmann, C., Bedford, F.K., 2006. The UBL domain of PLIC-1 regulates aggresome formation. *EMBO reports* 7**,** 1252-1258.

Higashiyama, H., Hirose, F., Yamaguchi, M., Inoue, Y.H., Fujikake, N., Matsukage, A., Kakizuka, A., 2002. Identification of ter94, Drosophila VCP, as a modulator of polyglutamine-induced neurodegeneration. *Cell Death Differ* 9**,** 264-273.

Hirabayashi, M., Inoue, K., Tanaka, K., Nakadate, K., Ohsawa, Y., Kamei, Y., Popiel, A.H., Sinohara, A., Iwamatsu, A., Kimura, Y., Uchiyama, Y., Hori, S., Kakizuka, A., 2001. VCP/p97 in abnormal protein aggregates, cytoplasmic vacuoles, and cell death, phenotypes relevant to neurodegeneration. *Cell Death Differ* 8**,** 977-984.

Hirsch, C., Gauss, R., Horn, S.C., Neuber, O., Sommer, T., 2009. The ubiquitylation machinery of the endoplasmic reticulum. *Nature* 458**,** 453-460.

Huang, O.W., Ma, X., Yin, J., Flinders, J., Maurer, T., Kayagaki, N., Phung, Q., Bosanac, I., Arnott, D., Dixit, V.M., Hymowitz, S.G., Starovasnik, M.A., Cochran, A.G., 2012. Phosphorylation-dependent activity of the deubiquitinase DUBA. *Nat Struct Mol Biol* 19**,** 171-175.

Hübener, J., Riess, O., 2010. Polyglutamine-induced neurodegeneration in SCA3 is not mitigated by non-expanded ataxin-3: conclusions from double-transgenic mouse models. *Neurobiol Dis* 38**,** 116-124.

Hübener, J., Vauti, F., Funke, C., Wolburg, H., Ye, Y., Schmidt, T., Wolburg-Buchholz, K., Schmitt, I., Gardyan, A., Driessen, S., Arnold, H.H., Nguyen, H.P., Riess, O., 2011. N-terminal ataxin-3 causes neurological symptoms with inclusions, endoplasmic reticulum stress and ribosomal dislocation. *Brain* 134**,** 1925-1942.

Hübener, J., Weber, J.J., Richter, C., Honold, L., Weiss, A., Murad, F., Breuer, P., Wullner, U., Bellstedt, P., Paquet-Durand, F., Takano, J., Saido, T.C., Riess, O., Nguyen, H.P., 2013. Calpain-mediated ataxin-3 cleavage in the molecular pathogenesis of spinocerebellar ataxia type 3 (SCA3). *Hum Mol Genet* 22**,** 508-518.

Humbert, S., Bryson, E.A., Cordelieres, F.P., Connors, N.C., Datta, S.R., Finkbeiner, S., Greenberg, M.E., Saudou, F., 2002. The IGF-1/Akt pathway is neuroprotective in Huntington's disease and involves Huntingtin phosphorylation by Akt. *Developmental cell* 2**,** 831-837.

Hunt, C.A., Schenker, L.J., Kennedy, M.B., 1996. PSD-95 is associated with the postsynaptic density and not with the presynaptic membrane at forebrain synapses. *J Neurosci* 16**,** 1380-1388.

Hunter, T., 2007. The age of crosstalk: phosphorylation, ubiquitination, and beyond. *Mol Cell* 28**,** 730-738.

Hunter, T., 2012. Why nature chose phosphate to modify proteins. *Philos Trans R Soc Lond B Biol Sci* 367**,** 2513-2516.

Huntley, M.A., Golding, G.B., 2004. Neurological proteins are not enriched for repetitive sequences. *Genetics* 166**,** 1141-1154.

Hutti, J.E., Turk, B.E., Asara, J.M., Ma, A., Cantley, L.C., Abbott, D.W., 2007. IkappaB kinase beta phosphorylates the K63 deubiquitinase A20 to cause feedback inhibition of the NF-kappaB pathway. *Mol Cell Biol* 27**,** 7451-7461.

Ichikawa, Y., Goto, J., Hattori, M., Toyoda, A., Ishii, K., Jeong, S.Y., Hashida, H., Masuda, N., Ogata, K., Kasai, F., Hirai, M., Maciel, P., Rouleau, G.A., Sakaki, Y., Kanazawa, I., 2001. The genomic structure and expression of MJD, the Machado-Joseph disease gene. *J Hum Genet* 46**,** 413-422.

Ikeda, F., Dikic, I., 2008. Atypical ubiquitin chains: new molecular signals. 'Protein Modifications: Beyond the Usual Suspects' review series. *EMBO reports* 9**,** 536-542.

Ikeda, H., Yamaguchi, M., Sugai, S., Aze, Y., Narumiya, S., Kakizuka, A., 1996. Expanded polyglutamine in the Machado-Joseph disease protein induces cell death in vitro and in vivo. *Nat Genet* 13**,** 196-202.

Ishikawa, A., Yamada, M., Makino, K., Aida, I., Idezuka, J., Ikeuchi, T., Soma, Y., Takahashi, H., Tsuji, S., 2002. Dementia and delirium in 4 patients with Machado-Joseph disease. *Arch Neurol* 59**,** 1804-1808.

Ito, Y., Tanaka, F., Yamamoto, M., Doyu, M., Nagamatsu, M., Riku, S., Mitsuma, T., Sobue, G., 1998. Somatic mosaicism of the expanded CAG trinucleotide repeat in mRNAs for the responsible gene of Machado-Joseph disease (MJD), dentatorubral-pallidoluysian atrophy (DRPLA), and spinal and bulbar muscular atrophy (SBMA). *Neurochem Res* 23**,** 25-32.

Jana, N.R., Dikshit, P., Goswami, A., Kotliarova, S., Murata, S., Tanaka, K., Nukina, N., 2005. Co-chaperone CHIP associates with expanded polyglutamine protein and promotes their degradation by proteasomes. *J Biol Chem* 280**,** 11635-11640.

Jana, N.R., Nukina, N., 2004. Misfolding promotes the ubiquitination of polyglutamine-expanded ataxin-3, the defective gene product in SCA3/MJD. *Neurotox Res* 6**,** 523-533.

Jellinger, K.A., 2009. Recent advances in our understanding of neurodegeneration. *Journal of neural transmission* 116**,** 1111-1162.

Jennekens, F.G., 2014. A short history of the notion of neurodegenerative disease. *J Hist Neurosci* 23**,** 85-94.

Jeub, M., Herbst, M., Spauschus, A., Fleischer, H., Klockgether, T., Wuellner, U., Evert, B.O., 2006. Potassium channel dysfunction and depolarized resting membrane potential in a cell model of SCA3. *Exp Neurol* 201**,** 182-192.

Jiang, M., Deng, L., Chen, G., 2004. High Ca(2+)-phosphate transfection efficiency enables single neuron gene analysis. *Gene therapy* 11**,** 1303-1311.

Jung, J., Xu, K., Lessing, D., Bonini, N.M., 2009. Preventing Ataxin-3 protein cleavage mitigates degeneration in a Drosophila model of SCA3. *Hum Mol Genet* 18**,** 4843-4852.

Kawaguchi, Y., Okamoto, T., Taniwaki, M., Aizawa, M., Inoue, M., Katayama, S., Kawakami, H., Nakamura, S., Nishimura, M., Akiguchi, I., et al., 1994. CAG expansions in a novel gene for Machado-Joseph disease at chromosome 14q32.1. *Nat Genet* 8**,** 221-228.

Kayed, R., Head, E., Thompson, J.L., McIntire, T.M., Milton, S.C., Cotman, C.W., Glabe, C.G., 2003. Common structure of soluble amyloid oligomers implies common mechanism of pathogenesis. *Science* 300**,** 486-489.

Kayed, R., Sokolov, Y., Edmonds, B., McIntire, T.M., Milton, S.C., Hall, J.E., Glabe, C.G., 2004. Permeabilization of lipid bilayers is a common conformation-dependent activity of soluble amyloid oligomers in protein misfolding diseases. *J Biol Chem* 279**,** 46363-46366.

Kazachkova, N., Raposo, M., Montiel, R., Cymbron, T., Bettencourt, C., Silva-Fernandes, A., Silva, S., Maciel, P., Lima, M., 2013. Patterns of mitochondrial DNA damage in blood and brain tissues of a transgenic mouse model of Machado-Joseph disease. *Neuro-degenerative diseases* 11**,** 206-214.

Kessler, B.M., Edelmann, M.J., 2011. PTMs in conversation: activity and function of deubiquitinating enzymes regulated via post-translational modifications. *Cell biochemistry and biophysics* 60**,** 21-38.

Khoshnan, A., Ko, J., Tescu, S., Brundin, P., Patterson, P.H., 2009. IKKalpha and IKKbeta regulation of DNA damage-induced cleavage of huntingtin. *PLoS One* 4**,** e5768.

Kieling, C., Prestes, P.R., Saraiva-Pereira, M.L., Jardim, L.B., 2007. Survival estimates for patients with Machado-Joseph disease (SCA3). *Clinical genetics* 72**,** 543-545.

Kim, E., Sheng, M., 2004. PDZ domain proteins of synapses. *Nat Rev Neurosci* 5**,** 771-781.

Kim, M.S., Kim, Y.K., Kim, Y.S., Seong, M., Choi, J.K., Baek, K.H., 2005. Deubiquitinating enzyme USP36 contains the PEST motif and is polyubiquitinated. *Biochem Biophys Res Commun* 330**,** 797-804.

Kim, M.W., Chelliah, Y., Kim, S.W., Otwinowski, Z., Bezprozvanny, I., 2009. Secondary structure of Huntingtin amino-terminal region. *Structure* 17**,** 1205-1212.

Kirkwood, T.B., 2008. A systematic look at an old problem. *Nature* 451**,** 644-647.

Koch, P., Breuer, P., Peitz, M., Jungverdorben, J., Kesavan, J., Poppe, D., Doerr, J., Ladewig, J., Mertens, J., Tuting, T., Hoffmann, P., Klockgether, T., Evert, B.O., Wullner, U., Brustle, O., 2011. Excitation-induced ataxin-3 aggregation in neurons from patients with Machado-Joseph disease. *Nature* 480**,** 543-546.

Komander, D., Clague, M.J., Urbe, S., 2009. Breaking the chains: structure and function of the deubiquitinases. *Nat Rev Mol Cell Biol* 10**,** 550-563.

Konno, A., Shuvaev, A.N., Miyake, N., Miyake, K., Iizuka, A., Matsuura, S., Huda, F., Nakamura, K., Yanagi, S., Shimada, T., Hirai, H., 2014. Mutant ataxin-3 with an abnormally expanded polyglutamine chain disrupts dendritic development and metabotropic glutamate receptor signaling in mouse cerebellar Purkinje cells. *Cerebellum* 13**,** 29-41.

Kopito, R.R., 2000. Aggresomes, inclusion bodies and protein aggregation. *Trends in cell biology* 10**,** 524-530.

Kowalski, J.R., Juo, P., 2012. The role of deubiquitinating enzymes in synaptic function and nervous system diseases. *Neural plasticity* 2012**,** 892749.

Kuhlbrodt, K., Janiesch, P.C., Kevei, E., Segref, A., Barikbin, R., Hoppe, T., 2011. The Machado-Joseph disease deubiquitylase ATX-3 couples longevity and proteostasis. *Nat Cell Biol* 13**,** 273-281.

La Spada, A.R., Taylor, J.P., 2003. Polyglutamines placed into context. *Neuron* 38**,** 681-684.

La Spada, A.R., Taylor, J.P., 2010. Repeat expansion disease: progress and puzzles in disease pathogenesis. *Nat Rev Genet* 11**,** 247-258.

Laço, M.N., Cortes, L., Travis, S.M., Paulson, H.L., Rego, A.C., 2012a. Valosin-containing protein (VCP/p97) is an activator of wild-type ataxin-3. *PLoS One* 7**,** e43563.

Laço, M.N., Oliveira, C.R., Paulson, H.L., Rego, A.C., 2012b. Compromised mitochondrial complex II in models of Machado-Joseph disease. *Biochim Biophys Acta* 1822**,** 139-149.

LaFevre-Bernt, M.A., Ellerby, L.M., 2003. Kennedy's disease. Phosphorylation of the polyglutamine-expanded form of androgen receptor regulates its cleavage by caspase-3 and enhances cell death. *J Biol Chem* 278**,** 34918-34924.

Lang, A.E., Rogaeva, E.A., Tsuda, T., Hutterer, J., St George-Hyslop, P., 1994. Homozygous inheritance of the Machado-Joseph disease gene. *Ann Neurol* 36**,** 443-447.

Lappe-Siefke, C., Loebrich, S., Hevers, W., Waidmann, O.B., Schweizer, M., Fehr, S., Fritschy, J.M., Dikic, I., Eilers, J., Wilson, S.M., Kneussel, M., 2009. The ataxia (axJ) mutation causes abnormal GABAA receptor turnover in mice. *PLoS genetics* 5**,** e1000631.

Lee, M.Y., Ajjappala, B.S., Kim, M.S., Oh, Y.K., Baek, K.H., 2008. DUB-1, a fate determinant of dynein heavy chain in B-lymphocytes, is regulated by the ubiquitin-proteasome pathway. *Journal of cellular biochemistry* 105**,** 1420-1429.

Lee, S.B., Bagley, J.A., Lee, H.Y., Jan, L.Y., Jan, Y.N., 2011. Pathogenic polyglutamine proteins cause dendrite defects associated with specific actin cytoskeletal alterations in Drosophila. *Proc Natl Acad Sci U S A* 108**,** 16795-16800.

Lerer, I., Merims, D., Abeliovich, D., Zlotogora, J., Gadoth, N., 1996. Machado-Joseph disease: correlation between the clinical features, the CAG repeat length and homozygosity for the mutation. *European journal of human genetics : EJHG* 4**,** 3-7.

Leroy, E., Boyer, R., Auburger, G., Leube, B., Ulm, G., Mezey, E., Harta, G., Brownstein, M.J., Jonnalagada, S., Chernova, T., Dehejia, A., Lavedan, C., Gasser, T., Steinbach, P.J., Wilkinson, K.D., Polymeropoulos, M.H., 1998. The ubiquitin pathway in Parkinson's disease. *Nature* 395**,** 451-452.

Li, F., Macfarlan, T., Pittman, R.N., Chakravarti, D., 2002. Ataxin-3 is a histone-binding protein with two independent transcriptional corepressor activities. *J Biol Chem* 277**,** 45004-45012.

Li, L.B., Yu, Z., Teng, X., Bonini, N.M., 2008. RNA toxicity is a component of ataxin-3 degeneration in Drosophila. *Nature* 453**,** 1107-1111.

Li, W., Tu, D., Brunger, A.T., Ye, Y., 2007. A ubiquitin ligase transfers preformed polyubiquitin chains from a conjugating enzyme to a substrate. *Nature* 446**,** 333-337.

Li, X., Moore, D.J., Xiong, Y., Dawson, T.M., Dawson, V.L., 2010. Reevaluation of phosphorylation sites in the Parkinson disease-associated leucine-rich repeat kinase 2. *J Biol Chem* 285**,** 29569-29576.

Lim, J., Hao, T., Shaw, C., Patel, A.J., Szabo, G., Rual, J.F., Fisk, C.J., Li, N., Smolyar, A., Hill, D.E., Barabasi, A.L., Vidal, M., Zoghbi, H.Y., 2006. A protein-protein interaction network for human inherited ataxias and disorders of Purkinje cell degeneration. *Cell* 125**,** 801-814.

Lobo, A.C., Gomes, J.R., Catarino, T., Mele, M., Fernandez, P., Inacio, A.R., Bahr, B.A., Santos, A.E., Wieloch, T., Carvalho, A.L., Duarte, C.B., 2011. Cleavage of the vesicular glutamate transporters under excitotoxic conditions. *Neurobiol Dis* 44**,** 292-303.

Lopes-Cendes, I., Maciel, P., Kish, S., Gaspar, C., Robitaille, Y., Clark, H.B., Koeppen, A.H., Nance, M., Schut, L., Silveira, I., Coutinho, P., Sequeiros, J., Rouleau, G.A., 1996. Somatic mosaicism in the central nervous system in spinocerebellar ataxia type 1 and Machado-Joseph disease. *Ann Neurol* 40**,** 199-206.

Lopes, T.M., D'Abreu, A., Franca, M.C., Jr., Yasuda, C.L., Betting, L.E., Samara, A.B., Castellano, G., Somazz, J.C., Balthazar, M.L., Lopes-Cendes, I., Cendes, F., 2013. Widespread

neuronal damage and cognitive dysfunction in spinocerebellar ataxia type 3. *Journal of neurology* 260**,** 2370-2379.

Louros, S.R., Hooks, B.M., Litvina, L., Carvalho, A.L., Chen, C., 2014. A role for stargazin in experience-dependent plasticity. *Cell reports* 7**,** 1614-1625.

Love, K.R., Catic, A., Schlieker, C., Ploegh, H.L., 2007. Mechanisms, biology and inhibitors of deubiquitinating enzymes. *Nature chemical biology* 3**,** 697-705.

Luo, S., Vacher, C., Davies, J.E., Rubinsztein, D.C., 2005. Cdk5 phosphorylation of huntingtin reduces its cleavage by caspases: implications for mutant huntingtin toxicity. *J Cell Biol* 169**,** 647-656.

Macedo-Ribeiro, S., Cortes, L., Maciel, P., Carvalho, A.L., 2009. Nucleocytoplasmic shuttling activity of ataxin-3. *PLoS One* 4**,** e5834.

Macek, B., Mann, M., Olsen, J.V., 2009. Global and site-specific quantitative phosphoproteomics: principles and applications. *Annual review of pharmacology and toxicology* 49**,** 199-221.

Maciel, P., Costa, M.C., Ferro, A., Rousseau, M., Santos, C.S., Gaspar, C., Barros, J., Rouleau, G.A., Coutinho, P., Sequeiros, J., 2001. Improvement in the molecular diagnosis of Machado-Joseph disease. *Arch Neurol* 58**,** 1821-1827.

Maciel, P., Gaspar, C., DeStefano, A.L., Silveira, I., Coutinho, P., Radvany, J., Dawson, D.M., Sudarsky, L., Guimaraes, J., Loureiro, J.E., et al., 1995. Correlation between CAG repeat length and clinical features in Machado-Joseph disease. *Am J Hum Genet* 57**,** 54-61.

Mao, Y., Senic-Matuglia, F., Di Fiore, P.P., Polo, S., Hodsdon, M.E., De Camilli, P., 2005. Deubiquitinating function of ataxin-3: insights from the solution structure of the Josephin domain. *Proc Natl Acad Sci U S A* 102**,** 12700-12705.

Marfany, G., Denuc, A., 2008. To ubiquitinate or to deubiquitinate: it all depends on the partners. *Biochemical Society transactions* 36**,** 833-838.

Markossian, K.A., Kurganov, B.I., 2004. Protein folding, misfolding, and aggregation. Formation of inclusion bodies and aggresomes. *Biochemistry (Mosc)* 69**,** 971-984.

Martin, K.H., Jeffery, E.D., Grigera, P.R., Shabanowitz, J., Hunt, D.F., Parsons, J.T., 2006. Cortactin phosphorylation sites mapped by mass spectrometry. *Journal of cell science* 119**,** 2851-2853.

Martins, S., Calafell, F., Gaspar, C., Wong, V.C., Silveira, I., Nicholson, G.A., Brunt, E.R., Tranebjaerg, L., Stevanin, G., Hsieh, M., Soong, B.W., Loureiro, L., Durr, A., Tsuji, S., Watanabe, M., Jardim, L.B., Giunti, P., Riess, O., Ranum, L.P., Brice, A., Rouleau, G.A., Coutinho, P., Amorim, A., Sequeiros, J., 2007. Asian origin for the worldwide-spread mutational event in Machado-Joseph disease. *Arch Neurol* 64**,** 1502-1508.

Martins, S., Soong, B.W., Wong, V.C., Giunti, P., Stevanin, G., Ranum, L.P., Sasaki, H., Riess, O., Tsuji, S., Coutinho, P., Amorim, A., Sequeiros, J., Nicholson, G.A., 2012. Mutational origin of Machado-Joseph disease in the Australian Aboriginal communities of Groote Eylandt and Yirrkala. *Arch Neurol* 69**,** 746-751.

Maruyama, H., Nakamura, S., Matsuyama, Z., Sakai, T., Doyu, M., Sobue, G., Seto, M., Tsujihata, M., Oh-i, T., Nishio, T., et al., 1995. Molecular features of the CAG repeats and clinical manifestation of Machado-Joseph disease. *Hum Mol Genet* 4**,** 807-812.

Masino, L., Musi, V., Menon, R.P., Fusi, P., Kelly, G., Frenkiel, T.A., Trottier, Y., Pastore, A., 2003. Domain architecture of the polyglutamine protein ataxin-3: a globular domain followed by a flexible tail. *FEBS Lett* 549**,** 21-25.

Masino, L., Nicastro, G., Calder, L., Vendruscolo, M., A., P., 2011. Functional interactions as a survival strategy against abnormal aggregation. *FASEB J* 25**,** 45-54.

Masino, L., Nicastro, G., Menon, R.P., Dal Piaz, F., Calder, L., Pastore, A., 2004. Characterization of the structure and the amyloidogenic properties of the Josephin domain of the polyglutamine-containing protein ataxin-3. *J Mol Biol* 344**,** 1021-1035.

Matos, C.A. (2009) Post-Translational Modifications of Ataxin-3, the Protein Involved in Machado-Joseph Disease: Evidences for Phosphorylation and Sumoylation. In: *Departamento de Zoologia, Faculdade de Ciências e Tecnologia*. Universidade de Coimbra: Coimbra.

Matos, C.A., de Macedo-Ribeiro, S., Carvalho, A.L., 2011. Polyglutamine diseases: the special case of ataxin-3 and Machado-Joseph disease. *Prog Neurobiol* 95**,** 26-48.

Matsumoto, M., Yada, M., Hatakeyama, S., Ishimoto, H., Tanimura, T., Tsuji, S., Kakizuka, A., Kitagawa, M., Nakayama, K.I., 2004. Molecular clearance of ataxin-3 is regulated by a mammalian E4. *EMBO J* 23**,** 659-669.

Mauri, P.L., Riva, M., Ambu, D., De Palma, A., Secundo, F., Benazzi, L., Valtorta, M., Tortora, P., Fusi, P., 2006. Ataxin-3 is subject to autolytic cleavage. *FEBS J* 273**,** 4277-4286.

Mayer, U., 2003. Integrins: redundant or important players in skeletal muscle? *J Biol Chem* 278**,** 14587-14590.

Mazzucchelli, S., De Palma, A., Riva, M., D'Urzo, A., Pozzi, C., Pastori, V., Comelli, F., Fusi, P., Vanoni, M., Tortora, P., Mauri, P., Regonesi, M.E., 2009. Proteomic and biochemical analyses unveil tight interaction of ataxin-3 with tubulin. *Int J Biochem Cell Biol* 41**,** 2485-2492.

McCampbell, A., Taylor, J.P., Taye, A.A., Robitschek, J., Li, M., Walcott, J., Merry, D., Chai, Y., Paulson, H., Sobue, G., Fischbeck, K.H., 2000. CREB-binding protein sequestration by expanded polyglutamine. *Hum Mol Genet* 9**,** 2197-2202.

Meray, R.K., Lansbury, P.T., Jr., 2007. Reversible monoubiquitination regulates the Parkinson disease-associated ubiquitin hydrolase UCH-L1. *J Biol Chem* 282**,** 10567-10575.

Metzler, M., Gan, L., Mazarei, G., Graham, R.K., Liu, L., Bissada, N., Lu, G., Leavitt, B.R., Hayden, M.R., 2010. Phosphorylation of huntingtin at Ser421 in YAC128 neurons is associated with protection of YAC128 neurons from NMDA-mediated excitotoxicity and is modulated by PP1 and PP2A. *J Neurosci* 30**,** 14318-14329.

Meulmeester, E., Kunze, M., Hsiao, H.H., Urlaub, H., Melchior, F., 2008. Mechanism and consequences for paralog-specific sumoylation of ubiquitin-specific protease 25. *Mol Cell* 30**,** 610-619.

Meusser, B., Hirsch, C., Jarosch, E., Sommer, T., 2005. ERAD: the long road to destruction. *Nat Cell Biol* 7**,** 766-772.

Miller, S.L., Malotky, E., O'Bryan, J.P., 2004. Analysis of the role of ubiquitin-interacting motifs in ubiquitin binding and ubiquitylation. *J Biol Chem* 279**,** 33528-33537.

Miller, V.M., Nelson, R.F., Gouvion, C.M., Williams, A., Rodriguez-Lebron, E., Harper, S.Q., Davidson, B.L., Rebagliati, M.R., Paulson, H.L., 2005. CHIP suppresses polyglutamine aggregation and toxicity in vitro and in vivo. *J Neurosci* 25**,** 9152-9161.

Mishra, R., Hoop, C.L., Kodali, R., Sahoo, B., van der Wel, P.C., Wetzel, R., 2012. Serine phosphorylation suppresses huntingtin amyloid accumulation by altering protein aggregation properties. *J Mol Biol* 424**,** 1-14.

Mizuno, E., Kitamura, N., Komada, M., 2007. 14-3-3-dependent inhibition of the deubiquitinating activity of UBPY and its cancellation in the M phase. *Experimental cell research* 313**,** 3624-3634.

Mori, F., Nishie, M., Piao, Y.S., Kito, K., Kamitani, T., Takahashi, H., Wakabayashi, K., 2005. Accumulation of NEDD8 in neuronal and glial inclusions of neurodegenerative disorders. *Neuropathol Appl Neurobiol* 31**,** 53-61.

Muchowski, P.J., Schaffar, G., Sittler, A., Wanker, E.E., Hayer-Hartl, M.K., Hartl, F.U., 2000. Hsp70 and hsp40 chaperones can inhibit self-assembly of polyglutamine proteins into amyloid-like fibrils. *Proc Natl Acad Sci U S A* 97**,** 7841-7846.

Muchowski, P.J., Wacker, J.L., 2005. Modulation of neurodegeneration by molecular chaperones. *Nat Rev Neurosci* 6**,** 11-22.

Mueller, T., Breuer, P., Schmitt, I., Walter, J., Evert, B.O., Wullner, U., 2009. CK2-dependent phosphorylation determines cellular localization and stability of ataxin-3. *Hum Mol Genet* 18**,** 3334-3343.

Mukhopadhyay, D., Riezman, H., 2007. Proteasome-independent functions of ubiquitin in endocytosis and signaling. *Science* 315**,** 201-205.

Murata, Y., Yamaguchi, S., Kawakami, H., Imon, Y., Maruyama, H., Sakai, T., Kazuta, T., Ohtake, T., Nishimura, M., Saida, T., Chiba, S., Oh-i, T., Nakamura, S., 1998. Characteristic magnetic resonance imaging findings in Machado-Joseph disease. *Arch Neurol* 55**,** 33-37.

Nagai, Y., Inui, T., Popiel, H.A., Fujikake, N., Hasegawa, K., Urade, Y., Goto, Y., Naiki, H., Toda, T., 2007. A toxic monomeric conformer of the polyglutamine protein. *Nat Struct Mol Biol* 14**,** 332-340.

Nakano, K.K., Dawson, D.M., Spence, A., 1972. Machado disease. A hereditary ataxia in Portuguese emigrants to Massachusetts. *Neurology* 22**,** 49-55.

Nascimento-Ferreira, I., Santos-Ferreira, T., Sousa-Ferreira, L., Auregan, G., Onofre, I., Alves, S., Dufour, N., Colomer Gould, V.F., Koeppen, A., Deglon, N., Pereira de Almeida, L., 2011. Overexpression of the autophagic beclin-1 protein clears mutant ataxin-3 and alleviates Machado-Joseph disease. *Brain* 134**,** 1400-1415.

Nguyen, L.K., Dobrzynski, M., Fey, D., Kholodenko, B.N., 2014. Polyubiquitin chain assembly and organization determine the dynamics of protein activation and degradation. *Frontiers in physiology* 5**,** 4.

Nicastro, G., Masino, L., Esposito, V., Menon, R.P., De Simone, A., Fraternali, F., Pastore, A., 2009. Josephin domain of ataxin-3 contains two distinct ubiquitin-binding sites. *Biopolymers* 91**,** 1203-1214.

Nicastro, G., Menon, R.P., Masino, L., Knowles, P.P., McDonald, N.Q., Pastore, A., 2005. The solution structure of the Josephin domain of ataxin-3: structural determinants for molecular recognition. *Proc Natl Acad Sci U S A* 102**,** 10493-10498.

Nicastro, G., Todi, S.V., Karaca, E., Bonvin, A.M., Paulson, H.L., Pastore, A., 2010. Understanding the role of the Josephin domain in the PolyUb binding and cleavage properties of ataxin-3. *PLoS One* 5**,** e12430.

Nijman, S.M., Luna-Vargas, M.P., Velds, A., Brummelkamp, T.R., Dirac, A.M., Sixma, T.K., Bernards, R., 2005. A genomic and functional inventory of deubiquitinating enzymes. *Cell* 123**,** 773-786.

Nishiyama, K., Murayama, S., Goto, J., Watanabe, M., Hashida, H., Katayama, S., Nomura, Y., Nakamura, S., Kanazawa, I., 1996. Regional and cellular expression of the Machado-Joseph disease gene in brains of normal and affected individuals. *Ann Neurol* 40**,** 776-781.

Nóbrega, C., Nascimento-Ferreira, I., Onofre, I., Albuquerque, D., Conceicao, M., Deglon, N., de Almeida, L.P., 2013. Overexpression of mutant ataxin-3 in mouse cerebellum induces ataxia and cerebellar neuropathology. *Cerebellum* 12**,** 441-455.

Okamura-Oho, Y., Miyashita, T., Nagao, K., Shima, S., Ogata, Y., Katada, T., Nishina, H., Yamada, M., 2003. Dentatorubral-pallidoluysian atrophy protein is phosphorylated by c-Jun NH2-terminal kinase. *Hum Mol Genet* 12**,** 1535-1542.

Ordway, J.M., Cearley, J.A., Detloff, P.J., 1999. CAG-polyglutamine-repeat mutations: independence from gene context. *Philos Trans R Soc Lond B Biol Sci* 354**,** 1083-1088.

Osaka, H., Wang, Y.L., Takada, K., Takizawa, S., Setsuie, R., Li, H., Sato, Y., Nishikawa, K., Sun, Y.J., Sakurai, M., Harada, T., Hara, Y., Kimura, I., Chiba, S., Namikawa, K., Kiyama, H., Noda, M., Aoki, S., Wada, K., 2003. Ubiquitin carboxy-terminal hydrolase L1 binds to and stabilizes monoubiquitin in neuron. *Hum Mol Genet* 12**,** 1945-1958.

Ouimet, C.C., Miller, P.E., Hemmings, H.C., Jr., Walaas, S.I., Greengard, P., 1984. DARPP-32, a dopamine- and adenosine 3':5'-monophosphate-regulated phosphoprotein enriched in dopamine-innervated brain regions. III. Immunocytochemical localization. *J Neurosci* 4**,** 111-124.

Ouyang, H., Ali, Y.O., Ravichandran, M., Dong, A., Qiu, W., MacKenzie, F., Dhe-Paganon, S., Arrowsmith, C.H., Zhai, R.G., 2012. Protein aggregates are recruited to aggresome by histone deacetylase 6 via unanchored ubiquitin C termini. *J Biol Chem* 287**,** 2317-2327.

Pak, D.T., Sheng, M., 2003. Targeted protein degradation and synapse remodeling by an inducible protein kinase. *Science* 302**,** 1368-1373.

Palazzolo, I., Burnett, B.G., Young, J.E., Brenne, P.L., La Spada, A.R., Fischbeck, K.H., Howell, B.W., Pennuto, M., 2007. Akt blocks ligand binding and protects against expanded polyglutamine androgen receptor toxicity. *Hum Mol Genet* 16**,** 1593-1603.

Palazzolo, I., Stack, C., Kong, L., Musaro, A., Adachi, H., Katsuno, M., Sobue, G., Taylor, J.P., Sumner, C.J., Fischbeck, K.H., Pennuto, M., 2009. Overexpression of IGF-1 in muscle attenuates disease in a mouse model of spinal and bulbar muscular atrophy. *Neuron* 63**,** 316-328.

Palop, J.J., Chin, J., Mucke, L., 2006. A network dysfunction perspective on neurodegenerative diseases. *Nature* 443**,** 768-773.

Pardo, R., Colin, E., Regulier, E., Aebischer, P., Deglon, N., Humbert, S., Saudou, F., 2006. Inhibition of calcineurin by FK506 protects against polyglutamine-huntingtin toxicity through an increase of huntingtin phosphorylation at S421. *J Neurosci* 26**,** 1635-1645.

Patrick, G.N., Bingol, B., Weld, H.A., Schuman, E.M., 2003. Ubiquitin-mediated proteasome activity is required for agonist-induced endocytosis of GluRs. *Current biology : CB* 13**,** 2073-2081.

Paulson, H.L., Das, S.S., Crino, P.B., Perez, M.K., Patel, S.C., Gotsdiner, D., Fischbeck, K.H., Pittman, R.N., 1997a. Machado-Joseph disease gene product is a cytoplasmic protein widely expressed in brain. *Ann Neurol* 41**,** 453-462.

Paulson, H.L., Perez, M.K., Trottier, Y., Trojanowski, J.Q., Subramony, S.H., Das, S.S., Vig, P., Mandel, J.L., Fischbeck, K.H., Pittman, R.N., 1997b. Intranuclear inclusions of expanded polyglutamine protein in spinocerebellar ataxia type 3. *Neuron* 19**,** 333-344.

Pawson, T., Scott, J.D., 2005. Protein phosphorylation in signaling--50 years and counting. *Trends in biochemical sciences* 30**,** 286-290.

Pearlman, S.M., Serber, Z., Ferrell, J.E., Jr., 2011. A mechanism for the evolution of phosphorylation sites. *Cell* 147**,** 934-946.

Pedroso, J.L., Franca, M.C., Jr., Braga-Neto, P., D'Abreu, A., Saraiva-Pereira, M.L., Saute, J.A., Teive, H.A., Caramelli, P., Jardim, L.B., Lopes-Cendes, I., Barsottini, O.G., 2013. Nonmotor and extracerebellar features in Machado-Joseph disease: a review. *Mov Disord* 28**,** 1200-1208.

Pennuto, M., Palazzolo, I., Poletti, A., 2009. Post-translational modifications of expanded polyglutamine proteins: impact on neurotoxicity. *Hum Mol Genet* 18**,** R40-47.

Perez, M.K., Paulson, H.L., Pendse, S.J., Saionz, S.J., Bonini, N.M., Pittman, R.N., 1998. Recruitment and the role of nuclear localization in polyglutamine-mediated aggregation. *J Cell Biol* 143**,** 1457-1470.

Perez, M.K., Paulson, H.L., Pittman, R.N., 1999. Ataxin-3 with an altered conformation that exposes the polyglutamine domain is associated with the nuclear matrix. *Hum Mol Genet* 8**,** 2377-2385.

Pickart, C.M., Eddins, M.J., 2004. Ubiquitin: structures, functions, mechanisms. *Biochim Biophys Acta* 1695**,** 55-72.

Pickart, C.M., Fushman, D., 2004. Polyubiquitin chains: polymeric protein signals. *Current opinion in chemical biology* 8**,** 610-616.

Popoli, M., Yan, Z., McEwen, B.S., Sanacora, G., 2012. The stressed synapse: the impact of stress and glucocorticoids on glutamate transmission. *Nat Rev Neurosci* 13**,** 22-37.

Pountney, D.L., Huang, Y., Burns, R.J., Haan, E., Thompson, P.D., Blumbergs, P.C., Gai, W.P., 2003. SUMO-1 marks the nuclear inclusions in familial neuronal intranuclear inclusion disease. *Exp Neurol* 184**,** 436-446.

Pozzi, C., Valtorta, M., Tedeschi, G., Galbusera, E., Pastori, V., Bigi, A., Nonnis, S., Grassi, E., Fusi, P., 2008. Study of subcellular localization and proteolysis of ataxin-3. *Neurobiol Dis* 30**,** 190-200.

Rangone, H., Poizat, G., Troncoso, J., Ross, C.A., MacDonald, M.E., Saudou, F., Humbert, S., 2004. The serum- and glucocorticoid-induced kinase SGK inhibits mutant huntingtin-induced toxicity by phosphorylating serine 421 of huntingtin. *The European journal of neuroscience* 19**,** 273-279.

Reiley, W., Zhang, M., Wu, X., Granger, E., Sun, S.C., 2005. Regulation of the deubiquitinating enzyme CYLD by IkappaB kinase gamma-dependent phosphorylation. *Mol Cell Biol* 25**,** 3886-3895.

Reina, C.P., Zhong, X., Pittman, R.N., 2010. Proteotoxic stress increases nuclear localization of ataxin-3. *Hum Mol Genet* 19**,** 235-249.

Renatus, M., Farady, C.J., 2012. Phosphorylation meets proteolysis. *Structure* 20**,** 570-571.

Reyes-Turcu, F.E., Ventii, K.H., Wilkinson, K.D., 2009. Regulation and cellular roles of ubiquitin-specific deubiquitinating enzymes. *Annu Rev Biochem* 78**,** 363-397.

Reyes-Turcu, F.E., Wilkinson, K.D., 2009. Polyubiquitin binding and disassembly by deubiquitinating enzymes. *Chem Rev* 109**,** 1495-1508.

Rieser, E., Cordier, S.M., Walczak, H., 2013. Linear ubiquitination: a newly discovered regulator of cell signalling. *Trends in biochemical sciences* 38**,** 94-102.

Riess, O., Rüb, U., Pastore, A., Bauer, P., Schöls, L. (2008) SCA3: neurological features, pathogenesis and animal models. In: *Cerebellum*. pp. 125-137.

Riley, B.E., Lougheed, J.C., Callaway, K., Velasquez, M., Brecht, E., Nguyen, L., Shaler, T., Walker, D., Yang, Y., Regnstrom, K., Diep, L., Zhang, Z., Chiou, S., Bova, M., Artis, D.R., Yao, N., Baker, J., Yednock, T., Johnston, J.A., 2013. Structure and function of Parkin E3 ubiquitin ligase reveals aspects of RING and HECT ligases. *Nature communications* 4**,** 1982.

Rivkin, E., Almeida, S.M., Ceccarelli, D.F., Juang, Y.C., MacLean, T.A., Srikumar, T., Huang, H., Dunham, W.H., Fukumura, R., Xie, G., Gondo, Y., Raught, B., Gingras, A.C., Sicheri, F., Cordes, S.P., 2013. The linear ubiquitin-specific deubiquitinase gumby regulates angiogenesis. *Nature* 498**,** 318-324.

Robert, X., Gouet, P., 2014. Deciphering key features in protein structures with the new ENDscript server. *Nucleic acids research* 42**,** W320-324.

Robertson, A.L., Bottomley, S.P., 2010. Towards the treatment of polyglutamine diseases: the modulatory role of protein context. *Curr Med Chem* 17**,** 3058-3068.

Rodrigues, A.J., Coppola, G., Santos, C., Costa Mdo, C., Ailion, M., Sequeiros, J., Geschwind, D.H., Maciel, P., 2007. Functional genomics and biochemical characterization of the C. elegans orthologue of the Machado-Joseph disease protein ataxin-3. *FASEB J* 21**,** 1126-1136.

Rodrigues, A.J., do Carmo Costa, M., Silva, T.L., Ferreira, D., Bajanca, F., Logarinho, E., Maciel, P., 2010. Absence of ataxin-3 leads to cytoskeletal disorganization and increased cell death. *Biochim Biophys Acta* 1803**,** 1154-1163.

Rosenberg, R.N., 1992. Machado-Joseph disease: an autosomal dominant motor system degeneration. *Mov Disord* 7**,** 193-203.

Rosenberg, R.N., Nyhan, W.L., Bay, C., Shore, P., 1976. Autosomal dominant striatonigral degeneration. A clinical, pathologic, and biochemical study of a new genetic disorder. *Neurology* 26**,** 703-714.

Ross, C.A., Poirier, M.A., 2004. Protein aggregation and neurodegenerative disease. *Nat Med* 10 Suppl**,** S10-17.

Ruano, L., Melo, C., Silva, M.C., Coutinho, P., 2014. The global epidemiology of hereditary ataxia and spastic paraplegia: a systematic review of prevalence studies. *Neuroepidemiology* 42**,** 174-183.

Rüb, U., Brunt, E.R., Deller, T., 2008. New insights into the pathoanatomy of spinocerebellar ataxia type 3 (Machado-Joseph disease). *Curr Opin Neurol* 21**,** 111-116.

Rüb, U., Brunt, E.R., Petrasch-Parwez, E., Schols, L., Theegarten, D., Auburger, G., Seidel, K., Schultz, C., Gierga, K., Paulson, H., van Broeckhoven, C., Deller, T., de Vos, R.A., 2006a. Degeneration of ingestion-related brainstem nuclei in spinocerebellar ataxia type 2, 3, 6 and 7. *Neuropathol Appl Neurobiol* 32**,** 635-649.

Rüb, U., de Vos, R.A., Brunt, E.R., Sebesteny, T., Schols, L., Auburger, G., Bohl, J., Ghebremedhin, E., Gierga, K., Seidel, K., den Dunnen, W., Heinsen, H., Paulson, H., Deller, T., 2006b. Spinocerebellar ataxia type 3 (SCA3): thalamic neurodegeneration occurs independently from thalamic ataxin-3 immunopositive neuronal intranuclear inclusions. *Brain Pathol* 16**,** 218-227.

Rüb, U., Schöls, L., Paulson, H., Auburger, G., Kermer, P., Jen, J.C., Seidel, K., Korf, H.W., Deller, T., 2013. Clinical features, neurogenetics and neuropathology of the polyglutamine spinocerebellar ataxias type 1, 2, 3, 6 and 7. *Prog Neurobiol* 104**,** 38-66.

Saigoh, K., Wang, Y.L., Suh, J.G., Yamanishi, T., Sakai, Y., Kiyosawa, H., Harada, T., Ichihara, N., Wakana, S., Kikuchi, T., Wada, K., 1999. Intragenic deletion in the gene encoding ubiquitin carboxy-terminal hydrolase in gad mice. *Nat Genet* 23**,** 47-51.

Saliba, R.S., Michels, G., Jacob, T.C., Pangalos, M.N., Moss, S.J., 2007. Activity-dependent ubiquitination of GABA(A) receptors regulates their accumulation at synaptic sites. *J Neurosci* 27**,** 13341-13351.

Saliba, R.S., Pangalos, M., Moss, S.J., 2008. The ubiquitin-like protein Plic-1 enhances the membrane insertion of GABAA receptors by increasing their stability within the endoplasmic reticulum. *J Biol Chem* 283**,** 18538-18544.

Saudou, F., Finkbeiner, S., Devys, D., Greenberg, M.E., 1998. Huntingtin acts in the nucleus to induce apoptosis but death does not correlate with the formation of intranuclear inclusions. *Cell* 95**,** 55-66.

Saunders, H.M., Bottomley, S.P., 2009. Multi-domain misfolding: understanding the aggregation pathway of polyglutamine proteins. *Protein Eng Des Sel* 22**,** 447-451.

Scaglione, K.M., Zavodszky, E., Todi, S.V., Patury, S., Xu, P., Rodriguez-Lebron, E., Fischer, S., Konen, J., Djarmati, A., Peng, J., Gestwicki, J.E., Paulson, H.L., 2011. Ube2w and ataxin-3 coordinately regulate the ubiquitin ligase CHIP. *Mol Cell* 43**,** 599-612.

Scarff, C.A., Sicorello, A., Tomé, R.J.L., Macedo-Ribeiro, S., Ashcroft, A.E., Radford, S.E., 2013. A tale of a tail: Structural insights into the conformational properties of the polyglutamine protein ataxin-3. *International Journal of Mass Spectrometry* 345-347**,** 63–70.

Schaefer, M.H., Wanker, E.E., Andrade-Navarro, M.A., 2012. Evolution and function of CAG/polyglutamine repeats in protein-protein interaction networks. *Nucleic acids research* 40**,** 4273-4287.

Schaffar, G., Breuer, P., Boteva, R., Behrends, C., Tzvetkov, N., Strippel, N., Sakahira, H., Siegers, K., Hayer-Hartl, M., Hartl, F.U., 2004. Cellular toxicity of polyglutamine expansion proteins: mechanism of transcription factor deactivation. *Mol Cell* 15**,** 95-105.

Scheel, H., Tomiuk, S., Hofmann, K., 2003. Elucidation of ataxin-3 and ataxin-7 function by integrative bioinformatics. *Hum Mol Genet* 12**,** 2845-2852.

Schilling, B., Gafni, J., Torcassi, C., Cong, X., Row, R.H., LaFevre-Bernt, M.A., Cusack, M.P., Ratovitski, T., Hirschhorn, R., Ross, C.A., Gibson, B.W., Ellerby, L.M., 2006. Huntingtin phosphorylation sites mapped by mass spectrometry. Modulation of cleavage and toxicity. *J Biol Chem* 281**,** 23686-23697.

Schindelin, J., Arganda-Carreras, I., Frise, E., Kaynig, V., Longair, M., Pietzsch, T., Preibisch, S., Rueden, C., Saalfeld, S., Schmid, B., Tinevez, J.Y., White, D.J., Hartenstein, V., Eliceiri, K., Tomancak, P., Cardona, A., 2012. Fiji: an open-source platform for biological-image analysis. *Nature methods* 9**,** 676-682.

Schmidt, T., Landwehrmeyer, G.B., Schmitt, I., Trottier, Y., Auburger, G., Laccone, F., Klockgether, T., Volpel, M., Epplen, J.T., Schols, L., Riess, O., 1998. An isoform of ataxin-3 accumulates in the nucleus of neuronal cells in affected brain regions of SCA3 patients. *Brain Pathol* 8**,** 669-679.

Schmidt, T., Lindenberg, K.S., Krebs, A., Schols, L., Laccone, F., Herms, J., Rechsteiner, M., Riess, O., Landwehrmeyer, G.B., 2002. Protein surveillance machinery in brains with spinocerebellar ataxia type 3: redistribution and differential recruitment of 26S proteasome subunits and chaperones to neuronal intranuclear inclusions. *Ann Neurol* 51**,** 302-310.

Schmitt, I., Linden, M., Khazneh, H., Evert, B.O., Breuer, P., Klockgether, T., Wuellner, U., 2007. Inactivation of the mouse Atxn3 (ataxin-3) gene increases protein ubiquitination. *Biochem Biophys Res Commun* 362**,** 734-739.

Schöls, L., Bauer, P., Schmidt, T., Schulte, T., Riess, O., 2004. Autosomal dominant cerebellar ataxias: clinical features, genetics, and pathogenesis. *Lancet Neurol* 3**,** 291-304.

Schöls, L., Paulson, H., Riess, O. 2000. Spinocerebellar Ataxia Type 3 Machado-Joseph Disease In: *Handbook of Ataxia Disorders*. pp. 385-423. Ed. T. Klockgether. CRC Press: New York.

Seidel, K., den Dunnen, W.F., Schultz, C., Paulson, H., Frank, S., de Vos, R.A., Brunt, E.R., Deller, T., Kampinga, H.H., Rüb, U., 2010. Axonal inclusions in spinocerebellar ataxia type 3. *Acta Neuropathol* 120**,** 449-460.

Seilhean, D., Takahashi, J., El Hachimi, K.H., Fujigasaki, H., Lebre, A.S., Biancalana, V., Durr, A., Salachas, F., Hogenhuis, J., de The, H., Hauw, J.J., Meininger, V., Brice, A., Duyckaerts, C., 2004. Amyotrophic lateral sclerosis with neuronal intranuclear protein inclusions. *Acta Neuropathol* 108**,** 81-87.

Seki, T., Gong, L., Williams, A.J., Sakai, N., Todi, S.V., Paulson, H.L., 2013. JosD1, a membrane-targeted deubiquitinating enzyme, is activated by ubiquitination and regulates membrane dynamics, cell motility, and endocytosis. *J Biol Chem* 288**,** 17145-17155.

Seo, J., Lee, K.J., 2004. Post-translational modifications and their biological functions: proteomic analysis and systematic approaches. *Journal of biochemistry and molecular biology* 37**,** 35-44.

Shakkottai, V.G., do Carmo Costa, M., Dell'Orco, J.M., Sankaranarayanan, A., Wulff, H., Paulson, H.L., 2011. Early changes in cerebellar physiology accompany motor dysfunction in the polyglutamine disease spinocerebellar ataxia type 3. *J Neurosci* 31**,** 13002-13014.

Shao, J., Diamond, M.I., 2007. Polyglutamine diseases: emerging concepts in pathogenesis and therapy. *Hum Mol Genet* 16 Spec No. 2**,** R115-123.

Silva-Fernandes, A., Costa Mdo, C., Duarte-Silva, S., Oliveira, P., Botelho, C.M., Martins, L., Mariz, J.A., Ferreira, T., Ribeiro, F., Correia-Neves, M., Costa, C., Maciel, P., 2010. Motor uncoordination and neuropathology in a transgenic mouse model of Machado-Joseph disease lacking intranuclear inclusions and ataxin-3 cleavage products. *Neurobiol Dis* 40**,** 163-176.

Simões, A.T., Goncalves, N., Koeppen, A., Deglon, N., Kugler, S., Duarte, C.B., Pereira de Almeida, L., 2012. Calpastatin-mediated inhibition of calpains in the mouse brain prevents mutant ataxin 3 proteolysis, nuclear localization and aggregation, relieving Machado-Joseph disease. *Brain* 135**,** 2428-2439.

Simões, A.T., Goncalves, N., Nobre, R.J., Duarte, C.B., Pereira de Almeida, L., 2014. Calpain inhibition reduces ataxin-3 cleavage alleviating neuropathology and motor impairments in mouse models of Machado-Joseph disease. *Hum Mol Genet*.

Slow, E.J., Graham, R.K., Osmand, A.P., Devon, R.S., Lu, G., Deng, Y., Pearson, J., Vaid, K., Bissada, N., Wetzel, R., Leavitt, B.R., Hayden, M.R., 2005. Absence of behavioral abnormalities and neurodegeneration in vivo despite widespread neuronal huntingtin inclusions. *Proc Natl Acad Sci U S A* 102**,** 11402-11407.

Sobue, G., Doyu, M., Nakao, N., Shimada, N., Mitsuma, T., Maruyama, H., Kawakami, S., Nakamura, S., 1996. Homozygosity for Machado-Joseph disease gene enhances phenotypic severity. *J Neurol Neurosurg Psychiatry* 60**,** 354-356.

Song, A.X., Zhou, C.J., Peng, Y., Gao, X.C., Zhou, Z.R., Fu, Q.S., Hong, J., Lin, D.H., Hu, H.Y., 2010. Structural transformation of the tandem ubiquitin-interacting motifs in ataxin-3 and their cooperative interactions with ubiquitin chains. *PLoS One* 5**,** e13202.

Soong, B., Cheng, C., Liu, R., Shan, D., 1997. Machado-Joseph disease: clinical, molecular, and metabolic characterization in Chinese kindreds. *Ann Neurol* 41**,** 446-452.

Soong, B.W., Liu, R.S., 1998. Positron emission tomography in asymptomatic gene carriers of Machado-Joseph disease. *J Neurol Neurosurg Psychiatry* 64**,** 499-504.

Sowa, M.E., Bennett, E.J., Gygi, S.P., Harper, J.W., 2009. Defining the human deubiquitinating enzyme interaction landscape. *Cell* 138**,** 389-403.

Sudarsky, L., Coutinho, P., 1995. Machado-Joseph disease. *Clin Neurosci* 3**,** 17-22.

Sugiura, A., Yonashiro, R., Fukuda, T., Matsushita, N., Nagashima, S., Inatome, R., Yanagi, S., 2010. A mitochondrial ubiquitin ligase MITOL controls cell toxicity of polyglutamine-expanded protein. *Mitochondrion* 11**,** 139-146.

Tait, D., Riccio, M., Sittler, A., Scherzinger, E., Santi, S., Ognibene, A., Maraldi, N.M., Lehrach, H., Wanker, E.E., 1998. Ataxin-3 is transported into the nucleus and associates with the nuclear matrix. *Hum Mol Genet* 7**,** 991-997.

Takahashi, J., Tanaka, J., Arai, K., Funata, N., Hattori, T., Fukuda, T., Fujigasaki, H., Uchihara, T., 2001. Recruitment of nonexpanded polyglutamine proteins to intranuclear aggregates in neuronal intranuclear hyaline inclusion disease. *J Neuropathol Exp Neurol* 60**,** 369-376.

Takahashi, T., Katada, S., Onodera, O., 2010. Polyglutamine diseases: where does toxicity come from? what is toxicity? where are we going? *Journal of molecular cell biology* 2**,** 180-191.

Takiyama, Y., Nishizawa, M., Tanaka, H., Kawashima, S., Sakamoto, H., Karube, Y., Shimazaki, H., Soutome, M., Endo, K., Ohta, S., et al., 1993. The gene for Machado-Joseph disease maps to human chromosome 14q. *Nat Genet* 4**,** 300-304.

Tanaka, M., Morishima, I., Akagi, T., Hashikawa, T., Nukina, N., 2001. Intra- and intermolecular beta-pleated sheet formation in glutamine-repeat inserted myoglobin as a model for polyglutamine diseases. *J Biol Chem* 276**,** 45470-45475.

Taniwaki, T., Sakai, T., Kobayashi, T., Kuwabara, Y., Otsuka, M., Ichiya, Y., Masuda, K., Goto, I., 1997. Positron emission tomography (PET) in Machado-Joseph disease. *Journal of the neurological sciences* 145**,** 63-67.

Tanno, H., Komada, M., 2013. The ubiquitin code and its decoding machinery in the endocytic pathway. *Journal of biochemistry* 153**,** 497-504.

Tao, R.S., Fei, E.K., Ying, Z., Wang, H.F., Wang, G.H., 2008. Casein kinase 2 interacts with and phosphorylates ataxin-3. *Neurosci Bull* 24**,** 271-277.

Tarlac, V., Storey, E., 2003. Role of proteolysis in polyglutamine disorders. *J Neurosci Res* 74**,** 406-416.

Tarrant, M.K., Cole, P.A., 2009. The chemical biology of protein phosphorylation. *Annu Rev Biochem* 78**,** 797-825.

Teixeira-Castro, A., Ailion, M., Jalles, A., Brignull, H.R., Vilaca, J.L., Dias, N., Rodrigues, P., Oliveira, J.F., Neves-Carvalho, A., Morimoto, R.I., Maciel, P., 2011. Neuron-specific proteotoxicity of mutant ataxin-3 in C. elegans: rescue by the DAF-16 and HSF-1 pathways. *Hum Mol Genet* 20**,** 2996-3009.

Terry, R.D., Masliah, E., Salmon, D.P., Butters, N., DeTeresa, R., Hill, R., Hansen, L.A., Katzman, R., 1991. Physical basis of cognitive alterations in Alzheimer's disease: synapse loss is the major correlate of cognitive impairment. *Ann Neurol* 30**,** 572-580.

Thompson, L.M., Aiken, C.T., Kaltenbach, L.S., Agrawal, N., Illes, K., Khoshnan, A., Martinez-Vincente, M., Arrasate, M., O'Rourke, J.G., Khashwji, H., Lukacsovich, T., Zhu, Y.Z., Lau, A.L., Massey, A., Hayden, M.R., Zeitlin, S.O., Finkbeiner, S., Green, K.N., LaFerla, F.M., Bates, G., Huang, L., Patterson, P.H., Lo, D.C., Cuervo, A.M., Marsh, J.L., Steffan, J.S., 2009. IKK phosphorylates Huntingtin and targets it for degradation by the proteasome and lysosome. *J Cell Biol* 187**,** 1083-1099.

Thorsness, P.E., Koshland, D.E., Jr., 1987. Inactivation of isocitrate dehydrogenase by phosphorylation is mediated by the negative charge of the phosphate. *J Biol Chem* 262**,** 10422-10425.

Todd, T.W., Lim, J., 2013. Aggregation formation in the polyglutamine diseases: protection at a cost? *Molecules and cells* 36**,** 185-194.

Todi, S.V., Laco, M.N., Winborn, B.J., Travis, S.M., Wen, H.M., Paulson, H.L., 2007. Cellular turnover of the polyglutamine disease protein ataxin-3 is regulated by its catalytic activity. *J Biol Chem* 282**,** 29348-29358.

Todi, S.V., Paulson, H.L., 2011. Balancing act: deubiquitinating enzymes in the nervous system. *Trends Neurosci* 34**,** 370-382.

Todi, S.V., Scaglione, K.M., Blount, J.R., Basrur, V., Conlon, K.P., Pastore, A., Elenitoba-Johnson, K., Paulson, H.L., 2010. Activity and cellular functions of the deubiquitinating enzyme and polyglutamine disease protein ataxin-3 are regulated by ubiquitination at lysine 117. *J Biol Chem* 285**,** 39303-39313.

Todi, S.V., Winborn, B.J., Scaglione, K.M., Blount, J.R., Travis, S.M., Paulson, H.L., 2009. Ubiquitination directly enhances activity of the deubiquitinating enzyme ataxin-3. *EMBO J* 28**,** 372-382.

Torashima, T., Koyama, C., Iizuka, A., Mitsumura, K., Takayama, K., Yanagi, S., Oue, M., Yamaguchi, H., Hirai, H., 2008. Lentivector-mediated rescue from cerebellar ataxia in a mouse model of spinocerebellar ataxia. *EMBO reports* 9**,** 393-399.

Trottier, Y., Cancel, G., An-Gourfinkel, I., Lutz, Y., Weber, C., Brice, A., Hirsch, E., Mandel, J.L., 1998. Heterogeneous intracellular localization and expression of ataxin-3. *Neurobiol Dis* 5**,** 335-347.

Tsai, Y.C., Fishman, P.S., Thakor, N.V., Oyler, G.A., 2003. Parkin facilitates the elimination of expanded polyglutamine proteins and leads to preservation of proteasome function. *J Biol Chem* 278**,** 22044-22055.

Tsou, W.L., Burr, A.A., Ouyang, M., Blount, J.R., Scaglione, K.M., Todi, S.V., 2013. Ubiquitination regulates the neuroprotective function of the deubiquitinase ataxin-3 in vivo. *J Biol Chem* 288**,** 34460-34469.

Tzvetkov, N., Breuer, P., 2007. Josephin domain-containing proteins from a variety of species are active de-ubiquitination enzymes. *Biol Chem* 388**,** 973-978.

Uchihara, T., Fujigasaki, H., Koyano, S., Nakamura, A., Yagishita, S., Iwabuchi, K., 2001. Non-expanded polyglutamine proteins in intranuclear inclusions of hereditary ataxias--triple-labeling immunofluorescence study. *Acta Neuropathol* 102**,** 149-152.

UniProt, C., 2014. Activities at the Universal Protein Resource (UniProt). *Nucleic acids research* 42**,** 7486.

Uversky, V.N., 2010. Mysterious oligomerization of the amyloidogenic proteins. *FEBS J* 277**,** 2940-2953.

Vale, J., Bugalho, P., Silveira, I., Sequeiros, J., Guimaraes, J., Coutinho, P., 2010. Autosomal dominant cerebellar ataxia: frequency analysis and clinical characterization of 45 families from Portugal. *European journal of neurology : the official journal of the European Federation of Neurological Societies* 17**,** 124-128.

van der Veen, A.G., Ploegh, H.L., 2012. Ubiquitin-like proteins. *Annu Rev Biochem* 81**,** 323-357.

Velazquez-Delgado, E.M., Hardy, J.A., 2012. Phosphorylation regulates assembly of the caspase-6 substrate-binding groove. *Structure* 20**,** 742-751.

Ventii, K.H., Wilkinson, K.D., 2008. Protein partners of deubiquitinating enzymes. *The Biochemical journal* 414**,** 161-175.

Verma, P., Chierzi, S., Codd, A.M., Campbell, D.S., Meyer, R.L., Holt, C.E., Fawcett, J.W., 2005. Axonal protein synthesis and degradation are necessary for efficient growth cone regeneration. *J Neurosci* 25**,** 331-342.

Villamil, M.A., Liang, Q., Chen, J., Choi, Y.S., Hou, S., Lee, K.H., Zhuang, Z., 2012. Serine phosphorylation is critical for the activation of ubiquitin-specific protease 1 and its interaction with WD40-repeat protein UAF1. *Biochemistry* 51**,** 9112-9123.

Wada, K., Kamitani, T., 2006. UnpEL/Usp4 is ubiquitinated by Ro52 and deubiquitinated by itself. *Biochem Biophys Res Commun* 342**,** 253-258.

Wang, G., Ide, K., Nukina, N., Goto, J., Ichikawa, Y., Uchida, K., Sakamoto, T., Kanazawa, I., 1997. Machado-Joseph disease gene product identified in lymphocytes and brain. *Biochem Biophys Res Commun* 233**,** 476-479.

Wang, G., Sawai, N., Kotliarova, S., Kanazawa, I., Nukina, N., 2000. Ataxin-3, the MJD1 gene product, interacts with the two human homologs of yeast DNA repair protein RAD23, HHR23A and HHR23B. *Hum Mol Genet* 9**,** 1795-1803.

Wang, H., Jia, N., Fei, E., Wang, Z., Liu, C., Zhang, T., Fan, J., Wu, M., Chen, L., Nukina, N., Zhou, J., Wang, G., 2007. p45, an ATPase subunit of the 19S proteasome, targets the polyglutamine disease protein ataxin-3 to the proteasome. *J Neurochem* 101**,** 1651-1661.

Wang, Q., Li, L., Ye, Y., 2006. Regulation of retrotranslocation by p97-associated deubiquitinating enzyme ataxin-3. *J Cell Biol* 174**,** 963-971.

Wang, Q., Li, L., Ye, Y., 2008. Inhibition of p97-dependent protein degradation by Eeyarestatin I. *J Biol Chem* 283**,** 7445-7454.

Wang, T., Yin, L., Cooper, E.M., Lai, M.Y., Dickey, S., Pickart, C.M., Fushman, D., Wilkinson, K.D., Cohen, R.E., Wolberger, C., 2009. Evidence for bidentate substrate binding as the basis for the K48 linkage specificity of otubain 1. *J Mol Biol* 386**,** 1011-1023.

Warby, S.C., Chan, E.Y., Metzler, M., Gan, L., Singaraja, R.R., Crocker, S.F., Robertson, H.A., Hayden, M.R., 2005. Huntingtin phosphorylation on serine 421 is significantly reduced in the striatum and by polyglutamine expansion in vivo. *Hum Mol Genet* 14**,** 1569-1577.

Warby, S.C., Doty, C.N., Graham, R.K., Shively, J., Singaraja, R.R., Hayden, M.R., 2009. Phosphorylation of huntingtin reduces the accumulation of its nuclear fragments. *Molecular and cellular neurosciences* 40**,** 121-127.

Warrick, J.M., Chan, H.Y., Gray-Board, G.L., Chai, Y., Paulson, H.L., Bonini, N.M., 1999. Suppression of polyglutamine-mediated neurodegeneration in Drosophila by the molecular chaperone HSP70. *Nat Genet* 23**,** 425-428.

Warrick, J.M., Morabito, L.M., Bilen, J., Gordesky-Gold, B., Faust, L.Z., Paulson, H.L., Bonini, N.M., 2005. Ataxin-3 suppresses polyglutamine neurodegeneration in Drosophila by a ubiquitin-associated mechanism. *Mol Cell* 18**,** 37-48.

Warrick, J.M., Paulson, H.L., Gray-Board, G.L., Bui, Q.T., Fischbeck, K.H., Pittman, R.N., Bonini, N.M., 1998. Expanded polyglutamine protein forms nuclear inclusions and causes neural degeneration in Drosophila. *Cell* 93**,** 939-949.

Watts, R.J., Hoopfer, E.D., Luo, L., 2003. Axon pruning during Drosophila metamorphosis: evidence for local degeneration and requirement of the ubiquitin-proteasome system. *Neuron* 38**,** 871-885.

Weeks, S.D., Grasty, K.C., Hernandez-Cuebas, L., Loll, P.J., 2011. Crystal structure of a Josephin-ubiquitin complex: evolutionary restraints on ataxin-3 deubiquitinating activity. *J Biol Chem* 286**,** 4555-4565.

Weissman, A.M., 2001. Themes and variations on ubiquitylation. *Nat Rev Mol Cell Biol* 2**,** 169-178.

Weissman, A.M., Shabek, N., Ciechanover, A., 2011. The predator becomes the prey: regulating the ubiquitin system by ubiquitylation and degradation. *Nat Rev Mol Cell Biol* 12**,** 605-620.

Welchman, R.L., Gordon, C., Mayer, R.J., 2005. Ubiquitin and ubiquitin-like proteins as multifunctional signals. *Nat Rev Mol Cell Biol* 6**,** 599-609.

Wellington, C.L., Ellerby, L.M., Hackam, A.S., Margolis, R.L., Trifiro, M.A., Singaraja, R., McCutcheon, K., Salvesen, G.S., Propp, S.S., Bromm, M., Rowland, K.J., Zhang, T., Rasper, D., Roy, S., Thornberry, N., Pinsky, L., Kakizuka, A., Ross, C.A., Nicholson, D.W., Bredesen, D.E., Hayden, M.R., 1998. Caspase cleavage of gene products associated with triplet expansion disorders generates truncated fragments containing the polyglutamine tract. *J Biol Chem* 273**,** 9158-9167.

Wen, F.C., Li, Y.H., Tsai, H.F., Lin, C.H., Li, C., Liu, C.S., Lii, C.K., Nukina, N., Hsieh, M., 2003. Down-regulation of heat shock protein 27 in neuronal cells and non-neuronal cells expressing mutant ataxin-3. *FEBS Lett* 546**,** 307-314.

Wilkinson, K.D., Ventii, K.H., Friedrich, K.L., Mullally, J.E., 2005. The ubiquitin signal: assembly, recognition and termination. Symposium on ubiquitin and signaling. *EMBO reports* 6**,** 815-820.

Williams, A.J., Paulson, H.L., 2008. Polyglutamine neurodegeneration: protein misfolding revisited. *Trends Neurosci* 31**,** 521-528.

Wilson, S.M., Bhattacharyya, B., Rachel, R.A., Coppola, V., Tessarollo, L., Householder, D.B., Fletcher, C.F., Miller, R.J., Copeland, N.G., Jenkins, N.A., 2002. Synaptic defects in ataxia mice result from a mutation in Usp14, encoding a ubiquitin-specific protease. *Nat Genet* 32**,** 420-425.

Winborn, B.J., Travis, S.M., Todi, S.V., Scaglione, K.M., Xu, P., Williams, A.J., Cohen, R.E., Peng, J., Paulson, H.L., 2008. The deubiquitinating enzyme ataxin-3, a polyglutamine disease protein, edits Lys63 linkages in mixed linkage ubiquitin chains. *J Biol Chem* 283**,** 26436-26443.

Witze, E.S., Old, W.M., Resing, K.A., Ahn, N.G., 2007. Mapping protein post-translational modifications with mass spectrometry. *Nature methods* 4**,** 798-806.

Woods, B.T., Schaumburg, H.H., 1972. Nigro-spino-dentatal degeneration with nuclear ophthalmoplegia. A unique and partially treatable clinico-pathological entity. *Journal of the neurological sciences* 17**,** 149-166.

Wullner, U., Reimold, M., Abele, M., Burk, K., Minnerop, M., Dohmen, B.M., Machulla, H.J., Bares, R., Klockgether, T., 2005. Dopamine transporter positron emission tomography in spinocerebellar ataxias type 1, 2, 3, and 6. *Arch Neurol* 62**,** 1280-1285.

Yamada, M., Hayashi, S., Tsuji, S., Takahashi, H., 2001. Involvement of the cerebral cortex and autonomic ganglia in Machado-Joseph disease. *Acta Neuropathol* 101**,** 140-144.

Ye, Y., Rape, M., 2009. Building ubiquitin chains: E2 enzymes at work. *Nat Rev Mol Cell Biol* 10**,** 755-764.

Yen, T.C., Tzen, K.Y., Chen, M.C., Chou, Y.H., Chen, R.S., Chen, C.J., Wey, S.P., Ting, G., Lu, C.S., 2002. Dopamine transporter concentration is reduced in asymptomatic Machado-Joseph disease gene carriers. *J Nucl Med* 43**,** 153-159.

Yi, J.J., Ehlers, M.D., 2007. Emerging roles for ubiquitin and protein degradation in neuronal function. *Pharmacological reviews* 59**,** 14-39.

Ying, Z., Wang, H., Fan, H., Zhu, X., Zhou, J., Fei, E., Wang, G., 2009. Gp78, an ER associated E3, promotes SOD1 and ataxin-3 degradation. *Hum Mol Genet* 18**,** 4268-4281.

Yoshizawa, T., Yamagishi, Y., Koseki, N., Goto, J., Yoshida, H., Shibasaki, F., Shoji, S., Kanazawa, I., 2000. Cell cycle arrest enhances the in vitro cellular toxicity of the truncated Machado-Joseph disease gene product with an expanded polyglutamine stretch. *Hum Mol Genet* 9**,** 69-78.

Yu, Y.C., Kuo, C.L., Cheng, W.L., Liu, C.S., Hsieh, M., 2009. Decreased antioxidant enzyme activity and increased mitochondrial DNA damage in cellular models of Machado-Joseph disease. *J Neurosci Res* 87**,** 1884-1891.

Yuan, J., Luo, K., Zhang, L., Cheville, J.C., Lou, Z., 2010. USP10 regulates p53 localization and stability by deubiquitinating p53. *Cell* 140**,** 384-396.

Yuasa-Kawada, J., Kinoshita-Kawada, M., Wu, G., Rao, Y., Wu, J.Y., 2009. Midline crossing and Slit responsiveness of commissural axons require USP33. *Nature neuroscience* 12**,** 1087-1089.

Zala, D., Colin, E., Rangone, H., Liot, G., Humbert, S., Saudou, F., 2008. Phosphorylation of mutant huntingtin at S421 restores anterograde and retrograde transport in neurons. *Hum Mol Genet* 17**,** 3837-3846.

Zhang, Z.R., Bonifacino, J.S., Hegde, R.S., 2013. Deubiquitinases sharpen substrate discrimination during membrane protein degradation from the ER. *Cell* 154**,** 609-622.

Zhong, X., Pittman, R.N., 2006. Ataxin-3 binds VCP/p97 and regulates retrotranslocation of ERAD substrates. *Hum Mol Genet* 15**,** 2409-2420.

Zhuo, S., Clemens, J.C., Hakes, D.J., Barford, D., Dixon, J.E., 1993. Expression, purification, crystallization, and biochemical characterization of a recombinant protein phosphatase. *J Biol Chem* 268**,** 17754-17761.

Zoghbi, H.Y., Orr, H.T., 2000. Glutamine repeats and neurodegeneration. *Annu Rev Neurosci* 23**,** 217-247.